frontiers | Research Topics

Novel ligands and receptors in endocrine disorders

Edited by
Huashan Zhao, Juxue Li, Peng Zhu, Stig Ove Bøe and Rujuan Zuo

Published in
Frontiers in Cell and Developmental Biology
Frontiers in Molecular Biosciences

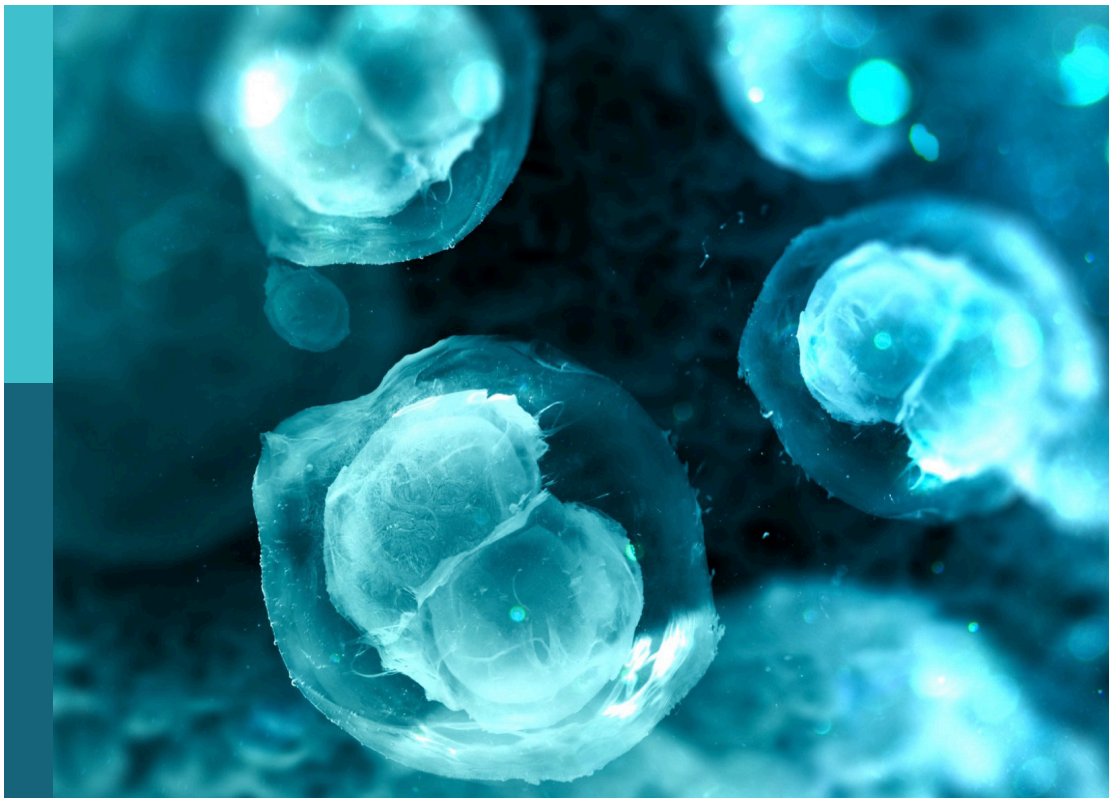

ISSN 1664-8714
ISBN 978-2-8325-2675-0
DOI 10.3389/978-2-8325-2675-0

About Frontiers

Frontiers is more than just an open access publisher of scholarly articles: it is a pioneering approach to the world of academia, radically improving the way scholarly research is managed. The grand vision of Frontiers is a world where all people have an equal opportunity to seek, share and generate knowledge. Frontiers provides immediate and permanent online open access to all its publications, but this alone is not enough to realize our grand goals.

Frontiers journal series

The Frontiers journal series is a multi-tier and interdisciplinary set of open-access, online journals, promising a paradigm shift from the current review, selection and dissemination processes in academic publishing. All Frontiers journals are driven by researchers for researchers; therefore, they constitute a service to the scholarly community. At the same time, the *Frontiers journal series* operates on a revolutionary invention, the tiered publishing system, initially addressing specific communities of scholars, and gradually climbing up to broader public understanding, thus serving the interests of the lay society, too.

Dedication to quality

Each Frontiers article is a landmark of the highest quality, thanks to genuinely collaborative interactions between authors and review editors, who include some of the world's best academicians. Research must be certified by peers before entering a stream of knowledge that may eventually reach the public - and shape society; therefore, Frontiers only applies the most rigorous and unbiased reviews. Frontiers revolutionizes research publishing by freely delivering the most outstanding research, evaluated with no bias from both the academic and social point of view. By applying the most advanced information technologies, Frontiers is catapulting scholarly publishing into a new generation.

What are Frontiers Research Topics?

Frontiers Research Topics are very popular trademarks of the *Frontiers journals series*: they are collections of at least ten articles, all centered on a particular subject. With their unique mix of varied contributions from Original Research to Review Articles, Frontiers Research Topics unify the most influential researchers, the latest key findings and historical advances in a hot research area.

Find out more on how to host your own Frontiers Research Topic or contribute to one as an author by contacting the Frontiers editorial office: frontiersin.org/about/contact

Novel ligands and receptors in endocrine disorders

Topic editors

Huashan Zhao — Shenzhen Institute of Advanced Technology, Chinese Academy of Sciences (CAS), China

Juxue Li — Nanjing Medical University, China

Peng Zhu — Anhui Medical University, China

Stig Ove Bøe — Oslo University Hospital, Norway

Rujuan Zuo — Oslo University Hospital, Norway

Citation

Zhao, H., Li, J., Zhu, P., Bøe, S. O., Zuo, R., eds. (2023). *Novel ligands and receptors in endocrine disorders*. Lausanne: Frontiers Media SA.

doi: 10.3389/978-2-8325-2675-0

The authors declare that the research was conducted in the absence of any commercial or financial relationships that could be construed as a potential conflict of interest

Table of contents

frontiers | Frontiers in Cell and Developmental Biology

TYPE Editorial
PUBLISHED 26 May 2023
DOI 10.3389/fcell.2023.1218271

OPEN ACCESS

EDITED AND REVIEWED BY
Graça Soveral,
University of Lisbon, Portugal

*CORRESPONDENCE
Huashan Zhao,
hs.zhao@siat.ac.cn

RECEIVED 06 May 2023
ACCEPTED 11 May 2023
PUBLISHED 26 May 2023

CITATION
Zhao H, Li J, Bøe SO, Zuo R and Zhu P (2023), Editorial: Novel ligands and receptors in endocrine disorders. *Front. Cell Dev. Biol.* 11:1218271. doi: 10.3389/fcell.2023.1218271

Editorial: Novel ligands and receptors in endocrine disorders

Huashan Zhao[1]*, Juxue Li[2], Stig Ove Bøe[3], Rujuan Zuo[4] and Peng Zhu[5]

[1]Center for Energy Metabolism and Reproduction, Shenzhen Institute of Advanced Technology, Chinese Academy of Sciences, Shenzhen, China, [2]State Key Laboratory of Reproductive Medicine and Offspring Health, Nanjing Medical University, Nanjing, Jiangsu, China, [3]Department of Microbiology, Oslo University Hospital, Oslo, Norway, [4]Laboratory for Stem Cell Dynamics, Department of Microbiology, Division of Laboratory Medicine, Oslo University Hospital, Rikshospitalet, Oslo, Norway, [5]Department of Maternal, Child and Adolescent Health, School of Public Health, Anhui Medical University, Hefei, China

KEYWORDS

ligands, receptors, endocrine disorders, reproductive endocrinology, environmental endocrine disrupting chemicals

Editorial on the Research Topic
Novel ligands and receptors in endocrine disorders

Abnormal interactions between ligands and receptors can promote various endocrine disorders. However, due to the complexity of endocrine systems and physiological processes, deciphering mechanisms for the diagnostic and treatment of these diseases remains a challenge. We thank authors from various research fields for their invaluable contributions to this Research Topic. The papers collected in this topic mainly encompass reproductive endocrine disorders, thereby enriching our knowledge on endocrine regulation involving well-known ligands and receptors in other systems. These identified targets shed light on further investigation of their mechanisms.

When an endogenous ligand binds to its receptor in the endocrine tissue cells, the ligand-receptor systems play an imperative role in regulating various physiological functions. Zhang et al. discovered that the chemerin-CMKLR1 system could regulate placental development and vascular remodeling during early pregnancy. Another Zhang et al. provided a comprehensive understanding of osteoprotegerin-RANK in endocrine regulation, reviewing the roles of osteoprotegerin in endocrine and metabolic disorders through the RANKL/RANK signaling. Furthermore, G protein-coupled receptors (GPCRs) family, as potential targets, contain many receptor candidates involved in endocrine disorders. For instance, Yin et al. reviewed the role of secretin/adhesion (Class B) GPCRs in placental development and preeclampsia. Lin et al. reviewed the emergent roles of GPR158 in regulating the endocrine system. And Luo et al. reviewed the effects of GPER on age-associated memory impairment induced by decreased estrogen levels. These three reviews highlight the multifaceted functions of GPCRs in endocrine disorders. In addition, Huang et al. discovered that the membrane ion channel protein, AQP8, could regulate ovarian secretion by modulating granulosa cell autophagy, suggesting that endocrine cells are not regulated solely by the ligand-receptor system.

Besides, receptors in endocrine cells can also be activated by exogenous ligands, including environmental endocrine disrupting chemicals (EDCs) and pharmaceutical molecules. In the field of exposure science, increasing studies focus on EDCs and their potential roles in endocrine disorders. As ligand analogs, EDCs disrupt endocrine hormone functions, leading to endocrine disorders and abnormal tissue development. Zhang et al. found that di-(2-ethylhexyl) phthalate (DEHP) exposure induced liver injury by promoting ferroptosis via downregulation of GPX4 in pregnant mice. Additionally, Zeng et al. reviewed the impact of early-life exposure to DEHP in

children with endocrine disorders. Similarly, pharmaceutical molecules could be used to treat endocrine disorders by activating corresponding receptors. Kong et al. reviewed recent advances in our understanding of the effects of *Salvia miltiorrhiza* active compounds on placenta-mediated pregnancy complications, indicating that many receptors play essential roles in the multiple endocrine events during pregnancy. These traditional Chinese medicine monomers could directly activate the corresponding receptors and improve the clinical symptoms, although the mechanism remains largely unknown.

Regarding research methods, Qu et al. established the three-dimensional visualization of mouse endometrial remodeling after superovulation, which is a valuable attempt. The response of the endometrial tissue to endocrine disturbance can be observed using the uterine 3D reconstruction technology.

In summary, this Research Topic aims to explore target ligands and receptors that regulate endocrine disorders, with a particular emphasis on the emerging roles of EDCs. Mechanism research, focusing on ligands or receptors, is still ongoing. It is hopeful that the discovery of more suitable drug targets, especially GPCRs, would aid in the treatment of endocrine disorders.

Author contributions

HZ drafted the manuscript. JL, SB, RZ, and PZ provided suggestions. HZ revised and finalized the manuscript. All authors contributed to the editorial and approved the submitted version.

Funding

This work was supported by Shenzhen Fundamental Research Program (JCYJ20220818102811025) and Open Project Fund of the Logistics Research Program (ZZBWS21J2001).

Acknowledgments

We thank all authors, reviewers and editors for their contributions to this Research Topic.

Conflict of interest

The authors declare that the research was conducted in the absence of any commercial or financial relationships that could be construed as a potential conflict of interest.

Publisher's note

frontiers | Frontiers in Cell and Developmental Biology

ORIGINAL RESEARCH
published: 17 May 2022
doi: 10.3389/fcell.2022.883636

The Regulatory Roles of Chemerin-Chemokine-Like Receptor 1 Axis in Placental Development and Vascular Remodeling During Early Pregnancy

Qingqing Zhang[1,2†], Zhonglin Xiao[3†], Cheuk-Lun Lee[1,2], Yong-Gang Duan[2], Xiujun Fan[3], William S. B. Yeung[1,2], Philip C. N. Chiu[1,2] and Jian V. Zhang[3,4,5*]*

[1]Shenzhen Key Laboratory of Fertility Regulation, The University of Hong Kong-Shenzhen Hospital, Shenzhen, China, [2]Department of Obstetrics and Gynecology, The University of Hong Kong, Hong Kong, Hong Kong SAR, China, [3]Center for Energy Metabolism and Reproduction, Shenzhen Institute of Advanced Technology, Chinese Academy of Sciences, Shenzhen, China, [4]Shenzhen Institute of Advanced Technology, Chinese Academy of Sciences, Shenzhen, China, [5]Shenzhen Key Laboratory of Metabolic Health, Shenzhen, China

OPEN ACCESS

Edited by:
Rujuan Zuo,
Oslo University Hospital, Norway

Reviewed by:
Min Chen,
Min Chen, China
Liyang Ma,
Albert Einstein College of Medicine, United States

***Correspondence:**
Philip C. N. Chiu
pchiucn@hku.hk
Jian V. Zhang
jian.zhang@siat.ac.cn

[†]These authors have contributed equally to this work and share first authorship

Specialty section:
This article was submitted to Cellular Biochemistry, a section of the journal Frontiers in Cell and Developmental Biology

Received: 25 February 2022
Accepted: 04 April 2022
Published: 17 May 2022

Citation:
Zhang Q, Xiao Z, Lee C-L, Duan Y-G, Fan X, Yeung WSB, Chiu PCN and Zhang JV (2022) The Regulatory Roles of Chemerin-Chemokine-Like Receptor 1 Axis in Placental Development and Vascular Remodeling During Early Pregnancy. Front. Cell Dev. Biol. 10:883636. doi: 10.3389/fcell.2022.883636

Chemerin is an adipokine that regulates metabolism in pregnancy. An elevation of serum chemerin level is associated with pregnancy complications. Consistently, we demonstrated that the chemerin expression was increased in placenta of preeclamptic patients at deliveries. The G protein-coupled receptor chemokine-like receptor 1 (CMKLR1) mediates the actions of chemerin. The functions of the chemerin-CMKLR1 axis in maintaining pregnancy are still unknown. In this study, we demonstrated that CMKLR1 was expressed in the decidual natural killer (dNK) cells and chorionic villi of human. Chemerin suppressed the proliferation of the dNK cells *in vitro*. Specific antagonist of CMKLR1, α-Neta abolished the suppressive effect of spent medium from chemerin-treated dNK cells culture on extravillous trophoblast invasion. Activation of the chemerin-CMKLR1 axis promoted fusion and differentiation of human cytotrophoblast to syncytiotrophoblast *in vitro*. We generated *Cmklr1* knockout mice and showed that the *Cmklr1* deficiency negatively affected pregnancy outcome in terms of number of implantation sites, litter size and fetal weight at birth. Histologically, the *Cmklr1* deficiency impaired formation of the syncytiotrophoblast layer II, induced enlargement of the maternal lacunae in the labyrinth, increased the diameter of the spiral arteries and increased trophoblast invasion in the decidua. The *Cmklr1* deficient placenta also displayed an increased number of dNK cells and serum IL-15 level. In summary, the chemerin-CMKLR1 axis regulated placental development and spiral artery remodeling in early pregnancy.

Keywords: chemerin, CMKLR1, placental development, trophoblast invasion, spiral artery remodeling

INTRODUCTION

Successful pregnancy depends on proper formation of the placenta, which forms the site of maternal-fetal exchange for nutrients and wastes (King et al., 2000; Ahokas and McKinney, 2008). The placenta comprises of trophoblastic layers with distinct ontogeny and function (Marsh and Blelloch, 2020). In mice, these layers arise from the spongiotrophoblast, trophoblast giant cells, and syncytiotrophoblasts in the labyrinth (Rossant and Cross, 2001). The development of labyrinth is initiated by fusion of the chorion with the allantois at around E8.5 (Cross et al., 2003), followed by invagination of the allantoic capillaries into the chorionic trophoblast layer that triggers the differentiation of syncytiotrophoblasts (Woods et al., 2018). Then the extensive process of branching morphogenesis forms an intricate network of syncytiotrophoblast-lined maternal blood spaces and allantoic mesoderm-derived fetal components of the placental vascular network (Maltepe and Fisher, 2015).

Trophoblast invasion is crucial to placentation which is achieved by the orchestrated effort of various cell types such as dNK cells, macrophages, and extravillous trophoblasts (EVTs) (Lyall, 2005; Whitley and Cartwright, 2009). After implantation, the cytotrophoblasts differentiate into EVTs and form the migratory cell columns that invade the decidua and contribute to the spiral arteries remodeling (Hiden et al., 2007). Disruption of this process in humans impairs placental blood flow and is associated with pregnancy complications such as recurrent pregnancy loss, fetal growth restriction, and preeclampsia (PE) (Jim and Karumanchi, 2017; Knöfler et al., 2019). *In vivo* studies demonstrated that the EVTs directly interact with the dNK cells during EVT invasion (Tilburgs et al., 2015), suggesting that their functions are modulated in the interactions (Co et al., 2013; Pollheimer et al., 2018). In addition, multiple dNK cells-derived factors regulate the EVTs-related processes *in vivo* as well as *in vitro* (Lash et al., 2006; Zhang et al., 2013; Pollheimer et al., 2018). However, much of the molecular mechanisms on the actions of decidual immune cells on EVT invasion and spiral artery remodeling remain unknown.

Chemerin, also known as tazarotene-induced gene 2 (TIG2), is secreted by various cell types, including adipocytes, epithelial and endothelial cells (ECs), fibroblasts, and trophoblasts (Carlino et al., 2012; Helfer and Wu, 2018; Xie et al., 2020). Chemokine-like receptor 1 (CMKLR1, encoded by the *Cmklr1* gene), also known as ChemR23, is a G protein-coupled receptor and the natural receptor of chemerin (Mariani and Roncucci, 2015). CMKLR1 is widely expressed in the whole body including the placenta, ECs, and immune cells (Carlino et al., 2012; Zabel et al., 2014; Cetin et al., 2017; Yang et al., 2018). Chemerin-CMKLR1 axis participates in various biological responses such as inflammation (Xie et al., 2020), insulin resistance (Sell et al., 2009), chemotaxis, endocytosis, and carbohydrate/fat metabolic process (Yoshimura and Oppenheim, 2011; Helfer and Wu, 2018). The serum levels of chemerin are notably increased during pregnancy, suggesting that the chemerin-CMKLR1 signaling may play a regulatory role in the process (Yang et al., 2018). Besides, the concentration of chemerin in maternal serum is significantly higher in preeclamptic patients than in normal pregnant women (Spradley et al., 2015; Cetin et al., 2017). However, the *in vivo* biological functions of chemerin-CMKLR1 in the maintenance of early pregnancy and placental development have not been elucidated.

To understand the role of the chemerin-CMKLR1 signaling in pregnancy, we generated *Cmklr1* knockout mice and demonstrated its regulatory roles in embryonic and placental development. In this study, we also investigated the role of the chemerin-CMKLR1 axis in trophoblast invasion, dNK cells proliferation, syncytiotrophoblast fusion, and differentiation *in vitro*.

MATERIALS AND METHODS

Immunohistochemistry of Chemerin for Human Placenta

The sections of term placentas of normal pregnancy and PE patients were subsequently de-waxed, rehydrated, the antigen was retrieved by using a 1× Universal HIER antigen retrieval reagent (ab208572, Abcam, MA 02453, United States) and incubated with 3% H_2O_2. Sections were then blocked with 10% goat serum (ab7481, Abcam) for 1 h at room temperature. The sections were incubated in chemerin (1: 100, ab72965, Abcam) overnight in the cold room. Chemerin staining was visualized using a DAB substrate kit for peroxidase from Vector Laboratories and counterstained and mounted as described above. Digital photographs at 4× and 10× were taken, and Image J software was used to quantify the H-score.

Isolation of Primary Human dNK Cells

This study was approved by the Institutional Review Board (IRB) of The University of Hong Kong/Hospital Authority Hong Kong West Cluster (IRB No: UW 17-057). Human dNK cells were isolated as described (Male et al., 2012; Lee et al., 2018) from late first-trimester decidual tissues collected from patients who had undergone surgical termination of pregnancy due to psychosocial reasons with written consent. The tissues were minced and digested with collagenase (300 U/ml) and DNase I (50 μg/ml), and the cells were passed through 100 and 40 μm filters followed by Ficoll-Paque (17,144,002, GE Healthcare Illinois, United States) density gradient centrifugation. The cells were then cultured on a plastic plate overnight. The non-adherent cells were collected, and dNK cells were further enriched using CD56 microbeads (Miltenyi Biotec, Germany). The isolated dNK were cultured with RPMI medium supplemented with 10% FBS and 1% penicillin-streptomycin under standard culture conditions in a 37°C and 5% CO_2 incubator.

Determination of Proliferation and Cytokine Secretions of Human dNK Cells

The CyQUANT® cell proliferation assay (CyQUANTTM NF Cell Proliferation assay kit, C35006, Invitrogen) was employed as a measurement of cell proliferation according to the manufacturer's instructions. Primary dNK cells (5×10^3 cells/well) were seeded in 96 well plate and cultured for 24 h with

0.5 μM chemerin (SRP6002, Sigma, St. Louis, UnitedStates), or 0.5 μM chemerin +1 μM 2-(alpha-Naphthoyl)ethyl trimethylammonium iodide (α-Neta, sc-221190A, Santa Cruz Biotechnology, United States) in RPMI1640 incomplete medium with 500 U/ml interleukin (IL)-2. The fluorescence intensity was measured using a fluorescence microplate reader (Infinite F Nano$^+$) with an excitation wavelength at 485 nm and an emission wavelength at 530 nm. The concentrations of IL-8, IL-10 and TNF-α in the spent medium of dNK cells were determined using commercially available enzyme-linked immunosorbent assay (ELISA) kits (KHC3012, BMS215-2 and KHC0081, Abgent, San Diego, CA, United States). The samples were analyzed in quadruplicate.

In Vitro Models to Study Human Trophoblast Invasion

JEG-3 cells (HTB-36, ATCC) were cultured in DMEM/Ham's F-12 medium (Sigma, St. Louis, MO) containing 10% fetal bovine serum (FBS) and 1% penicillin-streptomycin, at 37°C, in an atmosphere of 5% CO_2. The trophoblast invasion was measured by invasion assay (BD BioCoat™ Matrigel™ Invasion Assay, BD Biosciences). In brief, JEG3 cells (1×10^4 cells/well) were placed in the upper invasion chamber, with the spent medium from dNK cells (1×10^5 cells/well) treated with 0.5 μM chemerin, or 0.5 μM chemerin + 1 μM α-Neta treatment for 24 h were added into the upper chamber. FBS (10%) was added as a chemoattractive agent in the lower chamber. The invaded cells on the lower membrane of the chamber were stained with crystal violet, and images were acquired under light microscopy. The cells were then dissolved by 10% acetic acid, and the absorbance was measured at 595 nm.

In Vitro Models to Study Human Trophoblast Fusion and Differentiation

The BeWo cell line has been widely used as an *in vitro* model for studying trophoblast intercellular fusion and differentiation (Heaton et al., 2008). BeWo cells (CCL-98, ATCC) were cultured in DMEM/Ham's F-12 medium (Sigma, St. Louis, MO) containing 10% FBS and 1% penicillin-streptomycin, at 37°C, in an atmosphere of 5% CO_2. BeWo cells (1×10^6 cells/well) were plated in 6 well multi-dishes and maintained in culture until the cells were 70–80% confluent. Differentiation was induced by the addition of 20 μM forskolin (F6886, St. Louis, MO, as positive control) with or without 0.5 μM chemerin, or 0.5 μM chemerin +1 μM α-Neta, in a serum-free medium for 48 h. All experiments involving the cell treatment were accompanied in parallel by vehicle controls. The quantification of BeWo cell fusion under different stimulatory conditions was performed by calculating the fusion index in 20 randomly selected microscopic fields of each condition. The fusion index = number of nuclei in syncytia/total number of nuclei x 100%. The cells were harvested to measure the expression of relevant differentiation markers by qPCR.

Semi-Quantitative RT-PCR

Total RNA was extracted from placentas or BeWo cells after 48 h of treatment using Illustra RNAspin Mini RNA isolation kit (25-0500-71, GE Healthcare, United States). RT-PCR was performed following the protocol for Taqman Gold RT-PCR (Manufacturer). For cDNA amplifications, highly specific forward and reverse primers were used with initial heating at 95°C for 10 min, followed by 40 cycles of 95°C for 15 s and 60°C for 1 min. The TaqMan™ Gene Expression Assay primers were purchased from Life Technologies, including mouse Interleukin (IL)-6 (Mm00446191_m1); IL-8 (Mm04208136_m1); IL-10 (Mm01288386_m1); Tumor necrosis factor-alpha (TNF-α) (Mm00443258_m1); Matrix metalloproteinase-2 (MMP)2 (Mm01253624_m1); MMP9 (Mm00600157_g1); Human Glial Cells Missing-1 (GCM1) (Hs00961601_m1); syncytin-1 (Hs00835189_CE); Caudal-type homeobox gene 2 (CDX2) (Hs01078080_m1); Human leukocyte antigen G (HLA-G) (Hs00365950_g1); and CK7 (Hs00559840_m1).

Mouse Model

C57BL/6 mice (8 weeks) were obtained from the Guangdong Medical Laboratory Center (Guangdong, China). *Cmklr*1$^{-/-}$ mice were obtained from The Jackson Laboratory (Bar Harbor, ME United States). Estrous *Cmklr1*-deficient females were paired with *Cmklr*1$^{-/-}$ males to obtain timed pregnancy, and copulation plug detection the next morning was designated as gestation day (GD) 1. The same procedure was performed between wildtype mice. Animals were housed in a controlled environment where constant temperature, humidity, and a 12-h light-dark cycle with free access to chow diet and water were given. All animal usage has complied with the procedures approved by the Committee on the Use of Live Animals for Teaching and Research, Shenzhen Institutes of Advanced Technology, Chinese Academy of Sciences (Permit Number: SIAT-IRB-120223-A0009).

Measurement of Placental Layers

Undissected GD 12 mice enveloped within uterine tissue were collected. Tissue samples were fixed in fixative solution (Pyrocitric acid: formaldehyde: glacial acetic acid 15: 5: 1) and processed for embedding in paraffin. Paraffin-embedded tissues were sectioned into 5 μm for hematoxylin and eosin staining. Digital photographs of three central sections of each placenta were taken. Image J software was used to measure the relevant stained or unstained regions of each section. For each placental section, the area of the whole placenta, labyrinth, junctional, and decidua zone was measured.

Lectin Histochemistry for Fetal Blood Vessels and Mice dNK

The sections of GD12 placenta from both wildtype and *Cmklr*1-deficient pregnant mice mounted on glass slides were subsequently de-waxed, rehydrated, and incubated with 3% H_2O_2. It was then washed three times with PBS, and the antigen was retrieved by using a 1× Universal HIER antigen retrieval reagent (ab208572, Abcam, MA 02453, United States).

Sections were then blocked with 10% goat serum (ab7481, Abcam) for 1 h at room temperature. The sections were incubated in isolectin B4 (BSI-B4)(1: 100 in PBS, L-5391, Sigma-Aldrich, St Louis, United States) for fetal blood vessels and biotinylated-Dolichos biflorus (DBA) lectin (1: 1,000 in 1% BSA/PBS, L6533, Sigma Aldrich, Saint Louis, MO, United States) for dNK. The sections were incubated for 1 h and then washed three times in PBS. The lectin binding was detected by 30 min incubation with streptavidin-peroxidase (Extraditing-peroxidase; E2886, Sigma Aldrich, Saint Louis, MO, United States) and peroxidase-labeling kit (Vector Laboratories, city, country). The slides were then counterstained with hematoxylin, and then mounted followed by dehydration and clearing through a graded series of ethanol and xylene washes.

Immunofluorescent Staining of MCT4 for Syncytiotrophoblast II Development and TPBPA for the Glycogen Trophoblast Cells, Giant Cells and Spongiotrophoblasts in the Junctional Zone

For immunostaining, antigen retrieval was performed in the deparaffinized sections as described above. The sections were permeabilized by eBioscience™ Permeabilization Buffer (00-8333-56, Thermo Fisher Scientific, Massachusetts, United States), followed by blocking in 10% goat serum (ab7481, Abcam) for 1 h. The sections were incubated with anti-monocarboxylate transporter 4 (MCT4, 1: 100, AB3314P, Merck Millipore) or anti-trophoblast specific protein alpha (TPBPA, 1: 100, ab104401, Abcam) antibodies overnight. After incubation, sections were washed three times in PBS. Primary antibodies were detected with appropriate fluorescence-conjugated secondary antibodies (1: 500 dilutions in PBS) for 1-h incubation. After incubation, sections were washed by PBS three times for 15 min. Nuclei were then counterstained with 4',6-Diamidino-2-phenylindole dihydrochloride (DAPI, 1:500 dilution in PBS, D9542, MERCK, United States) for 2 min followed by washing with PBS five times. The sections were then mounted with a fluorescence mounting medium (S3023, DAKO, United States) and digital images were captured under a fluorescent microscope.

Immunohistochemistry of Cytokeratin 8 for Trophoblast

The sections were incubated with, anti-CK8 antibody (ab53280, Abcam). CK8 staining was visualized using a DAB substrate kit for peroxidase from Vector Laboratories and counterstained and mounted as described above. Digital photographs at 4× and 10× were taken, and Image J software was used to quantify the ratios of the invaded vessel to the amount vessels in wildtype and *Cmklr1* deficient decidual zone.

Serum IL-15 Measurement

The blood from wildtype and *Cmklr1*$^{-/-}$ mice in GD 12 were collected. Serum was collected and frozen at −20°C in aliquots. According to the manufacturer's protocol, serum IL-15 levels were measured using commercially available and sandwich enzyme-linked immunosorbent assay (ELISA) kits (R&D Systems, CA, United States). The samples were analyzed in triplicate.

Statistical Analysis

All values were expressed as mean ± SD. One-way ANOVA on Rank test was used to test the statistical differences between groups. Parametric Student's t-test or non-parametric Mann Whitney U test was used where appropriate as the post-test. GraphPad Prism 9.0 (GraphPad Software, La Jolla, CA, United States) was used for all statistical analyses. A p-value of less than 0.05 was considered significant.

RESULTS

Chemerin-CMKLR1 Axis Regulates the Proliferation and Cytokine Secretion of Human dNK Cells

Chemerin immunoreactivities were positively stained in the trophoblast layer of human placental tissues. Compared with normal pregnancy, the expression of chemerin was reduced in the term pregnancy placental villi from women who presented with PE (**Figure 1A**). The biological effects of chemerin are mediated by CMKLR1. By using flow cytometry and immunohistochemistry, we demonstrated CMKLR1 expressions in $CD16^{-}CD56^{+}$ dNK (**Figure 1B**) cells and chorionic villi (**Figure 1C**) of first-trimester pregnancies respectively. To determine the role of CMKLR1 in regulating dNK cell proliferation, dNK cells were treated with chemerin with or without α-Neta, a specific antagonist of CMKLR1 for 24 h. Our results showed that while 0.5 μM chemerin suppressed the proliferation of the dNK cells, the inclusion of 1 μM α-Neta abolished the suppressive effect of chemerin (**Figure 1D**). The results indicated that the interaction of chemerin-CMKLR1 inhibited dNK cell proliferation.

The dNK cells are in close proximity to EVTs and regulate EVT functions by secretory factors. For example, dNK cell-derived IL-6, IL-8, hepatocyte growth factor, granulocyte-macrophage colony-stimulating factor (GM-CSF), and interferon-inducible protein-10 have been demonstrated to regulate human EVT motility and/or invasion (Hanna et al., 2006; Wallace et al., 2012). Therefore, we investigated the possible roles of chemerin on IL-8, IL-10 and TNF-α secretions by dNK cells. Our data revealed that IL-8 (**Figure 1E**) production was downregulated, while IL-10 (**Figure 1F**) and TNF-α (**Figure 1G**) were upregulated in dNK cells after chemerin treatment. The inclusion of 1 μM α-Neta abolished the effect of chemerin, indicating the involvement of CMKLR1.

To further confirm the implication of chemerin-CMKLR1 interaction in the regulatory activities of dNK cells on EVT functions, the spent medium of dNK cells after chemerin treatment was collected and applied to the EVTs. The dNK cells without chemerin treatment or with chemerin treatment

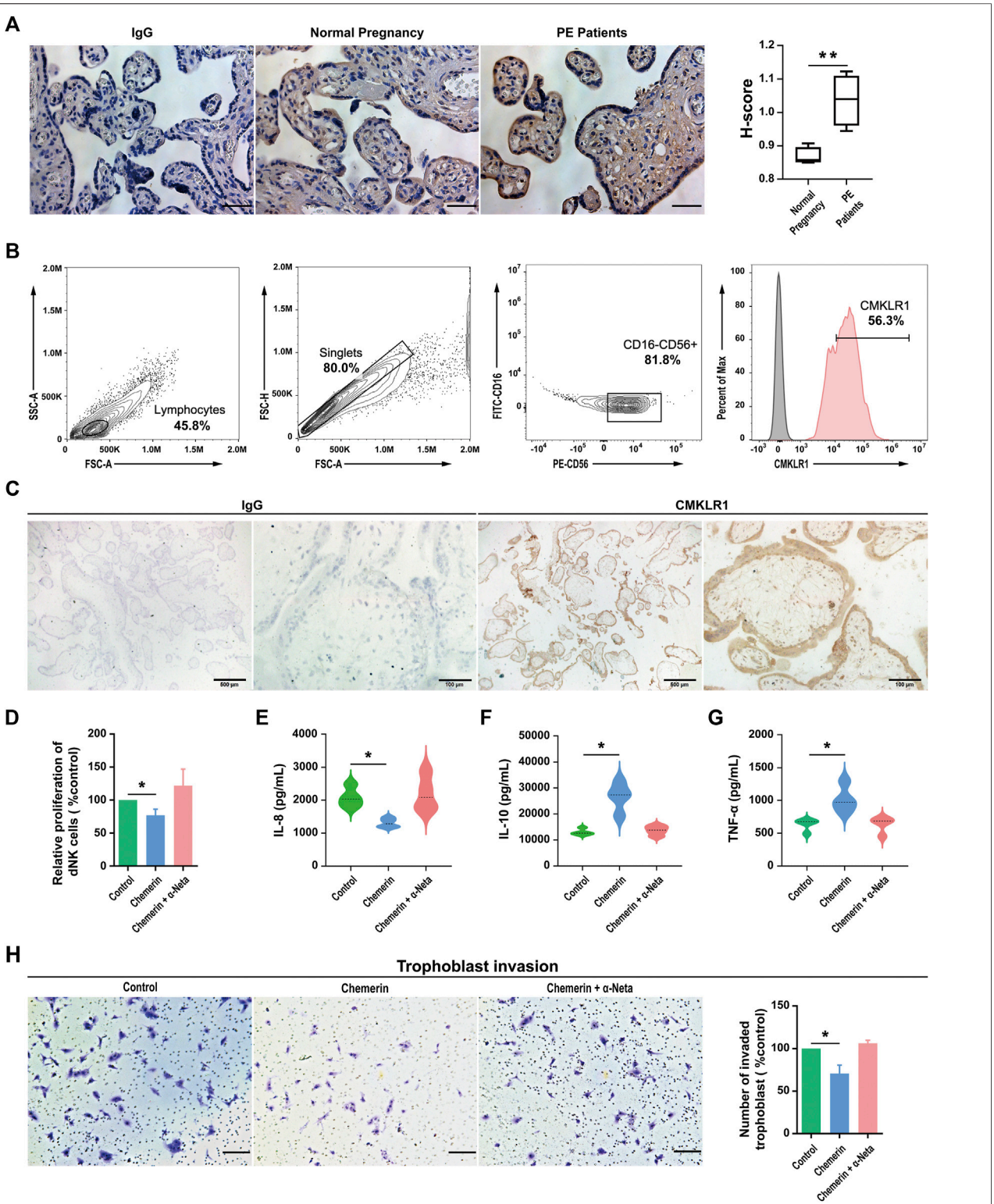

FIGURE 1 | Chemerin-CMKLR1 axis regulates the proliferation and cytokine secretion of human dNK cells **(A)** Representative chemerin staining in placentas and the H-score of the area displaying chemerin positivity. Scale bar = 100 μm **(B)** The expression of CMKLR1 was detected in human dNK cells ($CD56^{+}CD16^{-}$) using flow cytometry **(C)** Location of CMKLR1 in human villi in early pregnancy based on immunohistochemistry using antibodies specific for CMKLR1. Brown color indicates specific CMKLR1 staining **(D)** The proliferation of primary dNK cells after being treated with 0.5 μM chemerin, 0.5 μM chemerin +1 μM α-Neta or vehicle for 24 h was assessed by proliferation kit. The concentration of IL-8 **(E)**, IL-10 **(F)** and TNF-α **(G)** in spent medium of primary dNK cells after being treated with 0.5 μM chemerin,

(*Continued*)

FIGURE 1 | 0.5 μM chemerin +1 μM α-Neta or vehicle were measured by ELISA. As isotype controls, sections were incubated with Isotype IgG control **(H)** The effect of spent medium from dNK cells treated with 0.5 μM chemerin, 0.5 μM chemerin +1 μM α-Neta on trophoblast invasion in a transwell assay. Invasive cells were stained with crystal violet. Scale bar = 200 μm. The invasive index was calculated as the percentage of invasion in treatment groups to the percentage of control group invasion. The results were represented as Mean ± SD, analyzed by One-way ANOVA; *$p < 0.05$ and **$p < 0.01$ vs. Control group; $N = 5$. dNK: decidual Natural Killer.

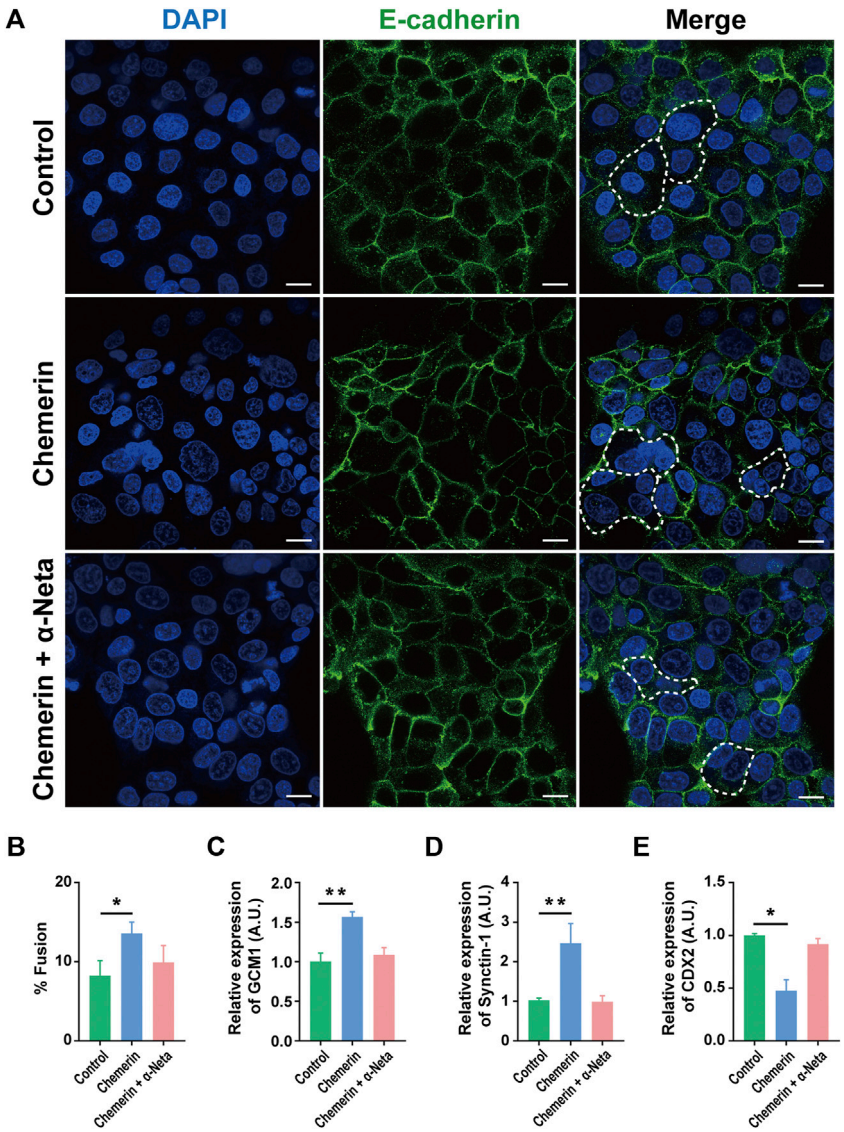

FIGURE 2 | Chemerin-CMKLR1 interaction promotes human trophoblast syncytialization **(A)** Immunofluorescence staining of BeWo cells was also used to quantify BeWo cell fusion under the different stimulatory conditions. There was a low level of spontaneous fusion of BeWo cells, but most cells were in a mononucleated state. Chemerin stimulated the fusion of BeWo cells while the presence of chemerin in combination with α-NETA showed that chemerin-induced cell fusion was inhibited by α-NETA **(B)** Fusion index of BeWo cells treated with the vehicle, 0.5 μM chemerin and 0.5 μM chemerin +1 μM α-Neta for 48 h **(C)** The relative expression of trophoblast differentiation maker GCM1 **(D)** syncytiotrophoblast markers Synctin-1 were quantified by quantitative real-time PCR **(E)** The relative expression of trophectoderm marker CDX2 was analyzed by real-time PCR. The results were represented as Mean ± SD, analyzed by One-way ANOVA; *$p < 0.05$ and ***$p < 0.001$ vs. Control group; $N = 5$. GCM1: Human Glial Cells Missing-1; Synctin-1; CDX2: caudal-type homeobox gene 2. Scale bar = 100 μm.

in the presence of α-Neta were served as control. Our results showed that the spent medium of chemerin-treated dNK cells significantly decreased EVT invasion when compared to the controls, and such effect was abolished by α-Neta (**Figure 1H**).

Chemerin-CMKLR1 Interaction Promotes Human Trophoblast Syncytialization

Fusion of the cytotrophoblasts forms the multinucleated syncytiotrophoblast responsible for hormone production and

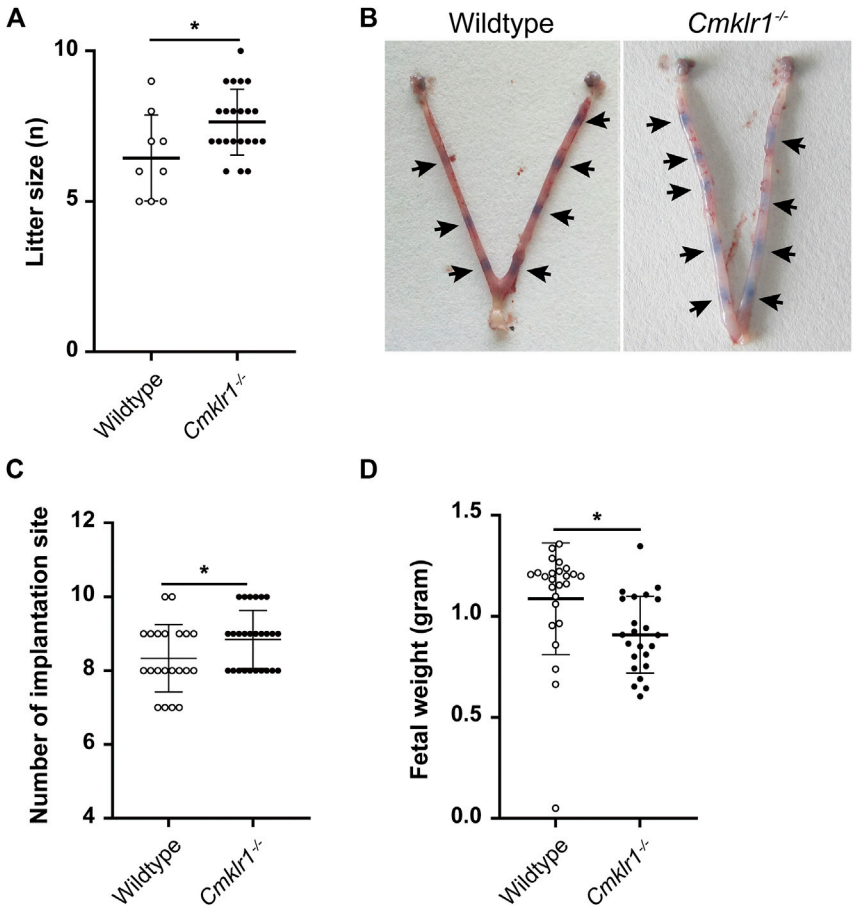

FIGURE 3 | *Cmklr1* knockout affects the pregnancy outcome *in vivo* **(A)** Quantification of average litter size (*N* = 20 pregnant mice/genotype) **(B)** Representative embryos within uteri in wildtype and *Cmklr1*$^{-/-}$ mice at GD5. Arrowheads indicate viable implantation sites visualized as blue bands by uptake of Chicago Blue dye **(C)** Quantification of average implantation sites at GD5 (*N* = 20 pregnant mice/genotype) **(D)** The fetus weight at birth from wildtype mice and *Cmklr1*$^{-/-}$ mice. The results were represented as mean ± SD, *n* = 5. **p* < 0.05. SD: standard deviation.

maintenance of homeostasis of pregnancy. By using BeWo cells, an established model of forskolin induced syncytialization of cytotrophoblasts (**Supplementary Figure S1**), we demonstrated that chemerin-CMKLR1 interaction reduced E-cadherin expression, and thereby promoted syncytialization (**Figures 2A,B**). The inclusion of 1 μM α-Neta abolished the stimulatory effect of chemerin on syncytialization, indicating the involvement of CMKLR1 in cytotrophoblast syncytialization. The observations were supported by the upregulation of GCM1 (a trophoblastic differentiation marker) and Synctin-1 (a syncytiotrophoblast marker), and downregulation of CDX2 (a trophectoderm marker) in BeWo cells after chemerin treatment.

Cmklr1 Knockout Affects the Pregnancy Outcome *in Vivo*

To assess the role of *Cmklr1* in placental development *in vivo*, a *Cmklr1*-deficient mouse model was generated (**Supplementary Figure S2A**). Successful ablation of *Cmklr1* was confirmed by PCR analysis (**Supplementary Figure S2B**). *Cmklr1* knockout had no effect on chemerin expression (**Supplementary Figure S2C**). The *Cmklr1* deficient mice exhibited larger litter size (**Figure 3A**) and more implantation sites (**Figures 3B,C**) but reduced fetal weight at birth (**Figure 3D**) when compared to the wildtype mice.

Cmklr1 Knockout Affects Placental Development and Spiral Arterial Remodeling *in Vivo*

Cellular morphology of the wildtype and the *Cmklr1*-deficient placentas were compared (**Figure 4A**) which showed a significant reduction of the junctional zone thickness as indicated by TPBPA staining, and thus a proportionally increased labyrinth zone in the *Cmklr1*-knockout placentas. Significant enlargement of the luminal diameter of the spiral artery was also observed in the *Cmklr1*$^{-/-}$ mice (**Figure 4B**) which was accompanied by accumulation of the CK8 positive trophoblast (**Figure 4C**). In contrast, there was no difference in size of the decidua basalis

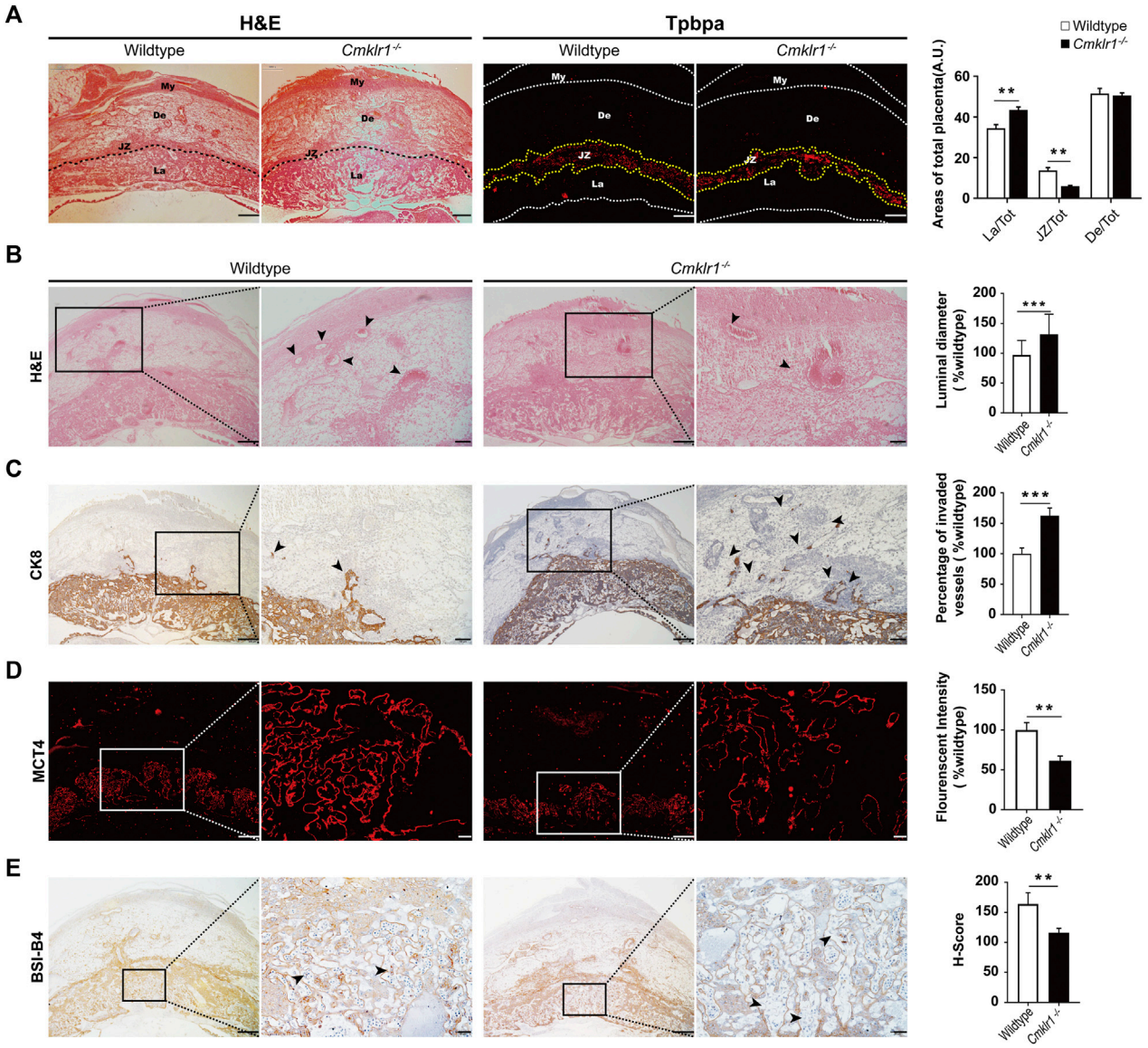

FIGURE 4 | *Cmklr1* knockout affects the placental development and spiral arterial remodeling *in vivo* **(A)** Representative H&E-stained transverse sections of placentas. The immunofluorescent staining of TPBPA for outlining the junctional zone. The ratio of the junctional zone, labyrinth layer, and decidual zone to total placental areas **(B)** H&E staining of placental sections from wildtype mice and *Cmklr1*$^{-/-}$ mice at GD12 in different magnifications. Quantification of the spiral arterial luminal diameter. The middle placenta section from each litter (four litters from four mothers per group) was used for analysis. The spiral arteries are indicated by arrowheads **(C)** The invasion ability of the trophoblast was examined. Transverse sections of wildtype and *Cmklr1*$^{-/-}$ placentas at GD12 were immunohistochemically stained with antibodies against trophoblast marker CK8 in different magnifications. Invading trophoblasts are indicated by arrowheads. The trophoblast invaded vessels percentage was analyzed in 3 mid-sagittal implantation site sections per mouse (n = 4/group) and averaged using ImageJ software. Quantification of the ratios of the invaded vessel to the amount vessels in wildtype and *Cmklr1*$^{-/-}$ decidua zone **(D)** Immunofluorescent staining with MCT4 showing the syncytiotrophoblast II in the transverse sections of placentas in wildtype and *Cmklr1*$^{-/-}$ mice at GD 12 in different magnifications. Quantification of the MCT4 expression in the labyrinth layers in wildtype and *Cmklr1*$^{-/-}$ placentas **(E)** Immunohistochemistry with isolectin BSI-B4 staining shows the fetal blood vessels in the transverse placenta's sections in wildtype and *Cmklr1*$^{-/-}$ mice at GD 12 in different magnifications. H-score of BSI-B4 positive staining in the labyrinth trophoblasts around fetal blood vessels in wildtype and *Cmklr1*$^{-/-}$ placentas. The maternal lacunae are indicated by arrowheads. The middle placenta section from each litter (four litters from four mothers per group) was used for analysis. The results were represented as the mean ± SD. *p < 0.05, **p < 0.01. Scale bar = 200 μm. BS1: isolectin BSI-B4 (GSL I-B4); MCT4: Monocarboxylate transporter 4; SD: standard deviation.

between the *Cmklr1*$^{-/-}$ and the wildtype pregnant mice (**Figure 4A**).

To determine syncytialization in the *Cmklr1*-knockout placenta, we stained for MCT4, a monocarboxylate transporter specifically expressed in the syncytiotrophoblast II layer. The thickness of the syncytiotrophoblast II layer and the MCT4 staining were significantly reduced in the *Cmklr1*-deficient labyrinth. As the syncytiotrophoblast II layer enclosed fetal

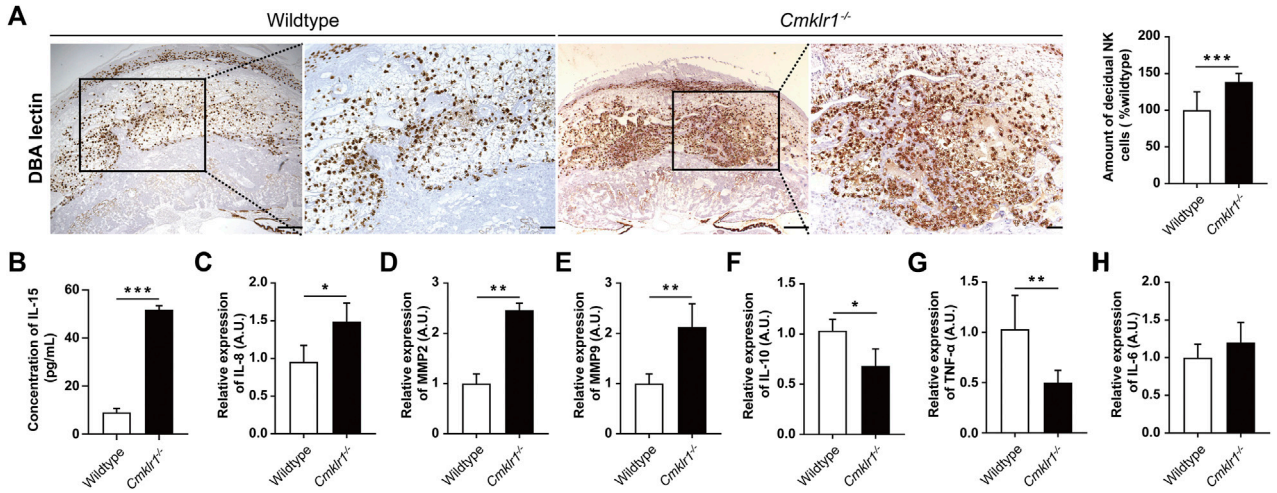

FIGURE 5 | *Cmklr1* knockout is associated with increased dNK cells. **(A)** The amount and distribution of dNK cells of wildtype and *Cmklr1*$^{-/-}$ were investigated by immunohistochemically staining with antibodies against DBA Lectin in different magnifications. Scale bar = 200 μm. Quantification of the number of dNK cells. **(B)** The concentration of IL-15 in serum of wildtype and *Cmklr1*$^{-/-}$ at GD 12 was measured by ELISA. Total RNA samples from wildtype and *Cmklr1*$^{-/-}$ placentas at GD12 were subjected to qRT-PCR. The middle placenta section from each litter (four litters from four mothers per group) was used for analysis. The expression of **(C)** IL-8, **(D)** MMP2, **(E)** MMP9, **(F)** IL-10, **(G)** TNF-α and **(H)** IL-6 were examined. The results were represented as mean ± SD, $n = 4$. *$p < 0.05$ and **$p < 0.01$. IL: Interleukin; TNF-α: Tumor necrosis factor-alpha; MMP: Matrix Metallopeptidase; TIMP: Tissue inhibitor of metalloproteinases. qRT-PCR: quantitative reverse-transcription polymerase chain reaction; SD: standard deviation. TPBPA: trophoblast-specific protein alpha.

blood vessels in the labyrinth, the reduced MCT4 staining suggested that the fetal blood vessels were not properly developed in the region (**Figure 4D**), consistent with the diminished BSI-B4 staining that outlines the matrix surrounding the fetal vessels in the *Cmklr1*-deficient placenta when compared to the wildtype (**Figure 4E**).

Cmklr1 Knockout Is Associated With Increased dNK Cells

Successful placental development and spiral arterial remodeling require dNK cells. The *Cmklr1*$^{-/-}$ mice had a significant increase in the number of DBA-lectin positive dNK cells (**Figure 5A**) in the decidual zone when compared to the wildtype. IL-15 is involved in activating the proliferation of the CD56^{Bright} NK cells (Felices et al., 2018). Therefore, we analyzed the serum IL-15 level of the *Cmklr1*$^{-/-}$ pregnant mice at GD 12. We detected a 5-fold increment in serum IL-15 level in the *Cmklr1*$^{-/-}$ mice when compared to the wildtype (**Figure 5B**). We also investigated the downstream factors responsible for the altered placental development in the *Cmklr1*-knockout placenta. These factors, including IL-6 (Champion et al., 2012), IL-8 (Jovanović et al., 2010), IL-10 (Pang et al., 2008), MMP2, MMP9 (Staun-Ram et al., 2004), and TNF-α have been associated with the regulatory activities of dNK cells on trophoblast functions. Our data revealed that IL-8 (**Figure 5C**), MMP2 (**Figure 5D**), and MMP9 (**Figure 5E**) were upregulated while IL-10 (**Figure 5F**) and TNF-α (**Figure 5G**) were downregulated. The expression of IL-6 was not significantly affected (**Figure 5H**).

DISCUSSION

The increased placental chemerin level was related to human PE and overexpression of chemerin in trophoblast contributed to the development of PE-like symptoms via its receptor CMKLR1 (Tan et al., 2022). Here, to elucidate the role of chemerin-CMKLR1 in pregnancy, we generated mice knockout for *Cmklr1*. We found that the weight of *Cmklr1*$^{-/-}$ fetus at birth was reduced by around 15%. It could be speculated that the reduced fetus growth was related to defective placental development. During labyrinth formation, the syncytiotrophoblast layers facilitate fetomaternal exchanges by intercrossing between the fetal vessel and maternal blood lacunae (Dupressoir et al., 2011). The extent of the trophoblast branch contributes to blood vessels in the mature labyrinth development (Watson and Cross, 2005). Here we demonstrated that the *Cmklr1*$^{-/-}$ mice showed 1) an increased total labyrinth area with enlarged maternal blood lacunae; 2) degenerative changes in interhemal trophoblasts; 3) defects in syncytial formation of the syncytiotrophoblast II, facing the embryonic vessels, which was confirmed by the ability of α-Neta in abolishment of observed effect on syncytialization. The defective syncytiotrophoblast II development may attenuate the interactions and functions of neighboring trophoblast cells leading to the observed reduced interhemal trophoblasts and disorganization of the maternal-fetal transferring network in the labyrinth, and finally to reduced fetal growth. As summarized above, we proposed the working model for CMKLR1 in placental development (**Figure 6**).

Patients suffering from hypertension and PE showed significantly higher serum chemerin concentrations (Cetin et al., 2017; Xie and Liu, 2022). The increased placental

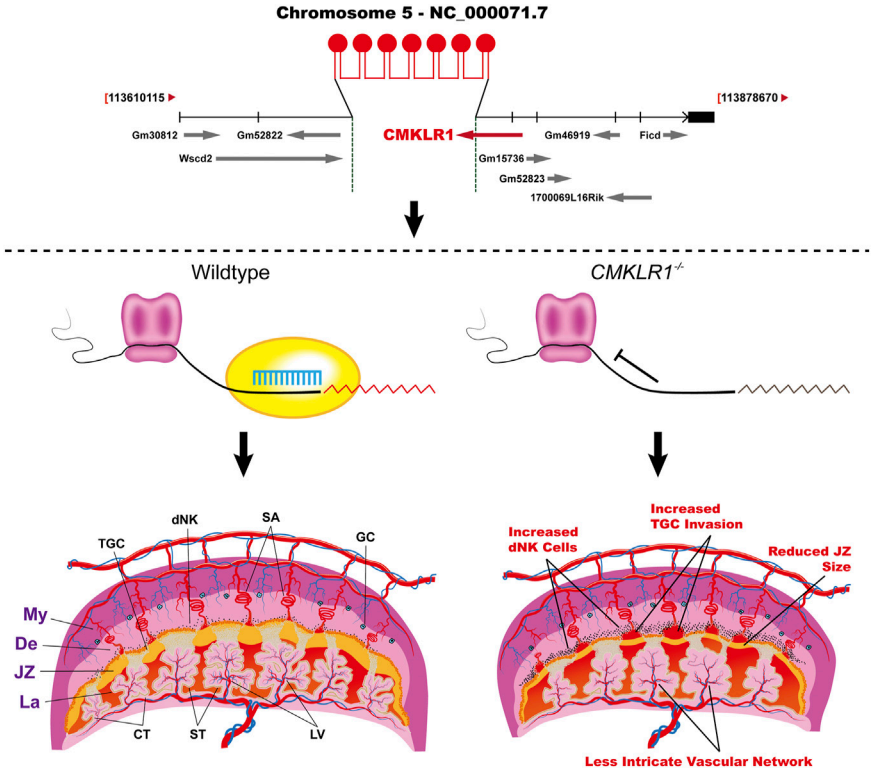

FIGURE 6 | The working model shows the regulation of CMKLR1 signaling during placental development. Upper: The strategy of *Cmklr1* gene knockout in mouse. Lower: *Cmklr1*$^{-/-}$ led to increased trophoblast invasion by increased proliferation of dNK cells and reduced JZ by reduced syncytiotrophoblast II differentiation. My: myometrium; De: decidua; JZ: junctional zone; La: Labyrinth; TGC: trophoblast giant cells; dNK: decidual Natural Killer; SA: spiral artery; GC: giant cells; CT: chronic trophoblast; ST: syncytiotrophoblast; LV: labyrinth vasculature.

chemerin was also found in the villi of preeclamptic women (Xu et al., 2014; Tan et al., 2022). Our findings demonstrated that *Cmklr1* knockout mice had more invaded trophoblasts and larger arteries in the decidua and myometrium than those in wildtype mice. Consistently, overexpression of trophoblastic chemerin diminishes trophoblast invasion (Tan et al., 2022). These observations indicate that CMKLR1 mediates the role of chemerin in pregnancy.

Trophoblast invasion and dNK cell functions are indispensable for spiral artery remodeling (James et al., 2010). During placental development, dNK cells (CD56^{bright}CD16^{-}) are the predominant lymphocyte population (around 70–80%) at the implantation sites (Liu et al., 2017), where trophoblast invasion and vascular remodeling happen (Hanna et al., 2006). Our data showed that CMKLR1 was expressed in the CD16^{-}CD56^{bright} NK cells, in line with a previous report (Carlino et al., 2012). The interaction of chemerin-CMKLR1 inhibited dNK cell proliferation and decreased EVTs invasion. These are in line with our *in-vivo* study showing increased trophoblast invasion deeply into the spiral artery in the *Cmklr1*-knockout mice placenta. The regulation of trophoblast invasion at the maternal-fetal interface is controlled by various factors, including cytokines, chemokines, growth factors, sex hormones, critical protease, and adhesion molecules (Harris et al., 2009) through autocrine or paracrine action (Bischoff et al., 2000). These factors are secreted from the trophoblast, decidual endothelial cells and dNK cells, suggesting a complex network to regulate trophoblast invasiveness (Knöfler, 2010). Based on the increased dNK cell number in the mouse placenta and the increased proliferation of human dNK cells treated with chemerin, the deep trophoblast invasion of the *Cmklr1*$^{-/-}$ mice placentas may be regulated by secretions of the dNK cells.

The dNK cells are well known to express killer cell immunoglobulin-like receptors and produce angiogenic cytokines and proteins such as TNF-α, interferon-γ, and vascular endothelial growth factor (VEGF) that regulate trophoblastic invasion, angiogenesis, and vascular remodeling (Ashkar et al., 2000; Fukui et al., 2012). The dNK cells also produce MMP2 and MMP9, which together with VEGF, placental growth factor (PGF), and angiopoietin are essential for maintenance of vessel stability (Smith et al., 2009). Consistently, both our *in vitro* and *in vivo* studies confirmed that chemerin-CMKLR1 axis is involved in regulating the productions of trophoblast regulatory factors from dNK cells, including TNF-α, IL-10 and IL8.

We observed upregulation of IL-15 in the *Cmklr1*$^{-/-}$ mice serum. IL-15 plays a role in development, survival, and activation of the NK cells, homeostasis of natural killer T (NKT) cells and intraepithelial lymphocytes, and maintenance of the naïve and memory CD8^{+} T cells (Koka et al., 2003). IL-15 and IL-15Rα-deficient mice lack NK cells and have severely reduced numbers of NKT cells, memory CD8^{+} T cells, and specific subsets of

intestinal intraepithelial lymphocytes (Koka et al., 2003; Terabe et al., 2008). The IL15$^{-/-}$ mice exhibited impaired remodeling of the spiral arteries, including decreased lumen diameters and thicker vessel walls (Ashkar et al., 2003). IL-15 might also participate in cytotrophoblast invasion, possibly related to the increased expression of MMP-1(Sharma et al., 2016). IL-15 is secreted by a large variety of tissues and cell types. Its expression in the endometrium is stronger during the secretory phase and first trimester pregnancy when compared to the proliferative phase, consistent with involvement of IL-15 in early placentation (Kitaya et al., 2000). Since IL-15 is also produced by placenta (Li et al., 2021), the increased serum IL-15 level in *Cmklr1* knockout mice may be contributed by both decidua and placental tissues. This IL-15 upregulation may activate the dNK cells and thereby modulate the trophoblast functions. These observations provide the cellular mechanism on how the dNK cell proliferation is related to the increased trophoblast invasion in the *Cmklr1*$^{-/-}$ mice.

In summary, CMKLR1 is required for placental development. The deletion of CMKLR1 decreased fetal vessel density, syncytiotrophoblast II development and enlarged maternal lacunae in the labyrinth while increased trophoblast invasion and enlarged spiral artery lumen in the decidua. The possible reasons for the observed beneficial effect of *Cmklr1* knockout on spiral artery remolding are increase in dNK cell proliferation and IL-15 production, upregulation of MMP2, MMP9, and reduction of TNF-α and IL-10, subsequently enhancement of trophoblast invasion. A major limitation of this study is the suppression of CMKLR1 is not placenta-specific, and the loss of CMKLR1 in other organs might have a confounding effect on the development of the placenta. Another limitation is that there is potential interference caused by the presence of endogenous chemerin from dNK cells in the *in vitro* experiments which might affect the result interpretation. Also, the specific CMKLR1 signaling cascade responsible for causing the phenotype is still unknown. Further investigation is required to define the exact molecular mechanisms how chemerin elevation can contribute to PE. It may associate with the dysregulation of transcription factor HOXA9 which has been reported to activate chemerin transcription, promote pyroptosis and inflammation of trophoblasts, and contributed to PE (Quan et al., 2021). The results of this study suggest that CMKLR1 expression may be used for the early prediction of placenta-associated complications with altered NK cell biology. Suppression of CMKLR1 via a specific antagonist could be a possible treatment for PE.

DATA AVAILABILITY STATEMENT

The original contributions presented in the study are included in the article/**Supplementary Material**, further inquiries can be directed to the corresponding authors.

ETHICS STATEMENT

The studies involving human participants were reviewed and approved by Institutional Review Board of The University of Hong Kong/Hospital Authority Hong Kong West Cluster (IRB No: UW 17-057). The patients/participants provided their written informed consent to participate in this study. The animal study was reviewed and approved by Committee on the Use of Live Animals for Teaching and Research, Shenzhen Institutes of Advanced Technology, Chinese Academy of Sciences (Permit Number: SIAT-IRB-120223-A0009).

AUTHOR CONTRIBUTIONS

PC and JZ designed this study and contributed to the research idea. QZ, ZX, C-LL, and PC contributed to the research data and wrote this manuscript. YD and XF revised and edited this manuscript. JZ was the guarantor of this work and, as such, had full access to all the data in the study and is responsible for the integrity of the data and the accuracy of the data analysis. All authors contributed to the article and approved the submitted version.

FUNDING

This study was supported by the Sanming Project of Medicine in Shenzhen (SZSM201612083), HKU-SZH Fund for Shenzhen Key Medical Discipline (SZXK2020089) and Shenzhen Key Laboratory of Metabolic Health (GrantNo: ZDSYS20210427152400v001).

ACKNOWLEDGMENTS

The authors are grateful to all the women who agreed to donate their tissue samples for this study. The authors acknowledge the project nurse and all gynecologists especially at Queen Mary Hospital and HKU-SZ Hospital for the collection of the samples. The authors are also grateful to the staff at Faculty Core Facility, the University of Hong Kong, for their technical assistance in this study.

SUPPLEMENTARY MATERIAL

The Supplementary Material for this article can be found online at: https://www.frontiersin.org/articles/10.3389/fcell.2022.883636/full#supplementary-material

REFERENCES

Ahokas, R. A., and McKinney, E. T. (2008). *Development and Physiology of the Placenta and Membranes*. Global Library Women's Medicine.

Ashkar, A. A., Di Santo, J. P., and Croy, B. A. (2000). Interferon γ Contributes to Initiation of Uterine Vascular Modification, Decidual Integrity, and Uterine Natural Killer Cell Maturation during Normal Murine Pregnancy. *J. Exp. Med.* 192 (2), 259–270. doi:10.1084/jem.192.2.259

Ashkar, A. A., Black, G. P., Wei, Q., He, H., Liang, L., Head, J. R., et al. (2003). Assessment of Requirements for IL-15 and IFN Regulatory Factors in Uterine NK Cell Differentiation and Function during Pregnancy. *J. Immunol.* 171 (6), 2937–2944. doi:10.4049/jimmunol.171.6.2937

Bischoff, P., Meisser, A., and Campana, A. (2000). Paracrine and Autocrine Regulators of Trophoblast Invasion- A Review. *Placenta* 21, S55–S60. doi:10.1053/plac.2000.0521

Carlino, C., Trotta, E., Stabile, H., Morrone, S., Bulla, R., Soriani, A., et al. (2012). Chemerin Regulates NK Cell Accumulation and Endothelial Cell Morphogenesis in the Decidua during Early Pregnancy. *J. Clin. Endocrinol. Metab.* 97 (10), 3603–3612. doi:10.1210/jc.2012-1102

Cetin, O., Kurdoglu, Z., Kurdoglu, M., and Sahin, H. G. (2017). Chemerin Level in Pregnancies Complicated by Preeclampsia and its Relation with Disease Severity and Neonatal Outcomes. *J. Obstet. Gynaecol.* 37 (2), 195–199. doi:10.1080/01443615.2016.1233947

Champion, H., Innes, B. A., Robson, S. C., Lash, G. E., and Bulmer, J. N. (2012). Effects of Interleukin-6 on Extravillous Trophoblast Invasion in Early Human Pregnancy. *Mol. Hum. Reprod.* 18 (8), 391–400. doi:10.1093/molehr/gas010

Co, E. C., Gormley, M., Kapidzic, M., Rosen, D. B., Scott, M. A., Stolp, H. A., et al. (2013). Maternal Decidual Macrophages Inhibit NK Cell Killing of Invasive Cytotrophoblasts during Human Pregnancy. *Biol. Reprod.* 88 (6155), 155–159. doi:10.1095/biolreprod.112.099465

Cross, J. C., Baczyk, D., Dobric, N., Hemberger, M., Hughes, M., Simmons, D. G., et al. (2003). Genes, Development and Evolution of the Placenta. *Placenta* 24 (2-3), 123–130. doi:10.1053/plac.2002.0887

Dupressoir, A., Vernochet, C., Harper, F., Guégan, J., Dessen, P., Pierron, G., et al. (2011). A Pair of Co-opted Retroviral Envelope Syncytin Genes Is Required for Formation of the Two-Layered Murine Placental Syncytiotrophoblast. *Proc. Natl. Acad. Sci. U.S.A.* 108 (46), E1164–E1173. doi:10.1073/pnas.1112304108

Felices, M., Lenvik, A. J., McElmurry, R., Chu, S., Hinderlie, P., Bendzick, L., et al. (2018). Continuous Treatment with IL-15 Exhausts Human NK Cells via a Metabolic Defect. *JCI Insight* 3 (3), e96219. doi:10.1172/jci.insight.96219

Fukui, A., Yokota, M., Funamizu, A., Nakamua, R., Fukuhara, R., Yamada, K., et al. (2012). Changes of NK Cells in Preeclampsia. *Am. J. Reprod. Immunol.* 67 (4), 278–286. doi:10.1111/j.1600-0897.2012.01120.x

Hanna, J., Goldman-Wohl, D., Hamani, Y., Avraham, I., Greenfield, C., Natanson-Yaron, S., et al. (2006). Decidual NK Cells Regulate Key Developmental Processes at the Human Fetal-Maternal Interface. *Nat. Med.* 12 (9), 1065–1074. doi:10.1038/nm1452

Harris, L. K., Jones, C. J. P., and Aplin, J. D. (2009). Adhesion Molecules in Human Trophoblast - A Review. II. Extravillous Trophoblast. *Placenta* 30 (4), 299–304. doi:10.1016/j.placenta.2008.12.003

Heaton, S. J., Eady, J. J., Parker, M. L., Gotts, K. L., Dainty, J. R., Fairweather-Tait, S. J., et al. (2008). The Use of BeWo Cells as an *In Vitro* Model for Placental Iron Transport. *Am. J. Physiol. Cell Physiol.* 295 (5), C1445–C1453. doi:10.1152/ajpcell.00286.2008

Helfer, G., and Wu, Q.-F. (2018). Chemerin: a Multifaceted Adipokine Involved in Metabolic Disorders. *J. Endocrinol.* 238 (2), R79–R94. doi:10.1530/joe-18-0174

Hiden, U., Bilban, M., Knöfler, M., and Desoye, G. (2007). Kisspeptins and the Placenta: Regulation of Trophoblast Invasion. *Rev. Endocr. Metab. Disord.* 8 (1), 31–39. doi:10.1007/s11154-007-9030-8

James, J. L., Whitley, G. S., and Cartwright, J. E. (2010). Pre-eclampsia: Fitting Together the Placental, Immune and Cardiovascular Pieces. *J. Pathol.* 221 (4), 363–378. doi:10.1002/path.2719

Jim, B., and Karumanchi, S. A. (2017). Preeclampsia: Pathogenesis, Prevention, and Long-Term Complications. *Semin. Nephrol.* 37, 386–397. doi:10.1016/j.semnephrol.2017.05.011

Jovanović, M., Stefanoska, I., Radojčić, L., and Vićovac, L. (2010). Interleukin-8 (CXCL8) Stimulates Trophoblast Cell Migration and Invasion by Increasing Levels of Matrix Metalloproteinase (MMP)2 and MMP9 and Integrins α5 and β1. *Reproduction* 139 (4), 789–798. doi:10.1530/rep-09-0341

King, A., Allan, D. S. J., Bowen, M., Powis, S. J., Joseph, S., Verma, S., et al. (2000). HLA-E Is Expressed on Trophoblast and Interacts with CD94/NKG2 Receptors on Decidual NK Cells. *Eur. J. Immunol.* 30 (6), 1623–1631. doi:10.1002/1521-4141(200006)30:6<1623::aid-immu1623>3.0.co;2-m

Kitaya, K., Yasuda, J., Yagi, I., Tada, Y., Fushiki, S., and Honjo, H. (2000). IL-15 Expression at Human Endometrium and Decidua. *Biol. Reprod.* 63 (3), 683–687. doi:10.1095/biolreprod63.3.683

Knöfler, M., Haider, S., Saleh, L., Pollheimer, J., Gamage, T. K. J. B., and James, J. (2019). Human Placenta and Trophoblast Development: Key Molecular Mechanisms and Model Systems. *Cell. Mol. Life Sci.* 76 (18), 3479–3496. doi:10.1007/s00018-019-03104-6

Knöfler, M. (2010). Critical Growth Factors and Signalling Pathways Controlling Human Trophoblast Invasion. *Int. J. Dev. Biol.* 54 (2-3), 269–280. doi:10.1387/ijdb.082769mk

Koka, R., Burkett, P. R., Chien, M., Chai, S., Chan, F., Lodolce, J. P., et al. (2003). Interleukin (IL)-15Rα-deficient Natural Killer Cells Survive in Normal but Not IL-15Rα-deficient Mice. *J. Exp. Med.* 197 (8), 977–984. doi:10.1084/jem.20021836

Lash, G. E., Otun, H. A., Innes, B. A., Kirkley, M., De Oliveira, L., Searle, R. F., et al. (2006). Interferon-γ Inhibits Extravillous Trophoblast Cell Invasion by a Mechanism that Involves Both Changes in Apoptosis and Protease Levels. *FASEB J.* 20 (14), 2512–2518. doi:10.1096/fj.06-6616com

Lee, C.-L., Vijayan, M., Wang, X., Lam, K. K. W., Koistinen, H., Seppala, M., et al. (2018). Glycodelin-A Stimulates the Conversion of Human Peripheral Blood CD16-CD56bright NK Cell to a Decidual NK Cell-like Phenotype. *Hum. Reprod.* 34, 689–701. doi:10.1093/humrep/dey378

Li, J., Li, Y., Zhou, X., Wei, L., Zhang, J., Zhu, S., et al. (2021). Upregulation of IL-15 in the Placenta Alters Trophoblasts Behavior Contributing to Gestational Diabetes Mellitus. *Cell Biosci.* 11 (1), 33. doi:10.1186/s13578-021-00533-4

Liu, S., Diao, L., Huang, C., Li, Y., Zeng, Y., and Kwak-Kim, J. Y. H. (2017). The Role of Decidual Immune Cells on Human Pregnancy. *J. Reprod. Immunol.* 124, 44–53. doi:10.1016/j.jri.2017.10.045

Lyall, F. (2005). Priming and Remodelling of Human Placental Bed Spiral Arteries during Pregnancy - A Review. *Placenta* 26, S31–S36. doi:10.1016/j.placenta.2005.02.010

Male, V., Gardner, L., and Moffett, A. (2012). Isolation of Cells from the Feto-Maternal Interface. *Curr. Protoc. Immunol.* Chapter 7, Unit 1-11.7. doi:10.1002/0471142735

Maltepe, E., and Fisher, S. J. (2015). Placenta: the Forgotten Organ. *Annu. Rev. Cel Dev. Biol.* 31, 523–552. doi:10.1146/annurev-cellbio-100814-125620

Mariani, F., and Roncucci, L. (2015). Chemerin/chemR23 axis in Inflammation Onset and Resolution. *Inflamm. Res.* 64 (2), 85–95. doi:10.1007/s00011-014-0792-7

Marsh, B., and Blelloch, R. (2020). Single Nuclei RNA-Seq of Mouse Placental Labyrinth Development. *eLife* 9, e60266. doi:10.7554/elife.60266

Pang, Z.-J., Zhou, J.-G., and Huang, L.-P. (2008). Interleukin-10 May Participate in Regulating Trophoblast Invasion in Human Placentae throughout Gestation. *Am. J. Reprod. Immunol.* 60 (1), 19–25. doi:10.1111/j.1600-0897.2008.00586.x

Pollheimer, J., Vondra, S., Baltayeva, J., Beristain, A. G., and Knöfler, M. (2018). Regulation of Placental Extravillous Trophoblasts by the Maternal Uterine Environment. *Front. Immunol.* 13 (9), 2597. doi:10.3389/fimmu.2018.02597

Quan, X.-Z., Ye, J.-H., Yang, X.-Z., and Xie, Y. (2021). HOXA9-induced Chemerin Signals through CMKLR1/AMPK/TXNIP/NLRP3 Pathway to Induce Pyroptosis of Trophoblasts and Aggravate Preeclampsia. *Exp. Cel Res.* 408 (2), 112802. doi:10.1016/j.yexcr.2021.112802

Rossant, J., and Cross, J. C. (2001). Placental Development: Lessons from Mouse Mutants. *Nat. Rev. Genet.* 2 (7), 538–548. doi:10.1038/35080570

Sell, H., Laurencikiene, J., Taube, A., Eckardt, K., Cramer, A., Horrighs, A., et al. (2009). Chemerin Is a Novel Adipocyte-Derived Factor Inducing Insulin Resistance in Primary Human Skeletal Muscle Cells. *Diabetes* 58 (12), 2731–2740. doi:10.2337/db09-0277

Sharma, S., Godbole, G., and Modi, D. (2016). Decidual Control of Trophoblast Invasion. *Am. J. Reprod. Immunol.* 75 (3), 341–350. doi:10.1111/aji.12466

Smith, S. D., Dunk, C. E., Aplin, J. D., Harris, L. K., and Jones, R. L. (2009). Evidence for Immune Cell Involvement in Decidual Spiral Arteriole Remodeling in Early Human Pregnancy. *Am. J. Pathol.* 174 (5), 1959–1971. doi:10.2353/ajpath.2009.080995

Spradley, F. T., Palei, A. C., and Granger, J. P. (2015). Increased Risk for the Development of Preeclampsia in Obese Pregnancies: Weighing in on the Mechanisms. *Am. J. Physiol. Regulatory Integr. Comp. Physiol.* 309 (11), R1326–R1343. doi:10.1152/ajpregu.00178.2015

Staun-Ram, E., Goldman, S., Gabarin, D., and Shalev, E. (2004). Expression and Importance of Matrix Metalloproteinase 2 and 9 (MMP-2 and -9) in Human Trophoblast Invasion. *Reprod. Biol. Endocrinol.* 2, 59. doi:10.1186/1477-7827-2-59

Tan, L., Chen, Z., Sun, F., Zhou, Z., Zhang, B., Wang, B., et al. (2022). Placental Trophoblast-specific Overexpression of Chemerin Induces Preeclampsia-like Symptoms. *Clin. Sci.* 136, 257–272. doi:10.1042/cs20210989

Terabe, M., Tagaya, Y., Zhu, Q., Granger, L., Roederer, M., Waldmann, T. A., et al. (2008). IL-15 Expands Unconventional CD8ααNK1.1+ T Cells but Not Vα14Jα18+ NKT Cells. *J. Immunol.* 180 (11), 7276–7286. doi:10.4049/jimmunol.180.11.7276

Tilburgs, T., Evans, J. H., Crespo, Â. C., and Strominger, J. L. (2015). The HLA-G Cycle Provides for Both NK Tolerance and Immunity at the Maternal-Fetal Interface. *Proc. Natl. Acad. Sci. U.S.A.* 112 (43), 13312–13317. doi:10.1073/pnas.1517724112

Wallace, A. E., Fraser, R., and Cartwright, J. E. (2012). Extravillous Trophoblast and Decidual Natural Killer Cells: a Remodelling Partnership. *Hum. Reprod. Update* 18 (4), 458–471. doi:10.1093/humupd/dms015

Watson, E. D., and Cross, J. C. (2005). Development of Structures and Transport Functions in the Mouse Placenta. *Physiology* 20, 180–193. doi:10.1152/physiol.00001.2005

Whitley, G. S. J., and Cartwright, J. E. (2009). Trophoblast-mediated Spiral Artery Remodelling: a Role for Apoptosis. *J. Anat.* 215 (1), 21–26. doi:10.1111/j.1469-7580.2008.01039.x

Woods, L., Perez-Garcia, V., and Hemberger, M. (2018). Regulation of Placental Development and its Impact on Fetal Growth-New Insights from Mouse Models. *Front. Endocrinol.* 9, 570. doi:10.3389/fendo.2018.00570

Xie, Y., and Liu, L. (2022). Role of Chemerin/ChemR23 axis as an Emerging Therapeutic Perspective on Obesity-Related Vascular Dysfunction. *J. Transl. Med.* 20 (1), 141. doi:10.1186/s12967-021-03220-7

Xie, Y., Huang, Y., Ling, X., Qin, H., Wang, M., and Luo, B. (2020). Chemerin/CMKLR1 Axis Promotes Inflammation and Pyroptosis by Activating NLRP3 Inflammasome in Diabetic Cardiomyopathy Rat. *Front. Physiol.* 11 (381). doi:10.3389/fphys.2020.00381

Xu, Q.-L., Zhu, M., Jin, Y., Wang, N., Xu, H.-X., Quan, L.-M., et al. (2014). The Predictive Value of the First-Trimester Maternal Serum Chemerin Level for Pre-eclampsia. *Peptides* 62, 150–154. doi:10.1016/j.peptides.2014.10.002

Yang, X., Yao, J., Wei, Q., Ye, J., Yin, X., Quan, X., et al. (2018). Role of chemerin/CMKLR1 in the Maintenance of Early Pregnancy. *Front. Med.* 12 (5), 525–532. doi:10.1007/s11684-017-0577-9

Yoshimura, T., and Oppenheim, J. J. (2011). Chemokine-like Receptor 1 (CMKLR1) and Chemokine (C-C Motif) Receptor-like 2 (CCRL2); Two Multifunctional Receptors with Unusual Properties. *Exp. Cel Res.* 317 (5), 674–684. doi:10.1016/j.yexcr.2010.10.023

Zabel, B. A., Kwitniewski, M., Banas, M., Zabieglo, K., Murzyn, K., and Cichy, J. (2014). Chemerin Regulation and Role in Host Defense. *Am. J. Clin. Exp. Immunol.* 3 (1), 1–19.

Zhang, J., Dunk, C. E., and Lye, S. J. (2013). Sphingosine Signalling Regulates Decidual NK Cell Angiogenic Phenotype and Trophoblast Migration. *Hum. Reprod.* 28 (11), 3026–3037. doi:10.1093/humrep/det339

Conflict of Interest: The authors declare that the research was conducted in the absence of any commercial or financial relationships that could be construed as a potential conflict of interest.

Publisher's Note: All claims expressed in this article are solely those of the authors and do not necessarily represent those of their affiliated organizations, or those of the publisher, the editors and the reviewers. Any product that may be evaluated in this article, or claim that may be made by its manufacturer, is not guaranteed or endorsed by the publisher.

frontiers | Frontiers in Cell and Developmental Biology

ORIGINAL RESEARCH
published: 29 June 2022
doi: 10.3389/fcell.2022.933852

Three-Dimensional Visualization of Mouse Endometrial Remodeling After Superovulation

*Yongcun Qu[1], Jia Zhang[2], Shanshan Guo[3], Liwen Zhang[3], Jingjing Qian[3], Xili Zhu[3], Enkui Duan[3] and Ying Zhang[2]**

[1]Institute of Artificial Intelligence in Sports, Capital University of Physical Education and Sports, Beijing, China, [2]College of Life Sciences, Beijing Normal University, Beijing, China, [3]Institute of Zoology, Chinese Academy of Sciences, Beijing, China

Uterine status determines pregnancy success. Although it is well known that superovulation operations can disrupt uterine function, our understanding of the morphological changes in the uterine endometrium at the three-dimensional (3D) level is limited. Here, combining the tissue clearing with 3D deep imaging, we reveal an increase in epithelial density and angiogenesis after ovarian stimulation, which is accompanied by a circulating surge in P4 levels. Using an ovariectomized mouse model, we further detected the separate regulatory effects of P4 and E2 on the uterine endometrium, with P4 promoting endothelial cell growth and E2 inducing epithelial proliferation. Additionally, we observed that the effects of E2 can be partially neutralized by P4, and vice versa. By analyzing the 3D uterine imaging, we discovered an interesting phenomenon in which the growing blood vessels closely surround the remodeling uterine epithelium, indicating a close relationship between angiogenesis and epithelial growth. These findings provide new insight into the uterine epithelial changes and angiogenesis at the 3D level, and explain a potential reason for endometrial changes due to the low implantation rate in patients undergoing clinic super-ovulation.

Keywords: superovulation, uterine clearing, 3D imaging, uterine endometrial angiogenesis, uterine gland, steroid hormone

OPEN ACCESS

Edited by:
Rujuan Zuo,
Oslo University Hospital, Norway

Reviewed by:
Qingqing Zhang,
The University of Hong Kong, Hong Kong, SAR China
Minmin Jiang,
Anhui Medical University, China

****Correspondence:***
Ying Zhang
yingzhanglab@gmail.com

Specialty section:
This article was submitted to Cellular Biochemistry, a section of the journal Frontiers in Cell and Developmental Biology

Received: *01 May 2022*
Accepted: *27 May 2022*
Published: *29 June 2022*

Citation:
Qu Y, Zhang J, Guo S, Zhang L, Qian J, Zhu X, Duan E and Zhang Y (2022) Three-Dimensional Visualization of Mouse Endometrial Remodeling After Superovulation. Front. Cell Dev. Biol. 10:933852. doi: 10.3389/fcell.2022.933852

INTRODUCTION

Although IVF (*in vitro* fertilization) has been widely used for over 40 years, a low implantation rate was found when fresh embryos were transferred after the superovulation cycle, especially in patients with ovarian hyperstimulation syndrome (Chen et al., 2016). Frozen embryo transfers can significantly increase the pregnancy rate (Chen et al., 2016; Shi et al., 2018), suggesting that the superovulation-induced abnormal uterine endometrial status is one of the main reasons for implantation failure.

In clinical and mouse-based researches, superovulation is a routine operation used to retrieve a large number of oocytes for pregnancy. However, this process usually induces an extensive ovulatory response and high levels of circulating steroid hormones. It is well known that progesterone (P4) and estrogen (E2) precisely regulate uterine functions, especially the changes in uterine blood vessels and the epithelium. For example, the induction of epithelial cell proliferation in mice is simply induced by E2 (O'Brien et al., 2006), but the regulatory effects of P4 and E2 on endometrial vasodilation and angiogenesis are more complex. It has been reported that E2 promotes uterine vascular permeability through its nuclear receptor ERα (Hyder et al., 2000), and stimulates VEGF and Flk1 expressions in

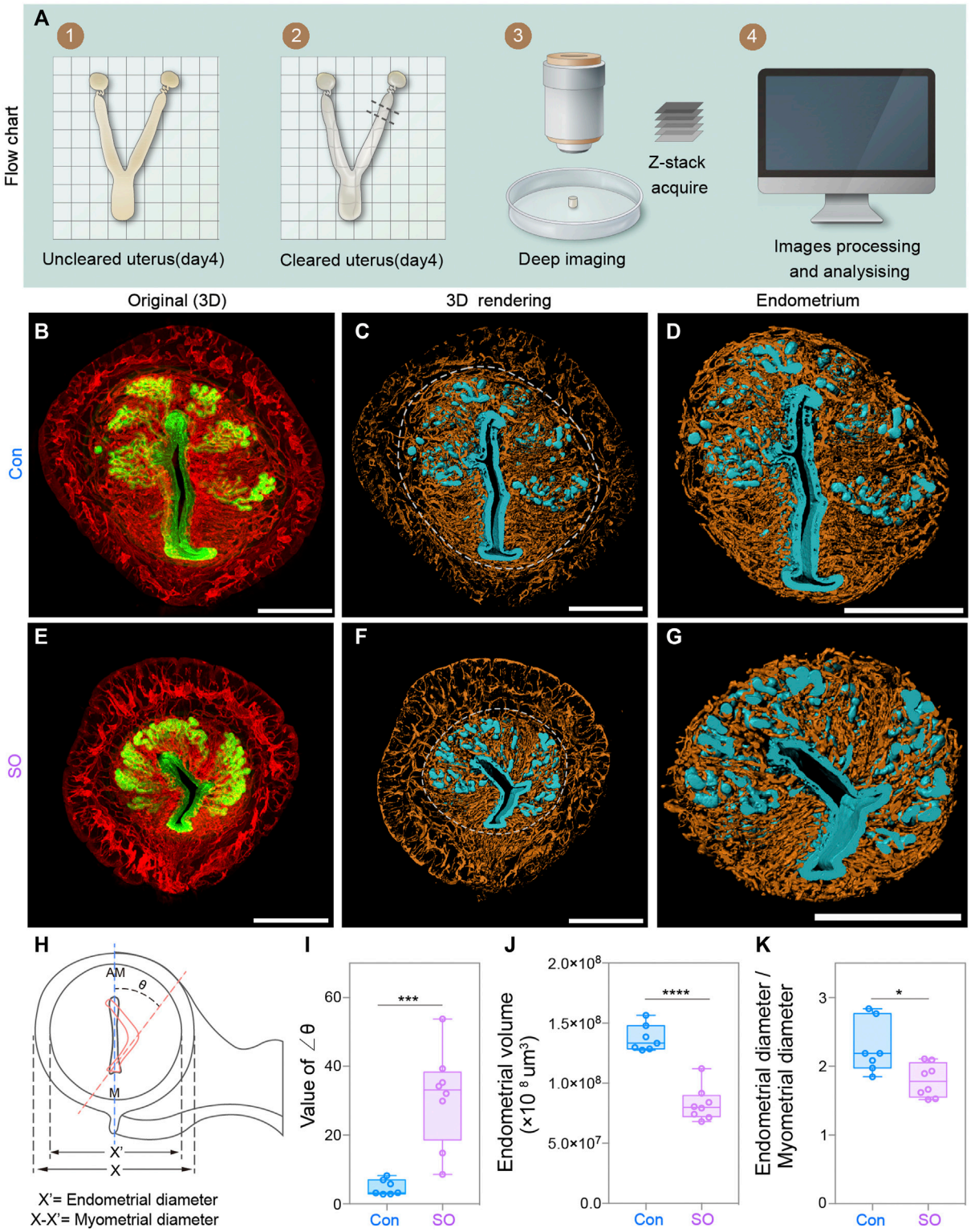

FIGURE 1 | Uterine endometrial changes in the 3D level after superovulation. **(A)** Experimental flow chart. **(B)** 3D reconstruction of the control uterus on day 4. **(C–D)** 3D rendering of the control uterus **(C)** and uterine endometrium **(D)** on day 4. **(E)** 3D reconstruction of the superovulation uterus on day 4. **(F–G)** 3D rendering of the superovulation uterus **(F)** and uterine endometrium **(G)** on day 4. **(H)** Schematic diagram illustrating the luminal orientation within the uterus and the diameter of the endometrium and myometrium. The normal luminal axis is parallel to the uterine M-AM axis in the control uteri, while the abnormal axis (delineated by the orange dashed line) is deflected from the uterine axis in the superovulation uteri. The angles of deviation are indicated as ∠θ. **(I)** Comparing the value of the ∠θ in the control and

(*Continued*)

FIGURE 1 | superovulation groups. **(J)** Comparing the endometrial volume on day 4 in control and Superovulation groups. **(K)** Comparing the ratio of the endometrial diameter/myometrial diameter in the control and superovulation groups. Scale bar of **(B–G)** = 350 μm. The results are shown as means ± SEM. *$p < 0.05$, **$p < 0.01$, ***$p < 0.001$, ****$p < 0.0001$. n ≥ 7.

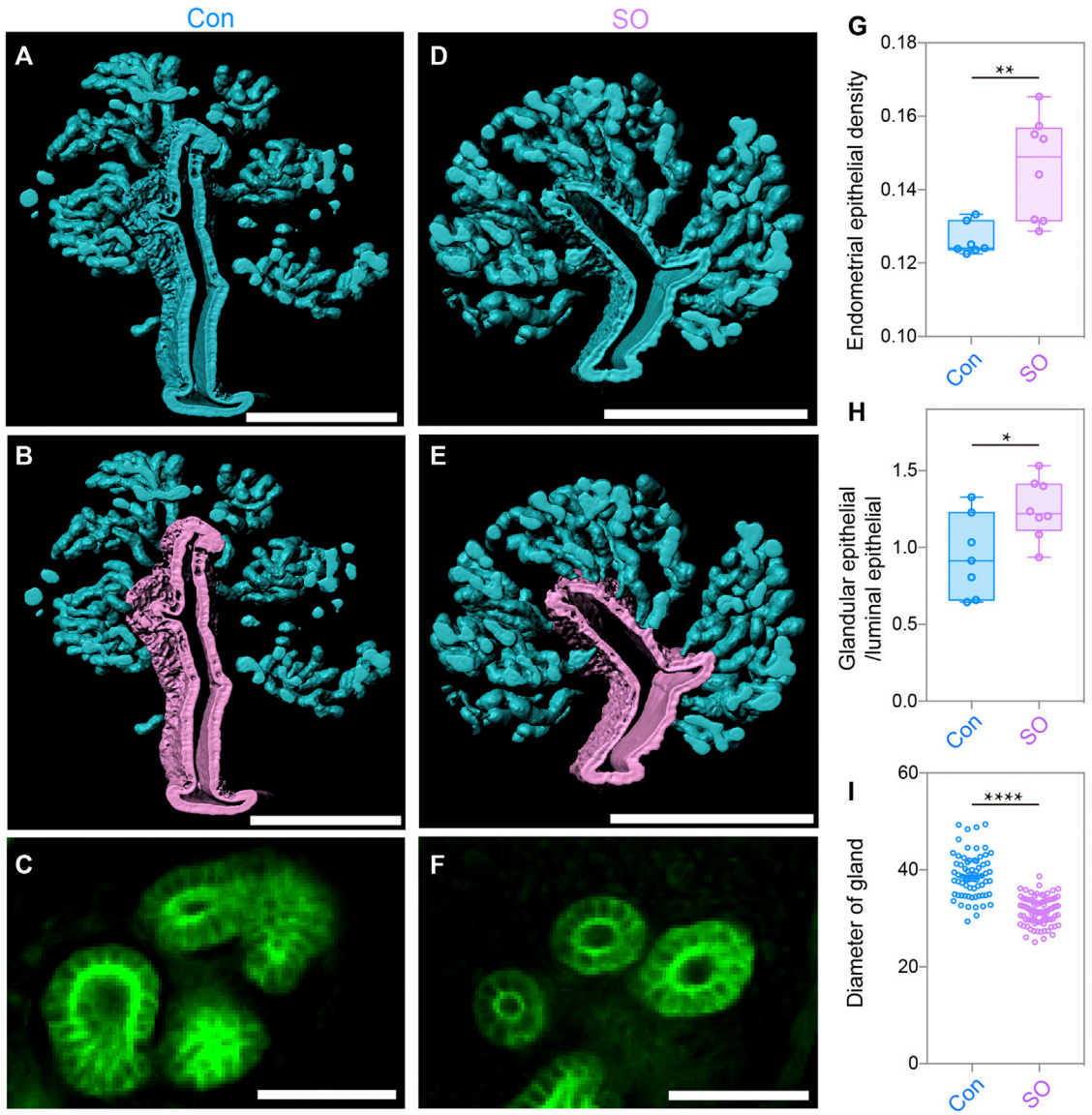

FIGURE 2 | Uterine epithelial changes in the 3D level after superovulation. **(A)** 3D rendering of uterine epithelium of the control group. **(B)** 3D rendering of glandular epithelium (blue) and luminal epithelium (purple) of the control group. **(C)** Light-section of the uterine gland in the control group. **(D)** 3D-rendering of the uterine epithelium of the superovulation group. **(E)** 3D rendering of the glandular epithelium (blue) and the luminal epithelium (purple) of the superovulation group. **(F)** Light-section of the uterine gland in the superovulation group. **(G)** Comparing endometrial epithelial density in the control and superovulation groups. **(H)** Comparing the ratio of glandular epithelium/total epithelium in the control and superovulation groups. **(I)** Comparing the glandular diameter in the control and superovulation groups. Scale bar of **(A,B,D,E)** = 350 μm. Scale bar of **(C,F)** = 50 μm. The results are shown as means ± SEM. *$p < 0.05$, **$p < 0.01$, ***$p < 0.001$, ****$p < 0.0001$. n ≥ 7.

the stromal bed (Ma et al., 2001), but profoundly attenuates uterine angiogenesis (Ma et al., 2001). P4 induces endothelial cell proliferation (Walter et al., 2005) and uterine angiogenesis but has little effect on vascular permeability (Ma et al., 2001). However, another study showed that E2 induces rapid proliferation of both the endothelial and stromal cells (Heryanto and Rogers, 2002), suggesting the angiogenic effect of E2. The differences between these results are not only due to

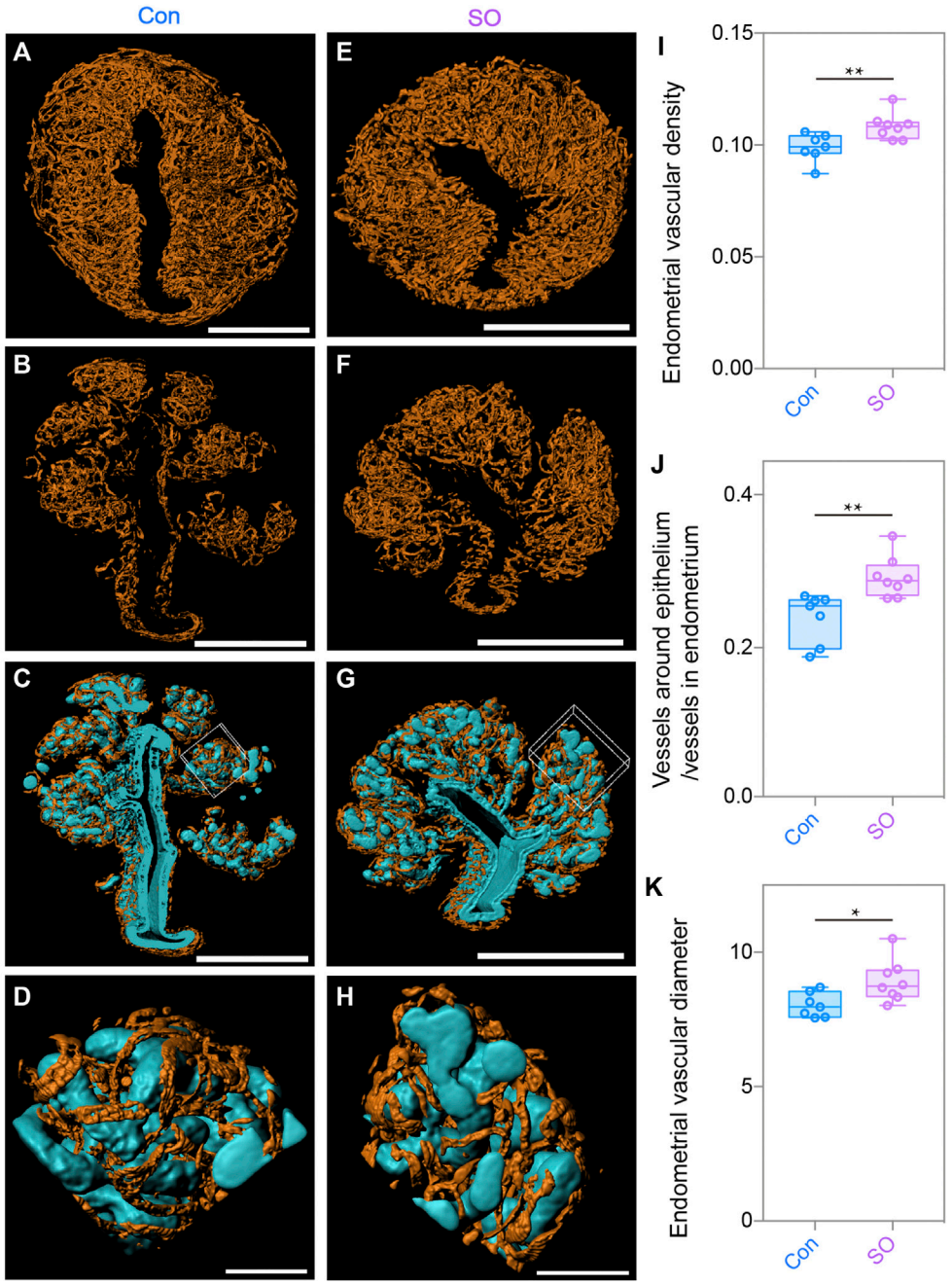

FIGURE 3 | Uterine endometrial angiogenesis in the 3D level after superovulation. **(A)** 3D rendering of the endometrial blood vessels of the control group. **(B)** 3D rendering of the vessels around the epithelium in the control group. **(C)** Blood vessels closely surrounded the epithelium in the control group. **(D)** Magnified detail at the boxed area of **(C)**. **(E)** 3D rendering of endometrial blood vessels of the superovulation group. **(F)** 3D rendering of vessels around the epithelium in the superovulation group. **(G)** Blood vessels closely surrounding the epithelium in the superovulation group. **(H)** Magnified detail at the boxed area of **(G)**. **(I)** Comparing endometrial vascular density in the control and superovulation groups. **(J)** Comparing the ratio of the vessels around the epithelium/vessels in the endometrium in the control and superovulation groups. **(K)** Comparing the endometrial vascular diameter in the control and superovulation groups. Scale bar of **(A–C,E–H)** = 350 μm. Scale bar of **(D,H)** = 60 μm. The results are shown as means ± SEM. $^{*}p < 0.05$, $^{**}p < 0.01$, $^{***}p < 0.001$, $^{****}p < 0.0001$. n ≥ 7.

the different mouse models used by the authors, but also due to the limitations of detection technology based on thin tissue sections, which can only provide local 2D information rather than 3D views. Moreover, although the adverse effects of superovulation and abnormal gene expression in the endometrium have been reported in the clinic (Haouzi et al.,

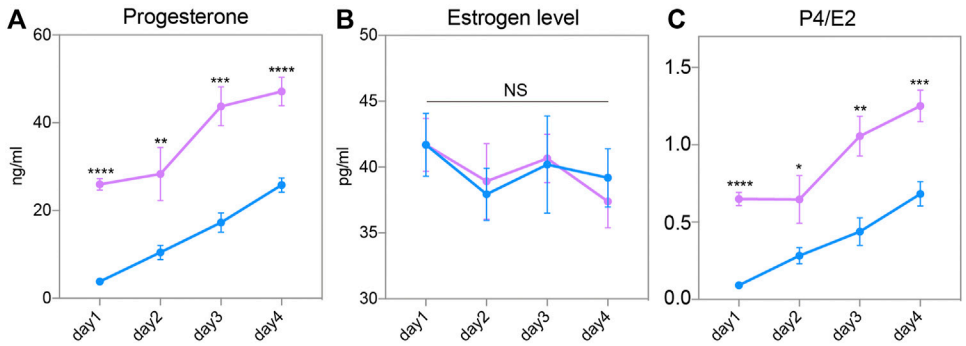

FIGURE 4 | Steroid hormone in response to superovulation. **(A)** Circulating progesterone (P4) levels in the control (blue) and superovulation (magenta) groups. **(B)** Circulating estrogen (E2) levels in the control (blue) and superovulation (magenta) groups. **(C)** The ratio of P4/E2 in control (blue) and superovulation (magenta) groups. The results are shown as means ± SEM. *$p < 0.05$, **$p < 0.01$, ***$p < 0.001$, ****$p < 0.0001$. n ≥ 5.

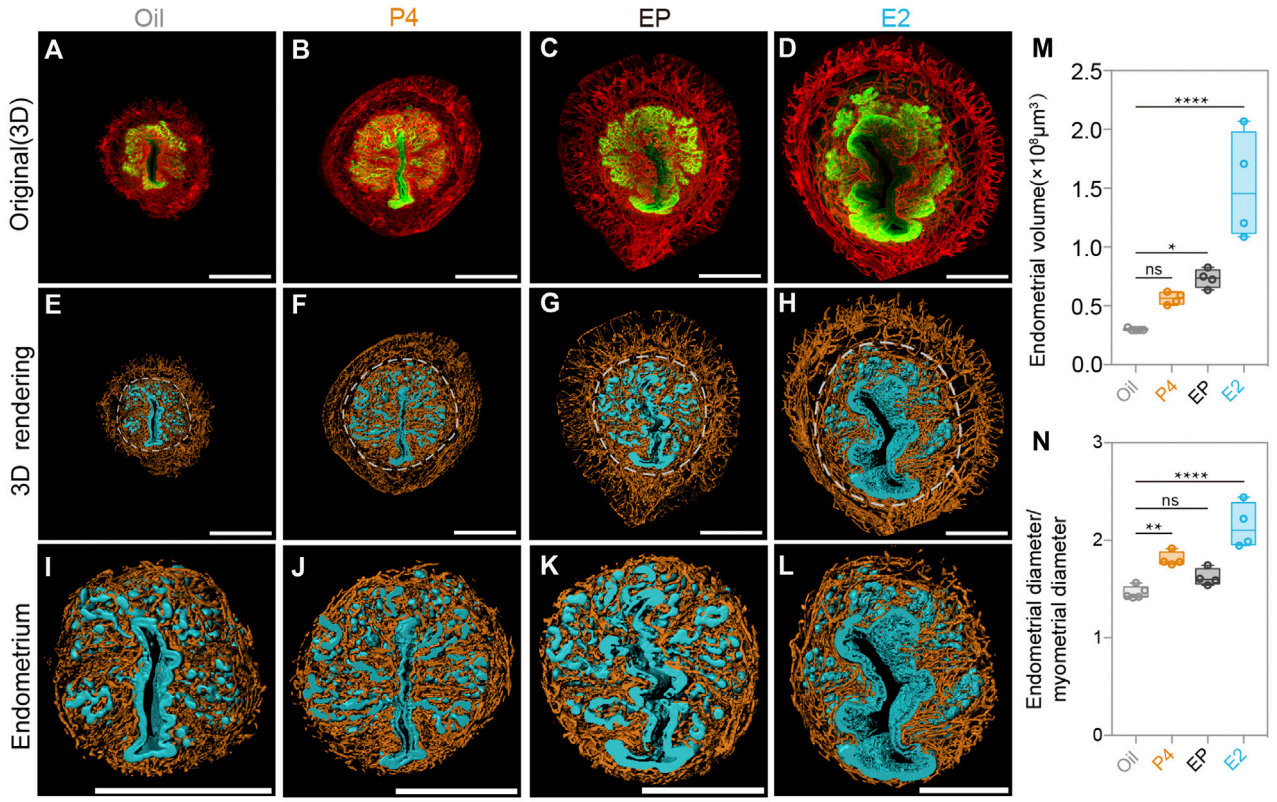

FIGURE 5 | Uterine endometrial changes in the 3D level after steroid hormone treatment in ovariectomized mice. **(A–D)** 3D reconstruction of the uterus after the oil-treated group **(A)**, P4-treated group **(B)**, E2 plus P4 (EP)-treated group **(C)**, and E2-treated group **(D)**. **(E–H)** 3D rendering of the uterus after the oil-treated group **(E)**, P4-treated group **(F)**, E2 plus P4 (EP) treated group **(G)**, and E2-treated group **(H)**. **(I–L)** 3D rendering of uterine endometrial after the oil-treated group **(I)**, P4-treated group **(J)**, E2 plus P4 (EP)-treated group **(K)**, and E2-treated group **(L)**. **(M)** Comparing endometrial volume with different steroid hormone treatments. **(N)** Comparing the ratio of the endometrial diameter/myometrial diameter with different steroid hormone treatments. Scale bar of **(A–L)** = 350 μm. The results are shown as means ± SEM. Different letters represent significant differences ($p < 0.05$). *$p < 0.05$, **$p < 0.01$, ***$p < 0.001$, ****$p < 0.0001$. n ≥ 4.

2009), the specific changes in uterine glands and endometrial blood vessels remain unclear, especially at the 3D level.

Here, by combining the tissue clearing method and deep imaging, we detected 3D changes in uterine endometrial angiogenesis and epithelial proliferation in the superovulated mouse endometrium compared with the control endometrium, showing a decreased endometrial volume and increased epithelial and vascular density. For superovulation-induced circulating P4

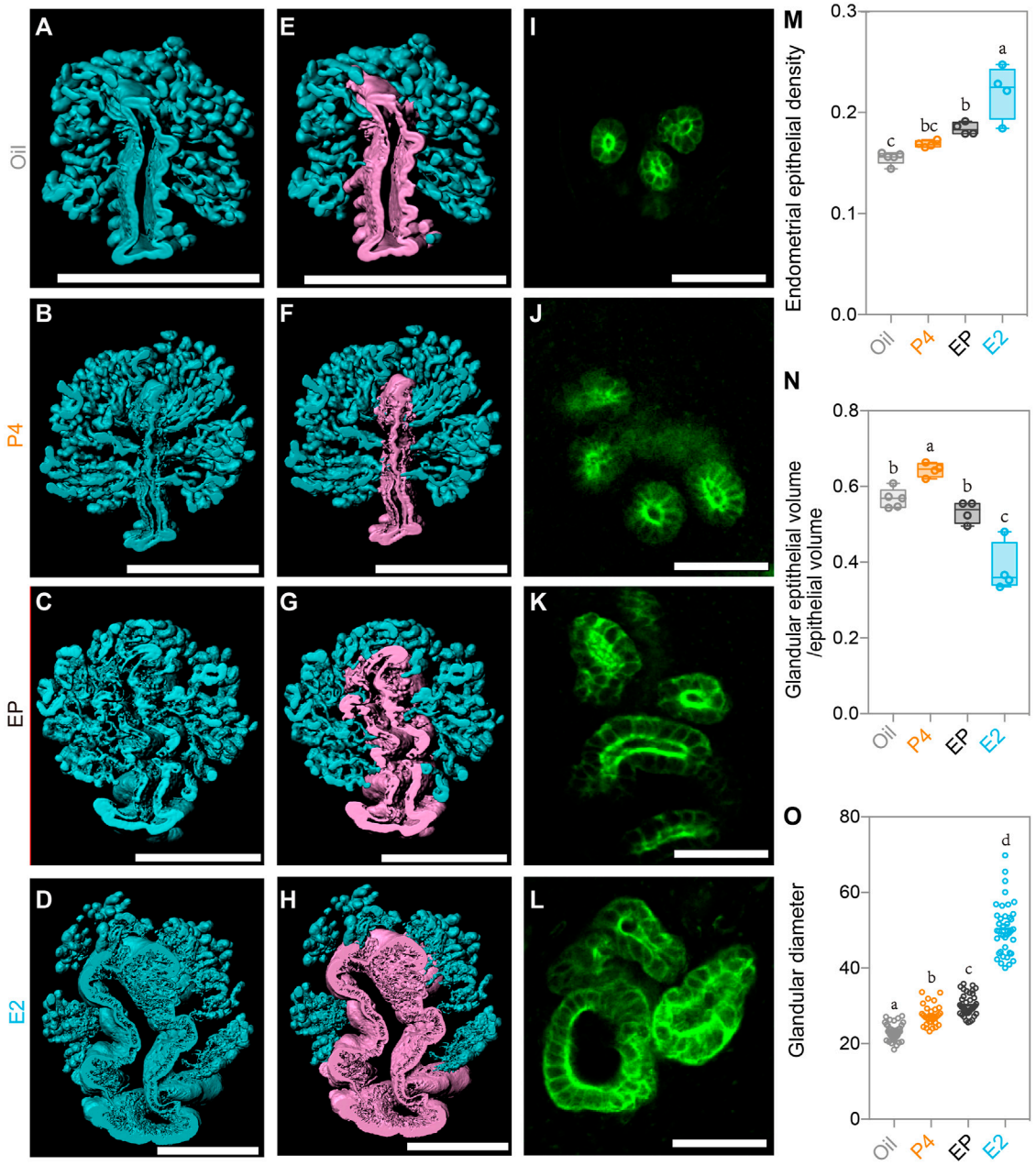

FIGURE 6 | Uterine epithelial alteration in the 3D level after steroid hormone treatment. **(A–D)** 3D rendering of the uterine epithelium of the oil-treated group **(A)**, P4-treated group **(B)**, E2 plus P4 (EP)-treated group **(C)**, and E2-treated group **(D)**. **(E–H)** 3D rendering of the glandular epithelium (blue) and luminal epithelium (purple) of the oil-treated group **(E)**, P4-treated group **(F)**, E2 plus P4 (EP)-treated group **(G)**, and E2-treated group **(H)**. **(I–L)** light-section of the uterine gland in the oil-treated group **(I)**, P4-treated group **(J)**, EP-treated group **(K)**, and E2-treated group **(L)**. **(M)** Comparing the endometrial epithelial density with different steroid hormone treatments. **(N)** Comparing the ratio of glandular epithelium/total epithelium with different steroid hormone treatments. **(O)** Comparing the glandular diameter with different steroid hormone treatments. Scale bar of **(A–H)** = 350 μm. Scale bar of **(I–L)** = 50 μm. The results are shown as means ± SEM. Different letters represent significant differences ($p < 0.05$). *$p < 0.05$, **$p < 0.01$, ***$p < 0.001$, ****$p < 0.0001$. n ≥ 4.

levels rather than E2 levels in mice, we also used the ovariectomized mouse model to detect the regulation by P4 and E2 in the endometrium separately. Moreover, we also observed an interesting network between blood vessel growth and epithelial lining proliferation, indicating a potential interaction between them in the endometrium.

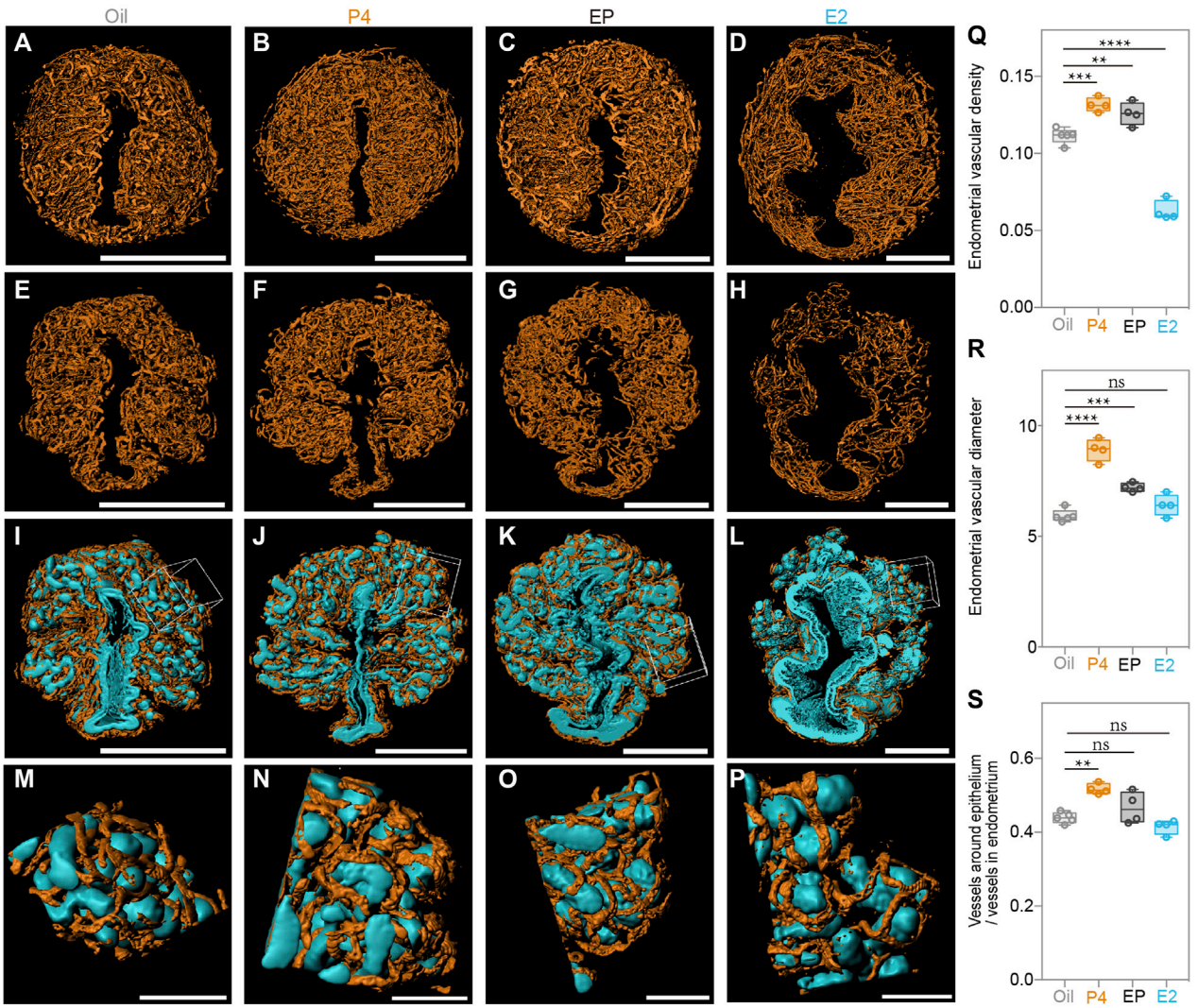

FIGURE 7 | Uterine endometrial angiogenesis in the 3D level after steroid hormone treatment. **(A–D)** 3D rendering of endometrial blood vessels in the oil-treated group **(A)**, P4-treated group **(B)**, E2 plus P4 (EP)-treated group **(C)**, and E2-treated group **(D)**. **(E–H)** 3D rendering of the vessels around the epithelium in the oil-treated group **(E)**, P4-treated group **(F)**, E2 plus P4 (EP)-treated group **(G)**, and E2 treated group **(H)**. **(I–L)** Blood vessels closely surrounding the epithelium in the oil-treated group **(I)**, P4-treated group **(J)**, E2 plus P4 (EP)-treated group **(K)** and E2-treated group **(L)**. **(M)** Magnified details at the boxed area of **(I)**. **(N)** Magnified details at the boxed area of **(N)**. **(O)** Magnified details at the boxed area of **(K)**. **(P)** Magnified details at the boxed area of **(L)**. **(Q)** Comparing the endometrial vascular density with different steroid hormone treatments. **(R)** Comparing the ratio of vessels around the epithelium/vessels in the endometrium with different steroid hormone treatments. **(S)** Comparing the endometrial vascular diameter with different steroid hormone treatments. Scale bar of **(A–L)** = 350 μm. Scale bar of **(M–P)** = 70 μm The results are shown as means ± SEM. Different letters represent significant differences ($p < 0.05$). $^{*}p < 0.05$, $^{**}p < 0.01$, $^{***}p < 0.001$, $^{****}p < 0.0001$. n ≥ 4.

RESULTS

Uterine 3D Imaging Revealed a Decreased Endometrial Volume Following Superovulation

To detect morphological changes in the pre-implantation mouse uterus in response to exogenous gonadotropin, we established a uterine-specific whole-organ clearing method (**Figure 1A**), which was optimized from a previous work (Arora et al., 2016). Uteri from both control (Con) and superovulation (SO) mice at gestational day 4 (Day 4) were collected and cleared by using clearing methods, during which FLK1 (VEGF receptor 2) and CK (cytokeratin) were used to label vascular endothelial and epithelial cells of the uteri, respectively (**Figures 1B–G**). Combining confocal imaging and 3D reconstruction, we found that the uterus of SO group was much smaller than that of the Con group (**Figures 1B,E**). To further examine the endometrial changes under superovulation, we computationally isolated the uterine endometrium and myometrium separately, and the results showed that endometrial volume and the ratio for the endometrial/myometrial diameter were all significantly decreased following superovulation (**Figures 1D,G,J,K**), suggesting that superovulation might disrupt endometrial proliferation at Day 4.

More interestingly, we noticed that, unlike the vertical lumen along the mesometrial–antimesometrial (M–AM) axis in the uteri of the Con group, that of the SO group showed an aberrant fold of the lumen, and the luminal axis was deflected from the uterine axis (**Figures 1H,I**). The angles of deviation were indicated as ∠θ, which was >20° in the SO group but <10° in the Con group (**Figure 1I**). Vertical luminal closure on Day 4 is responsible for the correct embryo orientation during the implantation process. This defect of luminal folds might lead to many "pitfalls" for blastocysts, as a previous study reported (Zhang et al., 2014), and causes a potentially disoriented uterine–embryonic axis after implantation, which might lead to developmental failure of the embryo post-implantation.

Superovulation Induced Epithelial Cell Proliferation and Endometrial Angiogenesis in Pre-implantation Uteri

To further quantitatively analyze the endometrial changes, 3D surface of the epithelial signals was generated after separating the endometrium (**Figures 2A,D**). The statistical results showed an increase in the endometrial epithelial density after superovulation (**Figure 2G**). We then computationally isolated 3D surfaces of the luminal epithelium and glandular epithelium, and the 3D surfaces were evaluated. The purple signal indicates the luminal epithelium and the blue signal indicates the glandular epithelium (**Figures 2B,E**). Compared to the Con group, the SO group had more glandular epithelium, and the ratio for glandular epithelial volume/epithelial volume was increased by approximately 1.2 times (**Figure 2H**). However, when amplifying the glandular epithelium at the 2D level (**Figures 2C,F**), we found that the diameter of the gland was much smaller in the SO uteri than in the Con group (**Figure 2I**). All these results suggested that ovarian stimulation led to more epithelial cell proliferation but with narrower glands.

With the same strategy, we also generated the 3D surface of blood vessels (orange) to quantitatively calculate the changes in the endometrial angiogenesis. As shown in **Figures 3A,E**, we noticed that the endometrial vascular density and diameter of the SO group were a marginally increased compared with those of the Con group (**Figures 3I,K**), showing an abnormal angiogenesis pattern of the stimulated cycles. A previous study reported that excessive angiogenesis and an abnormal vascular diameter in the peri-implantation endometrium were positively correlated with the occurrence of a miscarriage (Plaisier, 2011), suggesting that the low implantation rate caused by superovulation could be related to an abnormal endometrial vascular growth.

During the analysis, we unexpectedly noticed that the glands were closely intertwined with growing blood vessels (**Figures 3C,D,G,H**), suggesting that there might be crosstalk of the proliferation between epithelial cells and endothelial cells, as the direction of epithelial cell growth might be regulated by angiogenesis, or vice versa. Considering the topological relationship between blood vessels and the epithelium, we assumed that the number of blood vessels surrounding the epithelium might also increase because a higher epithelial density was found in the superovulated group. To test this hypothesis, we computationally separated the blood vessels twisting around the epithelium to measure their volumes and found more growth of the blood vessels around the epithelium in the SO uteri (**Figures 3B,F**). Additionally, the ratio of vessels around the epithelium to endometrial vessels was higher than that in Con group's uteri (**Figure 3J**). Taken together, the 3D-imaging results indicate that superovulation induced uterine epithelial cell proliferation and endometrial angiogenesis, which impaired the pre-implantation uterine milieu at the pre-implantation stage.

Superovulation Increased Circulating Progesterone Levels at the Early Stage of Pregnancy

To explore the mechanism of endometrial changes, we measured the circulating P4 and E2 levels of female mice after routine superovulation. After successful mating with wild-type male mice, the serum of pregnant female mice were collected from Day 1 to Day 4. The circulating P4 level continually increased from Day 1 to Day 4 in both groups. However, serum P4 was significantly higher in the SO group than in the Con group on these 4 days (**Figure 4A**). E2 showed relatively gentle changes in the pre-implantation stage, but there was no difference between the Con and SO groups (**Figure 4B**). Because the ratio of P4 to E2 is a key regulator of implantation, we also checked the changes in this ratio, and found a higher ratio in the SO group (**Figure 4C**), indicating that the superovulation-induced serum P4 level might be the cause of the endometrial changes.

Abnormal Endometrial Alterations Following Superovulation Were Mainly Regulated by Increased Progesterone

To further explore the regulatory role of P4 in endometrial changes at the 3D level, we established an ovariectomized mouse model (OV), and found that the ovariectomized uteri were much smaller than the normal uteri due to the lack of hormones, as previously reported. We treated the OV mice with sesame oil, P4, E2, and P4 plus E2 (EP) separately for 72 h. Then, the dissected uteri were collected and 3D imaging analyses as those for the SO and Con groups were performed. As shown in **Figures 5A–L**, the P4-, E2-, and EP-treatments all induced the proliferation of the uterine endometrium, which is consistent with previous reports. We also observed an increase in endometrial volume and the endometrium/myometrium ratio (**Figures 5M,N**). Among the hormone-treated groups, we noticed that although E2 treatment significantly promoted endometrial proliferation, the addition of P4 to E2 could partially counteract the E2 stimulatory effects (**Figures 5M,N**). This observation could explain the phenotype we found in the SO group that with the existence of E2, surged P4 decreased the endometrial volume during the pre-implantation stage.

We next detected changes in the endometrial glands. Although the E2 treatment induced endometrial gland growth as the endometrial epithelial density increased significantly, the administration of P4 plus E2 remarkably reduced the endometrial epithelial density (**Figure 6M**), indicating the inverse effect of P4 compared to E2. On the other hand, after isolating luminal and glandular epithelia separately as we did previously (**Figures 6A–H**), we found different effects between P4

and E2 on the glandular and luminal epithelia. The ratio of glandular epithelium/luminal epithelium was highest in the P4 group and lowest in the E2 group (**Figure 6N**), and P4 plus E2 neutralized the effect of administration of these two hormones alone (**Figure 6N**). A similar phenomenon was also found when analyzing the glandular diameter. E2 treatment alone induced the largest glandular diameter, but if treated with P4 plus E2, the glandular diameter was markedly decreased (**Figures 6I–L,O**). All these results suggested opposing the effects by P4 and E2 on epithelial cell growth, which can help us to understand the epithelial changes in the SO groups. In the Con group, the P4 level gradually increased from Day 1 to Day 4, while the E2 level remained stable during the pre-implantation stage. However, in the SO group, excess P4 was induced, while the E2 level was unchanged, which promoted glandular epithelial growth and resulted in an increase in the endometrial epithelial density and the glandular epithelium/luminal epithelium ratio.

Finally, we generated a 3D surface of the blood vessels in the endometrium of all the groups (**Figures 7A–D**), and observed that, compared to the oil-treated group, P4 significantly promoted endometrial blood vessel growth, while E2 inhibited this process. The endometrial vascular density and diameter were highest in the P4-treated group but lowest in the E2-treated group (**Figures 7Q,R**). It was not surprising to find that the P4 effects were attenuated by E2, and the endometrial vascular density and diameter of the EP-treated group were all between those of the P4 and E2 groups. Additionally, the ratio of the vessels around the epithelium/vessels in the endometrium was increased by P4 treatment (**Figures 7E–H,S**), suggesting that endometrial angiogenesis after superovulation could be regulated mainly by high P4 levels. In addition, blood vessels closely surrounded the epithelium in all groups as we found in the SO uteri (**Figures 7I–P**), suggesting that this topological relationship could play important roles in the endometrial function.

DISCUSSION

In the present study, we established a uterine-specific whole-organ clearing method and examined the 3D morphological changes in the superovulation mouse endometrium. We found a routine superovulation-induced epithelial cell proliferation and endometrial angiogenesis in the pre-implantation uteri, following a remarkable surge in circulating progesterone. We also revealed an essential finding that the growing blood vessels closely surrounded the remodeling uterine epithelium, which is the first morphological evidence of the close relationship between epithelial proliferation and angiogenesis at the 3D level.

Superovulation has been reported to cause many pregnancy disorders, among which defects in uterine receptivity are one of the main causes. Although most previous studies have focused on the molecular changes of uterine cells that regulate the receptivity establishment, the morphological differences of the uteri were more obvious to help us judge the uterine status. Here, by employing 3D imaging and quantitative analysis, we illustrated the changes in the endometrial glands and blood vessels following superovulation. It has been proved that uterine glands are essential for reproduction. The uterine gland knockout (UGKO) sheep and mice all showed infertility, and both had a defect in embryo implantation (Filant and Spencer, 2014). Moreover, the impaired uterine glands also affected glandular secretions, which are an important information mediator between the floating embryo and maternal uterus, and led to incorrect communication (Zhang et al., 2017). We observed the abnormal proliferation of the uterine gland after superovulation, indicating that glandular secretion might be changed. On the other hand, a previous study showed that the mouse uterus should show normal luminal closure along the M-AM direction on Day 4, to ensure that the embryo implants are in the right site, and if these processes are destroyed, aberrant embryo implantation will lead to a progressively disoriented embryonic–uterine axis and miscarriage (Zhang et al., 2014). Our findings in the superovulation mice showed an incorrect luminal structure in the SO uteri, suggesting potential adverse effects for embryo implantation.

Angiogenesis is another important event that regulates uterine receptivity. After the uterine arteries perfuse and branch into the myometrial layer, small vessels arrive at the endometrium. As early as 1940, two different endometrial vessels were described, including the straight arterioles that are in the basal layer and spiral arterioles that are in the functional layer. Among them, spiral arterioles have been found to be sensitive to progesterone (Karizbodagh et al., 2017). Here, we found that superovulation induced the endometrial angiogenesis, which is consistent with previous studies (Rashidi et al., 2017). Interestingly, we first discovered that the growing blood vessels closely surrounded the remodeling uterine glands at the 3D level, indicating the interaction between the epithelial cell proliferation and endothelial cell growth. Considering that the majority of endometrial VEGF is produced by glands (Gargett et al., 1999), there might be a higher expression of VEGF in the uterine gland proliferation site, which might direct the angiogenesis, but this hypothesis needs more study.

Progesterone and estrogen are the main regulators of the uterine status and the process of embryo implantation. It is well established that the function of these two hormones occurs primarily through their receptors via the activation of signaling cascades and adjustments to gene expression (Marquardt et al., 2019). During the pre-implantation stage, progesterone plays an essential role in establishing uterine receptivity, and supplementation with progesterone may extend uterine receptivity for implantation (Song et al., 2007). However, additional evidence has demonstrated that a high concentration of progesterone might impair uterine receptivity and implantation (Liang et al., 2018) and that an aberrant progesterone/estrogen ratio is also harmful to early pregnancy (Maclin et al., 1990), indicating that the concentration of progesterone should be in a suitable range to support implantation. Here, we discovered that a routine superovulation operation increases progesterone and the progesterone/estrogen ratio in mice, which was consistent with previous studies (Akinlosotu and Wilder, 1993). Considering the neutralization effects between E2 and P4, the adjustment of the serum P4/E2 ratio might be helpful in clinical treatments under a similar situation.

On the other hand, our study also has several limitations. Although superovulation-induced epithelial and vascular

abnormalities at the 3D level, the adverse effects of these changes on implantation and embryo development in later pregnancy are still unclear. Moreover, in our study, we only measured the serum progesterone and estrogen levels in pregnant mice after ovarian stimulation and did not include other steroid hormones. It has been reported that superovulation could robustly elevate the serum androgen levels, which could also promote epithelial proliferation via androgen receptors in the epithelium, suggesting that endometrial structural alterations may not only be due to a higher progesterone level. Furthermore, it is impossible to reveal the continuous changes of the endometrium in the 3D level for the limitations of tissue clearing methods, which have to use the fixed samples. It is worth expecting the real-time 3D imaging that helps us to have a direct view of the process of embryo implantation.

In summary, we used the uterine 3D reconstruction technology to discover that the superovulation operation increased the circulating progesterone and induced an abnormal epithelial cell proliferation and angiogenesis, which provides new insight for the evaluation of the impaired endometrial receptivity caused by ovarian stimulation at the 3D level, and also might provide a potential clinical index for predicting the outcome of IVF in the future.

MATERIALS AND METHODS

Mice

Eight-week-old adult CD1 mice were purchased from Charles River Laboratories China Inc. The mice were maintained with a 12:12-h light–dark cycle, and the health status is specific pathogen-free according to the Animal Care and Use Committee of Institute of Zoology, Chinese Academy of Sciences.

Superovulation Procedure and Conventional Mating

Virgin adult CD1 female mice were randomly divided into two groups; superovulation group of mice (SO) were injected with 7.5 IU PMSG (Pregnant Mare Serum Gonadotropin), following 7.5 IU HCG (Human Chorionic Gonadotrophin) 48 h later, and the control group (Con) were injected with a saline solution. Virgin adult CD1 female mice of the SO and Con groups were separately mated one-to-one with males overnight and the morning (08:00 a.m.) finding of the vaginal plug was designated as day 1 of pregnancy and then pregnant mice were sacrificed on day 4 (09:00 a.m.) of pregnancy.

Steroid Hormone Injection

Ovariectomized mice were respectively injected with sesame oil (0.1 ml/mouse), estradiol-17β (E2) (100 ng/mouse), P4 (2 mg/mouse), and E2 plus P4 at 9:00 a.m. every day, for 3 days, and then were sacrificed, and their uteri were collected 72 h after the first injection.

Measurement of Serum Hormone Levels

Blood samples of superovulation female pregnant mice and control female pregnant mice on day1–day4 were separately collected by eyeball extirpating under diethyl ether anesthesia. Blood samples were centrifuged at 3,000 rpm for 10 min at 4°C, and the serum was collected for estrogen and progesterone concentration detection using the electro-chemiluminescent immunoassay method.

Whole Mount Immunostaining

Whole mount immunostaining and tissue clearing methods were optimized as previously reported (Arora et al., 2016). Briefly, 1) all the female mice were sacrificed by cervical dislocation and the uteri were placed into fixative (DMSO:Methanol, 1:4) at −20°C overnight. 2) The fixed uteri were transferred to a 1:1, Methanol: PBT (PBS +1% Triton) solution at room temperature rocking on a nutator for 20 min 3) The uteri were transferred to 100% PBT at room temperature rocking on a nutator for 20 min 4) The uteri were blocked in PBSMT (PBS+1%Triton+2%powdered milk) at room temperature rocking on a nutator for 2 h 5) The uteri were subjected to immunostaining using primary antibodies at a dilution of (1:100) in PBSMT and incubated for 5 nights at 4°C on nutator. 6) After 5 days of incubation, the uteri were washed 7 times with PBSMT for 35 min on a nutator at room temperature. 7) The uteri were subjected to immunostaining using secondary antibodies at a dilution of (1:100) in PBSMT and incubated for 3 nights at 4°C on a nutator, and all the samples were covered with an aluminum foil to keep them in the dark. 8) After this step, the uteri were washed 7 times with PBSMT for 35 min on a nutator at room temperature.

Tissue Clearing Procedure

1) After immunofluorescence staining, the uteri were washed 7 times with PBSMT for 35 min on a nutator at room temperature. 2) The uteri were then transferred to 1:1, Methanol:PBT (PBS +1% Triton) solution for 5 min on a nutator at room temperature. 3) The uteri were transferred to a 100% methanol solution for 15 min each time on a nutator at room temperature, twice in total. 4) The uteri were cross-cut into 4 mm tissues and transferred to a 3% H_2O_2 solution (H_2O_2 diluted in methanol) and incubated 12 h on the nutator at 4°C. 5) All uterine tissues were then transferred to 100% methanol for 30 min at room temperature while rocking on a nutator. 6) All uterine tissues were put on filter papers to absorb the methanol completely and then immersed in BABB (Benzyl alcohol: Benzyl Benzoate, 1:2) until the tissues were transparent.

Image Data Obtaining and Analysis

Clarified uteri tissues were put upright on glass bottom culture dishes (NEST) and imaged with a Zeiss LSM 780 confocal microscope using 25X lenses. Tile scans were stitched using Zeiss software. The imaging data analysis, mainly performed with the Imaris software (8.4.1, Bitplane), and the Concrete analysis were as follows: The GFP signal and RFP signal were used to generate a surface of the epithelium and blood vessels separately for quantitative analysis. The surface gain size and diameter of the largest sphere were fit into the object, and the threshold value setting was consistent with the image signal. Under the 3D surface module, the uterine endometrium was circled according to uterine autofluorescence, and the

endometrial volume, epithelial volume, and vascular volume were also determined. The separation of the glandular epithelium and luminal epithelium, as well as the splitting of vessels around the epithelium was also under 3D surface module, whereas the diameter of vessels was detected under filament modules. In addition to the aforementioned analysis, the diameter of the uterine myometrium, endometrium ,and diameter of the gland, as well as the angle between the uterine vertical axis (AM–M axis) and the uterine luminal axis were determined by using ImageJ software.

Data Statistics

Quantitative data were subjected to analysis by using the two-tailed unpaired Student's t-test (2 groups), or an ordinary one-way ANOVA (>2 groups) with multiple comparisons test. The results were analyzed with GraphPad Prism 7 and presented as mean ±; statistical significance was set as $p < 0.05$.

DATA AVAILABILITY STATEMENT

The original contributions presented in the study are included in the article/Supplementary Material; further inquiries can be directed to the corresponding author.

ETHICS STATEMENT

The animal study was reviewed and approved by the Animal Care and Use Committee of Institute of Zoology, Chinese Academy of Sciences.

AUTHOR CONTRIBUTIONS

YZ and YQ conceived the project and designed the experiments. YQ and YZ wrote the manuscript with inputs from ED. YQ and SG performed mouse breeding, mouse mating experiments with the help of JQ and LZ. YQ performed 3D imaging with the help of XZ. Data analysis were performed by YQ and JZ under the supervision of YZ.

FUNDING

This work was funded by the National Key Research and Development Program of China (2019YFA0802600 and 2018YFC1004500 to YZ), the Natural Science Foundation of China (82122027 and 32171110 to YZ), and the Fundamental Research Funds for the Central Universities (2021NTST22 to YZ).

REFERENCES

Akinlosotu, B. A., and Wilder, C. D. (1993). Fertility and Blood Progesterone Levels Following LHRH-Induced Superovulation in FSH-Treated Anestrous Goats. *Theriogenology* 40, 895–904. doi:10.1016/0093-691x(93)90357-b

Arora, R., Fries, A., Oelerich, K., Marchuk, K., Sabeur, K., Giudice, L. C., et al. (2016). Insights from Imaging the Implanting Embryo and the Uterine Environment in Three Dimensions. *Development* 143, 4749–4754. doi:10.1242/dev.144386

Chen, Z.-J., Shi, Y., Sun, Y., Zhang, B., Liang, X., Cao, Y., et al. (2016). Fresh versus Frozen Embryos for Infertility in the Polycystic Ovary Syndrome. *N. Engl. J. Med.* 375, 523–533. doi:10.1056/nejmoa1513873

Ertzeid, G., and Storeng, R. (2001). The Impact of Ovarian Stimulation on Implantation and Fetal Development in Mice. *Hum. Reprod.* 16, 221–225. doi:10.1093/humrep/16.2.221

Filant, J., and Spencer, T. E. (2014). Uterine Glands: Biological Roles in Conceptus Implantation, Uterine Receptivity and Decidualization. *Int. J. Dev. Biol.* 58, 107–116. doi:10.1387/ijdb.130344ts

Gargett, C. E., Lederman, F. L., Lau, T. M., Taylor, N. H., and Rogers, P. A. (1999). Lack of Correlation between Vascular Endothelial Growth Factor Production and Endothelial Cell Proliferation in the Human Endometrium. *Hum. Reprod.* 14, 2080–2088. doi:10.1093/humrep/14.8.2080

Haouzi, D., Assou, S., Mahmoud, K., Tondeur, S., Reme, T., Hedon, B., et al. (2009). Gene Expression Profile of Human Endometrial Receptivity: Comparison between Natural and Stimulated Cycles for the Same Patients. *Hum. Reprod.* 24, 1436–1445. doi:10.1093/humrep/dep039

Heryanto, B., and Rogers, P. A. (2002). Regulation of Endometrial Endothelial Cell Proliferation by Oestrogen and Progesterone in the Ovariectomized Mouse. *Reproduction* 123, 107–113. doi:10.1530/rep.0.1230107

Hyder, S. M., Nawaz, Z., Chiappetta, C., and Stancel, G. M. (2000). Identification of Functional Estrogen Response Elements in the Gene Coding for the Potent Angiogenic Factor Vascular Endothelial Growth Factor. *Cancer Res.* 60, 3183–3190.

Karizbodagh, M. P., Rashidi, B., Sahebkar, A., Masoudifar, A., and Mirzaei, H. (2017). Implantation Window and Angiogenesis. *J. Cell Biochem.* 118, 4141–4151. doi:10.1002/jcb.26088

Liang, Y. X., Liu, L., Jin, Z. Y., Liang, X. H., Fu, Y. S., Gu, X. W., et al. (2018). The High Concentration of Progesterone Is Harmful for Endometrial Receptivity and Decidualization. *Sci. Rep.* 8, 712. doi:10.1038/s41598-017-18643-w

Ma, W., Tan, J., Matsumoto, H., Robert, B., Abrahamson, D. R., Das, S. K., et al. (2001). Adult Tissue Angiogenesis: Evidence for Negative Regulation by Estrogen in the Uterus. *Mol. Endocrinol.* 15, 1983–1992. doi:10.1210/mend.15.11.0734

Maclin, V. M., Radwanska, E., Binor, Z., and Dmowski, W. P. (1990). Progesterone: estradiol Ratios at Implantation in Ongoing Pregnancies, Abortions, and Nonconception Cycles Resulting from Ovulation Induction. *Fertil. Steril.* 54, 238–244. doi:10.1016/s0015-0282(16)53696-6

Marquardt, R. M., Kim, T. H., Shin, J. H., and Jeong, J. W. (2019). Progesterone and Estrogen Signaling in the Endometrium: What Goes Wrong in Endometriosis? *Int. J. Mol. Sci.* 20. doi:10.3390/ijms20153822

O'Brien, J. E., Peterson, T. J., Tong, M. H., Lee, E. J., Pfaff, L. E., Hewitt, S. C., et al. (2006). Estrogen-induced Proliferation of Uterine Epithelial Cells Is Independent of Estrogen Receptor Alpha Binding to Classical Estrogen Response Elements. *J. Biol. Chem.* 281, 26683–26692. doi:10.1074/jbc.m601522200

Plaisier, M. (2011). Decidualisation and Angiogenesis. *Best. Pract. Res. Clin. Obstet. Gynaecol.* 25, 259–271. doi:10.1016/j.bpobgyn.2010.10.011

Rashidi, B., Mardani, M., and Karizbodagh, M. P. (2017). Evaluation of Progesterone and Ovulation-Stimulating Drugs on the Glandular Epithelium and Angiogenesis in Mice. *Adv. Biomed. Res.* 6, 116. doi:10.4103/abr.abr_179_16

Senapati, S., Wang, F., Ord, T., Coutifaris, C., Feng, R., and Mainigi, M. (2018). Superovulation Alters the Expression of Endometrial Genes Critical to Tissue Remodeling and Placentation. *J. Assist. Reprod. Genet.* 35, 1799–1808. doi:10.1007/s10815-018-1244-z

Shi, Y., Sun, Y., Hao, C., Zhang, H., Wei, D., Zhang, Y., et al. (2018). Transfer of Fresh versus Frozen Embryos in Ovulatory Women. *N. Engl. J. Med.* 378, 126–136. doi:10.1056/nejmoa1705334

Song, H., Han, K., and Lim, H. (2007). Progesterone Supplementation Extends Uterine Receptivity for Blastocyst Implantation in Mice. *Reproduction* 133, 487–493. doi:10.1530/rep-06-0330

Van der Auwera, I., and D'Hooghe, T. (2001). Superovulation of Female Mice Delays Embryonic and Fetal Development. *Hum. Reprod.* 16, 1237–1243. doi:10.1093/humrep/16.6.1237

Walter, L. M., Rogers, P. A., and Girling, J. E. (2005). The Role of Progesterone in Endometrial Angiogenesis in Pregnant and Ovariectomised Mice. *Reproduction* 129, 765–777. doi:10.1530/rep.1.00625

Weinerman, R., Ord, T., Bartolomei, M. S., Coutifaris, C., and Mainigi, M. (2017). The Superovulated Environment, Independent of Embryo Vitrification, Results in Low Birthweight in a Mouse Model. *Biol. Reprod.* 97, 133–142. doi:10.1093/biolre/iox067

Zhang, S., Kong, S., Wang, B., Cheng, X., Chen, Y., Wu, W., et al. (2014). Uterine Rbpj Is Required for Embryonic-Uterine Orientation and Decidual Remodeling via Notch Pathway-independent and -dependent Mechanisms. *Cell Res.* 24, 925–942. doi:10.1038/cr.2014.82

Zhang, Y., Wang, Q., Wang, H., and Duan, E. (2017). Uterine Fluid in Pregnancy: A Biological and Clinical Outlook. *Trends Mol. Med.* 23, 604–614. doi:10.1016/j.molmed.2017.05.002

Conflict of Interest: The authors declare that the research was conducted in the absence of any commercial or financial relationships that could be construed as a potential conflict of interest.

Publisher's Note: All claims expressed in this article are solely those of the authors and do not necessarily represent those of their affiliated organizations, or those of the publisher, the editors, and the reviewers. Any product that may be evaluated in this article, or claim that may be made by its manufacturer, is not guaranteed or endorsed by the publisher.

frontiers | Frontiers in Cell and Developmental Biology

TYPE Original Research
PUBLISHED 23 August 2022
DOI 10.3389/fcell.2022.897666

OPEN ACCESS

EDITED BY
Rujuan Zuo,
Oslo University Hospital, Norway

REVIEWED BY
Huatao Chen,
Northwest A&F University, China
Yunfang Zhang,
Tongji University, China

*CORRESPONDENCE
He Zhang,
zhanghe0621@163.com

†These authors have contributed equally to this work

SPECIALTY SECTION
This article was submitted to Cellular Biochemistry,
a section of the journal
Frontiers in Cell and Developmental Biology

RECEIVED 16 March 2022
ACCEPTED 25 July 2022
PUBLISHED 23 August 2022

CITATION
Huang B, Jin L, Zhang L, Cui X, Zhang Z, Lu Y, Yu L, Ma T and Zhang H (2022), Aquaporin-8 transports hydrogen peroxide to regulate granulosa cell autophagy.
Front. Cell Dev. Biol. 10:897666.
doi: 10.3389/fcell.2022.897666

Aquaporin-8 transports hydrogen peroxide to regulate granulosa cell autophagy

Binbin Huang[1,2†], Lingling Jin[1†], Luodan Zhang[3†], Xiaolin Cui[1], Zhen Zhang[1], Yongqi Lu[2], Lujia Yu[2], Tonghui Ma[1] and He Zhang[1*]

[1]Department of Pathophysiology, College of Basic Medical Sciences, Dalian Medical University, Dalian, China, [2]Department of Maternal, Child and Adolescent Health, School of Public Health, Anhui Medical University, MOE Key Laboratory of Population Health Across Life Cycle, NHC Key Laboratory of Study on Abnormal Gametes and Reproductive Tract, Anhui Provincial Key Laboratory of Population Health and Aristogenics, Hefei, Anhui, China, [3]Department of Nephrology, Anhui Provincial Children's Hospital, Hefei, Anhui, China

Aquaporin-8 (AQP8), a member of the aquaporin family, is strongly expressed in follicular granulosa cells, which could affect the hormone secretion level in females. AQP8, as a membrane protein, could mediate H_2O_2 into cells, thereby triggering various biological events. The deficiency of *Aqp8* increases female fertility, resulting from the decrease in follicular atresia. The low cell death rate is related to the apoptosis of granulosa cells. However, the mechanism by which AQP8 regulates the autophagy of granulosa cells remains unclear. Thus, this study aimed to explore the effect of AQP8 on autophagy in follicular atresia. We found that the expression of the autophagy marker light-chain protein 3 was significantly downregulated in the granulosa cells of *Aqp8*-knockout ($Aqp8^{-/-}$) mice, compared with wild-type ($Aqp8^{+/+}$) mice. Immunofluorescence staining and transmission electron microscopic examination indicated that the number of autophagosomes in the granulosa cells of $Aqp8^{-/-}$ mice decreased. Using a follicular granulosa cell autophagy model, namely a follicular atresia model, we verified that the concentration of H_2O_2 significantly increased during the autophagy of granulosa cells, consistent with the *Aqp8* mRNA level. Intracellular H_2O_2 accumulation was modulated by endogenous AQP8 expression level, indicating that AQP8-mediated H_2O_2 was involved in the autophagy of granulosa cells. AQP8 deficiency impaired the elevation of H_2O_2 concentration through phosphorylated tyrosine activation. In addition, we carried out the analysis of transcriptome sequencing datasets in the ovary and found there were obvious differences in principal components, differentially expressed genes (DEGs) and KEGG pathways, which might be involved in AQP8-regulated follicular atresia. Taken together, these findings indicated that AQP8-mediated H_2O_2 transport could mediate the autophagy of granulosa cells. AQP8 might be a potential target for diseases related to ovarian insufficiency.

Abbreviations: AQP, aquaporin; ROS, reactive oxygen species; H_2O_2, hydrogen peroxide; LC3, light-chain protein 3; PMSG, pregnant mare serum gonadotropin; PCR, polymerase chain reaction; Akt, protein kinase B; PCD, programmed cell death.

KEYWORDS
AQP8, hydrogen peroxide, granulosa cell, autophagy, follicular atresia

Highlight

AQP8-mediated H_2O_2 was involved in the autophagy of granulosa cells.
AQP8 deficiency could impair the elevation of H_2O_2 concentration through P-Tyr activation.
AQP8-mediated extracellular H_2O_2 may promote follicular atresia.

Introduction

Aquaporin-8 (AQP8), as a transport facilitator, can control cellular oxidative stress by regulating H_2O_2 levels (Marchissio et al., 2012; Bertolotti et al., 2013). H_2O_2 is a reactive oxygen species (ROS) that serves as a secondary messenger in various signal transduction pathways. ROS and antioxidant deficiencies are involved in ovarian aging (Qian et al., 2016). Although high ROS levels are cytotoxic, low ROS levels are essential for cell physiology and survival. H_2O_2 transiently modulates tyrosine phosphatases and kinases and inhibits phosphatases to activate certain kinases (Finkel, 2011). H_2O_2 is generated *via* several approaches, such as oxidative phosphorylation in the mitochondria, oxidative protein folding in the endoplasmic reticulum, and NADPH oxidases in the plasma membrane (Kakihana et al., 2012). Some members of the aquaporin (AQP) family can transport H_2O_2 (Bienert et al., 2007; Miller et al., 2010). For instance, H_2O_2 can enter lymphoid cells through AQP8 and activate related growth factor signaling (Bertolotti et al., 2016). However, the mechanism by which AQP8 regulates the autophagy of ovary granulosa cells through H_2O_2 transport remains unclear.

Members of the AQP family can selectively and efficiently transport water molecules, and some of them transport small molecules, such as glycerol, urea, and H_2O_2, simultaneously. They are widely distributed in various animal tissues and serve important physiological functions. At present, few studies have concentrated on the roles of AQP in the reproductive system and various pathological processes (Sha et al., 2011; Zhang et al., 2012). Deletion of AQP3 affects sperm motility (Chen et al., 2011). Estrogen regulate the expression of AQP5 and AQP8 to abnormal embryo implantation (Zhang et al., 2015). A clinical study reported that the decreased uterine acceptance in patients with ovarian hyperstimulation is associated with decreased AQP2 expression in the endometrium (Zhang et al., 2016). And in yeast model, AQP8 can promote H_2O_2 transport (Bienert et al., 2007). Subsequently, studies have confirmed that AQP3 and AQP8 feature highly efficient H_2O_2 transport functions by systematically analyzing the H_2O_2 transport of various rat AQP family members overexpressed in HEK-293 cells (Miller et al., 2010). A recent study has shown that the migration of chemotactic T cells in skin contact hypersensitivity requires AQP3-mediated H_2O_2 transport (Hara-Chikuma et al., 2012). TNF stimulates the hyper H_2O_2 production of Nox2 on keratinized cell membranes, whereas the AQP3 synergistic transport of H_2O_2 regulating protein phosphatase 2A activates NF-KB signals to induce psoriasis (Hara-Chikuma et al., 2015). These results prove that some AQPs mediate the transport of H_2O_2 and regulate its harmful or beneficial functions.

We previously reported that *Aqp8*$^{-/-}$ mice have a more litter size (Su et al., 2010), with an increase in efficient follicles (Su et al., 2013). However, the mechanisms underlying these phenomena remain unclear. Previous studies have found that AQP8 is abundantly expressed in mouse (Su et al., 2010), rat (McConnell et al., 2002) and human (Li et al., 2013) ovaries. Thus, in this study, using *Aqp8*$^{-/-}$ mice and the follicular atresia model, we measured the intracellular H_2O_2 concentration and *Aqp8* expression level in granulosa cells and investigated the role of AQP8-transported H_2O_2 in the autophagy of granulosa cells.

Material and methods

Animal experiment

Aqp8$^{-/-}$ mice (C57BL/6 genetic background) were generated by targeted gene disruption (Yang et al., 2005). For this experiment, 5–6-week-old female mice were used. Mice were allowed free access to water and food in 12 h light and 12 h dark conditions. All animal experiments were reviewed and approved by the Committee on the Ethics of Animal Research of Dalian Medical University.

Follicular atresia mouse model

Aqp8$^{+/+}$ and *Aqp8*$^{-/-}$ were intraperitoneally injected with 0.1 ml pregnant mare serum gonadotropin (PMSG) (1000 IU in 10 ml 0.9% NaCl, Ningbo a second hormone factory) or vehicle control (0.9% NaCl, 0.1 ml) at 16:00 into the mice. Mice were killed by cervical dislocation 0, 1, 2, 3, 4, and 5 days after PMSG treatment, and the ovary samples were excised. The ovaries were used for the collection of granulosa cells.

Mouse primary granulosa cell collection and culture

Ovaries were excised from mice and placed in DMEM/F12 (GIBCO-BRL, 11039021) that was supplemented with 10% fetal

bovine serum (GIBCO-BRL), 10 mg/ml of streptomycin sulfate (Sigma), and 75 mg/ml of penicillin G (Sigma). Granulosa cells were harvested by follicle puncture using a 25-gauge needle. After follicle puncture, granulosa cells were suspended in the appropriate solution for immunoblotting or H_2O_2 concentration.

For *in vitro* culture of granulosa cells under serum-free conditions, ovaries were collected, and granulosa cells were collected by follicle puncture, as described previously. The cells were seeded in 24-well plates and were allowed to attach overnight. The next morning, the medium and unattached cells were removed and replaced with serum-free media. After 24 h, the granulosa cells were fixed for immunofluorescence.

Live cell station imaging of autophagic vacuoles

The adenovirus expressing GFP-LC3B (Ad-GFP-LC3B, C3006, Beyotime) was transfected into GCs grown on coverslips. After 24 h, cells were rinsed using PBS and then exposed to 2 h of H_2O_2 incubation. The distribution and fluorescence emitted by GFP-LC3B puncta were then observed under a live cell station (GE). Experiments were repeated three times.

Western blot analysis

Protein was isolated by the previous description (Huang et al., 2020a). The freshly isolated granulosa cells were lysed with ice-cold radioimmunoprecipitation assay (RIPA) buffer that was supplemented with a protease inhibitor PMSF (Beyotime). To facilitate the complete solubilization of the cellular proteins, the cell lysates were incubated on ice for 30 min and then centrifuged (13000 g at 4°C for 30 min). The protein concentration was tested by using a BCA Protein Assay Kit. The whole-cell lysates (20 mg/lane) were separated by sodium dodecyl sulfate (SDS)–polyacrylamide gel electrophoresis and transferred to a polyvinylidene difluoride (PVFD) membrane (Millipore). After the nonspecific binding sites were blocked with 5% skim milk, the membrane was treated with the anti-LC3 rabbit polyclonal antibody (1:2000, Novus Biologicals), cleaved caspase-3 rabbit polyclonal antibody (diluted 1:1000, Cell Signaling Technology), and β-actin (1:1000, Beyotime) overnight at 4°C. The primary antibodies for Akt, pAkt-Ser473, Bax, Bcl-2, and P-Tyr were obtained from Cell Signaling Technology (Beverly, MA). The primary antibodies for Atg3 were obtained from Proteintech (Wuhan, China), while Beclin-1 was obtained from Santa Cruz Biotechnology (Santa Cruz, CA, United States). The immunoreactive bands were demonstrated by incubation with horseradish peroxidase (HRP)-conjugated goat anti-rabbit IgG (1:10000, Zhongshan Biotechnology) at room temperature for 1 h. The peroxidase activity was visualized with the enhanced chemiluminescence detection system (WBKLS500, Millipore). Integrated optical intensities of the immunoreactive protein bands were detected by using the DNR bioimaging system MicroChemi 4.2 and the quantified analysis by ImageJ software, normalized to *β-actin* values.

Transmission electron microscopy test

To identify autophagic vacuoles at the ultrastructural level, the ovary was fixed with 2.5% glutaraldehyde in 0.1 M cacodylate buffer (pH 7.4) for more than 24 h at 4°C, rinsed in cacodylate buffer, postfixed in 1% OsO_4 in cacodylate buffer, dehydrated, and embedded in Epon. Ultrathin sections were briefly contrasted with uranyl acetate and photographed with a transmission electron microscope (Hitachi 7100 Japan).

Measurement of the intracellular hydrogen peroxide level

Intracellular hydrogen peroxide was measured by using the Hydrogen Peroxide Assay Kit (Beyotime, Nanjing, China). Briefly, 100–200 μl of hydrogen peroxide was added to detect the ratio of lysate to lysate. One million granulosa cells were treated with 100–200 μl of the hydrogen peroxide lysate, followed by sufficient homogenization to break and lyse the cells. It was then centrifuged at 12000 g at 4°C for 3–5 min, and the supernatant was collected. Then, 50 μl of the sample or standard was treated with 100 μl of the hydrogen peroxide detection reagent at room temperature (15–30°C). And then, it was immediately measured at A560 nm.

To evaluate intracellular H_2O_2 levels, 1×10^6 cells/ml were washed twice in HBSS and incubated with 20 μM 2′,7′-dichlorofluorescein diacetate (DCFH-DA) (sigma). Granulosa cells were incubated for 30 min at 37°C. DCFH-DA was a small nonpolar and nonfluorescent molecule that diffuses into the cells, where it is enzymatically deacetylated by intracellular esterases to a polar nonfluorescent compound, which is oxidized to the highly green fluorescent 2,7-dichlorofluorescein (DCF). DCF fluorescence was measured using a multiwell plate reader (Synergy Neo HTS multimode microplate reader, BioTek) at excitation and emission wavelengths of 485 and 535 nm, respectively.

RNA extraction and real-time PCR assay

Total RNA was isolated by the previous description (Huang et al., 2020b) using the TRIzol reagent (10296010,

Invitrogen) and quantified using a NanoVueTM Plus Spectrophotometer (GE Healthcare, Buckinghamshire, United Kingdom). The A260/A280 ratio of the optical density was measured using the NanoVueTM Plus Spectrophotometer. The ratio was between 1.9 and 2.1 for all samples, indicating a good quality of RNA purity and yield. cDNA was synthesized from 2 μg of total RNA using the RT reagent Kit with gDNA Eraser (TaKaRa, RR047A). The qPCR solution contained 1 μl of cDNA, 1 μl of specific primers, and 10 μl of a 2X PCR SuperMix (AS111, TransGen Biotech) in a final volume of 20 μl. All primers were produced by lifespan (Milan, Germany) and listed as follows in the 5′-3′ direction: *Aqp8-F: ACACCAATGTGTAGTATGGACCT*; *Aqp8-R: TGACCGATAGACATCCGATGAAG*; *β-actin-F: TGGAATCCTGTGGCATCCATGAAAC*; *β-actin-R: TAAAACGCAGCTCAGTAACAGTCCG*.

The reaction conditions were as follows: polymerase activation and DNA denaturation (one cycle at 95°C for 30 s); denaturation, annealing, and extension (40 cycles at 95°C for 10 s and 60°C for 30 s); melting curve (65°C, with the temperature, gradually increased 0.5°C up to 95°C). mRNA expression was normalized to the level of *β-actin* mRNA. Changes in mRNA expression were calculated according to the $2^{-\triangle\triangle Ct}$ method. The amplification of β-actin mRNA was utilized to normalize the data.

Analysis of transcriptome sequencing datasets

Raw transcriptome sequencing data were stored in FASTQ document format by Bcl2fastq (v2.17.1.14). Sequencing data quality was assessed by FastQC (v0.10.1). The raw data were preprocessed, the low-quality data were filtered, and the contamination and joint sequences were removed by cutadapt (version 1.9.1). Then, gene expressions were calculated by HTSeq (V 0.6.1) with FPKM (Fragments per Kilobase per Million reads) (Mortazavi et al., 2008). Differentially expressed genes (DEGs) in the ovary (group: control and PMSG with treatment for 2 days or 4 days) were analyzed by using the R package edgeR (v3.4.6) using |fold change|>2 and a p-value < 0.05.

Statistical analysis

Statistical analysis was performed by analysis of variance (ANOVA). Significant differences between treatment groups were determined by Duncan's multiple range tests. $p < 0.05$ was considered statistically significant. For statistical comparisons between two groups, an independent-sample t-test was used.

Results

Autophagy and apoptosis decrease in *Aqp8*$^{-/-}$ mouse follicular granulosa cells

Microtubule-associated light-chain protein 3 (LC3) is an autophagy marker used to evaluate granulosa cell autophagy. Granulosa cells freshly isolated from *Aqp8*$^{+/+}$ and *Aqp8*$^{-/-}$ mice were used. The results of Western blot analysis using specific antibodies against the autophagy marker LC3 and apoptosis marker cleaved caspase-3 were shown in Figure 1. Densitometric analysis normalized by the β-actin content indicated that the protein contents of LC3 and cleaved caspase-3 significantly decreased compared with the control, suggesting that AQP8 was involved in the development of follicular granulosa cells *via* autophagy and apoptosis.

Localization of autophagosomes in granulosa cells

Transmission electron micrographs showed that autophagosomes existed in the follicular granulosa cells of *Aqp8*$^{+/+}$ and *Aqp8*$^{-/-}$ mice. Fewer autophagosomes localized in the granulosa cells of the *Aqp8*$^{-/-}$ mice than in those of the *Aqp8*$^{+/+}$ mice (Figure 2).

Aquaporin-8 channel mediates H_2O_2 uptake and AQP8-dependent H_2O_2 permeability in granulosa cells

Considering that AQP8 is expressed on granulosa cells (Su et al., 2010), we used *Aqp8*$^{-/-}$ mice to determine whether or not AQP8 is required for the efficient entry of exogenous H_2O_2. To investigate H_2O_2 transport across the plasma membrane, we incubated DFCH-DA into granulosa cells. The addition of PBS or 50 μM H_2O_2 clearly activated DFCH-DA to DCF, as determined by 488/510 nm shifts on a microplate reader (Figure 3A). The aforementioned experiments provided additional evidence that H_2O_2 cannot freely permeate through the plasma membrane and identified AQP8 as an efficient transporter. Clearly, H_2O_2 import was severely impaired with AQP8 silencing.

Meanwhile, we investigated whether or not AQP8 can transport extracellular H_2O_2 into granulosa cells. Intracellular H_2O_2 was measured in primary granulosa cell cultures from *Aqp8*$^{+/+}$ and *Aqp8*$^{-/-}$ mice after the extracellular addition of 10–100 μM H_2O_2 using the fluorescent dye CM-H2DCFDA, which reacted with ROS, including H_2O_2. Results showed that the cellular H_2O_2 level was significantly higher in the granulosa cells of the *Aqp8*$^{+/+}$ mice than that in those of the Aqp8$^{-/-}$ mice (Figure 3B), indicating the involvement of AQP8 in H_2O_2

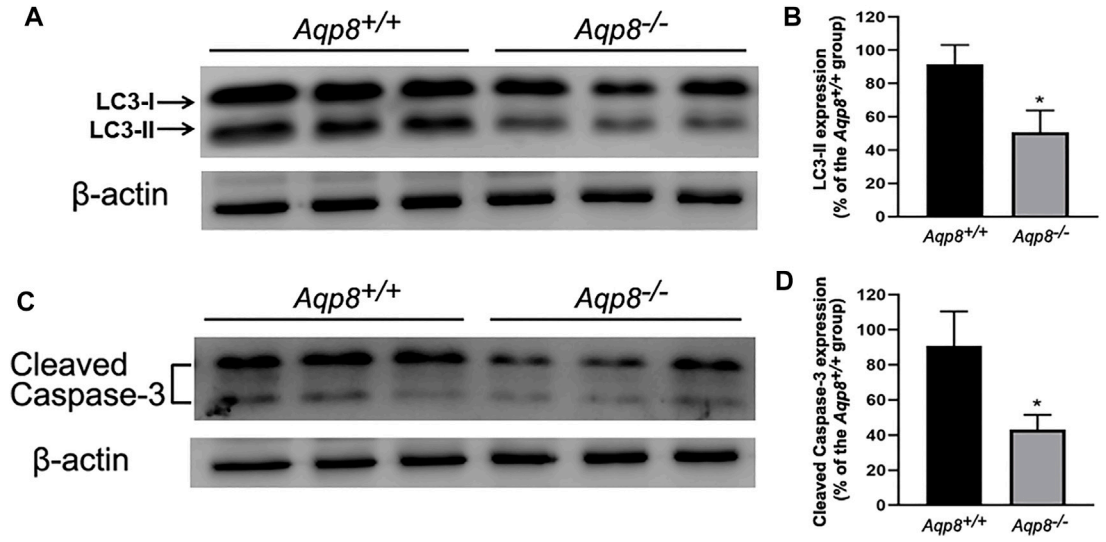

FIGURE 1
Autophagy and apoptosis decrease in *Aqp8*$^{-/-}$ mouse follicular granulosa cells. The expressions of cleaved caspase-3 and LC3-II proteins in granulosa cells from *Aqp8*$^{+/+}$ and *Aqp8*$^{-/-}$ mice. Densitometric quantification and representative immunoblots of LC3 proteins **(A,B)** or cleaved caspase-3 **(C,D)**. Experiments were repeated three times, and data were expressed as mean ± SD. **p* <0.05 were considered statistically significant.

transport in granulosa cells. The ability of AQP8 to transport H_2O_2 across the plasma membrane was tested. Figure 3B showed that the basal intracellular H_2O_2 level was significantly affected by AQP8, revealing that the channel activity of this AQP isoform modulated the entry of physiologically produced H_2O_2 into the cells.

Aquaporin-8 participates in granulosa cell autophagy during follicular development and atresia

Autophagy, as an important process of programmed cell death, regulates follicular homeostasis in rats (Choi et al., 2010). Follicular development and atresia *in vivo* model was established in immature mice. Granulosa cell autophagy was determined by measuring the expression levels of LC3-II/LC3-I. As shown in Figure 4A, LC3-II expression in the granulosa cells was significantly downregulated 1 and 2 days after PMSG injection compared with the granulosa cells of immature mice without the treatment of exogenous gonadotropin (day 0). LC3-II expression was upregulated on day 3 and maintained until day 5. Furthermore, the expression of *Aqp8* was measured. After PMSG injection, the expression of *Aqp8* was significantly downregulated on days 1 and 2 and then increased on days 3, 4, and 5 (Figure 4B). Ovarian granulosa cells were isolated from each stage of the atresia model, and the concentration of H_2O_2 in granulosa cells was measured. The concentration of H_2O_2 in granulosa cells decreased during follicular development but increased during atresia (Figure 4C), suggesting that AQP8 mediated H_2O_2 transport and autophagy in granulosa cells to regulate follicular development and atresia.

Aquaporin-8 inhibits pAkt and phosphorylated tyrosine signaling

The mechanism by which AQP8 regulates the autophagy of granulosa cells was further explored. Results showed that AQP8 can facilitate the absorption of H_2O_2 into granulosa cells and mediate downstream intracellular signaling. As shown in Figure 5A, the phosphorylation level of Akt in the granular cells of the *Aqp8*$^{-/-}$ mice was increased. The expression levels of proteins related to apoptosis (Bax and caspase-3) and autophagy (Beclin-1 and Atg-3) decreased in the granulosa cells of the *Aqp8*$^{-/-}$ mice. Meanwhile, phosphorylated tyrosine signaling was activated in the granulosa cells of the *Aqp8*$^{-/-}$ mice (Figure 5B). And the absorption of H_2O_2 in the granulosa cells of the *Aqp8*$^{+/+}$ mice inhibited the PI3K signaling pathway and promoted granulosa cell death and autophagy.

AQP8 mediated H_2O_2 uptake affects granulosa intracellular autophagy

We next investigated whether or not AQP8 influences autophagy by oxidative stress. An *in vitro* culture

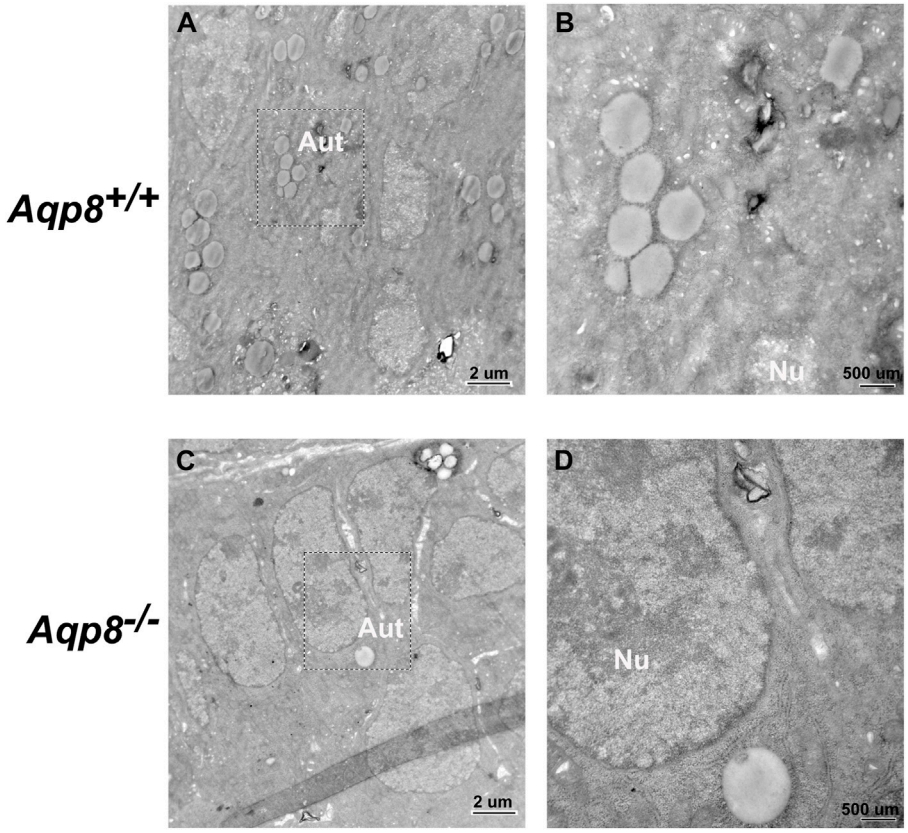

FIGURE 2
Transmission electron microscopic images of granulosa cells in *Aqp8*$^{+/+}$ and *Aqp8*$^{-/-}$ mice. Representative images from transmission electron microscopy of granulosa cells from *Aqp8*$^{+/+}$ **(A,B)** and *Aqp8*$^{-/-}$ **(C,D)** mice. High-magnification images indicated nucleus (Nu) and autophagosomes (Aut). The scale was indicated on the lower right corner of each image.

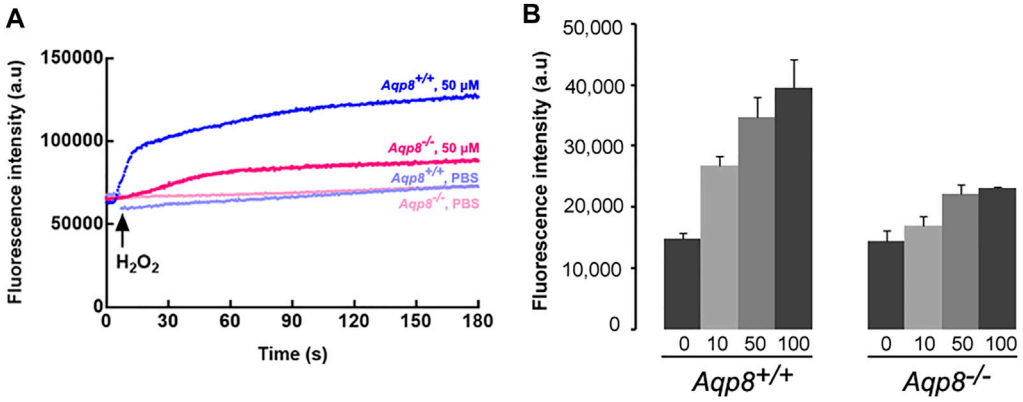

FIGURE 3
H_2O_2 uptake into primarily cultured granulosa cells. **(A)** Representative fluorescence intensity of CM-H2DCFDA. **(B)** Granulosa cells were incubated with H_2O_2 (0–100 mM), and cellular H_2O_2 was detected by CM-H2DCFDA fluorescence using a plate reader. Increased fluorescence intensity could be detected at 15 s after treatment with H_2O_2. Data were shown as mean ± SD.

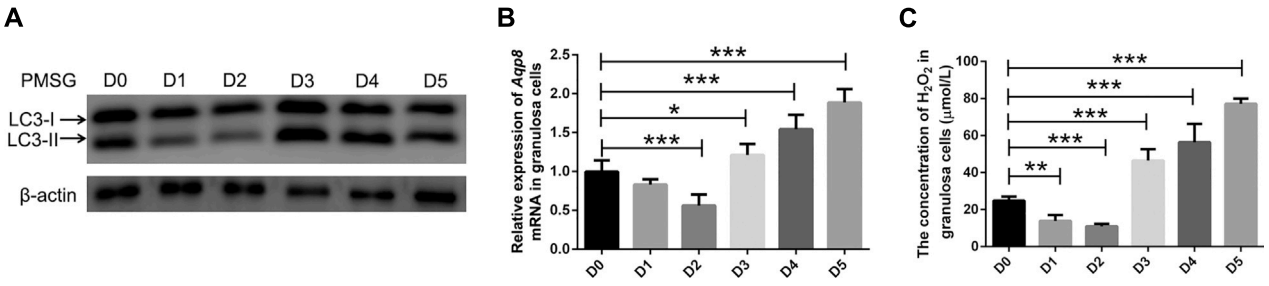

FIGURE 4
AQP8 involvement in granulosa cell autophagy during follicular development and atresia. **(A)** Expression of LC3-II proteins in granulosa cells from immature mice at different times (0–5 days) after pregnant mare serum gonadotropin injection (10 IU, intraperitoneally). **(B)** qRT-PCR was performed to measure the mRNA levels of *Aqp8* in GCs. The expression of *Aqp8* mRNA in granulosa cells from immature mice at different times (0–5 days) after pregnant mare serum gonadotropin injection. **(C)** Concentration of H_2O_2 in granulosa cells from immature $Aqp8^{+/+}$ mice at different times (0–5 days) after pregnant mare serum gonadotropin injection (10 IU, intraperitoneally). Values are presented as the means ± SD. $*p < 0.05$, $**p < 0.01$, and $***p < 0.001$.

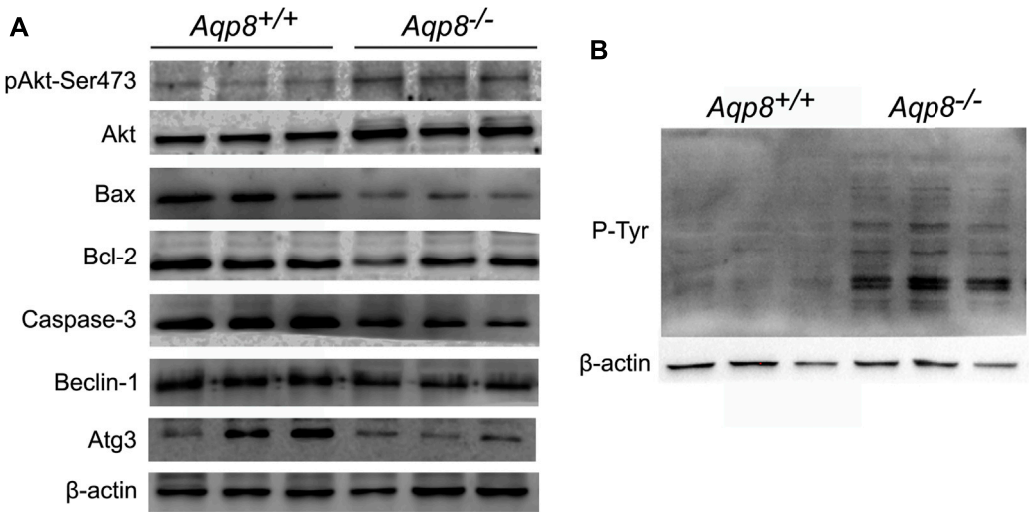

FIGURE 5
AQP8 inhibits pAkt and phosphorylated tyrosine (P-Tyr) signaling. **(A)** Western blot detection of the relevant signaling pathway. **(B)** Western blot of P-Tyr, which could be affected by H_2O_2.

experiment revealed that AQP8 was involved in granulosa cell autophagy through the transport of H_2O_2. Primary cultured GCs were transfected with the GFP-LC3B plasmid, incubated with or without 200 μM H_2O_2 for 2 h, and then rinsed with PBS. Immunofluorescence images of granulosa cells were obtained in a live cell station. As shown in Figure 6, AQP8 obviously induced autophagosome formation in the cells with H_2O_2 exposure, displaying that AQP8 facilitated intracellular autophagy of granulosa cells through H_2O_2 absorption.

Integrated analysis of the ovary transcriptome in mice with PMSG treatment

Transcriptome analysis of the ovary was performed in mice with PMSG treatment for 2 days or 4 days. Principal components, differentially expressed genes (DEGs), and KEGG pathways were analyzed. The principal components of each group between parents and offspring showed obvious differences (Figure 7A). To further study the mechanisms

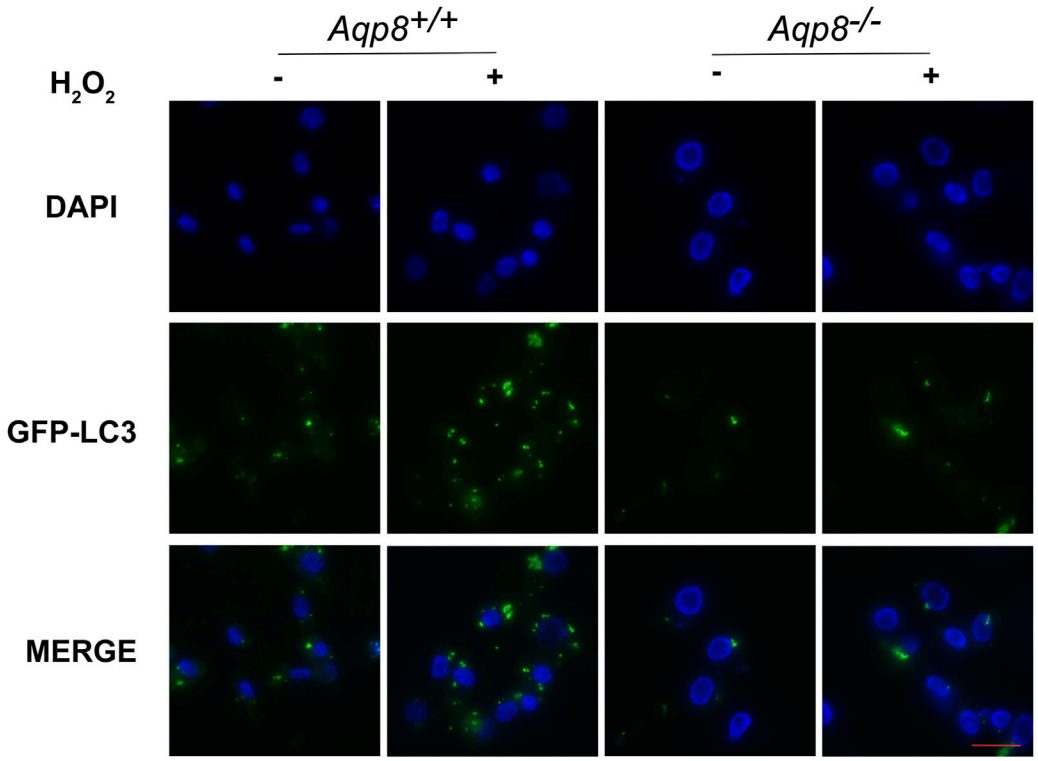

FIGURE 6
AQP8-mediated H_2O_2 uptake influences granulosa intracellular autophagy. GCs transfected with the GFP-LC3B plasmid for 24 h were incubated with 200 μM H_2O_2 for 1 h and rinsed in PBS. A live cell station was employed to observe the GFP fluorescent puncta in GCs. The nuclei were counterstained with DAPI (blue). Scale bar = 10 μm.

underlying follicular development and atresia, we analyzed the DEGs and KEGG pathways between different groups. In total, 1,421 DEGs with |fold change|> 2 and *p*-value < 0.05 were annotated in the ovary (groups: control and injected with PMSG for 2 days), of which 690 genes were upregulated and 731 genes were downregulated (Figure 7B). In total, 1,237 DEGs with |fold change| > 2 and *p* value < 0.05 were annotated in the ovary (groups: control and injected with PMSG for 4 days), of which 622 genes were upregulated and 615 genes were downregulated (Figure 7C). In addition, DEG analyses of the three cohorts (control, injected with PMSG for 2 days or 4 days) overlapped, with 52 common DEGs obtained (Figure 7D). KEGG pathway enrichment analysis was also performed to study the pathway with significant DEG enrichment. Functional enrichment results revealed that 30 KEGG pathways of DEGs in the ovaries of the mice injected with PMSG for 2 days or 4 days were statistically significantly enriched, respectively (Figures 7E,G). The KEGG pathways in the control mice and mice injected with PMSG for 2 days included five categories: organismal systems, metabolism, human diseases, environmental information processing, and cellular processes in the ovary (Figure 7F). The KEGG pathways in the control mice and mice injected with PMSG for 4 days included four categories: organismal systems, metabolism, human diseases, and environmental information processing in the ovary (Figure 7H). Organismal systems and metabolism are the most enriched pathways, suggesting that they might play important roles in follicular development and atresia.

Discussion

In the present study, we demonstrated that AQP8 induced autophagy by transporting H_2O_2 into granulosa cells during follicular atresia. During follicular growth and development, only less than 1% of oocytes sealed and protected by granular cells can form dominant follicles and be discharged from the body, whereas the remaining 99% of the follicles are degenerated, leading to atresia. Many studies have found that mammalian follicular development and atresia are primarily controlled by granulosa programmed cell death. In addition, at least five types of death ligands involved in programmed cell death induce particles, including TNF-alpha, Fas, TRAIL, APO-3, and PEG-5 ligands and their receptors (Manabe et al., 2004; Hurst et al.,

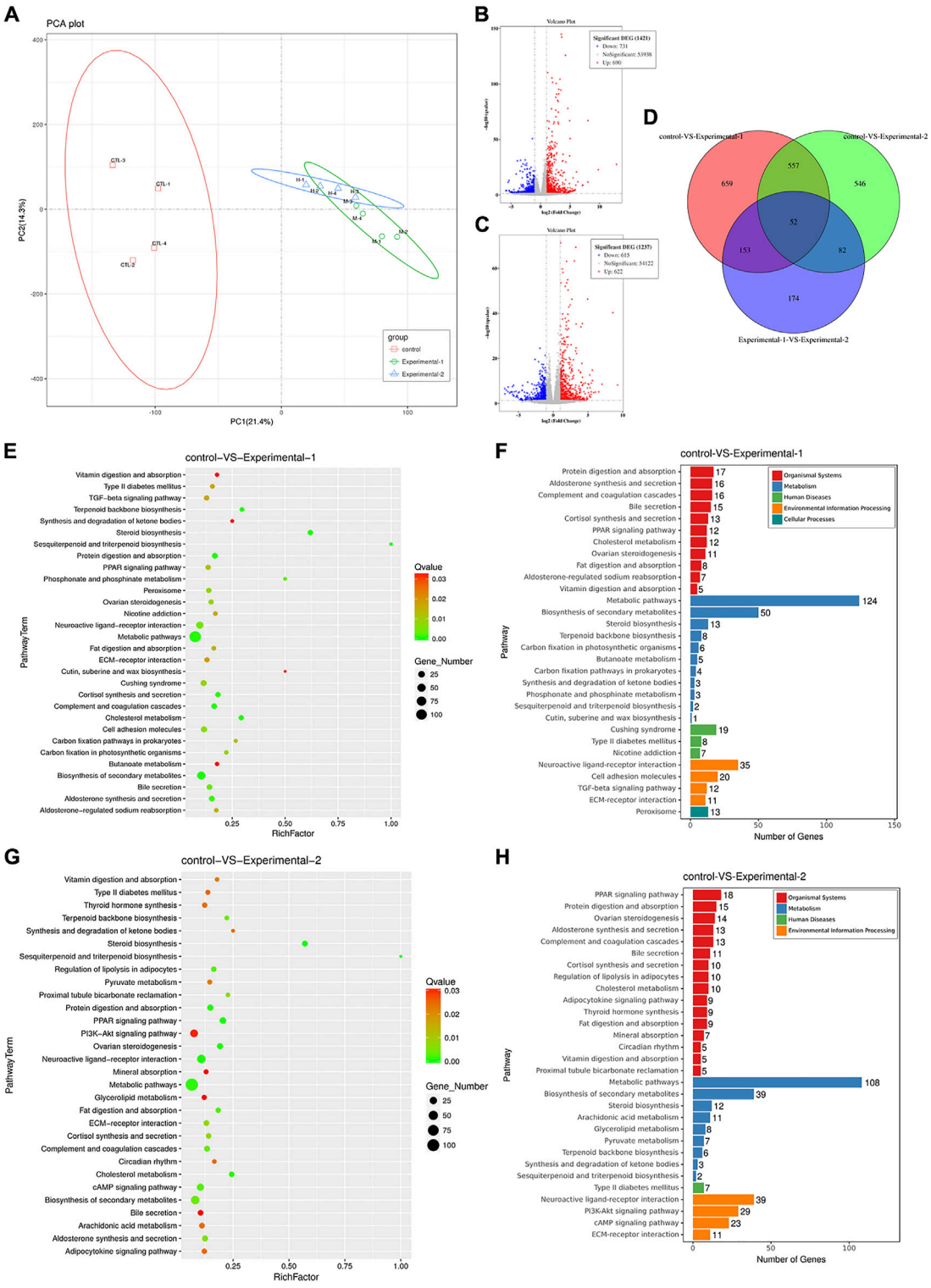

FIGURE 7
Analysis of the ovary transcriptome level after PMSG treatment. **(A)** Principal component analysis (PCA) was performed on the ovary (control, PMSG treatment for 2 days or 4 days), and the R function prcomp was used to analyze the samples at the transcriptome level. The volcano plot shows differentially expressed genes of three groups in the ovary with PMSG treatment for 2 days **(B)** and 4 days **(C)**. The red circle represents genes that are upregulated in gene expression, the blue circle represents genes that are downregulated in gene expression, and the gray circle represents insignificant genes. **(D)** Venn plot shows the correlation of differential genes expressed among three groups. The bubble plot represented the

(*Continued*)

FIGURE 7
enriched KEGG pathways of differentially expressed genes in the ovary with PMSG treatment for 2 days **(E,F)** and 4 days **(G,H)**. The red color indicated upregulated pathways, and the blue color indicated downregulated pathways. The bubble size represents the number of genes associated with pathways in each group, and the connected color indicates the *p*-value across the connected groups. Control, treatment with saline; experiment 1, treatment with PMSG for 2 days; experiment 2, treatment with PMSG for 4 days.

2006; Lin and Rui, 2010). However, the follicle selection process control of the molecular mechanism of granular cell death remains unclear.

During follicular development, granulosa cell apoptosis is not the only mechanism to control follicular atresia. Autophagy and cell necrosis have been observed in the follicles of other animals (Kovacs et al., 1992; D'Herde et al., 1996; Shao et al., 2022). In recent years, some studies have found that granulosa autophagy is also involved in follicular atresia (Choi et al., 2010; Choi et al., 2011; Matsuda et al., 2012; Zhou et al., 2019).Gonadotropin could reduce the granulosa cell autophagy by activating the PI3K/Akt signaling pathway with inhibition of mTOR (Choi et al., 2014), The expression of Beclin-1 and LC3 would increase in the ovary through the oxidative stress of mitochondrial damage after treatment with harmful chemical substances in cigarette (Gannon et al., 2013; Furlong et al., 2015). Conversely, inhibiting the expressions of Akt and mTOR proteins activate the AMPK pathway, which promotes granulosa autophagy and decreases the number of original follicles affecting reproduction (Shen et al., 2017; Shen et al., 2018). Exogenous addition of oxidizing LDL can trigger autophagy in human granulosa cells (Duerrschmidt et al., 2006). Furthermore, the circadian clock system is also involved in the granulosa cell autophagy through the regulation of nuclear receptor subfamily 1 group D member 1 (NR1D1) (Zhang et al., 2022). These findings indicate that autophagy is directly involved in the regulation of granulosa death during follicular development, whereas oxidative stress may play an important role in the regulation of granulosa autophagy.

The ROS content in mammalian cells is strictly controlled. ROS are the central elements of cell proliferation, apoptosis and other signal pathway. The H_2O_2 concentration decreases in the follicular fluids of animals, such as bovine (Gupta et al., 2011) and swine (Basini et al., 2008), with the follicular development, whereas the upper limit of the ROS concentration in human follicular fluids is strictly controlled (Jana et al., 2010). The balance between ROS and antioxidants in follicles plays an important role in follicular development. The physiological levels of ROS and antioxidants jointly regulate the follicular formation, and the continuous action or increase in the ROS concentration interferes with the intracellular redox reaction and leads to oxidative stress (Agarwal et al., 2008). Recent findings have shown that ROS exerts cytotoxic effects because of oxidative damage, and H_2O_2 activates apoptotic proteases through oxidative pressure or destroys cytochromes released by intracellular mitochondria to induce the apoptosis of Jurkat T lymphocytes (Hampton and Orrenius, 1997), which has the same effect on bovine follicular granulosa cells (Hennet et al., 2013). However, increasing evidence suggests that ROS, especially H_2O_2, can activate or inactivate multiple signaling pathways as signaling molecules by activating or inactivating phosphorylated proteins in cells (Rhee, 2006; Forman et al., 2010).

H_2O_2 is a relatively stable class of reactive oxygen molecules *in vivo*. H_2O_2 produced by NADPH oxidase on the cell surface can act as a secondary messenger responding to extracellular stimuli, such as growth factors, hormones, and cytokines (Bae et al., 1997; Rhee, 2006; Schroder and Eaton, 2008). As a signaling molecule, H_2O_2 activates ERK1/2 and the PI3K-Akt signaling pathway corresponding to the inhibition of PTP1B and PTEN pathways, whereas ERK and PTEN signaling pathways are crucial for ovulation (Blanc et al., 2003; Tonks, 2005). Therefore, the H_2O_2 concentration should be controlled and maintained to ensure its role in signal transduction. The concentration of H_2O_2 in non-atretic follicular fluids is higher than that in atretic follicles, suggesting that ROS in follicular fluids could regulate follicular atresia (Hennet et al., 2013). Exogenous H_2O_2 can activate the JNK signaling pathway and induce autophagy in mesenchymal stem cells (Liu et al., 2015). Intracellular H_2O_2 levels rapidly reach a certain threshold to play their molecular signaling function (Rhee, 2006). Extracellular H_2O_2 can enter cells through free diffusion, but free diffusion can not instantly increase the intracellular concentration of H_2O_2. Thus, the regulation of H_2O_2 transport possibly depends on selective membrane. The expression of Beclin-1 and LC3 would increase in the ovary through the oxidative stress of mitochondrial damage after treatment with harmful chemical substances in cigarette channel proteins (Rhee, 2006; Kruger et al., 2021).

The autophagy of granulosa cells increased during follicular atresia in the $Aqp8^{+/+}$ mice, whereas the autophagy and apoptosis of ovarian granulosa cells significantly decreased in the $Aqp8^{-/-}$ mice. Primary granulosa cells of the $Aqp8^{+/+}$ and $Aqp8^{-/-}$ mice were cultured *in vitro*, and different concentrations of H_2O_2 were added externally. The H_2O_2 concentration in the granulosa cells of the $Aqp8^{+/+}$ mice was significantly higher than that in the granulosa cells of the $Aqp8^{-/-}$ mice, indicating that AQP8 can mediate the efficient transport of H_2O_2 outside granulosa into cells. Further studies found that the H_2O_2 concentration in the granulosa cells increased during follicular atresia in mice. H_2O_2 transported by AQP8 can act as a secondary messenger to regulate intracellular signal transmission.

In conclusion, we provided a novel mechanism by which AQP8 transported extracellular H_2O_2 and induced cellular autophagy in granulosa cells, resulting in the increase of follicular atresia. This regulative mechanism may shed light on the treatment of ovarian insufficiency.

Data availability statement

The original contributions presented in the study are included in the article/Supplementary Material; further inquiries can be directed to the corresponding authors.

Ethics statement

The animal study was reviewed and approved by the Committee on the Ethics of Animal Research of Dalian Medical University.

Author contributions

HZ designed this study. HZ, BH, and LJ wrote this manuscript. HZ and BH contributed to the research design. LJ and LZ conducted animal and cell experiments. BH, XC, ZZ, YL, LY, TM, and HZ revised and edited this manuscript. HZ and BH was the guarantor of this work and, as such, had full access to all the data in the study and took responsibility for the integrity of the data and the accuracy of the data analysis. All authors contributed to the manuscript and approved the submitted version.

Funding

This study was supported by the National Natural Science Foundation of China (31600943 and 82103857), the Natural Science Foundation in Higher Education of Anhui (KJ 2020A0152), the Grants for Scientific Research of BSKY (XJ2020012), and the Grants for New Technology and New Project of Anhui Provincial Children's Hospital (2022118).

Conflict of interest

The authors declare that the research was conducted in the absence of any commercial or financial relationships that could be construed as a potential conflict of interest.

Publisher's note

All claims expressed in this article are solely those of the authors and do not necessarily represent those of their affiliated organizations, or those of the publisher, the editors, and the reviewers. Any product that may be evaluated in this article, or claim that may be made by its manufacturer, is not guaranteed or endorsed by the publisher.

Supplementary material

The Supplementary Material for this article can be found online at: https://www.frontiersin.org/articles/10.3389/fcell.2022.897666/full#supplementary-material

References

Agarwal, A., Gupta, S., Sekhon, L., and Shah, R. (2008). Redox considerations in female reproductive function and assisted reproduction: from molecular mechanisms to health implications. *Antioxid. Redox Signal.* 10, 1375–1403. doi:10.1089/ars.2007.1964

Bae, Y. S., Kang, S. W., Seo, M. S., Baines, I. C., Tekle, E., Chock, P. B., et al. (1997). Epidermal growth factor (EGF)-induced generation of hydrogen peroxide. Role in EGF receptor-mediated tyrosine phosphorylation. *J. Biol. Chem.* 272, 217–221. doi:10.1074/jbc.272.1.217

Basini, G., Simona, B., Santini, S. E., and Grasselli, F. (2008). Reactive oxygen species and anti-oxidant defences in swine follicular fluids. *Reprod. Fertil. Dev.* 20, 269–274. doi:10.1071/rd07147

Bertolotti, M., Bestetti, S., Garcia-Manteiga, J. M., Medrano-Fernandez, I., Dal Mas, A., Malosio, M. L., et al. (2013). Tyrosine kinase signal modulation: a matter of H2O2 membrane permeability? *Antioxid. Redox Signal.* 19, 1447–1451. doi:10.1089/ars.2013.5330

Bertolotti, M., Farinelli, G., Galli, M., Aiuti, A., and Sitia, R. (2016). AQP8 transports NOX2-generated H2O2 across the plasma membrane to promote signaling in B cells *J. Leukoc. Biol.*. doi:10.1189/jlb.2AB0116-045R

Bienert, G. P., Moller, A. L., Kristiansen, K. A., Schulz, A., Moller, I. M., Schjoerring, J. K., et al. (2007). Specific aquaporins facilitate the diffusion of hydrogen peroxide across membranes. *J. Biol. Chem.* 282, 1183–1192. doi:10.1074/jbc.M603761200

Blanc, A., Pandey, N. R., and Srivastava, A. K. (2003). Synchronous activation of ERK 1/2, p38mapk and PKB/Akt signaling by H2O2 in vascular smooth muscle cells: potential involvement in vascular disease (review). *Int. J. Mol. Med.* 11, 229–234. doi:10.3892/ijmm.11.2.229

Chen, Q., Peng, H., Lei, L., Zhang, Y., Kuang, H., Cao, Y., et al. (2011). Aquaporin3 is a sperm water channel essential for postcopulatory sperm osmoadaptation and migration. *Cell Res.* 21, 922–933. doi:10.1038/cr.2010.169

Choi, J. Y., Jo, M. W., Lee, E. Y., Yoon, B. K., and Choi, D. S. (2010). The role of autophagy in follicular development and atresia in rat granulosa cells. *Fertil. Steril.* 93, 2532–2537. doi:10.1016/j.fertnstert.2009.11.021

Choi, J., Jo, M., Lee, E., and Choi, D. (2011). Induction of apoptotic cell death via accumulation of autophagosomes in rat granulosa cells. *Fertil. Steril.* 95, 1482–1486. doi:10.1016/j.fertnstert.2010.06.006

Choi, J., Jo, M., Lee, E., and Choi, D. (2014). AKT is involved in granulosa cell autophagy regulation via mTOR signaling during rat follicular development and atresia. *Reproduction* 147, 73–80. doi:10.1530/REP-13-0386

D'Herde, K., De Prest, B., and Roels, F. (1996). Subtypes of active cell death in the granulosa of ovarian atretic follicles in the quail (*Coturnix coturnix* japonica). *Reprod. Nutr. Dev.* 36, 175–189. doi:10.1051/rnd:19960203

Duerrschmidt, N., Zabirnyk, O., Nowicki, M., Ricken, A., Hmeidan, F. A., Blumenauer, V., et al. (2006). Lectin-like oxidized low-density lipoprotein receptor-1-mediated autophagy in human granulosa cells as an alternative of programmed cell death. *Endocrinology* 147, 3851–3860. doi:10.1210/en.2006-0088

Finkel, T. (2011). Signal transduction by reactive oxygen species. *J. Cell Biol.* 194, 7–15. doi:10.1083/jcb.201102095

Forman, H. J., Maiorino, M., and Ursini, F. (2010). Signaling functions of reactive oxygen species. *Biochemistry* 49, 835–842. doi:10.1021/bi9020378

Furlong, H. C., Stampfli, M. R., Gannon, A. M., and Foster, W. G. (2015). Cigarette smoke exposure triggers the autophagic cascade via activation of the AMPK pathway in mice. *Biol. Reprod.* 93, 93. doi:10.1095/biolreprod.115.132183

Gannon, A. M., Stampfli, M. R., and Foster, W. G. (2013). Cigarette smoke exposure elicits increased autophagy and dysregulation of mitochondrial dynamics in murine granulosa cells. *Biol. Reprod.* 88, 63. doi:10.1095/biolreprod.112.106617

Gupta, S., Choi, A., Yu, H. Y., Czerniak, S. M., Holick, E. A., Paolella, L. J., et al. (2011). Fluctuations in total antioxidant capacity, catalase activity and hydrogen peroxide levels of follicular fluid during bovine folliculogenesis. *Reprod. Fertil. Dev.* 23, 673–680. doi:10.1071/RD10270

Hampton, M. B., and Orrenius, S. (1997). Dual regulation of caspase activity by hydrogen peroxide: implications for apoptosis. *FEBS Lett.* 414, 552–556. doi:10.1016/s0014-5793(97)01068-5

Hara-Chikuma, M., Chikuma, S., Sugiyama, Y., Kabashima, K., Verkman, A. S., Inoue, S., et al. (2012). Chemokine-dependent T cell migration requires aquaporin-3-mediated hydrogen peroxide uptake. *J. Exp. Med.* 209, 1743–1752. doi:10.1084/jem.20112398

Hara-Chikuma, M., Satooka, H., Watanabe, S., Honda, T., Miyachi, Y., Watanabe, T., et al. (2015). Aquaporin-3-mediated hydrogen peroxide transport is required for NF-κB signalling in keratinocytes and development of psoriasis. *Nat. Commun.* 6, 7454. doi:10.1038/ncomms8454

Hennet, M. L., Yu, H. Y., and Combelles, C. M. (2013). Follicular fluid hydrogen peroxide and lipid hydroperoxide in bovine antral follicles of various size, atresia, and dominance status. *J. Assist. Reprod. Genet.* 30, 333–340. doi:10.1007/s10815-012-9925-5

Huang, B., Zhao, H., Huang, C., Wu, L., Xiang, L., Chen, J., et al. (2020a). CMKLR1 deficiency attenuates androgen-induced lipid accumulation in mice. *Am. J. Physiol. Endocrinol. Metab.* 318, E371–E380. doi:10.1152/ajpendo.00176.2019

Huang, B., Zhu, W., Zhao, H., Zeng, F., Wang, E., Wang, H., et al. (2020b). Placenta-Derived osteoprotegerin is required for glucose homeostasis in gestational diabetes mellitus. *Front. Cell Dev. Biol.* 8, 563509. doi:10.3389/fcell.2020.563509

Hurst, P. R., Mora, J. M., and Fenwick, M. A. (2006). Caspase-3, TUNEL and ultrastructural studies of small follicles in adult human ovarian biopsies. *Hum. Reprod.* 21, 1974–1980. doi:10.1093/humrep/del109

Jana, S. K., Narendra Babu, K., Chattopadhyay, R., Chakravarty, B., and Chaudhury, K. (2010). Upper control limit of reactive oxygen species in follicular fluid beyond which viable embryo formation is not favorable. *Reprod. Toxicol.* 29, 447–451. doi:10.1016/j.reprotox.2010.04.002

Kakihana, T., Nagata, K., and Sitia, R. (2012). Peroxides and peroxidases in the endoplasmic reticulum: integrating redox homeostasis and oxidative folding. *Antioxid. Redox Signal.* 16, 763–771. doi:10.1089/ars.2011.4238

Kovacs, J., Forgo, V., and Peczely, P. (1992). The fine structure of the follicular cells in growing and atretic ovarian follicles of the domestic goose. *Cell Tissue Res.* 267, 561–569. doi:10.1007/BF00319379

Kruger, C., Waldeck-Weiermair, M., Kaynert, J., Pokrant, T., Komaragiri, Y., Otto, O., et al. (2021). AQP8 is a crucial H2O2 transporter in insulin-producing RINm5F cells. *Redox Biol.* 43, 101962. doi:10.1016/j.redox.2021.101962

Li, Y., Liu, H., Zhao, H., Xu, C., Zhao, Y., Ma, J., et al. (2013). Association of AQP8 in women with PCOS. *Reprod. Biomed. Online* 27, 419–422. doi:10.1016/j.rbmo.2013.07.001

Lin, P., and Rui, R. (2010). Effects of follicular size and FSH on granulosa cell apoptosis and atresia in porcine antral follicles. *Mol. Reprod. Dev.* 77, 670–678. doi:10.1002/mrd.21202

Liu, G. Y., Jiang, X. X., Zhu, X., He, W. Y., Kuang, Y. L., Ren, K., et al. (2015). ROS activates JNK-mediated autophagy to counteract apoptosis in mouse mesenchymal stem cells *in vitro*. *Acta Pharmacol. Sin.* 36, 1473–1479. doi:10.1038/aps.2015.101

Manabe, N., Goto, Y., Matsuda-Minehata, F., Inoue, N., Maeda, A., Sakamaki, K., et al. (2004). Regulation mechanism of selective atresia in porcine follicles: regulation of granulosa cell apoptosis during atresia. *J. Reprod. Dev.* 50, 493–514. doi:10.1262/jrd.50.493

Marchissio, M. J., Frances, D. E., Carnovale, C. E., and Marinelli, R. A. (2012). Mitochondrial aquaporin-8 knockdown in human hepatoma HepG2 cells causes ROS-induced mitochondrial depolarization and loss of viability. *Toxicol. Appl. Pharmacol.* 264, 246–254. doi:10.1016/j.taap.2012.08.005

Matsuda, F., Inoue, N., Manabe, N., and Ohkura, S. (2012). Follicular growth and atresia in mammalian ovaries: regulation by survival and death of granulosa cells. *J. Reprod. Dev.* 58, 44–50. doi:10.1262/jrd.2011-012

McConnell, N. A., Yunus, R. S., Gross, S. A., Bost, K. L., Clemens, M. G., and Hughes, F. M. (2002). Water permeability of an ovarian antral follicle is predominantly transcellular and mediated by aquaporins. *Endocrinology* 143, 2905–2912. doi:10.1210/endo.143.8.8953

Miller, E. W., Dickinson, B. C., and Chang, C. J. (2010). Aquaporin-3 mediates hydrogen peroxide uptake to regulate downstream intracellular signaling. *Proc. Natl. Acad. Sci. U. S. A.* 107, 15681–15686. doi:10.1073/pnas.1005776107

Mortazavi, A., Williams, B. A., Mccue, K., Schaeffer, L., and Wold, B. (2008). Mapping and quantifying mammalian transcriptomes by RNA-Seq. *Nat. Methods* 5, 621–628. doi:10.1038/nmeth.1226

Qian, Y., Shao, L., Yuan, C., Jiang, C. Y., Liu, J., Gao, C., et al. (2016). Implication of Differential peroxiredoxin 4 expression with age in ovaries of mouse and human for ovarian aging. *Curr. Mol. Med.* 16, 243–251. doi:10.2174/1566524016666160225151647

Rhee, S. G. (2006). Cell signaling. H2O2, a necessary evil for cell signaling. *Science* 312, 1882–1883. doi:10.1126/science.1130481

Schroder, E., and Eaton, P. (2008). Hydrogen peroxide as an endogenous mediator and exogenous tool in cardiovascular research: issues and considerations. *Curr. Opin. Pharmacol.* 8, 153–159. doi:10.1016/j.coph.2007.12.012

Sha, X. Y., Xiong, Z. F., Liu, H. S., Di, X. D., and Ma, T. H. (2011). Maternal-fetal fluid balance and aquaporins: from molecule to physiology. *Acta Pharmacol. Sin.* 32, 716–720. doi:10.1038/aps.2011.59

Shao, T., Ke, H., Liu, R., Xu, L., Han, S., Zhang, X., et al. (2022). Autophagy regulates differentiation of ovarian granulosa cells through degradation of WT1. *Autophagy*, 1–15. doi:10.1080/15548627.2021.2005415

Shen, M., Jiang, Y., Guan, Z., Cao, Y., Li, L., Liu, H., et al. (2017). Protective mechanism of FSH against oxidative damage in mouse ovarian granulosa cells by repressing autophagy. *Autophagy* 13, 1364–1385. doi:10.1080/15548627.2017.1327941

Shen, M., Cao, Y., Jiang, Y., Wei, Y., and Liu, H. (2018). Melatonin protects mouse granulosa cells against oxidative damage by inhibiting FOXO1-mediated autophagy: implication of an antioxidation-independent mechanism. *Redox Biol.* 18, 138–157. doi:10.1016/j.redox.2018.07.004

Su, W., Qiao, Y., Yi, F., Guan, X., Zhang, D., Zhang, S., et al. (2010). Increased female fertility in aquaporin 8-deficient mice. *IUBMB Life* 62, 852–857. doi:10.1002/iub.398

Su, W., Guan, X., Zhang, D., Sun, M., Yang, L., Yi, F., et al. (2013). Occurrence of multi-oocyte follicles in aquaporin 8-deficient mice. *Reprod. Biol. Endocrinol.* 11, 88. doi:10.1186/1477-7827-11-88

Tonks, N. K. (2005). Redox redux: revisiting PTPs and the control of cell signaling. *Cell* 121, 667–670. doi:10.1016/j.cell.2005.05.016

Yang, B., Song, Y., Zhao, D., and Verkman, A. S. (2005). Phenotype analysis of aquaporin-8 null mice. *Am. J. Physiol. Cell Physiol.* 288, C1161–C1170. doi:10.1152/ajpcell.00564.2004

Zhang, D., Tan, Y. J., Qu, F., Sheng, J. Z., and Huang, H. F. (2012). Functions of water channels in male and female reproductive systems. *Mol. Asp. Med.* 33, 676–690. doi:10.1016/j.mam.2012.02.002

Zhang, Y., Chen, Q., Zhang, H., Wang, Q., Li, R., Jin, Y., et al. (2015). Aquaporin-dependent excessive intrauterine fluid accumulation is a major contributor in hyper-estrogen induced aberrant embryo implantation. *Cell Res.* 25, 139–142. doi:10.1038/cr.2014.139

Zhang, D., Xu, G., Zhang, R., Zhu, Y., Gao, H., Zhou, C., et al. (2016). Decreased expression of aquaporin 2 is associated with impaired endometrial receptivity in controlled ovarian stimulation. *Reprod. Fertil. Dev.* 28, 499–506. doi:10.1071/RD13397

Zhang, J., Zhao, L., Li, Y., Dong, H., Zhang, H., Zhang, Y., et al. (2022). Circadian clock regulates granulosa cell autophagy through NR1D1-mediated inhibition of ATG5. *Am. J. Physiol. Cell Physiol.* 322, C231–C245. doi:10.1152/ajpcell.00267.2021

Zhou, J., Peng, X., and Mei, S. (2019). Autophagy in ovarian follicular Development and atresia. *Int. J. Biol. Sci.* 15, 726–737. doi:10.7150/ijbs.30369

frontiers | Frontiers in Cell and Developmental Biology

TYPE Mini Review
PUBLISHED 14 September 2022
DOI 10.3389/fcell.2022.959239

OPEN ACCESS

EDITED BY
Rujuan Zuo,
Oslo University Hospital, Norway

REVIEWED BY
Qingliang Zheng,
The Eighth Affiliated Hospital, Sun Yat-sen University, China
Linlin Sui,
Dalian Medical University, China

*CORRESPONDENCE
Jian V. Zhang,
jian.zhang@siat.ac.cn
Jianmin Niu,
njianmin@163.com

SPECIALTY SECTION
This article was submitted to Cellular Biochemistry, a section of the journal Frontiers in Cell and Developmental Biology

RECEIVED 01 June 2022
ACCEPTED 25 July 2022
PUBLISHED 14 September 2022

CITATION
Yin A, Guan X, Zhang JV and Niu J (2022), Focusing on the role of secretin/adhesion (Class B) G protein-coupled receptors in placental development and preeclampsia.
Front. Cell Dev. Biol. 10:959239.
doi: 10.3389/fcell.2022.959239

Focusing on the role of secretin/adhesion (Class B) G protein-coupled receptors in placental development and preeclampsia

Aiqi Yin[1], Xiaonian Guan[1], Jian V. Zhang[2,3,4]* and Jianmin Niu[1]*

[1]Department of Obstetrics, Shenzhen Maternity and Child Healthcare Hospital, The First School of Clinical Medicine, Southern Medical University, Shenzhen, China, [2]Center for Energy Metabolism and Reproduction, Shenzhen Institute of Advanced Technology, Chinese Academy of Sciences, Shenzhen, China, [3]Shenzhen Institute of Advanced Technology, Chinese Academy of Sciences, Shenzhen, China, [4]Shenzhen Key Laboratory of Metabolic Health, Shenzhen, China

Preeclampsia, a clinical syndrome mainly characterized by hypertension and proteinuria, with a worldwide incidence of 3–8% and high maternal mortality, is a risk factor highly associated with maternal and offspring cardiovascular disease. However, the etiology and pathogenesis of preeclampsia are complicated and have not been fully elucidated. Obesity, immunological diseases and endocrine metabolic diseases are high-risk factors for the development of preeclampsia. Effective methods to treat preeclampsia are lacking, and termination of pregnancy remains the only curative treatment for preeclampsia. The pathogenesis of preeclampsia include poor placentation, uteroplacental malperfusion, oxidative stress, endoplasmic reticulum stress, dysregulated immune tolerance, vascular inflammation and endothelial cell dysfunction. The notion that placenta is the core factor in the pathogenesis of preeclampsia is still prevailing. G protein-coupled receptors, the largest family of membrane proteins in eukaryotes and the largest drug target family to date, exhibit diversity in structure and function. Among them, the secretin/adhesion (Class B) G protein-coupled receptors are essential drug targets for human diseases, such as endocrine diseases and cardiometabolic diseases. Given the great value of the secretin/adhesion (Class B) G protein-coupled receptors in the regulation of cardiovascular system function and the drug target exploration, we summarize the role of these receptors in placental development and preeclampsia, and outlined the relevant pathological mechanisms, thereby providing potential drug targets for preeclampsia treatment.

KEYWORDS

preeclampsia (PE), pathogenesis, placenta, secretin GPCRs, adhesion GPCRs

Introduction

Preeclampsia (PE) is a multisystem pregnancy disorder characterized by new-onset hypertension after 20 weeks of gestation and affects the functions of multiple organ (Brown et al., 2018; Chappell et al., 2021). PE influences around 3–8% of the pregnant women and remains a key cause of maternal mortality, bringing about at least 42,000 maternal deaths each year (Abalos et al., 2013; Say et al., 2014). PE seriously threatens maternal and fetal life safety, leading to many severe complications such as acute renal failure, intracranial hemorrage, fetal growth restriction (FGR), abnormal fetal heart development and still birth (Adu-Bonsaffoh et al., 2013; Brown et al., 2018; Hutcheon et al., 2011). Furthermore, PE can bring substantial long-term cardiovascular and endocrine metabolic risks both to the mother and the child (Bellamy et al., 2007; Kajantie et al., 2009; Mongraw-Chaffin et al., 2010; Tuovinen et al., 2012). The strong evidence has demonstrated that aspirin can prevent the development of PE (Duley et al., 2019; Jin, 2021). However, once PE occurs, the existing treatments, such as antispasmodic and antihypertensive agents, cannot prevent the progression of the disease. The termination pf pregnancy is the only effective treatment for PE, which may leads to the delivery of premature fetus or low birth weight fetus, with high healthcare costs (Chappell et al., 2021; Liu et al., 2009). Thus, it is necessary to explore new treatments for PE to reduce the risk and safely prolong pregnancy.

The pathophysiological mechanisms of PE have been studied for a long time. The placenta is the key factor responsible for the development of PE. All maternal complications share a common pathophysiological feature focusing on placental abnormalities (Burton et al., 2019). The pathogenesis of PE contains poor placentation, uteroplacental malperfusion and endothelial cell dysfunction (Brennan et al., 2014; Redman and Staff, 2015). However, due to the heterogeneity of PE and the diversity of its clinical manifestations, the immunological, genetic and environmental mechanisms of PE are still not fully understood, and there is no great breakthrough regarding

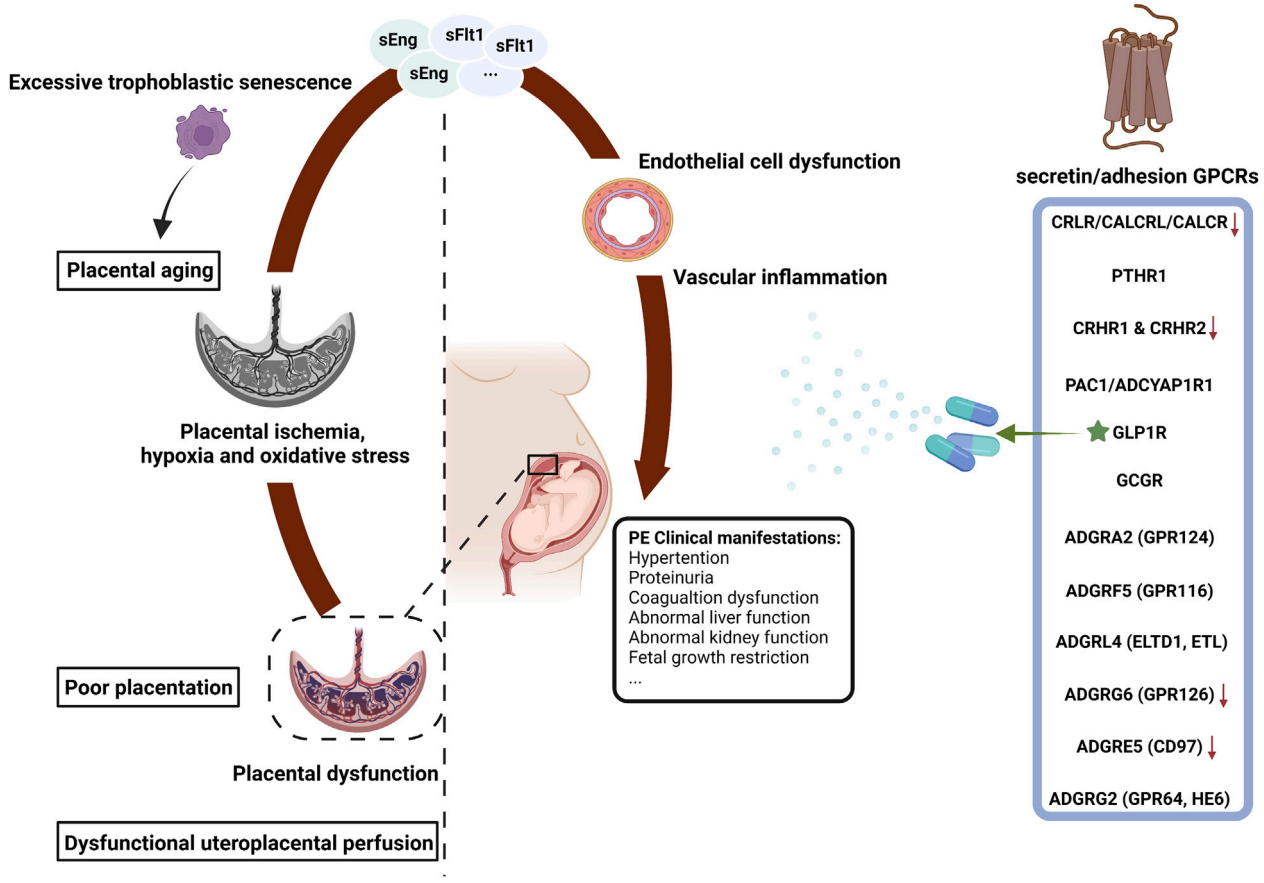

FIGURE 1
The secretin/adhesion GPCRs and the pathophysiology of preeclampsia. PE, preeclampsia; GPCRs, G protein-coupled receptors; sFlt-1, soluble fms-like tyrosine kinase 1; sEng, soluble endoglin; FGR, fetal growth restriction; ★, commercial drug; ↓, expressed at low levels in PE. The figure was created with BioRender.com.

TABLE 1 The secretin/adhesion (class B) GPCRs in placental development and PE.

Secretin (Class B) GPCRs	Species	GPCRs in placental development and PE	References
CRLR/CALCRL/CALCR	Human	Lowly expressed at the uterus and umbilical artery in pregnancy-induced hypertension	Makino et al. (2001)
	Human	Expressed at the vascular endothelial cells of placental chorionic villi in the first trimester	Tsatsaris et al. (2002)
	Mouse	Expressed in placenta and involved in blood flow	Dong et al. (2003)
	Human	Regulates human fetoplacental vascular tone	Dong et al. (2004)
	Human	Expressed in human trophoblast cell line JAr and HTR-8/SVneo	Zhang et al. (2005)
	Human	Decreasingly expressed in preeclamptic placenta	Dong et al. (2005)
		Affects vasodilation in PE	
	Mouse	Leads to hydrops fetalis, cardiovascular defects and embryonic lethality in CALCRL KO mouse	Dackor et al. (2006)
	Mouse	Shows a spatiotemporal pattern in rat female reproductive system	Li et al. (2010)
	Human	Results in autosomal recessive, hydrops fetalis and lymphatic dysplasia with CALCRL mutation	Mackie et al. (2018)
PTHR1	Human	Inhibits proliferation of JEG-3 cell line	Hellman et al. (1993)
	Mouse	Decreasingly expressed via CALCRL-associated RAMP2 regulation	Kadmiel et al. (2017)
	Human	Highly expressed in extravillous cytotrophoblast and decidua	Sirico et al. (2021)
		Expressed differently depending on maternal hyperglycemia type	
CRHR1 & CRHR2	Human	Expressed in syncytiotrophoblast cells and amniotic epithelium	Karteris et al. (1998)
	Human	Decreased expression of CRHR1 in PE and IUGR	Karteris et al. (2003)
		Influences vascular resistance	
	Human	Located in cultured human chorion trophoblast cells	Gao et al. (2007)
		Mediates expression of PGDH	Gao et al. (2008)
	Human	Expressed in placental trophoblasts	Gao et al. (2012)
		Regulates prostaglandin production	
	Human	Regulates estradiol and progesterone production in cultured human trophoblasts	Gao et al. (2012)
	Human	Regulates glucose transporters in cultured human placental trophoblasts	Gao et al. (2012)
	Human	Increasingly expressed via exogenous CRH stimulation in BeWo cells	Chen et al. (2013)
GCGR	Mouse	Causes hypoglycemia, hyperglucagonemia and fetoplacental defects in GCGR KO mouse	Ouhilal et al. (2012)
GLP1R	Mouse	Attenuates placental ischemia	Younes et al. (2020)
PAC1/ADCYAP1R1	Human/ mouse	Expressed in human and rat placenta	Scaldaferri et al. (2000)
	Mouse	As binding sites for PACAP in human tissue	Koh et al. (2003)
		Expressed in decidual cells, chorionic vessels and stromal cells	
		Dynamically expressed during gestation	
	Human	Expressed in stroma cells with spatiotemporal characteristics	Koh et al. (2005)
	Human	Regulates MAPK signaling pathways in cytotrophoblast cells	Reglodi et al. (2008)
Adhesion (Class B) GPCRs	**Species**	**GPCRs in placental development and preeclampsia**	**References**
ADGRA2 (*GPR124*)	Mouse	Causes embryonic lethality, CNS-specific angiogenesis arrest and hemorrhage in GPR124 KO mouse	Kuhnert et al. (2010)
	Mouse	Results in embryonic lethality in GPR124 global KO mouse and GPR124 conditional (endothelial-specific) KO mouse	Cullen et al. (2011)
	Human	Lowly expressed in early-onset PE with comparison of late-onset PE	Liang et al. (2016)
	Mouse	Leads to embryonic lethality in GPR124 KO mouse	Chang et al. (2017)
ADGRF5 (*GPR116*), *ADGRL4* (*ADGRG6* (*GPR126*))	Mouse	Causes vascular remodeling defects and postnatal kidney failure	Lu et al. (2017)
	Mouse	Possesses strict expression pattern	Moriguchi et al. (2004)
	Mouse	Required for embryonic development	Waller-Evans et al. (2010)
	Human	Related to placental angiogenesis in IUGR	Majewska et al. (2019)

(Continued on following page)

TABLE 1 (*Continued*) The secretin/adhesion (class B) GPCRs in placental development and PE.

Secretin (Class B) GPCRs	Species	GPCRs in placental development and PE	References
	Mouse/ zebrafish	Leads to embryonic lethality in GPR126 KO mouse	Torregrosa-Carrion et al. (2021)
		Expressed in trophoblast giant cells	
		Regulates trophoblast invasion and spiral artery remodeling	Bogias et al. (2022)
		Affects the expression of PE markers in GPR126 KO placenta	
	Human	Related to hypoxia at early pregnancy	
ADGRE5 (*CD97*)	Human	Lowly expressed in PE placenta	Shen et al. (2020)
		Promotes trophoblast invasion through PI3K/Akt/mTOR pathway	
ADGRG2 (*GPR64, HE6*)	Mouse	Expressed at epithelial and stromal cells in the uterus	Yoo et al. (2017)
		Reduces decidualization in GPR64 KO mouse	

Note: GPCRs, G protein-coupled receptors; PE, preeclampsia; KO, Knockout; RAMPs, Receptor activity-modifying protein 2; IUGR, intrauterine growth restriction; PGDH, 15-hydroxy prostaglandin dehydrogenase; CRH, Corticotropin-releasing hormone; PACAP, Pituitary adenylate cyclase-activating polypeptide; CNS, central nervous system.

the treatment for PE. Some research scholars advocate that PE should be reclassified using placenta-derived markers or new phenotypic combinations, which may assist in identifying high-risk patients, monitoring disease progression, and providing effective clinical interventions (Ferrazzi et al., 2018; Powers et al., 2012).

G protein-coupled receptors (GPCRs), the largest family of membrane proteins in eukaryotes, are involved in the regulation of almost all life processes and functions. GPCRs are the key factors for the occurrence and development of major diseases, including cardiometabolic diseases (Dorsam and Gutkind, 2007; Lappano and Maggiolini, 2011; Wang et al., 2018). Exploratory studies have revealed the essential functions of GPCRs in placental development and provided a sufficient theoretical basis that they can be used as potential targets for PE (Conrad, 2016; McGuane and Conrad, 2012; Quitterer and AbdAlla, 2021). Based on the classification by structure and phylogeny analysis of GPCRs, Class B GPCRs, which are structurally characterized by large extracellular regions, contain the following two families, secretin GPCRs and adhesion GPCRs. Secretin GPCRs are polypeptide hormone receptors that can mediate diverse physiological activities. Adhesion GPCRs are indispensable for human development, and their mutations are involved in all major tissues diseases. This review summarizes the pathophysiological mechanisms of PE and the biological role of secretin/adhesion (Class B) GPCRs in placental development and PE, aiming to find potential markers for the reclassification and treatment of PE.

Pathophysiology of PE: the two-stage placental model

The clinical symptoms of PE are immediately relieved once the placenta is delivered, suggesting that the placenta is crucial for the pathogenesis of PE. The two-stage placental model theory proposed by professor Redman is the most acceptable explanation for the pathogenesis of PE (Redman, 1991). In the first stage (preclinical and placental period), insufficient trophoblast infiltration causes the incomplete remodeling of the uterine spiral arteries, resulting in poor placentation and placental dysfunction. In the second stage (clinical and maternal disease period), placental ischemia, hypoxia and oxidative stress lead to the release of numerous inflammatory factors into the circulation, including soluble fms-like tyrosine kinase-1 (sFlt-1), soluble endoglin (sEng), trophoblast debris and reactive oxygen species (Levine et al., 2004; Maynard et al., 2003). These factors cause systemic vascular inflammation and extensive maternal endothelial cell dysfunction (Redman et al., 1999) and provoke diverse clinical manifestations such as maternal hypertension, proteinuria and FGR (Powe et al., 2011). This two-stage model is established on the assumption that poor placentation, predominantly leading to FGR, occurs in almost all PE cases (Avagliano et al., 2011). However, some of the late-onset PE patients with full delivery show unlimited neonatal growth, which suggests that poor placentation does not happens in all PE placenta (Xiong et al., 2002). The second placental cause of PE is uteroplacental malperfusion. The placenta capacity over the capacity of the uterus could compress the terminal villi and hinder intervillous perfusion, resulting in syncytiotrophoblast hypoxia and the subsequent placental dysfunction (Devisme et al., 2013). Increased syncytiotrophoblast apoptosis in the human full-term placenta may cause PE as well (Ishihara et al., 2002). Studies have shown that the angiogenesis-related factors secreted by syncytiotrophoblasts are expected to be circulating biomarkers for the diagnosis and prediction of PE (Droge et al., 2021). Excessive trophoblastic senescence increases placental cell stress, which may be a potential pathogenic factor for PE (Zaki et al., 2003; Zhang et al., 2021). Overall, syncytiotrophoblast stress is a common end point of both early-onset and late-onset PE pathways and is affected by maternal genetic, epigenetic and environmental factors. Syncytiotrophoblast stress signaling in the maternal

circulation may be the most specific biomarker of PE (Redman et al., 2022). The two-stage model summarizes the pathophysiological mechanisms of PE into two stages (placental dysfunction and clinical manifestations) and three ways (poor placentation, dysfunctional uteroplacental perfusion and placental aging) (Figure 1). In addition, it incorporates a range of pathophysiological mechanisms, including dysregulated immune tolerance, vascular inflammation, endoplasmic reticulum stress and oxidative stress (Sheppard and Bonnar, 1976). Maternal and pregnancy risk factors, such as primiparity, obesity and chronic prepregnancy disorders, are also considered (Alnaes-Katjavivi et al., 2016; Egeland et al., 2016; Skjaerven et al., 2002; Tannetta et al., 2015).

Role of GPCRs in PE

GPCRs, a superfamily of seven-transmembrane receptors, more than 800 of which are encoded in the human genome, constitute the largest family of cell surface receptors in mammalian cells. GPCRs were initially divided into A–F systems according to the structural similarity of their receptor size, ligand interaction points and phylogeny. Their prototype members are as follows: Class A (rhodopsin receptors), Class B (secretin/adhesion receptors), Class C (metabotropic glutamate receptors), Class D (fungal mating pheromone receptors), Class E (cyclic AMP receptors) and Class F (frizzled/smoothened receptors) (Attwood and Findlay, 1994; Bockaert and Pin, 1999). Fredriksson et al. provided a GRAFS classification approach based on an overall phylogenetic analysis of human tracks that consists of the following five families: rhodopsin (Class A), secretin/adhesion (Class B), glutamate (Class C), frizzled (Class F) and taste 2 (Class T) (Fredriksson et al., 2003). GPCRs can recognize various different ligands or stimuli, such as hormones, neurotransmitters and light, to regulate key physiological processes. Abnormal GPCR signaling can lead to various diseases, such as diabetes (Riddy et al., 2018; Wu et al., 2021), cardiovascular diseases (Wang et al., 2018) and cancers (Dorsam and Gutkind, 2007; Lappano and Maggiolini, 2011). More than 40% of commercial drugs exert their efficacy through GPCRs. Most drugs target rhodopsin GPCRs because they have various ligands, but other GPCRs also possess distinct therapeutic potential, such as more than 34 drugs targeting secretin GPCRs and 21 drugs targeting glutamate GPCRs (Hutchings, 2020). Furthermore, research on drugs targeting GPCRs are still increasing (Zhou and Wild, 2019).

The GPCRs-targeted drugs such as GLP-1, which belongs to secretin GPCRs, have been used for the treament of cardiovascular diseases and endocrine diseases. The GPCR-mediated regulation of vascular tone and circulating blood volume plays crucial roles in the maintenance of blood pressure homeostasis. PE is inextricably linked to endocrine and cardiovascular diseases. Recently, it's found GPCRs potentially contribute to maternal physiological adaptation to pregnancy and placental development. Several GPCRs such as calcitonin receptor-like receptor (CRLR) and angiotensin AT1/2 are potential therapeutic targets for PE. They can modulate systemic and/or uteroplacental vasodilation to alleviate hypertension in PE (Dong et al., 2006). Secretin and adhesion GPCRs, which belong to the class B GPCR family, present great potential in clinical use. Many studies are committed to investigate the fundamental role of Class B (secretin/adhesion) GPCRs in PE, so it is necessary to summarize the current research progress. A comprehensive summary of the researches in relation to Class B (secretin/adhesion) GPCRs in the field of placental development and PE is provided in the following part of this review (Table 1).

Secretin (Class B) GPCRs

The secretin family, a small part of GPCRs containing 15 members, has large extracellular domains that can bind to hormone and mainly regulates metabolism (Lagerstrom and Schioth, 2008).

Calcitonin receptor-like receptor (CRLR) is required for embryonic development (Chang and Hsu, 2013). Deficiency of CRLR causes extreme hydrops fetalis and embryonic death (Dackor et al., 2006; Mackie et al., 2018). CRLR is widely expressed in vascular endothelial cells of placental chorionic villi at the first trimester, human choriocarcinoma JAr cells and trophoblast HTR-8/svneo cells (Tsatsaris et al., 2002). It shows a spatiotemporal pattern in the female reproductive system of pregnant rats (Li et al., 2010). An analysis of mouse placenta obtained on E18 of pregnancy suggests that CRLR is predominantly expressed in trophoblast, syncytiotrophoblast and trophoblast giant cells (Chang and Hsu, 2013; Dong et al., 2003; Zhang et al., 2005). CRLR regulates trophoblast proliferation and differentiation in the implantation process (Tsatsaris et al., 2002). Existing research demonstrates that CRLR is decreasingly expressed at the uterus and umbilical artery tissues in pregnancy-induced hypertension patients (Makino et al., 2001) and at PE placenta (Dong et al., 2005). It also associates with PE in vascular remodeling (Chang and Hsu, 2013). The impairment of CRLR associated with calcitonin gene-related peptide (CGRP)-dependent vasodilation in PE (Dong et al., 2005) suggest their role in the control of human fetoplacental vascular tone. CGPR-mediated vascular dilation involves the activation of KATP channels, cAMP and nitric oxide pathway (Dong et al., 2004). The loss of CRLR associated receptor activity-modifying proteins (RAMPs) reduces the expression of parathyroid hormone 1 receptor (PTHR1) (Kadmiel et al., 2017). PTHR1 expresses differently depending on maternal hyperglycemia type. It's highly expressed in the extravillous cytotrophoblasts and decidua tissues, regulating the human

trophoblast-derived JEG-3 cell proliferation (Hellman et al., 1993), and committing to adverse pregnancy outcomes (Sirico et al., 2021).

Corticotropin releasing hormone (CRH) promotes embryo implantation (Makrigiannakis et al., 2001). It also control trophoblast invasion by downregulating the synthesis of carcinoembryonic antigen-related cell adhesion molecule 1 (CEACAM1) in extravillous trophoblast (EVT) cells (Bamberger et al., 2006). Abnormalities in trophoblast invasion may lead to abnormal placentation. The treatment of BeWo cells with exogenous CRH results in the elevation of cellular corticotropin releasing hormone receptor 1 (CRHR1) levels, which are significantly reduced in PE and intrauterine growth restriction (IUGR) (Chen et al., 2013; Karteris et al., 2003). CRHR1 and CRHR2 are expressed in placental trophoblasts, and they regulate estradiol and progesterone production as well as glucose transporters through distinct signaling pathways. They exert differential effects on 15 hydroxy prostaglandin dehydrogenase (PGDH) expression (Gao et al., 2007; Gao et al., 2008; Gao et al., 2012a; Gao et al., 2012b; Karteris et al., 1998). The deficiency of CRHR1 in uterine at early pregnancy implicates the pathogenesis of recurrent miscarriage, placenta accreta and PE (Kalantaridou et al., 2007).

The absence of the glucagon receptor (GCGR) gene during pregnancy leads to abnormal placentation and poor fetal growth, increasing occurrence rate of fetal and early postnatal death. The placenta affected by GCGR are characterized by extensive mineralization, fibrinoid necrosis, narrowing of the vascular channels and thickened interstitium associated with trophoblast hyperplasia. In addition, the lack of GCGR downregulates genes that control growth, vascularization and oxidative stress (Charron and Vuguin, 2015; Ouhilal et al., 2012). Regarding glucagon-like peptide receptors (GLPRs, including GLP1R and GLP2R), it's found that the GLP1R agonist liraglutide can increase nitric oxide production and decrease blood pressures. They function partially through activating nitric oxide synthase (NOS) and thus serve as a potential therapeutic option for PE (Younes et al., 2020).

Pituitary adenylate cyclase activating polypeptide receptor 1 (PAC1), expressed in both human and mouse placenta, has spatiotemporal expression characteristics in decidual cells, chorionic vessels and stromal cells (Koh et al., 2003; Koh et al., 2005; Scaldaferri et al., 2000). Its antagonist PACAP6-38 can activate MAPK signaling in human cytotrophoblasts, which suggests the possible role in gestational maintenance and fetal growth (Reglodi et al., 2008). Drugs designed on the basis of secretin GPCR have been developed and applied for clinical use, especially in the treatment of metabolic diseases, such as diabetes. Given diabetes and obesity are risk factors for PE, the prospect of secretin GPCRs in therapy of PE could be speculated.

Adhesion (Class B) GPCRs

The adhesion family of GPCRs, a large branch with 33 members, is the second largest family of GPCRs separated from secretin GPCRs. The International Union of Basic and Clinical Pharmacology (IUPHAR) rename adhesion GPCRs as ADGRs followed a letter and a number to denote their subfamily and subtype, respectively (Hamann et al., 2015). Adhesion GPCRs are paid close attention due to its specific biological function and structure. Most adhesion GPCRs have long diverse N termini, and their N termini are rich in functional domains that can be found in other proteins, such as cadherins, lectins and immunoglobulins. It's shown that the number and structure of these domains are essential for the specificity of receptor ligand binding interactions (Bjarnadottir et al., 2004; Purcell and Hall, 2018).

Several adhesion GPCRs participate in angiogenesis, a process that implicates in gestational physiology, placental development and the occurrence of PE (Masiero et al., 2013; Stehlik et al., 2004; Vallon and Essler, 2006; Wang et al., 2005). ADGRA2 (GPR124) deficiency leads to embryonic lethality due to the central nervous system (CNS)- specific angiogenesis and hemorrhage (Anderson et al., 2011; Chang et al., 2017; Cullen et al., 2011; Kuhnert et al., 2010). The loss of ADGRF5 (GPR116) and ADGRL4 (ELTD1, ETL) result in vascular remodeling defects (Lu et al., 2017). Both ADGRA2 (GPR124) and ADGRG6 (GPR126) are required for embryonic development (Chang et al., 2017; Waller-Evans et al., 2010). ADGRG6 (GPR126) has a strictly regulated expression pattern in mouse development (Moriguchi et al., 2004). A differential expression of ADGRG6 (GPR126) is found in IUGR placenta, which is correlated with placental angiogenesis (Majewska et al., 2019) and hypoxia in early pregnancy (Bogias et al., 2022). ADGRG6 (GPR126) mutant placenta shows a decreased expression of proteases associated with trophoblast invasion and maternal uterine vascular remodeling, leading to IUGR, PE and early miscarriage. Hence, ADGRG6 (GPR126) is essential in the trophoblast lineage for the promotion of spiral artery remodeling during placental development (Torregrosa-Carrion et al., 2021). Our research group previously analyzes the gene expression profiles at placentas in early-onset PE and late-onset PE. ADGRA2 (GPR124) is downregulated in early-onset PE and involve in cell surface receptor-related signaling (Liang et al., 2016). The specific role and mechanism of ADGRA2 (GPR124) in placental development and PE are still under investigation. ADGRE5 (CD97) is downregulated in PE placenta and promotes trophoblast invasion by targeting FOXC2 through PI3K/Akt/mTOR signaling pathway (Shen et al., 2020). ADGRG2 (GPR64, HE6) plays a crucial role in the decidualization of endometrial stromal cells (Yoo et al., 2017). Adhesion GPCRs are considered as suitable targets

for therapy, but the ligands of most members have not been found. And there are no associated drugs are currently approved by the FDA.

Conclusion and perspectives

In summary, the Class B (secretin/adhesion) GPCRs play crucial roles in placental development and PE, suggesting that the class B (secretin/adhesion) GPCRs could serve as therapeutic targets in PE. However, most of the studies mainly focus on their expression level and associated phenotype, whereas the molecular mechanisms still need to be paid much more attention. Deep comprehension on the mechanisms is required to provide solid rationale for the application of Class B (secretin/adhesion) GPCR-targeted drugs into PE.

Author contributions

JZ and JN conceived the manuscript. AY, JZ and JN wrote and revised the manuscript. XG prepared the figure and the table. All authors contributed to the article and approved the submitted version.

Funding

This work was supported by the National Natural Science Foundation of China (81830041 and 82001521), Guangdong Basic and Applied Basic Research Foundation (2019A1515110340), Shenzhen Science and Technology Program (JCYJ20190812170005666) and Shenzhen Key Laboratory of Metabolic Health (Grant No. ZDSYS20210427152400001).

Conflict of interest

The authors declare that the research was conducted in the absence of any commercial or financial relationships that could be construed as a potential conflict of interest.

Publisher's note

All claims expressed in this article are solely those of the authors and do not necessarily represent those of their affiliated organizations or those of the publisher, the editors and the reviewers. Any product that may be evaluated in this article or claim that may be made by its manufacturer is not guaranteed or endorsed by the publisher.

References

Abalos, E., Cuesta, C., Grosso, A. L., Chou, D., and Say, L. (2013). Global and regional estimates of preeclampsia and eclampsia: A systematic review. *Eur. J. Obstetrics Gynecol. Reproductive Biol.* 170 (1), 1–7. doi:10.1016/j.ejogrb.2013.05.005

Adu-Bonsaffoh, K., Oppong, S. A., Binlinla, G., and Obed, S. A. (2013). Maternal deaths attributable to hypertensive disorders in a tertiary hospital in Ghana. *Int. J. Gynecol. Obstetrics* 123 (2), 110–113. doi:10.1016/j.ijgo.2013.05.017

Alnaes-Katjavivi, P., Lyall, F., Roald, B., Redman, C. W., and Staff, A. C. (2016). Acute atherosis in vacuum suction biopsies of decidua basalis: An evidence based research definition. *Placenta* 37, 26–33. doi:10.1016/j.placenta.2015.10.020

Anderson, K. D., Pan, L., Yang, X. M., Hughes, V. C., Walls, J. R., Dominguez, M. G., et al. (2011). Angiogenic sprouting into neural tissue requires Gpr124, an orphan G protein-coupled receptor. *Proc. Natl. Acad. Sci. U.S.A.* 108 (7), 2807–2812. doi:10.1073/pnas.1019761108

Attwood, T. K., and Findlay, J. B. (1994). Fingerprinting G-protein-coupled receptors. *Protein Eng. Des. Sel.* 7 (2), 195–203. doi:10.1093/protein/7.2.195

Avagliano, L., Bulfamante, G. P., Morabito, A., and Marconi, A. M. (2011). Abnormal spiral artery remodelling in the decidual segment during pregnancy: From histology to clinical correlation. *J. Clin. Pathol.* 64 (12), 1064–1068. doi:10.1136/jclinpath-2011-200092

Bamberger, A. M., Minas, V., Kalantaridou, S. N., Radde, J., Sadeghian, H., Löning, T., et al. (2006). Corticotropin-releasing hormone modulates human trophoblast invasion through carcinoembryonic antigen-related cell adhesion molecule-1 regulation. *Am. J. Pathology* 168 (1), 141–150. doi:10.2353/ajpath.2006.050167

Bellamy, L., Casas, J. P., Hingorani, A. D., and Williams, D. J. (2007). Pre-eclampsia and risk of cardiovascular disease and cancer in later life: Systematic review and meta-analysis. *BMJ* 335 (7627), 974. doi:10.1136/bmj.39335.385301.BE

Bjarnadóttir, T. K., Fredriksson, R., Höglund, P. J., Gloriam, D. E., Lagerström, M. C., and Schiöth, H. B. (2004). The human and mouse repertoire of the adhesion family of G-protein-coupled receptors. *Genomics* 84 (1), 23–33. doi:10.1016/j.ygeno.2003.12.004

Bockaert, J., and Pin, J. P. (1999). Molecular tinkering of G protein-coupled receptors: An evolutionary success. *EMBO J.* 18 (7), 1723–1729. doi:10.1093/emboj/18.7.1723

Bogias, K. J., Pederson, S. M., Leemaqz, S., Smith, M. D., McAninch, D., Jankovic-Karasoulos, T., et al. (2022). Placental transcription profiling in 6-23 weeks' gestation reveals differential transcript usage in early development. *Ijms* 23 (9), 4506. doi:10.3390/ijms23094506

Brennan, L. J., Morton, J. S., and Davidge, S. T. (2014). Vascular dysfunction in preeclampsia. *Microcirculation* 21 (1), 4–14. doi:10.1111/micc.12079

Brown, M. A., Magee, L. A., Kenny, L. C., Karumanchi, S. A., McCarthy, F. P., Saito, S., et al. (2018). Hypertensive disorders of pregnancy. *Hypertension* 72 (1), 24–43. doi:10.1161/HYPERTENSIONAHA.117.10803

Burton, G. J., Redman, C. W., Roberts, J. M., and Moffett, A. (2019). Pre-eclampsia: Pathophysiology and clinical implications. *BMJ* 366, l2381. doi:10.1136/bmj.l2381

Chang, C. L., and Hsu, S. Y. (2013). Roles of CLR/RAMP receptor signaling in reproduction and development. *Cpps* 14 (5), 393–406. doi:10.2174/13892037113149990056

Chang, J., Mancuso, M. R., Maier, C., Liang, X., Yuki, K., Yang, L., et al. (2017). Gpr124 is essential for blood-brain barrier integrity in central nervous system disease. *Nat. Med.* 23 (4), 450–460. doi:10.1038/nm.4309

Chappell, L. C., Cluver, C. A., Kingdom, J., and Tong, S. (2021). Pre-eclampsia. *Lancet* 398 (10297), 341–354. doi:10.1016/S0140-6736(20)32335-7

Charron, M. J., and Vuguin, P. M. (2015). Lack of glucagon receptor signaling and its implications beyond glucose homeostasis. *J. Endocrinol.* 224 (3), R123–R130. doi:10.1530/JOE-14-0614

Chen, Y., Allars, M., Pan, X., Maiti, K., Angeli, G., Smith, R., et al. (2013). Effects of corticotrophin releasing hormone (CRH) on cell viability and differentiation in the human BeWo choriocarcinoma cell line: A potential syncytialisation inducer distinct from cyclic adenosine monophosphate (cAMP). *Reprod. Biol. Endocrinol.* 11, 30. doi:10.1186/1477-7827-11-30

Conrad, K. P. (2016). G-Protein-coupled receptors as potential drug candidates in preeclampsia: Targeting the relaxin/insulin-like family peptide receptor 1 for treatment and prevention. *Hum. Reprod. Update* 22 (5), 647–664. doi:10.1093/humupd/dmw021

Cullen, M., Elzarrad, M. K., Seaman, S., Zudaire, E., Stevens, J., Yang, M. Y., et al. (2011). GPR124, an orphan G protein-coupled receptor, is required for CNS-specific vascularization and establishment of the blood-brain barrier. *Proc. Natl. Acad. Sci. U.S.A.* 108 (14), 5759–5764. doi:10.1073/pnas.1017192108

Dackor, R. T., Fritz-Six, K., Dunworth, W. P., Gibbons, C. L., Smithies, O., and Caron, K. M. (2006). Hydrops fetalis, cardiovascular defects, and embryonic lethality in mice lacking the calcitonin receptor-like receptor gene. *Mol. Cell. Biol.* 26 (7), 2511–2518. doi:10.1128/MCB.26.7.2511-2518.2006

Devisme, L., Merlot, B., Ego, A., Houfflin-Debarge, V., Deruelle, P., and Subtil, D. (2013). A case-control study of placental lesions associated with pre-eclampsia. *Int. J. Gynecol. Obstetrics* 120 (2), 165–168. doi:10.1016/j.ijgo.2012.08.023

Dong, Y. L., Vegiraju, S., Chauhan, M., and Yallampalli, C. (2003). Expression of calcitonin gene-related peptide receptor components, calcitonin receptor-like receptor and receptor activity modifying protein 1, in the rat placenta during pregnancy and their cellular localization. *Mol. Hum. Reprod.* 9 (8), 481–490. doi:10.1093/molehr/gag058

Dong, Y. L., Vegiraju, S., Chauhan, M., Gangula, P. R., Hankins, G. D., Goodrum, L., et al. (2004). Involvement of calcitonin gene-related peptide in control of human fetoplacental vascular tone. *Am. J. Physiology-Heart Circulatory Physiology* 286 (1), H230–H239. doi:10.1152/ajpheart.00140.2003

Dong, Y. L., Green, K. E., Vegiragu, S., Hankins, G. D., Martin, E., Chauhan, M., et al. (2005). Evidence for decreased calcitonin gene-related peptide (CGRP) receptors and compromised responsiveness to CGRP of fetoplacental vessels in preeclamptic pregnancies. *J. Clin. Endocrinol. Metabolism* 90 (4), 2336–2343. doi:10.1210/jc.2004-1481

Dong, Y. L., Chauhan, M., Green, K. E., Vegiraju, S., Wang, H. Q., Hankins, G. D., et al. (2006). Circulating calcitonin gene-related peptide and its placental origins in normotensive and preeclamptic pregnancies. *Am. J. Obstetrics Gynecol.* 195 (6), 1657–1667. doi:10.1016/j.ajog.2006.04.006

Dorsam, R. T., and Gutkind, J. S. (2007). G-protein-coupled receptors and cancer. *Nat. Rev. Cancer.* 7 (2), 79–94. doi:10.1038/nrc2069

Dröge, L. A., Perschel, F. H., Stütz, N., Gafron, A., Frank, L., Busjahn, A., et al. (2021). Prediction of preeclampsia-related adverse outcomes with the sFlt-1 (soluble fms-like tyrosine kinase 1)/PlGF (placental growth factor)-ratio in the clinical routine. *Hypertension* 77 (2), 461–471. doi:10.1161/HYPERTENSIONAHA.120.15146

Duley, L., Meher, S., Hunter, K. E., Seidler, A. L., and Askie, L. M. (2019). Antiplatelet agents for preventing pre-eclampsia and its complications. *Cochrane Database Syst. Rev.* 2019 (10), CD004659. doi:10.1002/14651858.CD004659.pub3

Egeland, G. M., Klungsøyr, K., Øyen, N., Tell, G. S., Næss, O., and Skjærven, R. (2016). Preconception cardiovascular risk factor differences between gestational hypertension and preeclampsia. *Hypertension* 67 (6), 1173–1180. doi:10.1161/HYPERTENSIONAHA.116.07099

Ferrazzi, E., Stampalija, T., Monasta, L., Di Martino, D., Vonck, S., and Gyselaers, W. (2018). Maternal hemodynamics: A method to classify hypertensive disorders of pregnancy. *Am. J. Obstetrics Gynecol.* 218 (1), e1–124. doi:10.1016/j.ajog.2017.10.226

Fredriksson, R., Lagerström, M. C., Lundin, L. G., and Schiöth, H. B. (2003). The G-protein-coupled receptors in the human genome form five main families. Phylogenetic analysis, paralogon groups, and fingerprints. *Mol. Pharmacol.* 63 (6), 1256–1272. doi:10.1124/mol.63.6.1256

Gao, L., He, P., Sha, J., Liu, C., Dai, L., Hui, N., et al. (2007). Corticotropin-releasing hormone receptor type 1 and type 2 mediate differential effects on 15-hydroxy prostaglandin dehydrogenase expression in cultured human chorion trophoblasts. *Endocrinology* 148 (8), 3645–3654. doi:10.1210/en.2006-1212

Gao, L., Lu, C., Xu, C., Tao, Y., Cong, B., and Ni, X. (2008). Differential regulation of prostaglandin production mediated by corticotropin-releasing hormone receptor type 1 and type 2 in cultured human placental trophoblasts. *Endocrinology* 149 (6), 2866–2876. doi:10.1210/en.2007-1377

Gao, L., Lv, C., Xu, C., Li, Y., Cui, X., Gu, H., et al. (2012a). Differential regulation of glucose transporters mediated by CRH receptor type 1 and type 2 in human placental trophoblasts. *Endocrinology* 153 (3), 1464–1471. doi:10.1210/en.2011-1673

Gao, L., Tao, Y., Hu, T., Liu, W., Xu, C., Liu, J., et al. (2012b). Regulation of estradiol and progesterone production by CRH-R1 and -R2 is through divergent signaling pathways in cultured human placental trophoblasts. *Endocrinology* 153 (10), 4918–4928. doi:10.1210/en.2012-1453

Hellman, P., Hellman, B., Juhlin, C., Juppner, H., Rastad, J., Ridefelt, P., et al. (1993). Regulation of proliferation in JEG-3 cells by a 500-kDa Ca2+ sensor and parathyroid hormone-related protein. *Archives Biochem. Biophysics* 307 (2), 379–385. doi:10.1006/abbi.1993.1603

Hamann, J., Aust, G., Araç, D., Engel, F. B., Formstone, C., Fredriksson, R., et al. (2015). International union of basic and clinical Pharmacology. XCIV. Adhesion G protein-coupled receptors. *Pharmacol. Rev.* 67 (2), 338–367. doi:10.1124/pr.114.009647

Hutcheon, J. A., Lisonkova, S., and Joseph, K. S. (2011). Epidemiology of pre-eclampsia and the other hypertensive disorders of pregnancy. *Best Pract. Res. Clin. Obstetrics Gynaecol.* 25 (4), 391–403. doi:10.1016/j.bpobgyn.2011.01.006

Hutchings, C. J. (2020). A review of antibody-based therapeutics targeting G protein-coupled receptors: An update. *Expert Opin. Biol. Ther.* 20 (8), 925–935. doi:10.1080/14712598.2020.1745770

Ishihara, N., Matsuo, H., Murakoshi, H., Laoag-Fernandez, J. B., Samoto, T., and Maruo, T. (2002). Increased apoptosis in the syncytiotrophoblast in human term placentas complicated by either preeclampsia or intrauterine growth retardation. *Am. J. Obstetrics Gynecol.* 186 (1), 158–166. doi:10.1067/mob.2002.119176

Jin, J. (2021). Use of aspirin during pregnancy to prevent preeclampsia. *JAMA* 326 (12), 1222. doi:10.1001/jama.2021.15900

Kadmiel, M., Matson, B. C., Espenschied, S. T., Lenhart, P. M., and Caron, K. M. (2017). Loss of receptor activity-modifying protein 2 in mice causes placental dysfunction and alters PTH1R regulation. *PLoS One* 12 (7), e0181597. doi:10.1371/journal.pone.0181597

Kajantie, E., Eriksson, J. G., Osmond, C., Thornburg, K., and Barker, D. J. (2009). Pre-eclampsia is associated with increased risk of stroke in the adult offspring. *Stroke* 40 (4), 1176–1180. doi:10.1161/STROKEAHA.108.538025

Kalantaridou, S. N., Zoumakis, E., Makrigiannakis, A., Godoy, H., and Chrousos, G. P. (2007). The role of corticotropin-releasing hormone in blastocyst implantation and early fetal immunotolerance. *Horm. Metab. Res.* 39 (6), 474–477. doi:10.1055/s-2007-980190

Karteris, E., Grammatopoulos, D., Dai, Y., Olah, K. B., Ghobara, T. B., Easton, A., et al. (1998). The human placenta and fetal membranes express the corticotropin-releasing hormone receptor 1α (CRH-1α) and the CRH-C variant Receptor1. *J. Clin. Endocrinol. Metabolism* 83 (4), 1376–1379. doi:10.1210/jcem.83.4.4705

Karteris, E., Goumenou, A., Koumantakis, E., Hillhouse, E. W., and Grammatopoulos, D. K. (2003). Reduced expression of corticotropin-releasing hormone receptor type-1α in human preeclamptic and growth-restricted placentas. *J. Clin. Endocrinol. Metab.* 88 (1), 363–370. doi:10.1210/jc.2002-020375

Koh, P. O., Kwak, S. D., Kim, H. J., Roh, G., Kim, J. H., Kang, S. S., et al. (2003). Expression patterns of pituitary adenylate cyclase activating polypeptide and its type I receptor mRNAs in the rat placenta. *Mol. Reprod. Dev.* 64 (1), 27–31. doi:10.1002/mrd.10221

Koh, P. O., Won, C. K., Noh, H. S., Cho, G. J., and Choi, W. S. (2005). Expression of pituitary adenylate cyclase activating polypeptide and its type I receptor mRNAs in human placenta. *J. Vet. Sci.* 6 (1), 1–5. doi:10.4142/jvs.2005.6.1.1

Kuhnert, F., Mancuso, M. R., Shamloo, A., Wang, H. T., Choksi, V., Florek, M., et al. (2010). Essential regulation of CNS angiogenesis by the orphan G protein-coupled receptor GPR124. *Science* 330 (6006), 985–989. doi:10.1126/science.1196554

Lagerström, M. C., and Schiöth, H. B. (2008). Structural diversity of G protein-coupled receptors and significance for drug discovery. *Nat. Rev. Drug Discov.* 7 (4), 339–357. doi:10.1038/nrd2518

Lappano, R., and Maggiolini, M. (2011). G protein-coupled receptors: Novel targets for drug discovery in cancer. *Nat. Rev. Drug Discov.* 10 (1), 47–60. doi:10.1038/nrd3320

Levine, R. J., Maynard, S. E., Qian, C., Lim, K. H., England, L. J., Yu, K. F., et al. (2004). Circulating angiogenic factors and the risk of preeclampsia. *N. Engl. J. Med.* 350 (7), 672–683. doi:10.1056/NEJMoa031884

Li, L., Tang, F., and O, W. S. (2010). Coexpression of adrenomedullin and its receptor component proteins in the reproductive system of the rat during gestation. *Reprod. Biol. Endocrinol.* 8, 130. doi:10.1186/1477-7827-8-130

Liang, M., Niu, J., Zhang, L., Deng, H., Ma, J., Zhou, W., et al. (2016). Gene expression profiling reveals different molecular patterns in G-protein coupled receptor signaling pathways between early- and late-onset preeclampsia. *Placenta* 40, 52–59. doi:10.1016/j.placenta.2016.02.015

Liu, A., Wen, S. W., Bottomley, J., Walker, M. C., and Smith, G. (2009). Utilization of health care services of pregnant women complicated by preeclampsia in Ontario. *Hypertens. Pregnancy* 28 (1), 76–84. doi:10.1080/10641950802366252

Lu, S., Liu, S., Wietelmann, A., Kojonazarov, B., Atzberger, A., Tang, C., et al. (2017). Developmental vascular remodeling defects and postnatal kidney failure in mice lacking Gpr116 (Adgrf5) and Eltd1 (Adgrl4). *PLoS One* 12 (8), e0183166. doi:10.1371/journal.pone.0183166

Mackie, D. I., Al Mutairi, M. F., Davis, R. B., Kechele, D. O., Nielsen, N. R., Snyder, J. C., et al. (2018). HCALCRL mutation causes autosomal recessive nonimmune hydrops fetalis with lymphatic dysplasia. *J. Exp. Med.* 215 (9), 2339–2353. doi:10.1084/jem.20180528

Majewska, M., Lipka, A., Paukszto, L., Jastrzebski, J. P., Szeszko, K., Gowkielewicz, M., et al. (2019). Placenta transcriptome profiling in intrauterine growth restriction (IUGR). *Ijms* 20 (6), 1510. doi:10.3390/ijms20061510

Makino, Y., Shibata, K., Makino, I., Kangawa, K., and Kawarabayashi, T. (2001). Alteration of the adrenomedullin receptor components gene expression associated with the blood pressure in pregnancy-induced hypertension. *J. Clin. Endocrinol. Metabolism* 86 (10), 5079. doi:10.1210/jcem.86.10.8099

Makrigiannakis, A., Zoumakis, E., Kalantaridou, S., Coutifaris, C., Margioris, A. N., Coukos, G., et al. (2001). Corticotropin-releasing hormone promotes blastocyst implantation and early maternal tolerance. *Nat. Immunol.* 2 (11), 1018–1024. doi:10.1038/ni719

Masiero, M., Simões, F. C., Han, H. D., Snell, C., Peterkin, T., Bridges, E., et al. (2013). A core human primary tumor angiogenesis signature identifies the endothelial orphan receptor ELTD1 as a key regulator of angiogenesis. *Cancer Cell* 24 (2), 229–241. doi:10.1016/j.ccr.2013.06.004

Maynard, S. E., Min, J. Y., Merchan, J., Lim, K. H., Li, J., Mondal, S., et al. (2003). Excess placental soluble fms-like tyrosine kinase 1 (sFlt1) may contribute to endothelial dysfunction, hypertension, and proteinuria in preeclampsia. *J. Clin. Invest.* 111 (5), 649–658. doi:10.1172/JCI17189

McGuane, J., and Conrad, K. (2012). GPCRs as potential therapeutic targets in preeclampsia. *Drug Discov. Today Dis. Models* 9 (3), e119–e127. doi:10.1016/j.ddmod.2012.05.001

Mongraw-Chaffin, M. L., Cirillo, P. M., and Cohn, B. A. (2010). Preeclampsia and cardiovascular disease death. *Hypertension* 56 (1), 166–171. doi:10.1161/HYPERTENSIONAHA.110.150078

Moriguchi, T., Haraguchi, K., Ueda, N., Okada, M., Furuya, T., and Akiyama, T. (2004). DREG, a developmentally regulated G protein-coupled receptor containing two conserved proteolytic cleavage sites. *Genes cells.* 9 (6), 549–560. doi:10.1111/j.1356-9597.2004.00743.x

Ouhilal, S., Vuguin, P., Cui, L., Du, X. Q., Gelling, R. W., Reznik, S. E., et al. (2012). Hypoglycemia, hyperglucagonemia, and fetoplacental defects in glucagon receptor knockout mice: A role for glucagon action in pregnancy maintenance. *Am. J. Physiology-Endocrinology Metabolism* 302 (5), E522–E531. doi:10.1152/ajpendo.00420.2011

Powe, C. E., Levine, R. J., and Karumanchi, S. A. (2011). Preeclampsia, a disease of the maternal endothelium. *Circulation* 123 (24), 2856–2869. doi:10.1161/CIRCULATIONAHA.109.853127

Powers, R. W., Roberts, J. M., Plymire, D. A., Pucci, D., Datwyler, S. A., Laird, D. M., et al. (2012). Low placental growth factor Across pregnancy identifies a subset of women with preterm preeclampsia. *Hypertension* 60 (1), 239–246. doi:10.1161/HYPERTENSIONAHA.112.191213

Purcell, R. H., and Hall, R. A. (2018). Adhesion g Protein-Coupled receptors as drug targets. *Annu. Rev. Pharmacol. Toxicol.* 58, 429–449. doi:10.1146/annurev-pharmtox-010617-052933

Quitterer, U., and AbdAlla, S. (2021). Pathological AT1R-B2R protein aggregation and preeclampsia. *Cells* 10 (10), 2609. doi:10.3390/cells10102609

Redman, C. W. (1991). Pre-eclampsia and the placenta. *Placenta* 12 (4), 301–308. doi:10.1016/0143-4004(91)90339-h

Redman, C. W., Sacks, G. P., and Sargent, I. L. (1999). Preeclampsia: An excessive maternal inflammatory response to pregnancy. *Am. J. Obstetrics Gynecol.* 180 (2), 499–506. doi:10.1016/s0002-9378(99)70239-5

Redman, C., Staff, A. C., and Roberts, J. M. (2022). Syncytiotrophoblast stress in preeclampsia: The convergence point for multiple pathways. *Am. J. Obstetrics Gynecol.* 226, S907–S927. doi:10.1016/j.ajog.2020.09.047

Redman, C. W., and Staff, A. C. (2015). Preeclampsia, biomarkers, syncytiotrophoblast stress, and placental capacity. *Am. J. Obstetrics Gynecol.* 213 (4), e1–S9. S9-S11. doi:10.1016/j.ajog.2015.08.003

Reglodi, D., Borzsei, R., Bagoly, T., Boronkai, A., Racz, B., Tamas, A., et al. (2008). Agonistic behavior of PACAP6-38 on sensory nerve terminals and cytotrophoblast cells. *J. Mol. Neurosci.* 36 (1-3), 270–278. doi:10.1007/s12031-008-9089-z

Riddy, D. M., Delerive, P., Summers, R. J., Sexton, P. M., and Langmead, C. J. (2018). G Protein-Coupled receptors targeting insulin resistance, obesity, and type 2 diabetes mellitus. *Pharmacol. Rev.* 70 (1), 39–67. doi:10.1124/pr.117.014373

Say, L., Chou, D., Gemmill, A., Tunçalp, O., Moller, A. B., Daniels, J., et al. (2014). Global causes of maternal death: A WHO systematic analysis. *Lancet Glob. Health* 2 (6), e323–e333. doi:10.1016/S2214-109X(14)70227-X

Scaldaferri, M. L., Modesti, A., Palumbo, C., Ulisse, S., Fabbri, A., Piccione, E., et al. (2000). Pituitary adenylate cyclase-activating polypeptide (PACAP) and PACAP-receptor type 1 expression in rat and human Placenta1. *Endocrinology* 141 (3), 1158–1167. doi:10.1210/endo.141.3.7346

Shen, H., Jin, M., Gu, S., Wu, Y., Yang, M., and Hua, X. (2020). CD97 is decreased in preeclamptic placentas and promotes human trophoblast invasion through PI3K/Akt/mTOR signaling pathway. *Reprod. Sci.* 27 (8), 1553–1561. doi:10.1007/s43032-020-00183-w

Sheppard, B. L., and Bonnar, J. (1976). The ultrastructure of the arterial supply of the human placenta in pregnancy complicated by fetal growth retardation. *BJOG: An Int. J. O&G* 83 (12), 948–959. doi:10.1111/j.1471-0528.1976.tb00781.x

Sirico, A., Dell'Aquila, M., Tartaglione, L., Moresi, S., Farì, G., Pitocco, D., et al. (2021). PTH-rP and PTH-R1 expression in placentas from pregnancies complicated by gestational diabetes: New insights into the pathophysiology of hyperglycemia in pregnancy. *Diagnostics* 11 (8), 1356. doi:10.3390/diagnostics11081356

Skjærven, R., Wilcox, A. J., and Lie, R. T. (2002). The interval between pregnancies and the risk of preeclampsia. *N. Engl. J. Med.* 346 (1), 33–38. doi:10.1056/NEJMoa011379

Stehlik, C., Kroismayr, R., Dorfleutner, A., Binder, B. R., and Lipp, J. (2004). Vigr - a novel inducible adhesion family G-protein coupled receptor in endothelial cells. *FEBS Lett.* 569 (1-3), 149–155. doi:10.1016/j.febslet.2004.05.038

Tannetta, D. S., Hunt, K., Jones, C. I., Davidson, N., Coxon, C. H., Ferguson, D., et al. (2015). Syncytiotrophoblast extracellular Vesicles from pre-eclampsia placentas differentially affect platelet function. *PLoS One* 10 (11), e0142538. doi:10.1371/journal.pone.0142538

Torregrosa-Carrión, R., Piñeiro-Sabarís, R., Siguero-Álvarez, M., Grego-Bessa, J., Luna-Zurita, L., Fernandes, V. S., et al. (2021). Adhesion G protein-coupled receptor Gpr126/Adgrg6 is essential for placental development. *Sci. Adv.* 7 (46), j5445. doi:10.1126/sciadv.abj5445

Tsatsaris, V., Tarrade, A., Merviel, P., Garel, J. M., Segond, N., Jullienne, A., et al. (2002). Calcitonin gene-related peptide (CGRP) and CGRP receptor expression at the human implantation site. *J. Clin. Endocrinol. Metabolism* 87 (9), 4383–4390. doi:10.1210/jc.2002-020138

Tuovinen, S., Räikkönen, K., Pesonen, A. K., Lahti, M., Heinonen, K., Wahlbeck, K., et al. (2012). Hypertensive disorders in pregnancy and risk of severe mental disorders in the offspring in adulthood: The Helsinki Birth Cohort Study. *J. Psychiatric Res.* 46 (3), 303–310. doi:10.1016/j.jpsychires.2011.11.015

Vallon, M., and Essler, M. (2006). Proteolytically processed soluble tumor endothelial marker (TEM) 5 mediates endothelial cell survival during angiogenesis by linking integrin αvβ3 to glycosaminoglycans. *J. Biol. Chem.* 281 (45), 34179–34188. doi:10.1074/jbc.M605291200

Waller-Evans, H., Prömel, S., Langenhan, T., Dixon, J., Zahn, D., Colledge, W. H., et al. (2010). The orphan adhesion-GPCR GPR126 is required for embryonic development in the mouse. *PLoS One* 5 (11), e14047. doi:10.1371/journal.pone.0014047

Wang, T., Ward, Y., Tian, L., Lake, R., Guedez, L., Stetler-Stevenson, W. G., et al. (2005). CD97, an adhesion receptor on inflammatory cells, stimulates angiogenesis through binding integrin counterreceptors on endothelial cells. *Blood* 105 (7), 2836–2844. doi:10.1182/blood-2004-07-2878

Wang, J., Gareri, C., and Rockman, H. A. (2018). G-Protein-Coupled receptors in heart disease. *Circ. Res.* 123 (6), 716–735. doi:10.1161/CIRCRESAHA.118.311403

Wu, C. T., Hilgendorf, K. I., Bevacqua, R. J., Hang, Y., Demeter, J., Kim, S. K., et al. (2021). Discovery of ciliary G protein-coupled receptors regulating pancreatic islet insulin and glucagon secretion. *Genes Dev.* 35 (17-18), 1243–1255. doi:10.1101/gad.348261.121

Xiong, X., Demianczuk, N. N., Saunders, L. D., Wang, F. L., and Fraser, W. D. (2002). Impact of preeclampsia and gestational hypertension on birth weight by gestational age. *Am. J. Epidemiol.* 155 (3), 203–209. doi:10.1093/aje/155.3.203

Yoo, J. Y., Ahn, J. I., Kim, T. H., Yu, S., Ahn, J. Y., Lim, J. M., et al. (2017). G-protein coupled receptor 64 is required for decidualization of endometrial stromal cells. *Sci. Rep.* 7 (1), 5021. doi:10.1038/s41598-017-05165-8

Younes, S. T., Maeda, K. J., Sasser, J., and Ryan, M. J. (2020). The glucagon-like peptide 1 receptor agonist liraglutide attenuates placental ischemia-induced hypertension. *Am. J. Physiology-Heart Circulatory Physiology* 318 (1), H72–H77. doi:10.1152/ajpheart.00486.2019

Zaki, M., Greenwood, C., and Redman, C. W. (2003). The spontaneous reversal of pre-eclampsia associated with parvovirus-induced hydrops and the placental theory of pre-eclampsia: A case report. *BJOG Intern. J. Obs Gyn* 110 (12), 1125–1126. doi:10.1111/j.1471-0528.2003.03060.x

Zhang, X., Green, K. E., Yallampalli, C., and Dong, Y. L. (2005). Adrenomedullin enhances invasion by trophoblast cell Lines1. *Biol. Reprod.* 73 (4), 619–626. doi:10.1095/biolreprod.105.040436

Zhang, B., Kim, M. Y., Elliot, G., Zhou, Y., Zhao, G., Li, D., et al. (2021). Human placental cytotrophoblast epigenome dynamics over gestation and alterations in placental disease. *Dev. Cell* 56 (9), 1238–1252. doi:10.1016/j.devcel.2021.04.001

Zhou, J., and Wild, C. (2019). GPCR drug discovery: Emerging targets, novel approaches and future trends. *Curr. Top. Med. Chem.* 19 (16), 1363–1364. doi:10.2174/1568026619161908280935000

frontiers | Frontiers in Cell and Developmental Biology

TYPE Mini Review
PUBLISHED 03 November 2022
DOI 10.3389/fcell.2022.1005681

OPEN ACCESS

EDITED BY
Rujuan Zuo,
Oslo University Hospital, Norway

REVIEWED BY
Muhammad Khan,
University of the Punjab, Pakistan
Qingzheng Kang,
Shenzhen University, China

*CORRESPONDENCE
Maozhen Han,
hanmz@ahmu.edu.cn
Binbin Huang,
huangbb91@126.com

†These authors have contributed equally to this work

SPECIALTY SECTION
This article was submitted to Cellular Biochemistry, a section of the journal Frontiers in Cell and Developmental Biology

RECEIVED 28 July 2022
ACCEPTED 17 October 2022
PUBLISHED 03 November 2022

CITATION
Zhang L, Zeng F, Jiang M, Han M and Huang B (2022), Roles of osteoprotegerin in endocrine and metabolic disorders through receptor activator of nuclear factor kappa-B ligand/receptor activator of nuclear factor kappa-B signaling. *Front. Cell Dev. Biol.* 10:1005681. doi: 10.3389/fcell.2022.1005681

Roles of osteoprotegerin in endocrine and metabolic disorders through receptor activator of nuclear factor kappa-B ligand/receptor activator of nuclear factor kappa-B signaling

Luodan Zhang[1†], Fa Zeng[2†], Minmin Jiang[3,4], Maozhen Han[5*] and Binbin Huang[4*]

[1]Department of Nephrology, Anhui Provincial Children's Hospital, Children's Hospital of Anhui Medical University, Hefei, Anhui, China, [2]Shenzhen Longhua Maternity and Child Healthcare Hospital, Shenzhen, Guangdong, China, [3]Department of Occupational Health and Environmental Health, School of Public Health, Anhui Medical University, Hefei, Anhui, China, [4]Department of Maternal, Child and Adolescent Health, School of Public Health, Anhui Medical University, MOE Key Laboratory of Population Health Across Life Cycle, NHC Key Laboratory of Study on Abnormal Gametes and Reproductive Tract, Anhui Provincial Key Laboratory of Population Health and Aristogenics, Hefei, Anhui, China, [5]College of Life Science, Anhui Medical University, Hefei, Anhui, China

Endocrine and metabolic diseases show increasing incidence and high treatment costs worldwide. Due to the complexity of their etiology and mechanism, therapeutic strategies are still lacking. Osteoprotegerin (OPG), a member of the tumor necrosis factor receptor superfamily, appears to be a potential candidate for the treatment of these diseases. Studies based on clinical analysis and rodent animal models reveal the roles of OPG in various endocrine and metabolic processes or disorders, such as bone remodeling, vascular calcification, and β-cell proliferation, through the receptor activator of nuclear factor kappa-B ligand (RANKL) and the receptor activator of NF-κB (RANK). Thus, in this review, we mainly focus on relevant diseases, including osteoporosis, cardiovascular disease (CVD), diabetes, and gestational diabetes mellitus (GDM), to summarize the effects of the RANKL/RANK/OPG system in endocrine and metabolic tissues and diseases, thereby providing a comprehensive insight into OPG as a potential drug for endocrine and metabolic diseases.

KEYWORDS

nuclear factor kappa-B ligand, receptor activator of NF-κB, osteoprotegerin, osteoporosis, cardiovascular disease, gestational diabetes mellitus

Introduction

Endocrine and metabolic disorders have become global health challenges due to their complications in physiological and pathological processes in multiple endocrine and metabolic tissues, which are risk factors for many diseases, such as osteoporosis, cardiovascular disease, diabetes mellitus, and pregnancy complications (Khosla and Hofbauer, 2017; Schafer et al., 2017; Helfer and Wu, 2018). To date, some key signaling systems responsible for the regulation of endocrine and metabolic processes have been revealed. Among them, RANKL/RANK signaling is a critical participant in endocrine metabolism (Kiechl et al., 2013; Kondegowda et al., 2015).

RANKL, a transmembrane ligand belonging to the TNF superfamily, is a crucial regulator of bone resorption and is a type II transmembrane glycoprotein composed of 317 amino acid residues (Anderson et al., 1997). RANKL can bind to RANK on neighboring cells and activate NF-κB signaling to regulate biological processes, such as the cell cycle, proliferation, differentiation, and apoptosis (Blomberg Jensen et al., 2021). RANKL is involved in regulating many processes, such as immune surveillance, bone resorption, monocyte chemotaxis, fibrosis, β-cell proliferation, and glucose homeostasis (Bernardi et al., 2016; Huang et al., 2020). RANKL can be found in membrane-bound and soluble forms, in which RANKL binds to two other RANKL molecules to form a trimer that binds to the receptor RANK (Rinotas et al., 2020). RANKL/RANK acts as a major regulator of BRCA1/BRCA2 mutations and is involved in controlling the development of breast cancer by inhibiting NF-κB activation and EGFR signaling (Galluzzi et al., 2016; Sirinian et al., 2018). RANKL mRNA in the bone marrow and lymphoid tissues with high expression, especially through the specific receptor RANK on osteoclast cells, promotes osteoclast maturation and inhibits osteoclast apoptosis. One study using a RANKL monoclonal antibody to block the specific binding of RANKL and RANK verified that the inhibition of osteoclasts could significantly increase the bone density of each place with a low bone mass after menopause and effectively reduce the conversion rate of bones (Kostenuik et al., 2009).

OPG acts as a soluble secreted glycoprotein first discovered by Simon et al. in the intestine of rats in 1997. OPG is a new member of the tumor necrosis factor receptor superfamily that can inhibit differentiation and maturation in osteoclasts and increase the bone density (Simonet et al., 1997). OPG is expressed in the healthy and pathological statuses of various tissues, including the bone, heart, blood vessels, kidney, liver, spleen, thymus, lymph nodes, placenta, adipose tissue, and pancreas (Shen et al., 2012; Bernardi et al., 2016). Indeed, OPG is a fusion receptor that selectively binds to RANKL and inhibits bone resorption, acting as a decoy receptor (Kwon et al., 1998; Akinci et al., 2011).

Receptor activator of nuclear factor kappa-B ligand/receptor activator of nuclear factor kappa-B system regulates bone development

The bone is a special endocrine tissue that can protect the body organs and the hematopoietic bone marrow, providing structural support for muscles and maintaining the balance of ions and factors in vertebrates (Siddiqui and Partridge, 2016). The most striking function of the bone is paracrine signaling originating from bone cells. Current research has confirmed that the bone can be used as an endocrine organ (Zhou et al., 2021). The main components of a bone include osteoblasts, osteocytes, marrow adipocyte tissue, and mineralized fibrous tissue (Zhang et al., 2015; Lecka-Czernik et al., 2017). The RANKL/RANK/OPG system participates in pathological and physiological processes by secreting bone-derived hormones (Ferron et al., 2008; DiGirolamo et al., 2012; Wei et al., 2015; Zhang et al., 2015; Bernardi et al., 2016). RANKL can activate RANK in osteoclast precursor cells by residing in bone-forming cells and inducing osteoclastogenesis to promote bone resorption (Ikebuchi et al., 2018). Moreover, OPG acts as a natural inhibitor of RANKL and protects against bone loss in a mouse model (Simonet et al., 1997). OPG binds to RANKL and blocks the activation of RANK, which prevents bone resorption by differentiation and activation in osteoclasts (Ono et al., 2020). In clinics, there is a drug targeting RANKL, denosumab (Dmab), a monoclonal antibody that has been broadly used to treat osteoporosis and decrease the risk of fractures (McCloskey et al., 2012). Collectively, both osteogenesis and bone resorption are two key processes for bone remodeling, which is regulated by RANKL in osteocytes, suggesting that it is possible to use OPG as a natural biological inhibitor of RANKL for the treatment of bone-related diseases.

Osteoprotegerin ameliorates cardiovascular disorders through the receptor activator of nuclear factor kappa-B ligand/receptor activator of nuclear factor kappa-B signaling

Cardiovascular diseases (CVDs) remain the leading cause of death and premature disability. In 2019, there were more than 523 million patients with CVD worldwide, of which approximately 18.6 million died from CVD (Roth et al., 2020). By 2020, cardiovascular diseases, such as atherosclerosis, had become the main cause of the total disease burden (Mozaffarian, 2016). These findings reinforce

the need for diagnostic and prognostic tools that are helpful for CVD interventions. OPG levels were strongly correlated with arterial stiffness and the number of atherosclerotic sites in dysmetabolic patients (Monseu et al., 2016). Plasma OPG levels were increased in hypertensive patients compared to normal blood pressure volunteers, and serum OPG levels were significantly correlated with inflammation and hypertension, which may be used as a predictive indicator of hypertensive vascular endothelial dysfunction (Stepien et al., 2011; Arnold et al., 2019). Moreover, hypertensive patients with high plasma OPG levels are significantly more likely to have three or more target organ (cardiac, vascular, and renal) lesions at 10 years of cardiovascular risk for hypertensive retinopathy (Blazquez-Medela et al., 2012). These studies indicate that an increase in OPG levels might play a potential role in cardiovascular diseases. Recent research studies have indicated that vascular calcification is likely to be traditionally associated with the OPG/RANKL signaling system, which regulates bone remodeling. RANKL promoted vascular calcification, a disorder that causes blood vessel hardening and dysfunction (Lee et al., 2019), acting as a significant risk factor for type 2 diabetes mellitus, which is strongly associated with cardiovascular complications. Vascular calcification can be blocked by OPG acting as a RANKL decoy receptor (Ndip et al., 2011; Harper et al., 2016). An OPG-knockout mouse model showed aortic calcification, suggesting that OPG could protect large blood vessels from medial calcification (Callegari et al., 2013). These studies indicate that OPG could prevent vascular calcification.

In addition, experimental studies have shown that OPG can promote the adhesion of immune cells on endothelial cells, which is an important barrier to maintain the integrity of the inner surface of blood vessels, and its damage is the beginning of atherosclerosis, while the lack of OPG can cause endothelial cell damage (Rochette et al., 2018). With high OPG concentrations, endothelial cells stimulated by the vascular endothelial growth factor are more likely to survive. However, the mechanisms of OPG and RANKL remain to be determined and remain controversial in cardiovascular diseases. Hence, there might be an underlying mechanism involved in cardiovascular functions along with RANKL/RANK/OPG signaling.

Osteoprotegerin affects glucose homeostasis

Diabetes results in insufficient absolute insulin secretion, resulting in higher blood glucose and causing metabolic disorders and even damage to multiple systems. Diabetes kills more than 3 million people worldwide each year, making it the third leading cause of death from cardiovascular diseases and tumors (Corona et al., 2011). Diabetes can be divided into type 1 and 2 diabetes, according to the etiology of diabetes. Moderate-type diabetes accounts for more than 90% of the total incidence. Insulin deficiency and insulin resistance are two indispensable causes of diabetes. In insulin-dependent diabetes mellitus, islet cells can secrete a certain amount of insulin, but the sensitivity of insulin is reduced, resulting in relative insulin deficiency in the body and causing metabolic disorders in the body and hyperglycemia. The main pathogenesis of diabetes is the inability of β-cells to secrete insulin required for metabolism, resulting in an imbalance in blood glucose homeostasis (Arnes and Sussel, 2015). Bone metabolism has received increasing attention regarding the regulation of blood glucose homeostasis. In a clinical study, an increase in serum OPG levels was reported in both patients with type 1 and type 2 diabetes mellitus compared to normal controls by different groups of investigators (Browner et al., 2001; Knudsen et al., 2003; Galluzzi et al., 2005; Giovannini et al., 2017). There is a strong potential association between OPG and diabetes. Rodent animal models reveal that OPG is a common gene upregulated in islets involved in β-cell replication from the models of β-cell expansion that include pregnancy, obesity, insulin resistance, and β-cell regeneration (Rieck et al., 2009). OPG regulated the proliferation of β-cells in young and old rodent models of diabetes mellitus through prolactin (Kondegowda et al., 2015). OPG-knockout mice and the inflammation induced by lipopolysaccharides (LPS) in a mouse model show an obvious decline in insulin secretion and impaired glucose tolerance. After the artificial addition of exogenous OPG, the symptoms are evidently improved, suggesting that OPG can increase the secretion of insulin, which regulates blood glucose homeostasis (Kuroda et al., 2016). In addition, in animal experiments, a high-fat diet can induce the upregulation of OPG levels in mice. In contrast, after exogenous injection of human OPG molecular protein, the blood glucose of mice is disturbed and their glucose tolerance is significantly impaired, resulting in impaired insulin secretion in mice (Toffoli et al., 2011; Bernardi et al., 2014). Human OPG induces inflammation in mice, leading to the death of cells, which has the opposite effect, with the consequence of disordered regulation of glucose metabolism (Kondegowda et al., 2015). Whether Dmab, as a targeted drug for osteoporosis, can control glucose remains to be deeply investigated in the future.

Osteoprotegerin attenuated symptoms in gestational diabetes mellitus

Previously, different studies have elucidated the specific role of the RANKL/RANK/OPG system in mammary tissues, including gland physiology and hormone-driven epithelial proliferation during pregnancy (Infante et al., 2019). In

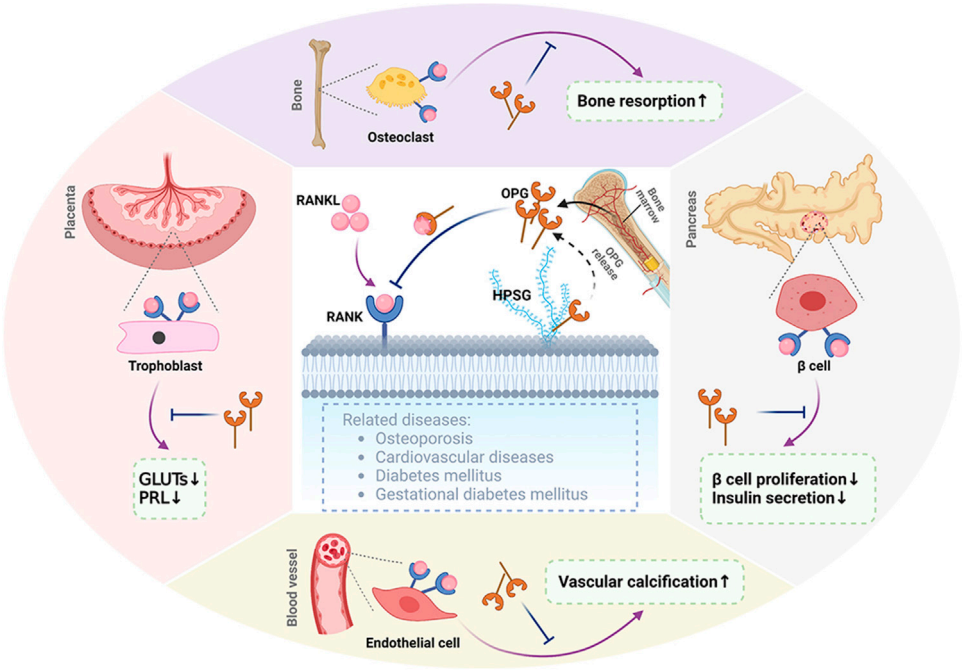

FIGURE 1
Representation of RANKL/RANK/OPG. RANKL binds to its receptor RANK, which can be found in membrane-bound molecules involved in bone resorption in osteoclasts, decreasing GLUT and PRL expression levels in the placenta, vascular calcification in blood vessels, and inhibiting β-cell proliferation and insulin secretion in islets. Osteoprotegerin (OPG), as a decoy receptor for RANKL, is secreted by the bone marrow and as a secreted glycoprotein. OPG competitively binds to RANKL to inhibit some functions of RANKL/RANK signaling in the bone, placenta, blood vessels, and pancreas. In addition, OPG binds to glycosaminoglycans such as heparin sulfate proteoglycans (HSPGs). OPG, osteoprotegerin; RANK, receptor activator of nuclear factor kappa-B; RANKL, receptor activator of nuclear factor kappa-B ligand; GLUTs, glucose transport proteins; PRL, prolactin. The figure was created with BioRender.com.

addition, progesterone induces RANKL expression levels in both mice and humans (Liu et al., 2019), suggesting that RANKL might play roles in physiological processes during pregnancy. Regarding pregnancy complications, we mainly referred to hypertension and hyperglycemia during pregnancy. There was a significant increase in OPG during pregnancy, and the serum OPG rapidly decreased to the prepregnancy level after delivery, which is consistent with a previous experiment on mice (Yano et al., 2001; Naylor et al., 2003).

Pregnant women are first tested for impaired glucose tolerance and are diagnosed with GDM. Complications associated with gestational diabetes include overweight newborn infants or excessive babies, increased perinatal mortality, and risk of type 2 diabetes in offspring (Canouil et al., 2021). According to the International Diabetes Federation (IDF), the incidence of GDM has reached 16.8% in recent years. Retrospective clinical studies showed that the circulating levels of OPG in women with a history of GDM were significantly increased compared to normal women later in life, and they were positively correlated with various metabolic diseases with a high incidence later in life (Akinci et al., 2011; Telejko et al., 2015). We also have proven that placenta-derived OPG could regulate β-cell proliferation and glucose metabolism in placental glucose involved in glucose homeostasis in pregnant mice (Huang et al., 2020). OPG could promote glucose homeostasis during pregnancy, while there is no direct evidence to prove that OPG regulates hypertension during pregnancy. Taken together, these findings indicate that OPG seems to be a potential natural biology inhibitor for the treatment of pregnancy complications.

Conclusion and prospects

In summary, the RANKL/RANK/OPG system is important for homeostasis, CVD, bone diseases, and diabetes and has been one of the most important advances in physiology and biology in the past decade, as shown in Figure 1. The discovery of RANKL, RANK, and OPG has led to the development of specific inhibitors of RANKL, such as OPG, and a monoclonal antibody to RANKL has been tested in humans in clinical trials. Whether there are adverse effects on these tissues, especially on immune response,

still needs to be clarified for the application of the RANKL/RANK/OPG system as a drug target.

Data availability statement

The original contributions presented in the study are included in the article/supplementary material. Further inquiries can be directed to the corresponding authors.

Author contributions

LZ and BH wrote this manuscript. BH, MH, FZ, MJ, and LZ revised and edited this manuscript. All authors contributed to the article and approved the submitted version.

Funding

This study was supported by the National Natural Science Foundation of China (82103857 and 82003419), the Natural Science Foundation in Higher Education of Anhui (KJ2020A0152 and KJ2021A0244), the Anhui Provincial Natural Science Foundation (2208085QH231), the Grants for Scientific Research of BSKY (XJ2020012), and research on the clinical prevention and control model of birth defects based on accurate information management (2022061).

Conflict of interest

The authors declare that the research was conducted in the absence of any commercial or financial relationships that could be construed as a potential conflict of interest.

Publisher's note

All claims expressed in this article are solely those of the authors and do not necessarily represent those of their affiliated organizations, or those of the publisher, the editors, and the reviewers. Any product that may be evaluated in this article, or claim that may be made by its manufacturer, is not guaranteed or endorsed by the publisher.

References

Akinci, B., Celtik, A., Yuksel, F., Genc, S., Yener, S., Secil, M., et al. (2011). Increased osteoprotegerin levels in women with previous gestational diabetes developing metabolic syndrome. *Diabetes Res. Clin. Pract.* 91 (1), 26–31. doi:10.1016/j.diabres.2010.09.028

Anderson, D. M., Maraskovsky, E., Billingsley, W. L., Dougall, W. C., Tometsko, M. E., Roux, E. R., et al. (1997). A homologue of the TNF receptor and its ligand enhance T-cell growth and dendritic-cell function. *Nature* 390 (6656), 175–179. doi:10.1038/36593

Arnes, L., and Sussel, L. (2015). Epigenetic modifications and long noncoding RNAs influence pancreas development and function. *Trends Genet.* 31 (6), 290–299. doi:10.1016/j.tig.2015.02.008

Arnold, N. D., Pickworth, J. A., West, L. E., Dawson, S., Carvalho, J. A., Casbolt, H., et al. (2019). A therapeutic antibody targeting osteoprotegerin attenuates severe experimental pulmonary arterial hypertension. *Nat. Commun.* 10 (1), 5183. doi:10.1038/s41467-019-13139-9

Bernardi, S., Bossi, F., Toffoli, B., and Fabris, B. (2016). Roles and clinical applications of OPG and TRAIL as biomarkers in cardiovascular disease. *Biomed. Res. Int.* 2016, 1752854. doi:10.1155/2016/1752854

Bernardi, S., Fabris, B., Thomas, M., Toffoli, B., Tikellis, C., Candido, R., et al. (2014). Osteoprotegerin increases in metabolic syndrome and promotes adipose tissue proinflammatory changes. *Mol. Cell. Endocrinol.* 394 (1-2), 13–20. doi:10.1016/j.mce.2014.06.004

Blazquez-Medela, A. M., Garcia-Ortiz, L., Gomez-Marcos, M. A., Recio-Rodriguez, J. I., Sanchez-Rodriguez, A., Lopez-Novoa, J. M., et al. (2012). Osteoprotegerin is associated with cardiovascular risk in hypertension and/or diabetes. *Eur. J. Clin. Invest.* 42 (5), 548–556. doi:10.1111/j.1365-2362.2011.02619.x

Blomberg Jensen, M., Andreassen, C. H., Jorgensen, A., Nielsen, J. E., Juel Mortensen, L., Boisen, I. M., et al. (2021). RANKL regulates male reproductive function. *Nat. Commun.* 12 (1), 2450. doi:10.1038/s41467-021-22734-8

Browner, W. S., Lui, L. Y., and Cummings, S. R. (2001). Associations of serum osteoprotegerin levels with diabetes, stroke, bone density, fractures, and mortality in elderly women. *J. Clin. Endocrinol. Metab.* 86 (2), 631–637. doi:10.1210/jcem.86.2.7192

Callegari, A., Coons, M. L., Ricks, J. L., Yang, H. L., Gross, T. S., Huber, P., et al. (2013). Bone marrow- or vessel wall-derived osteoprotegerin is sufficient to reduce atherosclerotic lesion size and vascular calcification. *Arterioscler. Thromb. Vasc. Biol.* 33 (11), 2491–2500. doi:10.1161/ATVBAHA.113.301755

Canouil, M., Khamis, A., Keikkala, E., Hummel, S., Lobbens, S., Bonnefond, A., et al. (2021). Epigenome-wide association study reveals methylation loci associated with offspring gestational diabetes mellitus exposure and maternal methylome. *Diabetes Care* 44 (9), 1992–1999. doi:10.2337/dc20-2960

Corona, G., Monami, M., Rastrelli, G., Aversa, A., Sforza, A., Lenzi, A., et al. (2011). Type 2 diabetes mellitus and testosterone: A meta-analysis study. *Int. J. Androl.* 34, 528–540. doi:10.1111/j.1365-2605.2010.01117.x

DiGirolamo, D. J., Clemens, T. L., and Kousteni, S. (2012). The skeleton as an endocrine organ. *Nat. Rev. Rheumatol.* 8 (11), 674–683. doi:10.1038/nrrheum.2012.157

Dorota, D. K., Bogdan, K. G., Mieczyslaw, G., Bozena, L. G., and Jan, O. (2012). The concentrations of markers of bone turnover in normal pregnancy and preeclampsia. *Hypertens. Pregnancy* 31 (1), 166–176. doi:10.3109/10641955.2010.484084

Ferron, M., Hinoi, E., Karsenty, G., and Ducy, P. (2008). Osteocalcin differentially regulates beta cell and adipocyte gene expression and affects the development of metabolic diseases in wild-type mice. *Proc. Natl. Acad. Sci. U. S. A.* 105 (13), 5266–5270. doi:10.1073/pnas.0711119105

Galluzzi, F., Stagi, S., Salti, R., Toni, S., Piscitelli, E., Simonini, G., et al. (2005). Osteoprotegerin serum levels in children with type 1 diabetes: A potential modulating role in bone status. *Eur. J. Endocrinol.* 153 (6), 879–885. doi:10.1530/eje.1.02052

Galluzzi, L., Buque, A., and Kroemer, G. (2016). Prevention of breast cancer by RANKL/RANK blockade. *Cell Res.* 26 (7), 751–752. doi:10.1038/cr.2016.79

Giovannini, S., Tinelli, G., Biscetti, F., Straface, G., Angelini, F., Pitocco, D., et al. (2017). Serum high mobility group box-1 and osteoprotegerin levels are associated with peripheral arterial disease and critical limb ischemia in type 2 diabetic subjects. *Cardiovasc. Diabetol.* 16 (1), 99. doi:10.1186/s12933-017-0581-z

Harper, E., Forde, H., Davenport, C., Rochfort, K. D., Smith, D., and Cummins, P. M. (2016). Vascular calcification in type-2 diabetes and cardiovascular disease: Integrative roles for OPG, RANKL and TRAIL. *Vasc. Pharmacol.* 82, 30–40. doi:10.1016/j.vph.2016.02.003

Helfer, G., and Wu, Q. F. (2018). Chemerin: A multifaceted adipokine involved in metabolic disorders. *J. Endocrinol.* 238 (2), R79–R94. doi:10.1530/JOE-18-0174

Huang, B., Zhu, W., Zhao, H., Zeng, F., Wang, E., Wang, H., et al. (2020). Placenta-derived osteoprotegerin is required for glucose homeostasis in gestational diabetes mellitus. *Front. Cell Dev. Biol.* 8, 563509. doi:10.3389/fcell.2020.563509

Ikebuchi, Y., Aoki, S., Honma, M., Hayashi, M., Sugamori, Y., Khan, M., et al. (2018). Coupling of bone resorption and formation by RANKL reverse signalling. *Nature* 561 (7722), 195–200. doi:10.1038/s41586-018-0482-7

Infante, M., Fabi, A., Cognetti, F., Gorini, S., Caprio, M., and Fabbri, A. (2019). RANKL/RANK/OPG system beyond bone remodeling: Involvement in breast cancer and clinical perspectives. *J. Exp. Clin. Cancer Res.* 38 (1), 12. doi:10.1186/s13046-018-1001-2

Khosla, S., and Hofbauer, L. C. (2017). Osteoporosis treatment: Recent developments and ongoing challenges. *Lancet. Diabetes Endocrinol.* 5 (11), 898–907. doi:10.1016/S2213-8587(17)30188-2

Kiechl, S., Wittmann, J., Giaccari, A., Knoflach, M., Willeit, P., Bozec, A., et al. (2013). Blockade of receptor activator of nuclear factor-κB (RANKL) signaling improves hepatic insulin resistance and prevents development of diabetes mellitus. *Nat. Med.* 19 (3), 358–363. doi:10.1038/nm.3084

Knudsen, S., Foss, C., Poulsen, P., Andersen, N., Mogensen, C., and Rasmussen, L. (2003). Increased plasma concentrations of osteoprotegerin in type 2 diabetic patients with microvascular complications. *Diabetes* 52, A21.

Kondegowda, N. G., Fenutria, R., Pollack, I. R., Orthofer, M., Garcia-Ocana, A., Penninger, J. M., et al. (2015). Osteoprotegerin and denosumab stimulate human beta cell proliferation through inhibition of the receptor activator of NF-kappa B ligand pathway. *Cell Metab.* 22 (1), 77–85. doi:10.1016/j.cmet.2015.05.021

Kostenuik, P. J., Nguyen, H. Q., McCabe, J., Warmington, K. S., Kurahara, C., Sun, N., et al. (2009). Denosumab, a fully human monoclonal antibody to RANKL, inhibits bone resorption and increases BMD in knock-in mice that express chimeric (Murine/Human) RANKL. *J. Bone Min. Res.* 24 (2), 182–195. doi:10.1359/jbmr.081112

Kuroda, Y., Maruyama, K., Fujii, H., Sugawara, I., Ko, S. B. H., Yasuda, H., et al. (2016). Osteoprotegerin regulates pancreatic beta-cell homeostasis upon microbial invasion. *Plos One* 11 (1). e0146544 doi:10.1371/journal.pone.0146544

Kwon, B. S., Wang, S., Udagawa, N., Haridas, V., Lee, Z. H., Kim, K. K., et al. (1998). TR1, a new member of the tumor necrosis factor receptor superfamily, induces fibroblast proliferation and inhibits osteoclastogenesis and bone resorption. *FASEB J.* 12 (10), 845–854. doi:10.1096/fasebj.12.10.845

Lecka-Czernik, B., Stechschulte, L. A., Czernik, P. J., Sherman, S. B., Huang, S., and Krings, A. (2017). Marrow adipose tissue: Skeletal location, sexual dimorphism, and response to sex steroid deficiency. *Front. Endocrinol.* 8, 188. doi:10.3389/fendo.2017.00188

Lee, G. L., Yeh, C. C., Wu, J. Y., Lin, H. C., Wang, Y. F., Kuo, Y. Y., et al. (2019). TLR2 promotes vascular smooth muscle cell chondrogenic differentiation and consequent calcification via the concerted actions of osteoprotegerin suppression and IL-6-mediated RANKL induction. *Arterioscler. Thromb. Vasc. Biol.* 39 (3), 432–445. doi:10.1161/ATVBAHA.118.311874

Liu, S., Yin, P., Kujawa, S. A., Coon, J. S. T., Okeigwe, I., and Bulun, S. E. (2019). Progesterone receptor integrates the effects of mutated MED12 and altered DNA methylation to stimulate RANKL expression and stem cell proliferation in uterine leiomyoma. *Oncogene* 38 (15), 2722–2735. doi:10.1038/s41388-018-0612-6

McCloskey, E. V., Johansson, H., Oden, A., Austin, M., Siris, E., Wang, A., et al. (2012). Denosumab reduces the risk of osteoporotic fractures in postmenopausal women, particularly in those with moderate to high fracture risk as assessed with FRAX. *J. Bone Min. Res.* 27 (7), 1480–1486. doi:10.1002/jbmr.1606

Monseu, M., Dubois, S., Boursier, J., Aube, C., Gagnadoux, F., Leftheriotis, G., et al. (2016). Osteoprotegerin levels are associated with liver fat and liver markers in dysmetabolic adults. *Diabetes Metab.* 42 (5), 364–367. doi:10.1016/j.diabet.2016.02.004

Mozaffarian, M. (2016). Heart disease and stroke statistics-2016 update: A report from the American heart association. *Circulation* 133 (15), E599. doi:10.1161/Cir.0000000000000409

Naylor, K. E., Rogers, A., Fraser, R. B., Hall, V., Eastell, R., Blumsohn, A., et al. (2003). Serum osteoprotegerin as a determinant of bone metabolism in a longitudinal study of human pregnancy and lactation. *J. Clin. Endocrinol. Metab.* 88 (11), 5361–5365. doi:10.1210/jc.2003-030486

Ndip, A., Williams, A., Jude, E. B., Serracino-Inglott, F., Richardson, S., Smyth, J. V., et al. (2011). The RANKL/RANK/OPG signaling pathway mediates medial arterial calcification in diabetic charcot neuroarthropathy. *Diabetes* 60 (8), 2187–2196. doi:10.2337/db10-1220

Ono, T., Hayashi, M., Sasaki, F., and Nakashima, T. (2020). RANKL biology: Bone metabolism, the immune system, and beyond. *Inflamm. Regen.* 40, 2. doi:10.1186/s41232-019-0111-3

Rieck, S., White, P., Schug, J., Fox, A. J., Smirnova, O., Gao, N., et al. (2009). The transcriptional response of the islet to pregnancy in mice. *Mol. Endocrinol.* 23 (10), 1702–1712. doi:10.1210/me.2009-0144

Rinotas, V., Papakyriakou, A., Violitzi, F., Papaneophytou, C., Ouzouni, M. D., Alexiou, P., et al. (2020). Discovery of small-molecule inhibitors of receptor activator of nuclear factor-κb ligand with a superior therapeutic index. *J. Med. Chem.* 63 (20), 12043–12059. doi:10.1021/acs.jmedchem.0c01316

Rochette, L., Meloux, A., Rigal, E., Zeller, M., Cottin, Y., and Vergely, C. (2018). The role of osteoprotegerin in the crosstalk between vessels and bone: Its potential utility as a marker of cardiometabolic diseases. *Pharmacol. Ther.* 182, 115–132. doi:10.1016/j.pharmthera.2017.08.015

Roth, G. A., Mensah, G. A., Johnson, C. O., Addolorato, G., Ammirati, E., Baddour, L. M., et al. (2020). Global burden of cardiovascular diseases and risk factors, 1990-2019: Update from the GBD 2019 study. *J. Am. Coll. Cardiol.* 76 (25), 2982–3021. doi:10.1016/j.jacc.2020.11.010

Schafer, M. J., Miller, J. D., and LeBrasseur, N. K. (2017). Cellular senescence: Implications for metabolic disease. *Mol. Cell. Endocrinol.* 455, 93–102. doi:10.1016/j.mce.2016.08.047

Shen, P., Gong, Y., Wang, T., Chen, Y., Jia, J., Ni, S., et al. (2012). Expression of osteoprotegerin in placenta and its association with preeclampsia. *PLoS One* 7 (8), e44340. doi:10.1371/journal.pone.0044340

Siddiqui, J. A., and Partridge, N. C. (2016). Physiological bone remodeling: Systemic regulation and growth factor involvement. *Physiol. (Bethesda)* 31 (3), 233–245. doi:10.1152/physiol.00061.2014

Simonet, W. S., Lacey, D. L., Dunstan, C. R., Kelley, M., Chang, M. S., Luthy, R., et al. (1997). Osteoprotegerin: A novel secreted protein involved in the regulation of bone density. *Cell* 89 (2), 309–319. doi:10.1016/S0092-8674(00)80209-3

Sirinian, C., Papanastasiou, A. D., Schizas, M., Spella, M., Stathopoulos, G. T., Repanti, M., et al. (2018). RANK-c attenuates aggressive properties of ER-negative breast cancer by inhibiting NF-κB activation and EGFR signaling. *Oncogene* 37 (37), 5101–5114. doi:10.1038/s41388-018-0324-y

Stepien, E., Wypasek, E., Stopyra, K., Konieczynska, M., Przybylo, M., and Pasowicz, M. (2011). Increased levels of bone remodeling biomarkers (osteoprotegerin and osteopontin) in hypertensive individuals. *Clin. Biochem.* 44 (10-11), 826–831. doi:10.1016/j.clinbiochem.2011.04.016

Telejko, B., Kalejta, K., Kuzmicki, M., Wawrusiewicz-Kurylonek, N., Lipinska, D., Pliszka, J., et al. (2015). The association of bone turnover markers with pro- and anti-inflammatory adipokines in patients with gestational diabetes. *Ann. Agric. Environ. Med.* 22 (2), 307–312. doi:10.5604/12321966.1152085

Toffoli, B., Bernardi, S., Candido, R., Sabato, N., Carretta, R., Corallini, F., et al. (2011). Osteoprotegerin induces morphological and functional alterations in mouse pancreatic islets. *Mol. Cell. Endocrinol.* 331 (1), 136–142. doi:10.1016/j.mce.2010.08.019

Wei, J., Flaherty, S., and Karsenty, G. (2015). Searching for additional endocrine functions of the skeleton: Genetic approaches and implications for therapeutics. *Expert Rev. Endocrinol. Metab.* 10 (4), 413–424. doi:10.1586/17446651.2015.1058152

Yano, K., Shibata, O., Mizuno, A., Kobayashi, F., Higashio, K., Morinaga, T., et al. (2001). Immunological study on circulating murine osteoprotegerin/osteoclastogenesis inhibitory factor (OPG/OCIF): Possible role of OPG/OCIF in the prevention of osteoporosis in pregnancy. *Biochem. Biophys. Res. Commun.* 288 (1), 217–224. doi:10.1006/bbrc.2001.5745

Zhang, Q., Riddle, R. C., and Clemens, T. L. (2015). Bone and the regulation of global energy balance. *J. Intern. Med.* 277 (6), 681–689. doi:10.1111/joim.12348

Zhou, R., Guo, Q., Xiao, Y., Guo, Q., Huang, Y., Li, C., et al. (2021). Endocrine role of bone in the regulation of energy metabolism. *Bone Res.* 9 (1), 25. doi:10.1038/s41413-021-00142-4

frontiers | Frontiers in Cell and Developmental Biology

TYPE Original Research
PUBLISHED 10 November 2022
DOI 10.3389/fcell.2022.1014243

OPEN ACCESS

EDITED BY
Rujuan Zuo,
Oslo University Hospital, Norway

REVIEWED BY
Zhenxing Mao,
Zhengzhou University, China
Liyang Ma,
Albert Einstein College of Medicine, United States
Yajie Chen,
University of Yamanashi, Japan

*CORRESPONDENCE
Binbin Huang,
huangbb91@126.com
Minmin Jiang,
jiangmm0205@ahmu.edu.cn

†These authors contributed equally to this work and share first authorship

SPECIALTY SECTION
This article was submitted to Cellular Biochemistry, a section of the journal Frontiers in Cell and Developmental Biology

RECEIVED 08 August 2022
ACCEPTED 25 October 2022
PUBLISHED 10 November 2022

CITATION
Zhang F, Zhen H, Cheng H, Hu F, Jia Y, Huang B and Jiang M (2022), Di-(2-ethylhexyl) phthalate exposure induces liver injury by promoting ferroptosis via downregulation of GPX4 in pregnant mice.
Front. Cell Dev. Biol. 10:1014243.
doi: 10.3389/fcell.2022.1014243

Di-(2-ethylhexyl) phthalate exposure induces liver injury by promoting ferroptosis *via* downregulation of GPX4 in pregnant mice

Fan Zhang[1†], Hualong Zhen[1†], Hengshun Cheng[1], Fengying Hu[1], Yunfei Jia[1], Binbin Huang[2,3,4*] and Minmin Jiang[1*]

[1]Department of Occupational Health and Environmental Health, School of Public Health, Anhui Medical University, Hefei, China, [2]MOE Key Laboratory of Population Health Across Life Cycle, Department of Maternal, Child and Adolescent Health, School of Public Health, Anhui Medical University, Hefei, China, [3]NHC Key Laboratory of Study on Abnormal Gametes and Reproductive Tract, Department of Maternal, Child and Adolescent Health, School of Public Health, Anhui Medical University, Hefei, China, [4]Anhui Provincial Key Laboratory of Population Health and Aristogenics, Department of Maternal, Child and Adolescent Health, School of Public Health, Anhui Medical University, Hefei, China

As one kind of endocrine disrupting chemical, di-(2-ethylhexyl) phthalate (DEHP) has been reported to cause liver dysfunction in epidemiological and experimental studies. Abnormal liver function in pregnancy is associated with adverse maternal and perinatal outcomes. Few studies have investigated the potential effect of gestational DEHP exposure on the liver in pregnant mice, and the underlying mechanisms remain unclear. In the present study, pregnant ICR mice were exposed to doses (0, 500, 1,000 mg/kg/day) of DEHP in the presence or absence of 5 mg/kg/day ferrostatin-1 (Fer-1, ferroptosis inhibitor) by oral gavage from gestation day 4 to day 18. HepG2 cells were exposed to different doses of monoethylhexyl phthalate (MEHP, a major metabolite of DEHP) *in vitro*. Hepatic function and pathologic changes were observed. Oxidative stress, iron metabolism, and ferroptosis-related indicators and genes were evaluated both *in vivo* and *in vitro*. The results showed that gestational DEHP exposure induced disordered liver function and hepatocyte morphology changes in pregnant mice, along with increased malondialdehyde (MDA) and Fe^{2+} content and decreased glutathione (GSH) levels. The expression levels of the selected ferroptosis-related genes *Slc7a11*, *Gpx4*, and *Nfr2* were significantly decreased, and *Ptgs2* and *Lpcat3* were significantly increased. Notably, Fer-1 attenuated DEHP-induced liver injury and ferroptosis. Furthermore, MEHP exhibited a synergistic effect with RSL3 (a GPX4 inhibitor) in promoting ferroptosis *in vitro*. Taken together, the results demonstrated that DEHP induced liver injury and ferroptosis in pregnant mice, probably by inhibiting the GPX4 pathway through lipid peroxidation and iron accumulation.

KEYWORDS

DEHP, liver injury, ferroptosis, endocrine disrupting chemical, pregnancy

Introduction

Di-(2-ethylhexyl) phthalate (DEHP), one of the most commonly used phthalates, has been widely used in the manufacture of PVC plastics and household products. Humans, even pregnant women and children are widely exposed to DEHP in everyday life *via* ingestion of food, inhalation, skin contact, and medical devices. Growing epidemiological evidence has highlighted the association between phthalate exposure and a higher risk for liver injury (Yu et al., 2021; Midya et al., 2022). As an endocrine disrupting chemical (EDC), DEHP is reported to be toxic to rodent liver, leading to lipid metabolism disorder, liver injury and nonalcoholic fatty liver disease (Chen et al., 2016; Zhao et al., 2020; Liu et al., 2021). Abnormal liver function in pregnancy is associated with adverse maternal and perinatal outcomes (Lao, 2020; Sarkar et al., 2020). However, the effects of DEHP exposure on the liver and the potential mechanism are currently understudied in pregnant mice.

Ferroptosis is a form of iron-dependent cell death characterized by the accumulation of intracellular reactive oxygen species (ROS) and lipid peroxidation (Dixon, 2012; Yang and Stockwell, 2016). Ferroptosis has been reported to play an important role in the pathogenesis of liver injury (Chen et al., 2022). Reports from *in vivo* and *in vitro* experiments have revealed that DEHP exposure triggers ferroptosis in mouse testes, spleen and murine hepatocyte cell line AML12 cells (Dai et al., 2021; Han et al., 2022; Wu et al., 2022). Yin et al. investigated the effects of acute exposure to DEHP on Oryzias melastigma, and the results indicated the occurrence of ferroptosis in the liver (Yin et al., 2021). DEHP is metabolized to mono(2-ethylhexyl) phthalate (MEHP) in the liver, but whether ferroptosis plays a potential role in DEHP-induced liver injury in pregnant mice remains unknown.

Glutathione peroxidase 4 (GPX4), as a central regulator of ferroptosis, is a common mechanism shared by multiple independent small molecule scaffolds (Yang et al., 2014). GPX4 uses glutathione (GSH) to repair lipids and converts toxic lipid hydroperoxides into nontoxic lipid alcohols, which have been functionally characterized as critical protectors of hepatic function (Carlson et al., 2016). In the presence of catalytically active iron, any disturbance to the system x_c^-/GSH/GPX4 axis may induce lipid peroxidation and result in cellular membrane damage and eventually ferroptosis (Seibt et al., 2019). The balance between oxidative stress and antioxidant response is very important during the normal course of pregnancy. As an exogenous compound, DEHP was reported to trigger oxidative stress with a decrease in GSH activity and an increase in ROS and MDA levels (Zhao et al., 2021). Therefore, we hypothesize that the oxidant/antioxidant imbalance caused by exogenous DEHP exposure may mediate liver injury by decreasing GPX4 activity and triggering ferroptosis. The present study aims to explore the effects of gestational DEHP exposure on the liver in pregnant mice and the potential role of ferroptosis in the mechanism.

Materials and methods

Animals and treatment

Specific pathogen-free ICR mice were purchased from the Animal Experimental Research Center of Anhui Medical University (Anhui, China). Before the formal experiment, the mice were adaptively fed for 1 week. All mice had free access to food and water under a 12:12-h light-dark cycle at 22 ± 1 °C. Then, 7-week-old ICR female mice were mated with fertile 10 to 12-week-old ICR males (female: male = 2:1). A vaginal plug was detected at next day after mating (the presence of a vaginal plug is defined as gestational day 0, GD0). Pregnant mice were randomly divided into four groups (n = 6 per group) and exposed to the following interventions from GD4 to GD18: 1) control group (DEHP 0 mg/kg), mice treated with corn oil; 2) DEHP 500 mg/kg group, mice treated with DEHP at a dose of 500 mg/kg/day by gavage; 3) DEHP 1000 mg/kg group, mice treated with DEHP at a dose of 1,000 mg/kg/day by gavage; 4) DEHP + Fer-1 group, mice treated with 1,000 mg/kg/day of DEHP and 5 mg/kg/day of ferroptosis inhibitor ferrostatin-1 (Fer-1). Dosage information and design in this experiment were based on recent previous research (Li et al., 2012; Zhao et al., 2021). All mice were sacrificed by cervical dislocation under diethyl ether anesthesia on GD18. Schematic diagram of experimental design in mice is shown in Figure 1A. All animal experiments were carried out with the approval of the Experimental Animal Ethics Committee of Anhui Medical University (No: 20190302).

Sample collection and preparation

On GD18, the mice were euthanized. Blood samples were collected and centrifuged to separate the serum. Liver tissue was excised and weighed immediately and divided into two parts: one for histological assays by fixing in 4% paraformaldehyde and the other for western blotting by freezing in liquid nitrogen for 20 min. All blood and liver samples were stored at −80°C for further experiments.

Chemicals and reagents

DEHP, MEHP, and RSL3 were purchased from Aladdin (Shanghai, China). Fer-1 was purchased from Sigma–Aldrich (Shanghai, China). Alanine aminotransferase (ALT), aspartate aminotransferase (AST), MDA, GSH detection kits and glucose kits (glucose oxidase method) were purchased from Nanjing Jiancheng Bioengineering Institute (Nanjing, China). A hematoxylin and eosin (H&E) staining kit, BCA protein assay kit, lysis buffer and Reactive Oxygen Species Assay Kit were purchased from Beyotime Technology (Shanghai, China). CCK8 was purchased

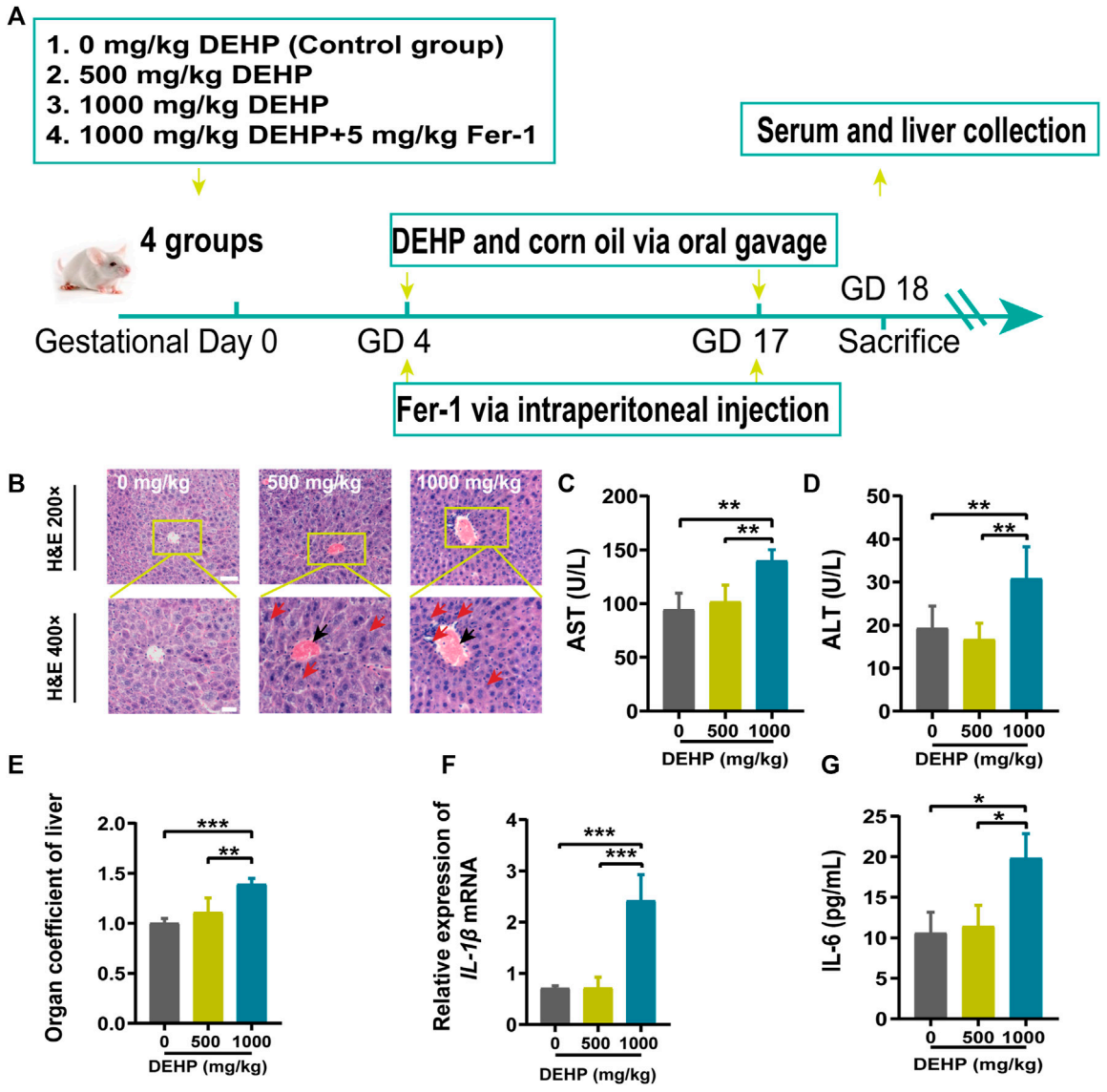

FIGURE 1
DEHP exposure resulted in liver injury in pregnant mice. **(A)** The treatment schedule performed in mice. **(B)** Liver sections were stained with H&E. H&E magnification, first row, 200 × (scale bar = 100 μm); second row, 400 × (scale bar = 50 μm). The red arrow indicates hepatocyte swelling, necrosis, and inflammatory cell infiltration, and the black arrow indicates hyperemia in the central vein in the DEHP-treated groups. **(C,D)** Serum levels of AST and ALT. **(E)** The ratio of the liver weight to the body weight. **(F,G)** RT-qPCR of the inflammatory factor *IL-1β* and the serum levels of IL-6. All serum indexes were tested by kits. Data are presented as the mean ± SD. AST, aspartate aminotransferase; ALT, alanine aminotransferase; H&E, hematoxylin and eosin; IL-6, inflammatory factor interleukin-6; IL-1β, inflammatory factor interleukin-1β; *$p < 0.05$, **$p < 0.01$, ***$p < 0.001$.

from Apex-Bio (Houston, United States). DMEM was purchased from Gibco (New York, United States). Antibodies for solute carrier family 7 member 11 (SLC7A11) and GPX4 were purchased from Abcam (MA, United States). All horseradish peroxidase (HRP)-conjugated secondary antibodies were purchased from Zen Bio (Chengdu, China). TRIzol® reagent was purchased from Invitrogen (San Giuliano Milanese, Italy), and the SYBR Green kit was purchased from Life Science Biotechnology (Beijing, China). Primers for detecting *Fth1, Ftl, Gpx4, Lpcat3, Slc7a11, Ptgs2, Lpcat3, Nrf2, and β-actin* were synthesized by Invitrogen (San Giuliano Milanese, Italy).

Biochemical analysis

Serum AST and ALT levels were measured by using an automatic biochemistry analyzer (Hitachi Automatic analyzer, Japan).

Histological analysis

Samples of liver tissue were collected and fixed with 4% paraformaldehyde, embedded in paraffin, and sectioned for H&E staining. The histopathological observations were performed using a Microscope (Tissue FAXS-S plus, TG, Austria). First, the hepatic lobule structure was found under a ×4 objective lens. Second, the size, morphological structure, and arrangement of hepatocytes were observed under ×20 and ×40 objective lenses.

Hepatic iron accumulation was assessed by Perl's Prussian Blue (PPB) staining. Paraffin-embedded liver tissue sections were deparaffinized and rehydrated through graded alcohols in water. The paraffin sections were stained with Prussian blue (10 mg/ml) for 15 min, washed in running water for 1 min and counterstained with 0.5% aqueous neutral red solution for 1 min. Tissue cells showing bright blue dots in the cytoplasm were examined under a phase-contrast microscope. Subsequent dehydration steps used exact timings to maintain consistent counterstain intensity and distribution. Each slice was randomly selected, and the percentage of Prussian blue-stained area was measured by image analysis (Tissue FAXS-S plus, TG, Austria).

Ferrous iron and lipid peroxidation assay

The liver ferrous iron (Fe^{2+}) concentration was assessed with an Iron Assay Kit (Solarbio Life Science Institute, China). Liver tissue (0.1 g) was added to 1 ml of extracting solution for ice bath homogenization and centrifuged at 4,000 × *g* for 10 min at 4°C. The supernatant was collected for further testing according to the manufacturer's instructions. The absorbance of the supernatant was measured on an EnSight multimode detection platform (EnSight, PE, United States) at a wavelength of 520 nm.

The concentration of GSH, GSH/GSSG ratio, and MDA in liver homogenized supernatant were measured to evaluate the antioxidant status and lipid peroxidation. The liver homogenate was prepared as previously described. The total protein concentration in the supernatant was also determined by the BCA assay. All operations were performed according to the manufacturer's instructions.

Cell culture

HepG2 cells were cultured in Dulbecco's Modified Eagle's Medium (DMEM, Gibco, USA) with 10% fetal bovine serum (FBS, BI, Israel) and 1% penicillin–streptomycin. The HepG2 cell line was maintained in a humidified incubator at 37 °C with 5% CO_2. The cells were then separated into five groups: control (DMSO), 100 μM (MEHP), 200 μM (MEHP), 1 μM RSL3 (GPX4 inhibitor), and 200 μM (MEHP)+RSL3. HepG2 cells were pretreated in serum-free medium for 6 h and then incubated with MEHP for 24 h. All reagents were dissolved in DMSO (Sigma, United States) before use. Cells were treated with DMSO in the control group.

Cell counting kit-8 assay

To investigate the effect of MEHP and RSL3 on HepG2 cell viability, HepG2 cells were inoculated at a density of 10^4 cells/well in 96-well plates and then incubated in cell culture media containing 100–500 μM MEHP concentrations for 24 h. After 24 h of incubation, cell proliferation was evaluated using the Cell Counting Kit-8 kit, following the manufacturer's instructions. Cell viability% = (absorbance of experimental group - absorbance of blank)/(absorbance of control group - absorbance of blank) × 100%.

Glucose levels analysis

To measure glucose metabolism in HepG2 cells treated with MEHP. The glucose levels were measured by following the manufacturer's instructions. We also analyzed cell viability to measure the glucose consumption ratio after MEHP treatment.

ROS assay

ROS levels in HepG2 cells were measured by the fluorescent probe DCFH-DA. HepG2 cells were inoculated in 6-well plates using a Reactive Oxygen Species Assay Kit (Beyotime, Shanghai, China) and subjected to various treatments for 24 h. The culture medium was switched to serum-free medium, and 10 mol/L dichloro-fluorescein diacetate was incubated for 30 min in the dark. Finally, flow cytometry and fluorescence microscopy were used to estimate the ROS level in the cells.

RNA extraction and real-time PCR analysis

Total RNA was extracted from liver tissues using TRIzol reagent (Invitrogen, USA) according to the manufacturer's instructions and standardized to 1 μg/μL. The purification of RNA was performed according to the ratio of absorbance at 260 nm and 280 nm. The reaction solution was configured according to the instructions mentioned in the Reverse Transcription Kit (Roche, Switzerland). Then, RT-PCR was performed with SYBR Green Master Mix (Roche, Switzerland). The relative concentration of mRNA levels was normalized by the comparative Ct ($2^{-\Delta\Delta Ct}$) with β-actin as an internal reference. The specific primer sequences applied in this study are presented in Table 1.

TABLE 1 The specific primer sequences.

Symbol	Forward primer	Reverse primer
Gpx4	CCTCCCCAGTACTGCAACAG	GGCTGAGAATTCGTGCATGG
Fth1	TGCCTCCTACGTCTATCTGTC	GTCATCACGGTCTGGTTTCTTT
Ftl	AGGGCGTAGGCCACTTCTT	CTGGGTTTTACCCCATTCATCTT
Ptgs2	CTGCGCCTTTTCAAGGATGG	GGGGATACACCTCTCCACCA
Slc7a11	AGGGCATACTCCAGAACACG	GGACCAAAGACCTCCAGAATG
Lpcat3	GCCGTTATTACTACCCTTTGCT	ACACAGCCCAATTAGCTTCAG
Nrf2	TCCGCTGCCATCAGTCAGTC	ATTGTGCCTTCAGCGTGCTTC
IL-1β	GATGATAACCTGCTGGTGTGTGA	GTTGTTCATCTCGGAGCCTGTAG
Tfrc	GTTTCTGCCAGCCCCTTATTAT	GCAAGGAAAGGATATGCAGCA
β-actin	ATCTGGCACCACACCTTCT	GGGGTGTTGAAGGTCTCAAA

Protein extraction and western blotting analysis

Total proteins were extracted from the liver and quantified using the BCA Protein Assay Kit (Beyotime Biotechnology, China). Proteins were separated by 10% sodium dodecyl sulfate (SDS)-polyacrylamide gel electrophoresis (PAGE) and transferred to polyvinylidene fluoride membranes, blocked with skimmed milk powder, and incubated at 4 °C overnight with primary antibodies. The membranes were washed with Tris-buffered saline with Tween 20 (TBST) and incubated with secondary antibodies conjugated with HRP. Antibody-protein complexes were detected using an ECL Prime Western Blotting Detection Reagent (Advansta, California, USA) and visualized using a Tanon digital imaging system (Fine-do X6, Shanghai, China). β-actin was used as an internal control protein.

Statistical analysis

All independent experiments were repeated at least 3 times, and the data are expressed as the mean ± standard deviation (SD). Student's *t* test or one-way analysis of variance (ANOVA) was used to compare significant differences among groups, and Dunnett's test was used for multiple comparisons using GraphPad Prism eight software. $p < 0.05$ (*), $p < 0.01$ (**), and $p < 0.001$ (***) indicated a statistically significant difference.

Results

DEHP exposure resulted in liver injury in pregnant mice

The results of H&E staining, inflammatory cytokine levels, and liver function parameters are shown in Figure 1. H&E staining was performed to observe histopathological changes in the liver. Representative micrographs from H&E-stained liver sections revealed swollen hepatocytes, necrosis, inflammatory cell infiltration (red arrow), and hyperemia in the central vein (black arrow) in mice treated with 1,000 mg/kg DEHP (Figure 1B). The liver is the key target organ of DEHP exposure. AST is mainly found in the liver cytoplasm and hepatocyte mitochondria. ALT is mainly distributed in the liver cytoplasm. The levels of AST and ALT were significantly elevated ($p < 0.01$) in the 1,000 mg/kg DEHP group, which suggested damage to the liver parenchyma (Figures 1C,D). We found that the liver weight/body ratio was markedly increased ($p < 0.001$) in the DEHP-exposed group compared to the control group (Figure 1E), the expression of the inflammatory factor interleukin-1β (IL-1β) was significantly evaluated, and the level of the inflammatory factor interleukin-6 (IL-6) in liver tissue was much higher in the 1,000 mg/kg DEHP group ($p < 0.05$) (Figures 1F,G). From the above results, it has been demonstrated that gestational DEHP exposure induces liver injury in pregnant mice.

DEHP exposure disrupted iron metabolism and increased oxidative stress in mice livers

To explore the effects of DEHP exposure on iron metabolism in the livers of pregnant mice. Liver Fe^{2+} concentration and PPB staining were performed. The level of Fe^{2+} was significantly elevated, and PPB staining showed increasing iron accumulation in the liver tissue (red arrow) in the 1,000 mg/kg DEHP group ($p < 0.01$, Figures 2A–C). Moreover, the MDA content was significantly increased ($p < 0.05$) in the livers of mice in the 1,000 mg/kg DEHP-exposed group (Figure 2D). To assess hepatic redox homeostasis after DEHP exposure, GSH and the GSH/GSSG ratio were also measured. They were markedly

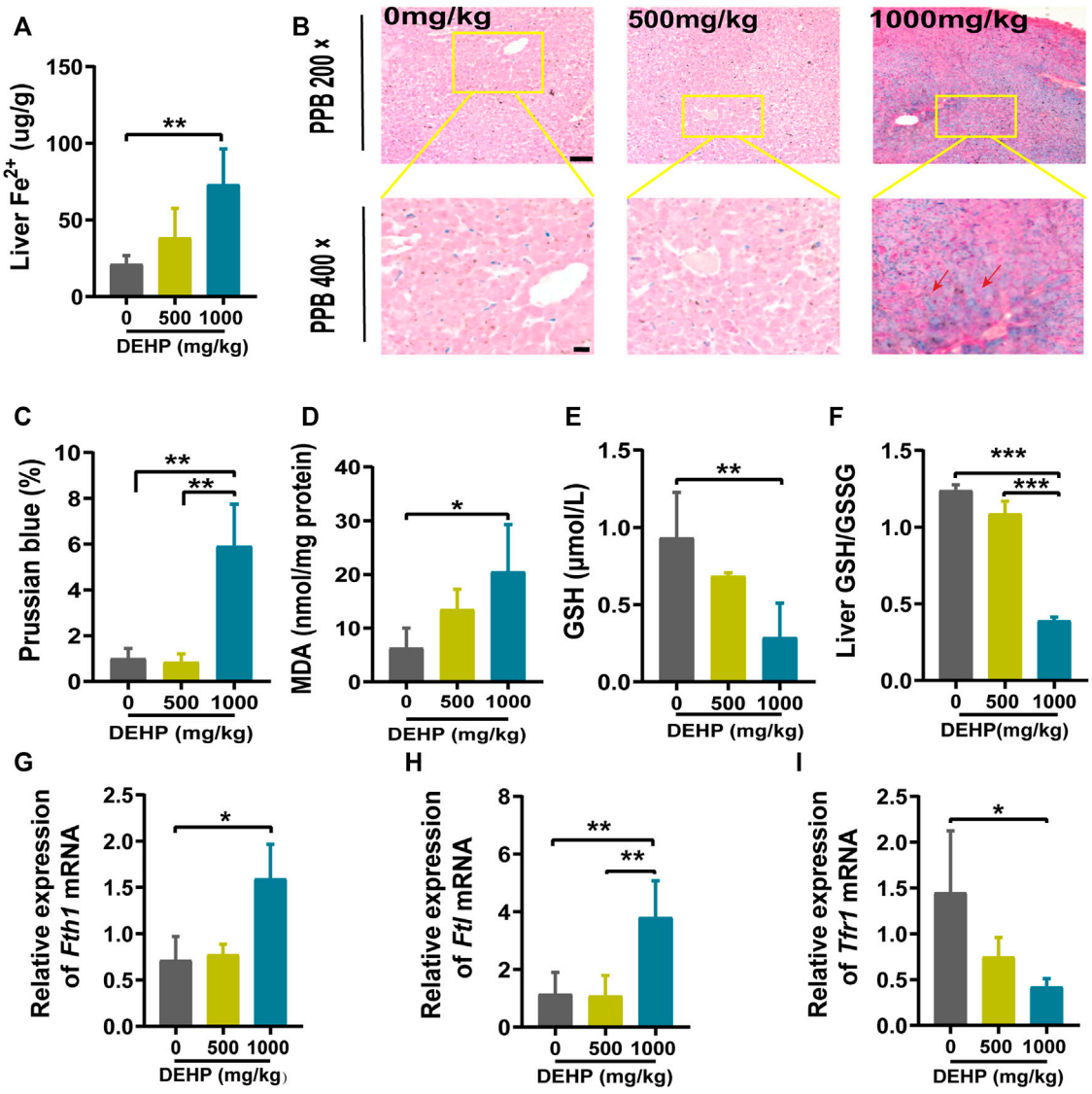

FIGURE 2
DEHP exposure disrupted iron metabolism and increased oxidative stress in mice livers. **(A)** The level of Fe^{2+} in the liver. **(B)** Representative micrographs from PPB staining. First row, 200 × (scale bar = 100 μm); second row, 400 × (scale bar = 50 μm). The red arrow indicates the accumulation of iron in the liver tissue. **(C)** Quantification of PPB staining for iron in hepatocytes. **(D)** MDA content in the livers of mice. **(E)** GSH content in the livers of mice. **(F)** Liver GSH/GSSG ratio. **(G–I)** RT–qPCR of the iron metabolism-related genes *Fth1, Ftl,* and *Tfr1* in mouse livers. Data are presented as the mean ± SD. PPB, Perl's Prussian blue; MDA, malondialdehyde; GSH, glutathione. *$p < 0.05$, **$p < 0.01$, ***$p < 0.001$.

decreased in the 1,000 mg/kg DEHP-exposed group compared to the control group (Figures 2E,F).

Iron metabolism-related genes were analyzed by qPCR. We found that the *Ftl* and *Fth1* genes were highly expressed ($p < 0.05$, $p < 0.01$), and the *Tfr1* gene was expressed at low levels in the 1,000 mg/kg DEHP-exposed group ($p < 0.05$, Figures 2G–I). Collectively, these results suggested that gestational DEHP exposure might alter iron metabolism in the liver and promote lipid peroxidation.

DEHP exposure led to ferroptosis in mice livers

To further determine whether DEHP exposure could induce ferroptosis in mice livers, ferroptosis-related genes and proteins were detected. We found that the ferroptosis-related genes *Gpx4, Slc7a11, and Nrf2* were significantly downregulated, and *Ptgs2 and Lpcat3* were significantly highly expressed in the 1,000 mg/kg DEHP-exposed group (Figures 3A–E). Since *Gpx4* is the key gene in

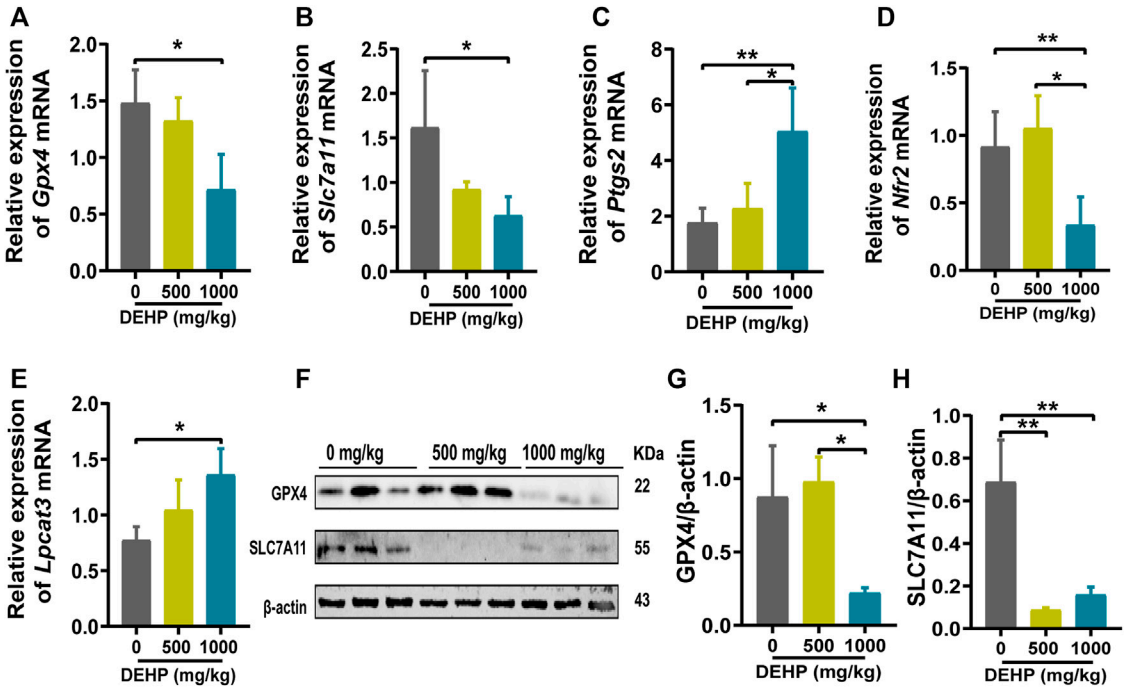

FIGURE 3
DEHP exposure led to ferroptosis in mice livers. **(A–E)** mRNA levels were evaluated by RT–qPCR of the selected ferroptosis genes *Gpx4, Slc7a11, Ptgs2, Nrf2, and Lpcat3*, and β-actin was used as the reference gene. **(F)** Protein levels of GPX4 and SLC7A11 in the livers of mice; β-actin was used as the reference protein. **(G,H)** Quantification of the protein levels of GPX4 and SLC7A11 in the livers of mice. Experiments were repeated at least three times. Data are presented as the mean ± SD. *$p < 0.05$, **$p < 0.01$, ***$p < 0.001$.

ferroptosis, we further conducted western blotting and revealed that the protein levels of GPX4 and SLC7A11 were markedly downregulated ($p < 0.05$, Figures 3F–H). The above results indicated that gestational DEHP exposure may lead to iron overload and further induce ferroptosis in mouse livers.

Fer-1 alleviated DEHP-induced liver injury in pregnant mice

To determine whether ferroptosis plays a potential role in DEHP-induced liver injury. Fer-1 was injected into mice before DEHP exposure. Compared with the 1,000 mg/kg DEHP-exposed group, the levels of AST and ALT and the organ coefficient of the liver were significantly decreased in the 1,000 mg/kg DEHP + Fer-1 group ($p < 0.05$, Figures 4A–C). The level of liver Fe^{2+} was not significantly changed compared to that in the DEHP-exposed group (Figure 4D). Furthermore, the infiltration of inflammatory cells and hyperemia in the central vein was diminished after Fer-1 treatment (Figure 4E). In addition, the level of MDA in the liver was decreased ($p < 0.05$) in the 1,000 mg/kg DEHP + Fer-1 group, and the levels of GSH and the GSH/GSSG ratio were not markedly increased (Figures 4F–H). Overall, the data further indicated that Fer-1 was able to alleviate liver injury in DEHP-exposed mice.

Fer-1 attenuated DEHP-induced ferroptosis and the activation of ferroptosis-related gene expression

In addition, ferroptosis-related genes and proteins were detected in DEHP-exposed mouse livers after treatment with Fer-1. Compared with the 1,000 mg/kg DEHP-espoused group, the mRNA level of *Slc7a11* was significantly increased and *Ptgs2* was obviously decreased ($p < 0.05$), while the expression of *Nrf2* and *Gpx4* showed an increasing trend that was not significantly different in the DEHP + Fer-1 group (Figures 5A–D). In addition, the protein levels of SLC7A11 and GPX4 were markedly increased ($p < 0.05$) in the DEHP + Fer-1 group (Figures 5E–G). In conclusion, the results demonstrated that DEHP may promote ferroptosis through the SLC7A11/GPX4-related pathway in pregnant mice livers.

MEHP induced ferroptosis in HepG2 cells

To further determine the role of ferroptosis in MEHP-induced hepatotoxicity, an *in vitro* study was conducted in HepG2 cells. RSL3 (a specific GPX4 inhibitor) was utilized to explore the potential molecular mechanism. We evaluated

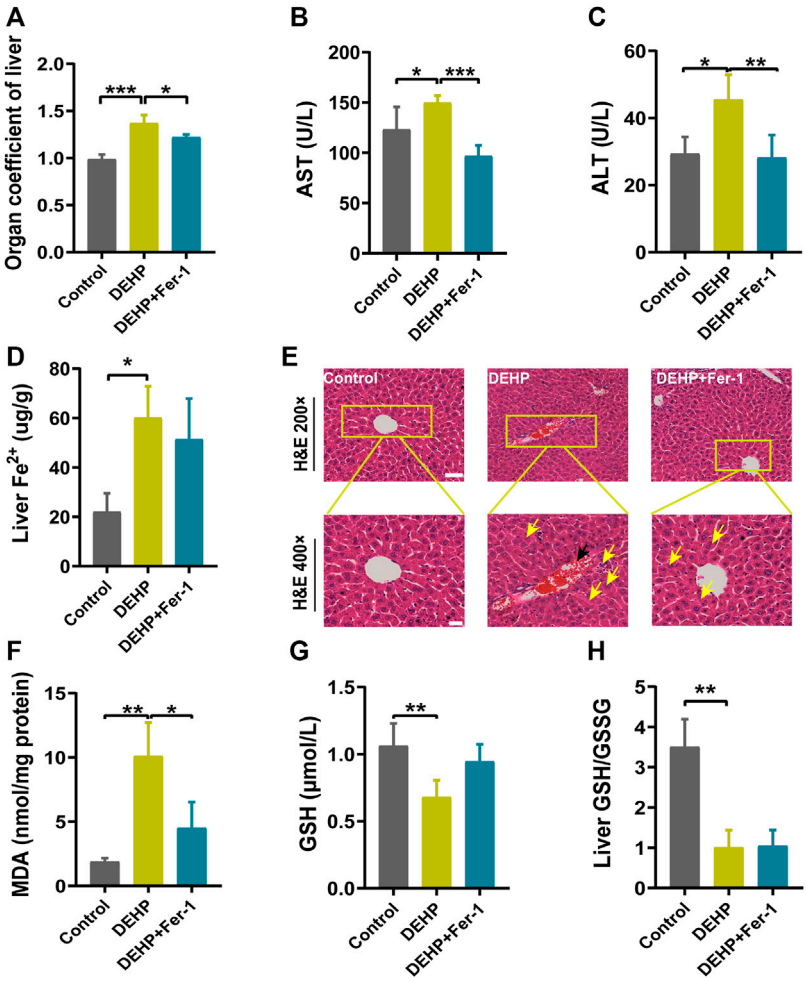

FIGURE 4
Fer-1 alleviated DEHP-induced liver injury in pregnant mice. **(A)** Liver weight/body ratio. **(B)** Serum levels of AST. **(C)** Serum levels of ALT. **(D)** The level of Fe^{2+} in the liver. **(E)** Liver sections were stained with H&E in the normal control, DEHP, and DEHP + Fer-1 group. H&E magnification, first row, 200 × (scale bar = 100 μm); second row, 400 × (scale bar = 50 μm). The black arrow indicates hyperemia in the central vein. The yellow arrow indicates swollen hepatocytes, focal necrosis, and inflammatory cell infiltration. DEHP + Fer-1-treated liver sections showed that the severe signs of liver damage induced by DEHP were significantly attenuated. **(F)** MDA content in the livers of mice. **(G)** GSH content in the livers of mice. **(H)** Liver GSH/GSSG ratio. Data are presented as the mean ± SD. AST, aspartate aminotransferase; ALT, alanine aminotransferase; H&E, hematoxylin and eosin; MDA, malondialdehyde; GSH, glutathione. *$p < 0.05$, **$p < 0.01$, ***$p < 0.001$.

cell viability after treatment with MEHP and RSL3 (Figures 6A,B). In addition, we measured the glucose levels in the cell lines (Figures 6C,D), and the results suggested the occurrence of abnormal glucose metabolism in the MEHP-treated group. After evaluating the level of ROS, we found that the ROS level was higher in the MEHP + RSL3 group than in the RSL3-treated group (Figures 6E–H). Furthermore, we also discovered that the protein expression of GPX4, SLC7A11 and Nrf2 was significantly downregulated after treatment with MEHP + RSL3 (Figures 6I-L). These *in vitro* data support the idea that ferroptosis is involved in the molecular mechanism of MEHP-induced hepatotoxicity.

Discussion

DEHP, as a typical EDC, is a widely used plasticizer. EDCs are well known to change the functions of the endocrine system and consequently induce adverse health effects in an intact organism (Koch et al., 2003; Caldwell, 2012; Heindel and Blumberg, 2019). In the present study, we observed that gestational DEHP exposure induced liver injury in pregnant mice. In addition, gestational DEHP exposure resulted in iron overload, leading to ferroptosis in mouse livers with the downregulation of GPX4. These findings suggested that ferroptosis might play a potential role in DEHP-induced liver injury.

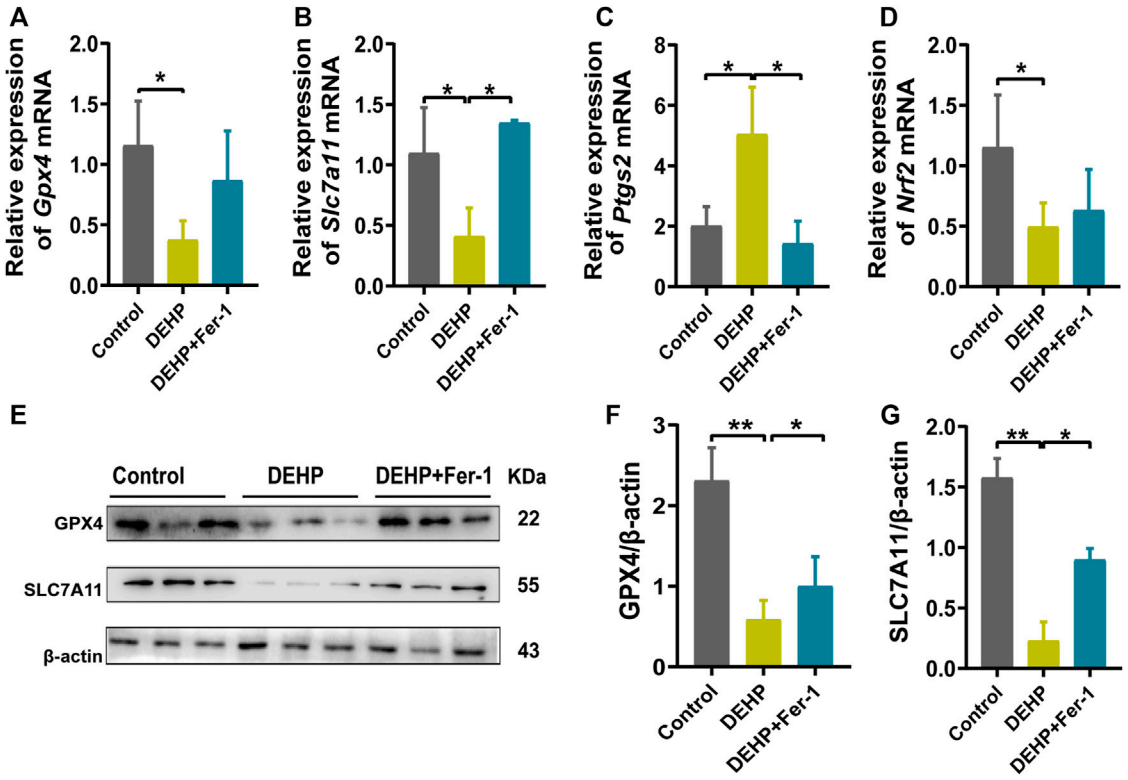

FIGURE 5
Fer-1 attenuated DEHP-induced ferroptosis and the activation of ferroptosis related gene expression. **(A–D)** mRNA levels evaluated by RT–qPCR of the selected ferroptosis genes *Gpx4, Slc7a11, Ptgs2, and Nrf2* in the control, DEHP, and DEHP+Fer-1 group. β-actin was used as the reference gene. **(E)** Protein levels of GPX4 and SLC7A11 in the livers of mice; β-actin was used as the reference protein. **(F, G)** Quantification of the protein levels of GPX4 and SLC7A11 in the livers of mice. Experiments were repeated at least three times. Data are presented as the mean ± SD. $^{*}p < 0.05$, $^{**}p < 0.01$, $^{***}p < 0.001$.

Epidemiological studies have suggested that urinary phthalate metabolite concentrations are associated with elevated markers of liver injury, such as serum ALT AST, gamma-glutamyl transferase (GGT) and alkaline phosphatase (ALP), indicating the potential toxic effect of phthalate exposure on the liver. (Yu et al., 2021; Midya et al., 2022). Animal experiments have also reported that DEHP exacerbates nonalcoholic fatty liver in rats. Huang et al. concluded that DEHP induced lipid metabolism disorder in the liver by activating the LXR/SREBP-1c/PPARα/γ and NF-κB signaling pathways. Lo et al. found that DEHP induced injury in liver FL83B cells (Lo et al., 2014; Chen et al., 2016; Huang et al., 2022). Consistent with previous studies, we discovered elevated ALT and AST and hepatocyte morphology changes after gestational DEHP exposure in pregnant mice.

Ferroptosis is a form of regulated cell death that is characterized by the iron-dependent accumulation of lipid peroxidation to lethal levels (Stockwell et al., 2017; Jiang et al., 2021). Emerging evidence suggests that ferroptosis can be triggered by downregulation of system x_c^- activity, inhibition of GPX4, and accumulation of lipid ROS (Duan et al., 2021). Ferritin is a hollow iron storage protein composed of 24 highly symmetrical subunits of ferritin heavy chain (FTH1) and ferritin light chain (FTL) (Lee JH, 2009; N. Zhang et al., 2021). A previous study reported that IL-6 could enhance the synthesis of FTH1 and FTL in hepatocytes (Naz et al., 2013). It has been reported that inflammatory factors, such as IL-6 and IL-1β, have isozyme-specific effects on glutathione peroxidase (GPX) expression (Shou et al., 2021; Wang et al., 2022). They increase GPX2 transcript concentration and decrease GPX4 transcript concentration. Ferroptosis can be induced by IL-6, which also impairs iron homeostasis and causes an increase in reactive oxygen species (Han et al., 2021). Inhibitors of ferroptosis may alleviate inflammation as well as pathological indicators such as liver injury (Tsurusaki et al., 2019; Li et al., 2020). In an epidemiological study, increased iron levels, accompanied by elevated ROS levels, were reported to be associated with an increased risk of GDM (Bothwell, 2000; Ding et al., 2021). In our study, gestational DEHP exposure

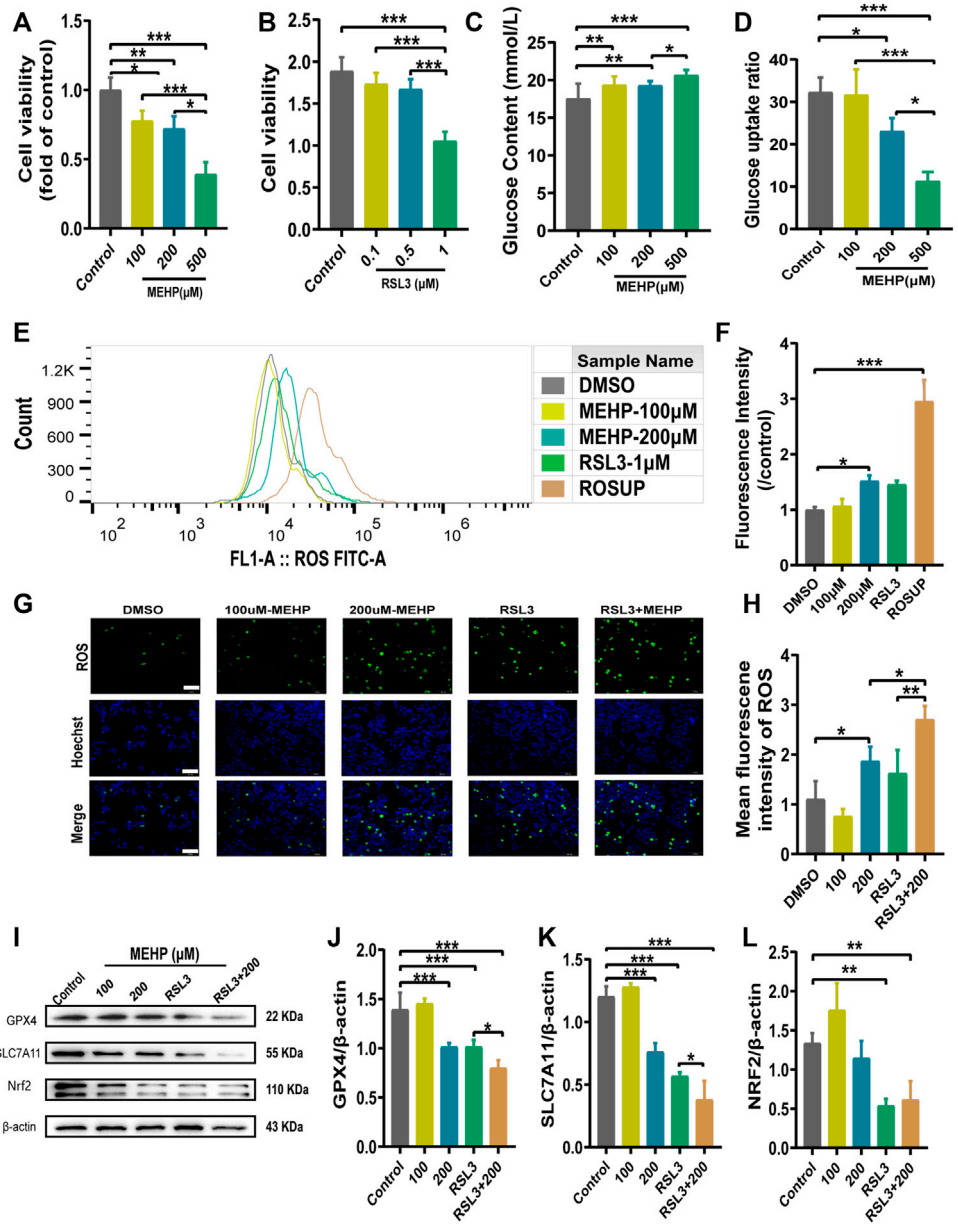

FIGURE 6
MEHP induced ferroptosis in HepG2 cells. **(A,B)** Cell viability was detected by CCK8 assays. **(C,D)** The glucose level and glucose uptake ratio were assessed by assays. **(E–H)** The intracellular ROS level was analyzed by a DCFH-DA probe on a fluorescence microscope and flow cytometry. **(I)** Protein levels of GPX4, SLC7A11, and Nrf2 in HepG2 cells; β-actin was used as the reference protein. **(J–L)** Quantification of the protein levels of GPX4, SLC7A11, and Nrf2 in HepG2 cells. Experiments were repeated at least three times. Data are presented as the mean ± SD. $*p < 0.05$, $**p < 0.01$, $***p < 0.001$.

induced upregulation of inflammatory factors and hepatic genes involved in iron transport and storage, including *Fth1 and Ftl*. Inflammation and the oxidative stress response were upregulated in mouse livers, which is known to stimulate the expression of iron metabolism genes (Evstatiev and Gasche, 2012; X. Li et al., 2020; Xiao et al., 2021). It has been reported that defects in Tfr1 cause systemic iron overload and hemochromatosis through downregulation of hepcidin (Kawabata, 2019). Therefore, the determination of iron accumulation is crucial in diagnosing the occurrence and progression of many liver and iron-related diseases (van Vuren et al., 2020). In this study, consistent with previous findings, we found that iron accumulated and elevated the Fe^{2+} concentration in liver tissue, and MDA, as one of the final products of lipid peroxidation in cell membranes, was

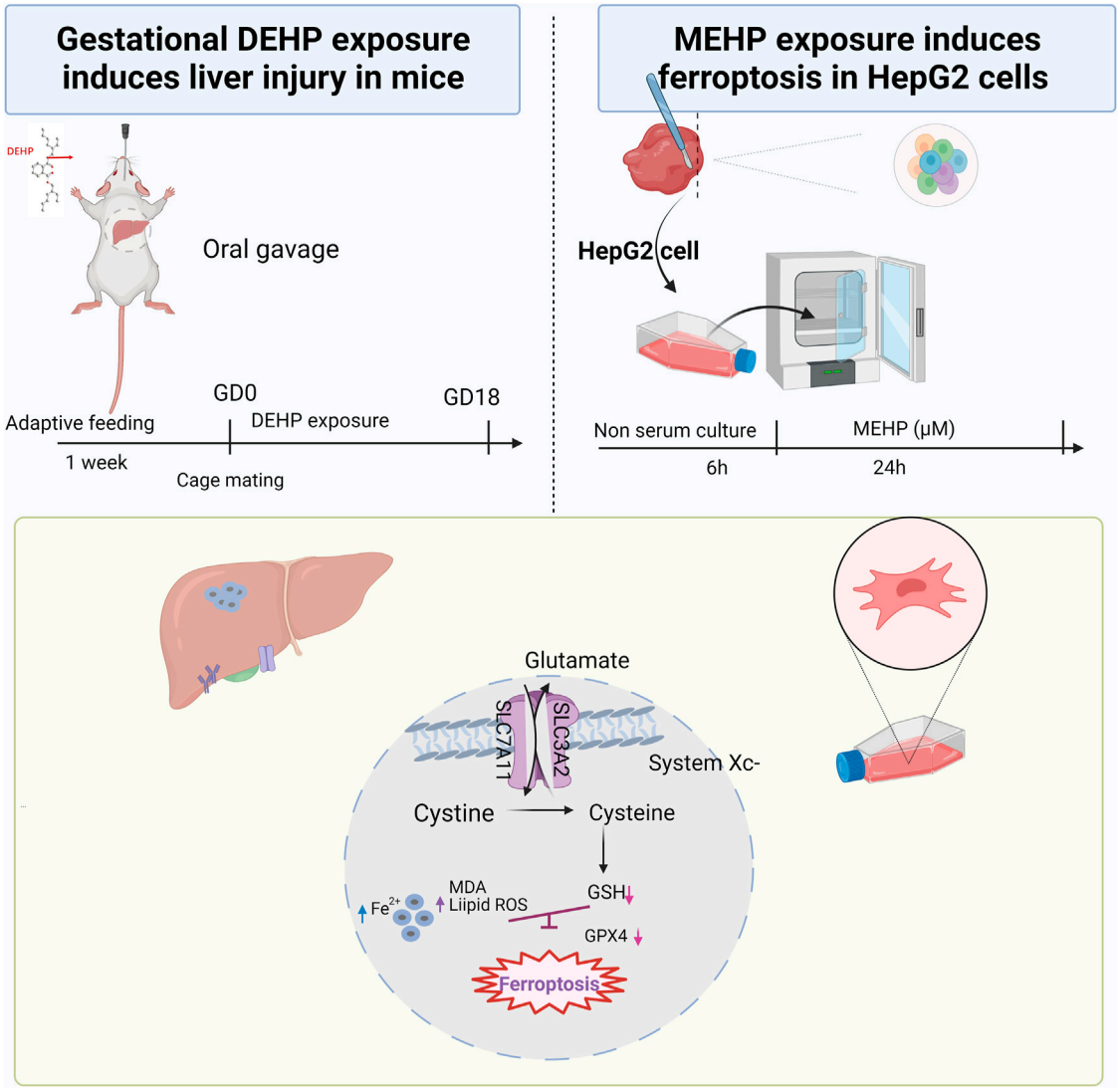

FIGURE 7
Summary of the experiment conducted in mice and HepG2 cells and the proposed pathway of DEHP-induced liver injury. DEHP or MEHP exposure induces ferroptosis by promoting iron metabolism, accelerating GPX4 proteasomal degradation and inducing excessive oxidative stress in hepatic cells. The figure was partly generated using Bio-Render, and confirmation of publication and licensing rights was provided by Bio-Render.

significantly increased. The levels of GSH and the GSH/GSSG ratio in the mouse livers decreased significantly in the DEHP-exposed group. Ferrous iron can participate in the Fenton reaction with H_2O_2, which could cause oxidative damage to DNA, protein, and membrane lipids and promote lipid peroxidation (Lunova M, 2014; Meynard D, 2014; Zhuang et al., 2014).

In addition to the liver, it was reported previously that DEHP could trigger ferroptosis in mouse testes and spleen (Dai et al., 2021; Wu et al., 2022). The exact molecular mechanism of DEHP-induced ferroptosis has not been fully clarified. The x_c^-/GPX4 antioxidant system and HIF-1α/HO-1 signaling pathway were suggested to play pivotal roles in DEHP-induced ferroptosis. According to previous studies, the System x_c^-/GPX4 pathway is a key pathway in removing lipid ROS to regulate ferroptosis. In mammals, GPX4 plays a major role in antioxidant defense by regulating responses to oxidative stress. Furthermore, loss of function of GPX4 protein and depletion of GSH levels are the key mechanisms for triggering ferroptosis.

The current study examined the expression of genes related to the System x_c^-/GPX4 axis and discovered that the mRNA levels of *Slc7a11*, *Gpx4* and *Nrf2* were significantly decreased, and *Ptgs2* was increased in the 1,000 mg/kg DEHP-exposed

group. A previous study indicated that Nrf2 protects cells from ferroptosis by increasing GSH production (Kerins and Ooi, 2018). Nevertheless, the administration of Fer-1 significantly increased the expression of *Slc7a11 and Gpx4* while decreasing the expression of *Ptgs2*. *Nrf2* was not improved significantly, and liver GSH was also not markedly changed in the Fer-1 group compared with the DEHP-exposed group. In an *in vitro* study, Nrf2 was obviously downregulated, which suggests that other signaling pathways and factors might be altered by the treatments and contribute to the resulting changes in the liver and should be investigated for causality in the future (Dong et al., 2020; Cheng et al., 2021). Currently, the results of our study suggest that DEHP exposure causes the accumulation of iron and lipid oxidation and further triggers ferroptosis in the liver through the SLC7A11/GPX4 pathway. The proposed pathway of DEHP-induced liver injury in our study is shown in Figure 7. Further studies are needed to explore the exact molecular mechanism.

The limitations of this study are as follows. First, the exposure doses of DEHP in mice in this study were comparatively high, which were not representative of the actual DEHP exposure dose of the general population in daily life. The findings may not be suitable for extrapolation to the general population. However, the effects of high-dose DEHP exposure on glucose metabolism in particular occupational populations should be given more attention (Xia et al., 2018). Further studies are expected to establish low-dose DEHP exposure animal models to model actual environmental exposure in the general population. Second, we did not measure the long-term effects of DEHP exposure on liver function in offspring. Third, we identified the role of ferroptosis in liver injury in this study, but whether DEHP exposure during pregnancy triggers ferroptosis through SLC7A11/GPX4 or Nrf2/GPX4-related pathways needs to be investigated.

Conclusion

In conclusion, this study revealed that gestational exposure to DEHP induced liver injury *in vivo* and *in vitro* and that ferroptosis may play a potential role in the mechanism of toxicity. In particular, DEHP exposure prompted ferroptosis in mice livers by downregulating the expression of GPX4. These findings provide new insight into the underlying mechanism of DEHP-induced liver injury in gestation.

Data availability statement

The data supporting the conclusion of this study are included in the article/Supplementary Material, further inquiries can be directed to the corresponding author.

Ethics statement

The animal study was reviewed and approved by the Experimental Animal Ethics Committee of Anhui Medical University (No: 20190302).

Author contributions

FZ and HZ wrote the manuscript. FZ, HC, and HZ. performed the experiments and data analysis. FH and YJ performed the related experiments in animals. MJ and BH reviewed and revised the article. MJ guided the project. All authors contributed to the article and approved the submitted version.

Funding

This work was supported by the National Natural Science Foundation of China (82003419 and 82103857) and the Key Project of the Natural Science Foundation of Education Department of Anhui Province (KJ 2019A0228).

Acknowledgments

We would like to thank the Platform of Environmental Exposure and Life Health Research at Anhui Medical University for experimental assistance during the studies.

Conflict of interest

The authors declare that the research was conducted in the absence of any commercial or financial relationships that could be construed as a potential conflict of interest.

Publisher's note

Supplementary material

The Supplementary Material for this article can be found online at: https://www.frontiersin.org/articles/10.3389/fcell.2022.1014243/full#supplementary-material

References

Bothwell, T. H. (2000). Iron requirements in pregnancy and strategies to meet them. *Am. J. Clin. Nutr.* 72, 257S–264S. doi:10.1093/ajcn/72.1.257S

Caldwell, J. C. (2012). Dehp: Genotoxicity and potential carcinogenic mechanisms—a review. *Mutat. Res.* 751, 82–157. doi:10.1016/j.mrrev.2012.03.001

Carlson, B. A., Tobe, R., Yefremova, E., Tsuji, P. A., Hoffmann, V. J., Schweizer, U., et al. (2016). Glutathione peroxidase 4 and vitamin E cooperatively prevent hepatocellular degeneration. *Redox Biol.* 9, 22–31. doi:10.1016/j.redox.2016.05.003

Chen, H., Zhang, W., Rui, B. B., Yang, S. M., Xu, W. P., and Wei, W. (2016). Di(2-ethylhexyl) phthalate exacerbates nonalcoholic fatty liver in rats and its potential mechanisms. *Environ. Toxicol. Pharmacol.* 42, 38–44. doi:10.1016/j.etap.2015.12.016

Chen, J., Li, X., Ge, C., Min, J., and Wang, F. (2022). The multifaceted role of ferroptosis in liver disease. *Cell Death Differ.* 29, 467–480. doi:10.1038/s41418-022-00941-0

Cheng, K., Huang, Y., and Wang, C. (2021). 1, 25$(OH)_2D_3$ inhibited ferroptosis in zebrafish liver cells (ZFL) by regulating keap1-nrf2-GPx4 and NF-κB-hepcidin Axis. *Int. J. Mol. Sci.* 22, 11334. doi:10.3390/ijms222111334

Dai, X., Zhu, S., Li, M., Talukder, M., Zhao, Y., and Li, J. (2021). Potential role of lycopene in the inhibition of di(2-ethylhexyl) phthalate-induced ferroptosis in spleen via modulation of iron ion homeostasis. *ACS Pharmacol. Transl. Sci.* 4, 386–395. doi:10.1021/acsptsci.1c00001

Ding, S., Qi, W., Xu, Q., Zhao, T., Li, X., Yin, J., et al. (2021). Relationships between di-(2-ethylhexyl) phthalate exposure and lipid metabolism in adolescents: Human data and experimental rat model analyses. *Environ. Pollut.* 286, 117570–117579. doi:10.1016/j.envpol.2021.117570

Dixon, S. J. E. A., Lemberg, K. M., Lamprecht, M. R., Skouta, R., Zaitsev, E. M., Gleason, C. E., et al. (2012). Ferroptosis: An iron-dependent form of nonapoptotic cell death. *Cell* 149, 1060–1072. doi:10.1016/j.cell.2012.03.042

Dong, H., Qiang, Z., Chai, D., Peng, J., Xia, Y., Hu, R., et al. (2020). Nrf2 inhibits ferroptosis and protects against acute lung injury due to intestinal ischemia reperfusion via regulating SLC7A11 and HO-1. *Aging (Albany NY)* 12, 12943–12959. doi:10.18632/aging.103378

Duan, J., Lin, X., Xu, F., Shan, S., Guo, B., Li, F., et al. (2021). Ferroptosis and its potential role in metabolic diseases: A curse or revitalization? *Front. Cell Dev. Biol.* 9, 701788–788. doi:10.3389/fcell.2021.701788

Evstatiev, R., and Gasche, C. (2012). Iron sensing and signalling. *Gut* 61, 933–952. doi:10.1136/gut.2010.214312

Han, D., Yao, Y., Chen, L., Miao, Z., and Xu, S. (2022). Apigenin ameliorates di(2-ethylhexyl) phthalate-induced ferroptosis: The activation of glutathione peroxidase 4 and suppression of iron intake. *Food Chem. Toxicol.* 164, 113089. doi:10.1016/j.fct.2022.113089

Han, F., Li, S., Yang, Y., and Bai, Z. (2021). Interleukin-6 promotes ferroptosis in bronchial epithelial cells by inducing reactive oxygen species-dependent lipid peroxidation and disrupting iron homeostasis. *Bioengineered* 12, 5279–5288. doi:10.1080/21655979.2021.1964158

Heindel, J. J., and Blumberg, B. (2019). Environmental obesogens: Mechanisms and controversies. *Annu. Rev. Pharmacol. Toxicol.* 59, 89–106. doi:10.1146/annurev-pharmtox-010818-021304

Huang, Y. Q., Tang, Y. X., Qiu, B. H., Talukder, M., Li, X. N., and Li, J. L. (2022). Di-2-ethylhexyl phthalate (DEHP) induced lipid metabolism disorder in liver via activating the LXR/SREBP-1c/PPARα/γ and NF-κB signaling pathway. *Food Chem. Toxicol.* 165, 113119–119. doi:10.1016/j.fct.2022.113119

Jiang, X., Stockwell, B. R., and Conrad, M. (2021). Ferroptosis: Mechanisms, biology and role in disease. *Nat. Rev. Mol. Cell Biol.* 22, 266–282. doi:10.1038/s41580-020-00324-8

Kawabata, H. (2019). Transferrin and transferrin receptors update. *Free Radic. Biol. Med.* 133, 46–54. doi:10.1016/j.freeradbiomed.2018.06.037

Kerins, M. J., and Ooi, A. (2018). The roles of nrf2 in modulating cellular iron homeostasis. *Antioxid. Redox Signal.* 29, 1756–1773. doi:10.1089/ars.2017.7176

Koch, H. M., Drexler, H., and Angerer, J. (2003). An estimation of the daily intake of di(2-ethylhexyl) phthalate (DEHP) and other phthalates in the general population. *Int. J. Hyg. Environ. Health* 206, 77–83. doi:10.1078/1438-4639-00205

Lao, T. T. (2020). Implications of abnormal liver function in pregnancy and nonalcoholic fatty liver disease. *Best. Pract. Res. Clin. Obstet. Gynaecol.* 68, 2–11. doi:10.1016/j.bpobgyn.2020.02.011

Lee Jh, J. H. C. E., Jang, H., Cho, E. J., and Youn, H. D. (2009). Ferritin binds and activates p53 under oxidative stress. *Biochem. Biophys. Res. Commun.* 3, 399–404. doi:10.1016/j.bbrc.2009.08.125

Li, R., Yu, C., Gao, R., Liu, X., Lu, J., Zhao, L., et al. (2012). Effects of DEHP on endometrial receptivity and embryo implantation in pregnant mice. *J. Hazard. Mat.* 241, 231–240. doi:10.1016/j.jhazmat.2012.09.038

Li, X., Wang, T. X., Huang, X., Li, Y., Sun, T., Zang, S., et al. (2020). Targeting ferroptosis alleviates methionine-choline deficient (mcd)-diet induced NASH by suppressing liver lipotoxicity. *Liver Int.* 40, 1378–1394. doi:10.1111/liv.14428

Liu, R. J., He, Y. J., Liu, H., Zheng, D. D., Huang, S. W., and Liu, C. H. (2021). Protective effect of lycium barbarum polysaccharide on di-(2-ethylhexyl) phthalate-induced toxicity in rat liver. *Environ. Sci. Pollut. Res. Int.* 28, 23501–23509. doi:10.1007/s11356-020-11990-8

Lo, D., Wang, Y. T., and Wu, M. C. (2014). Hepatoprotective effect of silymarin on di(2-ethylhexyl) phthalate (DEHP)-induced injury in liver fl83b cells. *Environ. Toxicol. Pharmacol.* 38, 112–118. doi:10.1016/j.etap.2014.05.005

Lunova, M. G. C. K. D., Goehring, C., Kuscuoglu, D., Mueller, K., Chen, Y., Walther, P., et al. (2014). Hepcidin knockout mice fed with iron-rich diet develop chronic liver injury and liver fibrosis due to lysosomal iron overload. *J. Hepatol.* 3, 633–641. doi:10.1016/j.jhep.2014.04.034

Meynard D, B. J. L. H., Babitt, J. L., and Lin, H. Y. (2014). The liver: Conductor of systemic iron balance. *Blood* 2, 168–176. doi:10.1182/blood-2013-06-427757

Midya, V., Colicino, E., Conti, D. V., Berhane, K., Garcia, E., Stratakis, N., et al. (2022). Association of prenatal exposure to endocrine-disrupting chemicals with liver injury in children. *JAMA Netw. Open* 5, e2220176–e27. doi:10.1001/jamanetworkopen.2022.20176

Naz, N., Moriconi, F., Ahmad, S., Amanzada, A., Khan, S., Mihm, S., et al. (2013). Ferritin l is the sole serum ferritin constituent and a positive hepatic acute-phase protein. *Shock* 39, 520–526. doi:10.1097/SHK.0b013e31829266b9

Sarkar, M., Grab, J., Dodge, J. L., Gunderson, E. P., Rubin, J., Irani, R. A., et al. (2020). Nonalcoholic fatty liver disease in pregnancy is associated with adverse maternal and perinatal outcomes. *J. Hepatol.* 73, 516–522. doi:10.1016/j.jhep.2020.03.049

Seibt, T. M., Proneth, B., and Conrad, M. (2019). Role of GPX4 in ferroptosis and its pharmacological implication. *Free Radic. Biol. Med.* 133, 144–152. doi:10.1016/j.freeradbiomed.2018.09.014

Shou, Y., Yang, L., Yang, Y., and Xu, J. (2021). Inhibition of keratinocyte ferroptosis suppresses psoriatic inflammation. *Cell Death Dis.* 12, 1009. doi:10.1038/s41419-021-04284-5

Stockwell, B. R., Friedmann, A. J., Bayir, H., Bush, A. I., Conrad, M., Dixon, S. J., et al. (2017). Ferroptosis: A regulated cell death nexus linking metabolism, redox biology, and disease. *Cell* 171, 273–285. doi:10.1016/j.cell.2017.09.021

Tsurusaki, S., Tsuchiya, Y., Koumura, T., Nakasone, M., Sakamoto, T., Matsuoka, M., et al. (2019). Hepatic ferroptosis plays an important role as the trigger for initiating inflammation in nonalcoholic steatohepatitis. *Cell Death Dis.* 10, 449–452. doi:10.1038/s41419-019-1678-y

van Vuren, A. J., van Wijk, R., van Beers, E. J., and Marx, J. J. M. (2020). Liver iron retention estimated from utilization of oral and intravenous radioiron in various anemias and hemochromatosis in humans. *Int. J. Mol. Sci.* 21, E1077–E1078. doi:10.3390/ijms21031077

Wang, X., Liu, Z., Peng, P., Gong, Z., Huang, J., and Peng, H. (2022). Astaxanthin attenuates osteoarthritis progression via inhibiting ferroptosis and regulating mitochondrial function in chondrocytes. *Chem. Biol. Interact.* 366, 110148–148. doi:10.1016/j.cbi.2022.110148

Wu, Y., Wang, J., Zhao, T., Chen, J., Kang, L., Wei, Y., et al. (2022). Di-(2-ethylhexyl) phthalate exposure leads to ferroptosis via the hif-1α/ho-1 signaling pathway in mouse testes. *J. Hazard. Mat.* 426, 127807–127814. doi:10.1016/j.jhazmat.2021.127807

Xia, M., Ouyang, X., Wang, X., Shen, X., and Zhan, Y. (2018). Occupational exposure assessment of phthalate esters in indoor and outdoor microenvironments. *J. Environ. Sci.* 72, 75–88. doi:10.1016/j.jes.2017.12.013

Xiao, Z., Kong, B., Fang, J., Qin, T., Dai, C., Shuai, W., et al. (2021). Ferrostatin-1 alleviates lipopolysaccharide-induced cardiac dysfunction. *Bioengineered* 12, 9367–9376. doi:10.1080/21655979.2021.2001913

Yang, W. S., Sriram Ratnam, R., Welsch, M. E., Shimada, K., Skouta, R., Viswanathan, V. S., et al. (2014). Regulation of ferroptotic cancer cell death by gpx4. *Cell* 156, 317–331. doi:10.1016/j.cell.2013.12.010

Yang, W. S., and Stockwell, B. R. (2016). Ferroptosis: Death by lipid peroxidation. *Trends Cell Biol.* 26, 165–176. doi:10.1016/j.tcb.2015.10.014

Yin, X., Zeb, R., Wei, H., and Cai, L. (2021). Acute exposure of di(2-ethylhexyl) phthalate (DEHP) induces immune signal regulation and ferroptosis in oryzias melastigma. *Chemosphere* 265, 129053. doi:10.1016/j.chemosphere.2020.129053

Yu, L., Yang, M., Cheng, M., Fan, L., Wang, X., Xu, T., et al. (2021). Associations between urinary phthalate metabolite concentrations and markers of liver injury in the us adult population. *Environ. Int.* 155, 106608. doi:10.1016/j.envint.2021.106608

Zhang, N., Yu, X., Xie, J., and Xu, H. (2021). New insights into the role of ferritin in iron homeostasis and neurodegenerative diseases. *Mol. Neurobiol.* 58, 2812–2823. doi:10.1007/s12035-020-02277-7

Zhao, Y., Bao, R., Zhu, S., Talukder, M., Cui, J., Zhang, H., et al. (2021). Lycopene prevents DEHP-induced hepatic oxidative stress damage by crosstalk between AHR-Nrf2 pathway. *Environ. Pollut.* 285, 117080. doi:10.1016/j.envpol.2021.117080

Zhao, Y., Ma, D. X., Wang, H. G., Li, M. Z., Talukder, M., Wang, H. R., et al. (2020). Lycopene prevents DEHP-induced liver lipid metabolism disorder by inhibiting the HIF-1α-induced pparα/pparγ/fxr/lxr system. *J. Agric. Food Chem.* 68, 11468–11479. doi:10.1021/acs.jafc.0c05077

Zhuang, T., Han, H., and Yang, Z. (2014). Iron, oxidative stress and gestational diabetes. *Nutrients* 6, 3968–3980. doi:10.3390/nu6093968

frontiers | Frontiers in Cell and Developmental Biology

TYPE Mini Review
PUBLISHED 18 November 2022
DOI 10.3389/fcell.2022.1034348

OPEN ACCESS

EDITED BY
Sandra Donnini,
University of Siena, Italy

REVIEWED BY
Paul J. Kammermeier,
University of Rochester, United States
Valerio Ciccone,
University of Siena, Italy

*CORRESPONDENCE
Xiaohua Lei,
xh.lei@siat.ac.cn
Huashan Zhao,
hs.zhao@siat.ac.cn

†These authors have contributed equally to this work

SPECIALTY SECTION
This article was submitted to Cellular Biochemistry, a section of the journal Frontiers in Cell and Developmental Biology

RECEIVED 01 September 2022
ACCEPTED 08 November 2022
PUBLISHED 18 November 2022

CITATION
Lin J, Li Q, Lei X and Zhao H (2022), The emerging roles of GPR158 in the regulation of the endocrine system. *Front. Cell Dev. Biol.* 10:1034348. doi: 10.3389/fcell.2022.1034348

The emerging roles of GPR158 in the regulation of the endocrine system

Jinju Lin†, Qin Li†, Xiaohua Lei* and Huashan Zhao*

Center for Energy Metabolism and Reproduction, Shenzhen Institute of Advanced Technology, Chinese Academy of Sciences, Shenzhen, China

G protein-coupled receptor 158 (GPR158) is a member of class C G protein-coupled receptors (GPCRs) and is highly expressed in the central nervous system (CNS) while lowly expressed in peripheral tissues. Previous studies have mainly focused on its functions in the CNS, such as regulating emotions, memory, and cognitive functions, whereas studies on its role in the non-nervous system are limited. It has been recently reported that GPR158 is directly involved in adrenal regulation, suggesting its role in peripheral tissues. Moreover, GPR158 is a stable dimer coupled to the regulator of G protein signaling protein 7 (RGS7) that forms the GPR158-RGS7-Gβ5 complex. Given that the RGS7-Gβ5 complex is implicated in endocrine functions, we speculate that GPR158 might be an active component of the endocrine system. Herein, we reviewed the relevant literature on GPR158, including its molecular structure, regulatory molecules, expression, and functions, and highlighted its roles in endocrine regulation. These findings not only enhance our understanding of GPR158 from an endocrine perspective but also provide valuable insights into drug exploration targeting GPR158 and their applicability in endocrine disorders.

KEYWORDS

GPR158, endocrine, glucocorticoid, prostate, adrenal gland, energy metabolism

Introduction

GPR158 was first identified in 2005; Bjarnadóttir et al. searched for genes encoding class C GPCRs in four vertebrates and four invertebrates and classified them into four phylogenetic groups (Group I-IV). GPR158, together with γ-aminobutyric acid (GABA), belongs to Group III (Bjarnadóttir et al., 2005). It plays a pivotal role in modulating physiological function and are targets of several investigational drugs (Ellaithy et al., 2020). To date, the ligand of GPR158 remains unknown, and thus studies on the deorphanization of GPR158 are ongoing (Fu et al., 2022).

According to the Genotype-Tissue Expression database, GPR158 is highly expressed in the CNS, including the cortex, hippocampus, and hypothalamus, while its expression level is lower in peripheral tissues (Obri et al., 2018). Therefore, researchers have predominantly focused on the role of GPR158 in the CNS. Notably, an increasing number of studies indicate that GPR158 is related to endocrine regulation. For instance,

glucocorticoid disorders could lead to depression *via* the modulation of GPR158 levels (Sutton et al., 2018). Moreover, the up-regulation of GPR158 in prostate cancer (PCa) and ovarian carcinoma indirectly affects the endocrine system (Patel et al., 2015; Engqvist et al., 2019).

Thus, in this review, literature in PubMed was searched with the keyword "GPR158," and 43 articles and eight reviews were retrieved. Among them, 15 articles were related to endocrine alterations and the correlation between GPR158 and the endocrine system, such as its structure, regulatory molecules, expression profile, and endocrine-related functions.

Structural characteristics of GPR158-RGS7-Gβ5 complex

In 2012, Orlandi et al. (2012) reported that GPR158 binds with RGS7 to target the RGS7-Gβ5 complex in the plasma membrane in the CNS. Extracellularly, GPR158 contains a leucine repeat region and a calcium-binding EGF-like domain at the N-terminal and lacks the Venus flytrap module, which is necessary for ligand binding and receptor activation in class C GPCRs. Meanwhile, silico analysis signaled that GPR158 has a signature motif of the metabolic glutamate receptor family at the beginning of the 7th helix, and the N-terminal contains several N-glycosylation sites. Similar to many GPCRs, GPR158 contains cysteine residues at analogous locations between extracellular loop (EL)1 and EL2 that are responsible for ligand recognition (Patel et al., 2013). Moreover, the C-terminal of GPR158 contains three conservative regions similar to other known G protein regulators, which are crucial for binding to RGS7 and enhancing its function in regulating GTPase-activating proteins (Ross and Wilkie, 2000). Knockout of GPR158 in mice led to post-transcriptional destabilization of RGS7 and its inability to localize to the membrane, suggesting that GPR158 is an essential regulator of RGS7 in the CNS and plays a key role in controlling its expression, membrane localization, and catalytic activity (Orlandi et al., 2015). In 2022, Patil et al. (2022) analyzed the near-atomic-level structure of GPR158 *via* single-particle cryo-electron microscopy and described that GPR158 is a homodimeric organization stabilized by phosphatidylinositol and phosphatidylethanolamine. Its N-terminal is the characteristic cache domain fold, an unusual ligand-binding domain in GPCRs. In contrast, its C-terminal directly binds to RGS7, which subsequently binds to Gβ5. This anchoring differs from the classical GPCRs that require the participation of the α subunit of G protein, implying that the GPR158-RGS7-Gβ5 complex may have its unique signaling pathway. Interestingly, RGS7-Gβ5 is also expressed in the corticotroph-derived pituitary AtT-20 cell line, pituitary gland, and pancreatic islets (Nini et al., 2012). A previous study described that overexpression of RGS7-Gβ5 in pancreatic β cells promoted insulin synthesis *via* stimulation of the muscarinic cholinergic receptor M3, indicating that the RGS7-Gβ5 complex plays a decisive role in the endocrine system (Wang et al., 2017).

Regulatory molecules of GPR158

Although GPR158 is regarded as an orphan receptor, some putative ligands or regulatory molecules have been reported to be associated with it, including polypeptides, intracellular binding proteins, steroid hormones, glycosaminoglycans, and microRNAs (Table 1). Osteocalcin (OCN), as the putative ligand of GPR158, can improve mouse hippocampus-dependent memory (Khrimian et al., 2017), in which the histone-binding protein RbAp48 is an active component (Kosmidis et al., 2018). In nerve growth factor-induced neurite outgrowth of PC12 cells, OCN interacts with GPR158 and promotes PC12 cell proliferation, differentiation, and survival (Ando et al., 2021). Embryonic OCN/GPR158 signals determine lifelong adrenal steroidogenesis and homeostasis in the adrenal gland of mice (Yadav et al., 2022). Indeed, steroid hormones, such as glucocorticoids and androgens, can interact with GPR158. In trabecular meshwork cells (TBM), glucocorticoids can stimulate the expression of GPR158, which promotes proliferation and reduces the permeability of TBM (Patel et al., 2013). Under chronic stress conditions, GPR158 responds to glucocorticoids and induces depression (Sutton et al., 2018). In the early stage of PCa, androgen can upregulate the expression of GPR158 (Patel et al., 2015). Besides the aforementioned hormones, GPC4, as a heparan sulfate proteoglycan (HSPG), interacts with GPR158 in the hippocampal CA3 region and organizes mossy fiber-CA3 synapse density and size (Condomitti et al., 2018). In addition, some microRNAs could also govern the expression of GPR158. In glioma, microRNA-449a down-regulates the expression of GPR158 to regulate neural differentiation and apoptosis (Li et al., 2018). In osteosarcoma, miR613 inhibits the expression of GPR158, leading to the inhibition of the proliferation and angiogenesis of osteosarcoma (Wang et al., 2022). Collectively, the deorphanization of GPR158 still necessitates further investigation in order to identify novel molecules regulating the endocrine system.

Expression of GPR158 in endocrine-related tissues

In situ hybridization and qPCR have revealed that GPR158 is highly expressed in the CA3 region of the hippocampus, cortex, midbrain, brainstem, and cerebellum

TABLE 1 Overview of GPR158 regulatory molecules.

Classification	Regulatory molecules	Species/cell types	Location	Function	References
Peptide hormone	OCN	mouse	Hippocampal CA3 region	Improves hippocampal-dependent memory	Khrimian et al. (2017)
		Rat pheochromocytoma cell line PC12	—	Promotes proliferation, differentiation, and survival of PC12 cells	Ando et al. (2021)
		mouse	Adrenal gland	Determines adrenal steroidogenesis and homeostasis[a]	Yadav et al. (2022)
Intracellular binding protein	RGS7	HEK293T/17 cells	membrane	Targets RGS7 to the plasma membrane and augments the activity of GTPase-activating proteins[a]	Orlandi et al. (2012)
	RbAp48	mouse	Hippocampal CA3 region and dentate gyrus	Improves age-related memory loss	Kosmidis et al. (2018)
Steroid hormone	Glucocorticoid	human	Trabecular meshwork cell (TBM)	Promotes proliferation and differentiation of TBM and increases the barrier function of monolayer cells[a]	Patel et al. (2013)
		mouse	Prefrontal cortex	Leads to depression[a]	Sutton et al. (2018)
	Androgen (DHT)	PHPECs and LNCaP cells	—	Stimulates androgen receptor and prostate-specific antigen expression[a]	Patel et al. (2015)
Glycosaminoglycan	Heparan sulfate proteoglycan (HSPG) glypican (GPC4)	HEK293T cells	Hippocampal granule cell axons (mossy fibers)	Organizes mossy fiber-CA3 synapse density and size	Condomitti et al. (2018)
microRNA	microRNA-449a	mouse	glioma	Antagonizes neural differentiation and apoptosis of glioma stem cells	Li et al. (2018)
	miR613	Human osteosarcoma cell lines (U2OS and MG63)	—	Inhibits the proliferation and angiogenesis of osteosarcoma	Wang et al. (2022)

[a]Indicates association with endocrine function.

(Khrimian et al., 2017). Nevertheless, its expression in the hypothalamus has not been explored so far. In 2007, gene expression profiling analysis of the metastatic process of PCa determined the expression of GPR158 in peripheral glands (Chandran et al., 2007). Using affymetrix oligonucleotide arrays to analyze 24 androgen-ablation-resistant metastatic samples and 64 primary prostate tumor samples, the authors found that GPR158 is up-regulated during PCa metastasis. In the female reproductive system, 17 of 29 mucinous ovarian cancer samples (59%) were GPR158-positive (Engqvist et al., 2019). In estrogen-sensitive breast cancer, the expression of GPR158 is down-regulated following the withdrawal of estrogen or the use of estrogen antagonists (Salazar et al., 2011), suggesting that GPR158 may be a novel biomarker for the prognosis of ovarian carcinoma and breast cancer. Recently, a study on OCN regulation of adrenal steroidogenesis in mice revealed that GPR158 is expressed in the adrenal gland, and the expression level is significantly higher than in the hypothalamus and pituitary gland (Yadav et al., 2022). Overall, despite the expression level of GPR158 in peripheral endocrine tissues being lower than that in nervous tissue, this does not influence its physiological role owing to the powerful effects of hormones.

Endocrine-related functions of GPR158

GPR158 affects cognition through bone-derived hormone OCN

OCN, as a putative ligand of GPR158, was first discovered by Khrimian et al. (2017) in 2017. By injecting plasma from young mice into aged mice with evident hippocampal-dependent memory impairments, they found that the memory and anxiety-like behaviors were significantly ameliorated. Contrastingly, the absence of this effect in the plasma of OCN knockout (KO) mice confirmed that OCN can improve memory and cognitive abilities. Furthermore, the failure of plasma from OCN KO mice to improve cognitive functions and memory in aged mice was not illustrated by the accumulation of β2-microglobulin, a progeronic molecule in plasma. This phenotype could be reversed by supplementing mouse recombinant uncarboxylated OCN exogenously into the plasma of OCN KO mice. Meanwhile, tissue metalloproteinase inhibitor 2 (TIMP2), a beneficial molecule on cognition in the hippocampus, does not mediate this effect. These results signify that OCN signaling

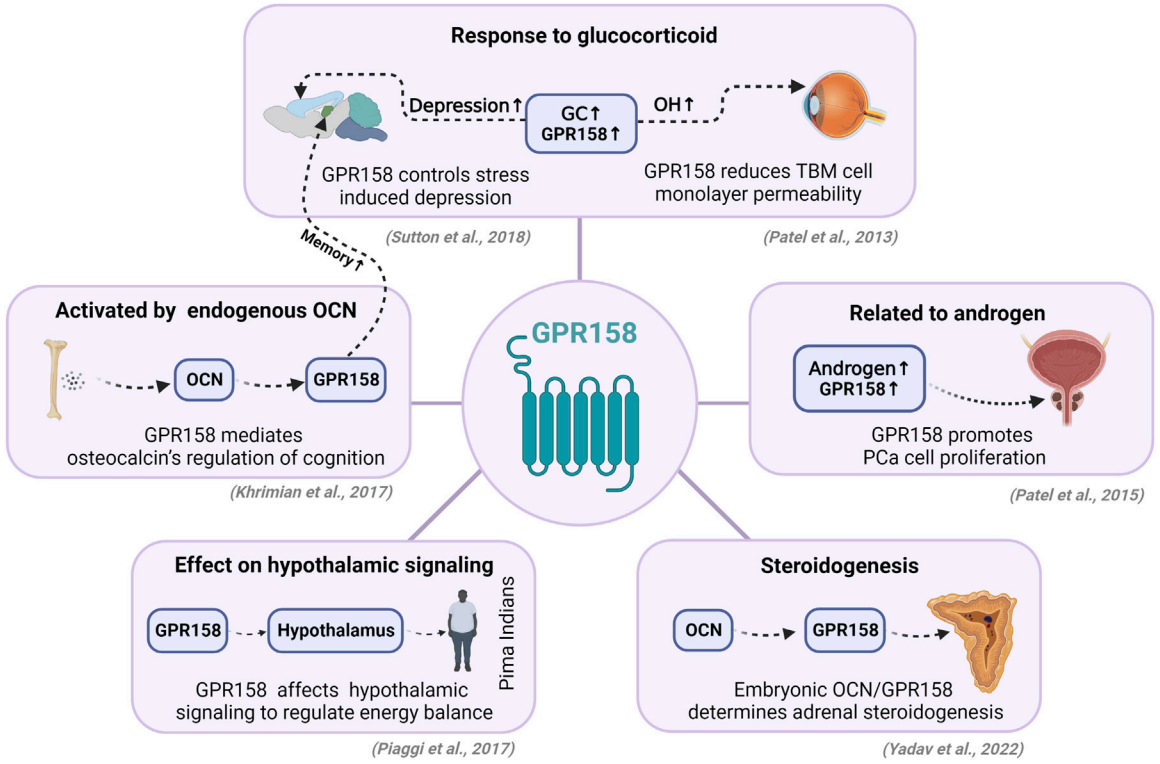

FIGURE 1
Endocrine-related functions of GPR158. GPR158 is abundantly expressed in the nervous system and participates in the pathogenesis of depression, glaucoma, *etc.*, but some studies indicate that GPR158 is related to endocrine pathways. In the nervous system, GC is directly involved in GPR158-mediated depression and alterations in intraocular pressure. The peripheral bone-derived hormone OCN can affect cognitive functions *via* GPR158. Moreover, a study in Pima Indians confirmed that GPR158 regulates energy balance by affecting hypothalamic signaling. In peripheral tissues, GPR158 is also closely associated with androgen and androgen receptors, thereby regulating the proliferation of prostate cancer cells. Interestingly, the relatively high expression of GPR158 in the adrenal gland can directly affect the generation of adrenocorticosteroids through OCN. GC, glucocorticoid; OH, ocular hypertension; TBM, trabecular meshwork; OCN, osteocalcin; PCa, prostate cancer. GC, glucocorticoid; OH, ocular hypertension; TBM, trabecular meshwork; OCN, osteocalcin; PCa, prostate cancer. The figure was created with BioRender.com.

in the brain is independent of β2-microglobulin and TIMP2 and may function through the hormonal pathway. In contrast, GPR158 can interact with OCN in the CA3 region to promote the expression of brain-derived neurotrophic factor (BDNF), thereby improving hippocampal-dependent memory in mice and demonstrating that GPR158 is involved in enhancing memory and cognitive processes. Intracellularly, OCN binds to GPR158 and Gαq on the hippocampal cell membrane, while the amount of pull down of Gαq is significantly decreased in GPR158 KO mice. Furthermore, OCN can upregulate the expression of inositol triphosphate (IP3) but does not affect cAMP expression, indicating that OCN acts through the Gαq-IP3 signaling pathway (Khrimian et al., 2017). Lastly, RbAp48 is required for GPR158/OCN signaling to improve age-related memory decline (Kosmidis et al., 2018).

GPR158 determines adrenal steroidogenesis through OCN

Glucocorticoid hormones are secreted by cells in the adrenal cortex zona fasciculata, and their synthesis and secretion are regulated by the hypothalamic-pituitary-adrenal axis (Gjerstad et al., 2018). Clinically, glucocorticoids are primarily used to treat various allergic diseases, but excessive use of glucocorticoids can cause numerous side effects, such as osteoporosis (Henneicke et al., 2014). Glucocorticoids inhibit the function of osteoblasts and further attenuate the secretion of OCN. Conversely, OCN enhances the function of glucocorticoids through a classical hormonal feedback loop. GPR158 is expressed in the zona fasciculata and zona globule of the adrenal cortex but not in the adrenal medulla. The binding of embryonic OCN to GPR158 promotes the proliferation of adrenal cells and

increases the expression of SF1, a transcription factor essential for adrenal gland development. Embryonic adrenal cells express SF1 and generate Gli1-positive adrenal cortical progenitors in the adrenal capsule, which differentiate into glucocorticoid-producing cells. The hormones released from these cells eventually control blood pressure, blood K+ concentration, and circulating corticosterone levels in acute stress conditions. However, GPR158 KO in the hypothalamus does not affect the expression levels of corticosterone and aldosterone in mice, suggesting that OCN promotes adrenal steroid hormone secretion independently of the hypothalamic-pituitary axis (Yadav et al., 2022).

GPR158 exacerbates ocular hypertension after glucocorticoid treatment

Ocular hypertension is a severe side effect of glucocorticoid overdose (Dibas and Yorio, 2016). Glucocorticoid drugs, including dexamethasone and triamcinolone acetonide, drive the activity of the GPR158 promoter, thereby increasing its transcription level. In the post-transcription stage, two separate bands (~70 kDa and ~55 kDa) can be detected using the C-terminal antibody; likewise, two bands (~95 -kDa and ~80-kDa) can be detected using the N-terminal antibody, consistent with those found in prostate cells. This observation indicates that the hydrolysis of GPR158 overexpression occurs in two different locations: EL2 and the C-terminal surrounding the cytosolic tail of the 8th helix. These GPR158 molecular fragments at the C-terminal might participate in GPR158 nuclear entry (Patel et al., 2013). The localization of GPR158 to the nucleus is essential for its function. Following treatment with two different endocytic inhibitors, ConA and CPZ, GPR158 is localized to the plasma membrane. The 8th helical region of GPR158 contains a bipartite nuclear localization signal (NLS), and a different mutant part of NLS in GPR158 would disturb its location in the nucleus. This indicates the necessity of bipartite NLS for GPR158 transfer into the nucleus (Patel et al., 2013). GPR158 enhances TBM cell proliferation by regulating the expression of cyclin D1, a key protein in the transition from the G1 to the S phase of the cell cycle. GPR158 reduces TBM cell monolayer permeability by increasing the expression of tight junction-specific proteins, resulting in the obstruction of aqueous humor backflow and the occurrence of ocular hypertension, which may eventually lead to primary open-angle glaucoma. Glaucoma is treated by lowering the intraocular pressure (IOP). Several different GPCRs can be used as the target of IOP-lowering drugs, such as β-adrenergic antagonists, including atenolol, betaxolol, and carteolo (Toris, 2010). Owing to the pressure regulation of GPR158 in TBM cells, it could be reckoned that inhibition of GPR158 expression may be a new strategy for the treatment of glaucoma.

GPR158 controls stress-induced depression by responding to glucocorticoid

The medial prefrontal cortex (mPFC) is the region regulating emotion in the brain. Exposure to chronic stress can lead to major depressive disorders (MDD). Glucocorticoids are continuously released during chronic stress conditions, which can lead to the development of maladaptive responses (Myers et al., 2014). Patel et al. (2013) reported that glucocorticoids induce GPR158 expression during chronic stress conditions. Exposure to chronic physical restraint stress subsequently up-regulates GPR158 expression in the glutamatergic neurons of mPFC, thereby leading to depression. Analysis of GPR158 expression in the dorsolateral PFC (dlPFC) of MDD subjects uncovered that GPR158 expression was significantly higher in the dlPFC of MDD patients than that of control subjects, suggesting that GPR158 may regulate the occurrence of depression through neuropathological mechanisms. Deficiency of GPR158 increases the spine density of glutamatergic neurons in the layers of 2/3 of the mPFC and improves expression levels of AMPAR and BDNF, thereby exerting antidepressant effects (Duman and Monteggia, 2006; Autry et al., 2011). GPR158 knockdown also increased the expression of cAMP in the mPFC. As previously mentioned, GPR158 binding to OCN initiates the Gαq-IP3 signaling pathway, which is independent of cAMP (Khrimian et al., 2017). Under chronic stress conditions, glucocorticoid stimulation increases the transcription of GPR158, which links stress, depression, and synaptic plasticity at the molecular level (Sutton et al., 2018), suggesting that GPR158 may be closely related to the neuroendocrine through BDNF.

GPR158 aggravates PCa progression after stimulation of androgen

The early stage of PCa is androgen-dependent and hence can be treated by androgen deprivation. Nonetheless, in the later stage of cancer, it becomes androgen-independent, also referred to as castration-resistant PCa (Desai et al., 2021). GPR158 overexpression can promote PCa cell proliferation, while endogenous GPR158 siRNA treatment can inhibit cell growth. Administration of the androgen receptor (AR) antagonist bicalutamide inhibited DHT-mediated GPR158 expression in primary human prostate epithelial cells. This also signifies that GPR158 needs to be localized in the nucleus to execute its function. *Pten* is a tumor suppressor gene, and *Pten* KO mice are an accepted PCa animal model. GPR158 is up-

regulated in *Pten* KO PCa models co-localized with AR, implying that the expression of GPR158 during androgen deprivation therapy sensitizes PCa to low androgen conditions, thereby accelerating PCa progression (Wang et al., 2003; Patel et al., 2015). The development of castration-resistant PCa includes multiple pathways, including AR co-activation and co-inhibitory protein expression (Shiota et al., 2011). GPR158 co-localizes with AR, illustrating that GPR158 may act as a co-activator of AR and promote the development of PCa. GPR158 expression is associated with a neuroendocrine cell phenotype present in scattered foci of prostate cancer. In LNCaP cells, a human PCa cell line, GPR158 also promoted colony formation, indicating that GPR158 may increase tumorigenicity. Collectively, androgens are necessary to maintain normal physiological functions, but the role of GPR158 in influencing the secretion of AR under physiological conditions remains to be elucidated. In PCa, GPR158 aggravates tumor progression, and its role in regulating other diseases caused by androgen secretion disorders remains unknown.

GPR158 participates in energy metabolism

GPR158 is involved in the regulation of energy metabolism in both animal models and humans. In 2016, a microarray analysis of mRNAs in the micro-dissected hypothalamic and thalamic control areas yielded 17,745 expression values for RNAs representing protein-coding genes that could be assigned annotated gene names. High relative values of genes are expressed in the medial habenula (MHb), lateral habenula (LHb), and thalamus. Notably, LHb is genetically more closely related to the thalamus than MHb. The study pointed out that GPR158 is up-regulated in the habenular region, suggesting its involvement in regulating food and energy expenditure (Wagner et al., 2016). In 2017, a genome-wide association study using a custom genotyping array found that the GPR158 variant is associated with energy expenditure (EE) in Pima Indians. By analyzing rs11014566, DNA fragments of GPR158, they demonstrated the correlation between GPR158 and EE. GPR158 impacts the obesity genes RGS7 and N-type voltage-gated calcium channel (CACNA1B). Custom genotype analysis of Pima Indians identified a new gene locus in GPR158 that affects EE and predisposition to weight gain. PCR results show that GPR158 is predominantly expressed in the whole brain, hypothalamus, pituitary gland, and liver (Piaggi et al., 2017). Taken together, GPR158 interacts with RGS7 and CACNA1B in the CNS, suggesting that it may influence the body's food intake and energy metabolism by affecting the hypothalamic-pituitary axis.

Conclusion

With the discovery of various regulatory molecules, the functions of GPR158 in peripheral tissue are constantly being updated, especially its role in the endocrine system, despite its low expression levels in the peripheral system (Figure 1). There are still questions to be addressed. For instance, given the expression level of GPR158 in ovarian cancer, GPR158 might have a similar effect through estrogen as that of androgen in PCa. RGS7-Gβ5 is involved in the regulation of the endocrine system, and therefore the endocrine function of the GPR158-RGS7-Gβ5 complex necessitates further exploration. Novel drugs targeting GPR158 showed great promise, but the number of drugs targeting it remains limited. We have established a drug delivery system targeting GPR158 in the brain for either cell labeling or therapeutic purposes (Zhao et al., 2021), which is a preliminary study lacking a thorough exploration of the underlying mechanism. Despite studies on GPR158 being underway, existing studies suggest that GPR158 might be a potential target for endocrine diseases.

Author contributions

HZ and XL conceived the manuscript. JL, QL, XL, and HZ wrote and revised the manuscript. JL prepared the figure and the table. All authors contributed to the article and approved the submitted version.

Funding

This work was supported by Shenzhen Fundamental Research Program (JCYJ202208183000694), National Key Research and Development Program of China (2021YFA0719303), Natural Science Foundation of Guangdong Province (2022A1515010952) and China Manned Space Flight Technology Project Chinese Space Station (YYWT-0901-EXP- 15, to XL).

Conflict of interest

The authors declare that the research was conducted in the absence of any commercial or financial relationships that could be construed as a potential conflict of interest.

Publisher's note

References

Ando, E., Higashi, S., Mizokami, A., Watanabe, S., Hirata, M., and Takeuchi, H. (2021). Osteocalcin promotes proliferation, differentiation, and survival of PC12 cells. *Biochem. Biophys. Res. Commun.* 557, 174–179. doi:10.1016/j.bbrc.2021.03.146

Autry, A. E., Adachi, M., Nosyreva, E., Na, E. S., Los, M. F., Cheng, P. F., et al. (2011). NMDA receptor blockade at rest triggers rapid behavioural antidepressant responses. *Nature* 475 (7354), 91–95. doi:10.1038/nature10130

Bjarnadóttir, T. K., Fredriksson, R., and Schiöth, H. B. (2005). The gene repertoire and the common evolutionary history of glutamate, pheromone (V2R), taste(1) and other related G protein-coupled receptors. *Gene* 362, 70–84. doi:10.1016/j.gene.2005.07.029

Chandran, U. R., Ma, C., Dhir, R., Bisceglia, M., Lyons-Weiler, M., Liang, W., et al. (2007). Gene expression profiles of prostate cancer reveal involvement of multiple molecular pathways in the metastatic process. *BMC Cancer* 7, 64. doi:10.1186/1471-2407-7-64

Condomitti, G., Wierda, K. D., Schroeder, A., Rubio, S. E., Vennekens, K. M., Orlandi, C., et al. (2018). An input-specific orphan receptor gpr158-HSPG interaction organizes hippocampal mossy fiber-CA3 synapses. *Neuron* 100 (1), 201–215. doi:10.1016/j.neuron.2018.08.038

Desai, K., Mcmanus, J. M., and Sharifi, N. (2021). Hormonal therapy for prostate cancer. *Endocr. Rev.* 42 (3), 354–373. doi:10.1210/endrev/bnab002

Dibas, A., and Yorio, T. (2016). Glucocorticoid therapy and ocular hypertension. *Eur. J. Pharmacol.* 787, 57–71. doi:10.1016/j.ejphar.2016.06.018

Duman, R. S., and Monteggia, L. M. (2006). A neurotrophic model for stress-related mood disorders. *Biol. Psychiatry* 59 (12), 1116–1127. doi:10.1016/j.biopsych.2006.02.013

Ellaithy, A., Gonzalez-Maeso, J., Logothetis, D. A., and Levitz, J. (2020). Structural and biophysical mechanisms of class C G protein-coupled receptor function. *Trends biochem. Sci.* 45 (12), 1049–1064. doi:10.1016/j.tibs.2020.07.008

Engqvist, H., Parris, T. Z., Kovács, A., Nemes, S., Werner Rönnerman, E., De Lara, S., et al. (2019). Immunohistochemical validation of COL3A1, GPR158 and PITHD1 as prognostic biomarkers in early-stage ovarian carcinomas. *BMC Cancer* 19 (1), 928. doi:10.1186/s12885-019-6084-4

Fu, X., Wei, S., Wang, T., Fan, H., Zhang, Y., Costa, C. D., et al. (2022). Research status of the orphan G protein coupled receptor 158 and future perspectives. *Cells* 11 (8), 1334. doi:10.3390/cells11081334

Gjerstad, J. K., Lightman, S. L., and Spiga, F. (2018). Role of glucocorticoid negative feedback in the regulation of HPA axis pulsatility. *Stress* 21 (5), 403–416. doi:10.1080/10253890.2018.1470238

Henneicke, H., Gasparini, S. J., Brennan-Speranza, T. C., Zhou, H., and Seibel, M. J. (2014). Glucocorticoids and bone: Local effects and systemic implications. *Trends Endocrinol. Metab.* 25 (4), 197–211. doi:10.1016/j.tem.2013.12.006

Khrimian, L., Obri, A., Ramos-Brossier, M., Rousseaud, A., Moriceau, S., Nicot, A. S., et al. (2017). Gpr158 mediates osteocalcin's regulation of cognition. *J. Exp. Med.* 214 (10), 2859–2873. doi:10.1084/jem.20171320

Kosmidis, S., Polyzos, A., Harvey, L., Youssef, M., Denny, C. A., Dranovsky, A., et al. (2018). RbAp48 protein is a critical component of GPR158/OCN signaling and ameliorates age-related memory loss. *Cell Rep.* 25 (4), 959–973. doi:10.1016/j.celrep.2018.09.077

Li, N., Zhang, Y., Sidlauskas, K., Ellis, M., Evans, I., Frankel, P., et al. (2018). Inhibition of GPR158 by microRNA-449a suppresses neural lineage of glioma stem/progenitor cells and correlates with higher glioma grades. *Oncogene* 37 (31), 4313–4333. doi:10.1038/s41388-018-0277-1

Myers, B., Mcklveen, J. M., and Herman, J. P. (2014). Glucocorticoid actions on synapses, circuits, and behavior: Implications for the energetics of stress. *Front. Neuroendocrinol.* 35 (2), 180–196. doi:10.1016/j.yfrne.2013.12.003

Nini, L., Zhang, J. H., Pandey, M., Panicker, L. M., and Simonds, W. F. (2012). Expression of the Gβ5/R7-RGS protein complex in pituitary and pancreatic islet cells. *Endocrine* 42 (1), 214–217. doi:10.1007/s12020-012-9611-5

Obri, A., Khrimian, L., Karsenty, G., and Oury, F. (2018). Osteocalcin in the brain: From embryonic development to age-related decline in cognition. *Nat. Rev. Endocrinol.* 14 (3), 174–182. doi:10.1038/nrendo.2017.181

Orlandi, C., Posokhova, E., Masuho, I., Ray, T. A., Hasan, N., Gregg, R. G., et al. (2012). GPR158/179 regulate G protein signaling by controlling localization and activity of the RGS7 complexes. *J. Cell Biol.* 197 (6), 711–719. doi:10.1083/jcb.201202123

Orlandi, C., Xie, K., Masuho, I., Fajardo-Serrano, A., Lujan, R., and Martemyanov, K. A. (2015). Orphan receptor GPR158 is an allosteric modulator of RGS7 catalytic activity with an essential role in dictating its expression and localization in the brain. *J. Biol. Chem.* 290 (22), 13622–13639. doi:10.1074/jbc.M115.645374

Patel, N., Itakura, T., Gonzalez, J. M., Jr., Schwartz, S. G., and Fini, M. E. (2013). GPR158, an orphan member of G protein-coupled receptor family C: Glucocorticoid-stimulated expression and novel nuclear role. *PLoS One* 8 (2), e57843. doi:10.1371/journal.pone.0057843

Patel, N., Itakura, T., Jeong, S., Liao, C. P., Roy-Burman, P., Zandi, E., et al. (2015). Expression and functional role of orphan receptor GPR158 in prostate cancer growth and progression. *PLoS One* 10 (2), e0117758. doi:10.1371/journal.pone.0117758

Patil, D. N., Singh, S., Laboute, T., Strutzenberg, T. S., Qiu, X., Wu, D., et al. (2022). Cryo-EM structure of human GPR158 receptor coupled to the RGS7-Gβ5 signaling complex. *Science* 375 (6576), 86–91. doi:10.1126/science.abl4732

Piaggi, P., Masindova, I., Muller, Y. L., Mercader, J., Wiessner, G. B., Chen, P., et al. (2017). A genome-wide association study using a custom genotyping array identifies variants in GPR158 associated with reduced energy expenditure in American Indians. *Diabetes* 66 (8), 2284–2295. doi:10.2337/db16-1565

Ross, E. M., and Wilkie, T. M. (2000). GTPase-activating proteins for heterotrimeric G proteins: regulators of G protein signaling (RGS) and RGS-like proteins. *Annu. Rev. Biochem.* 69, 795–827. doi:10.1146/annurev.biochem.69.1.795

Salazar, M. D., Ratnam, M., Patki, M., Kisovic, I., Trumbly, R., Iman, M., et al. (2011). During hormone depletion or tamoxifen treatment of breast cancer cells the estrogen receptor apoprotein supports cell cycling through the retinoic acid receptor α1 apoprotein. *Breast Cancer Res.* 13 (1), R18. doi:10.1186/bcr2827

Shiota, M., Yokomizo, A., and Naito, S. (2011). Increased androgen receptor transcription: A cause of castration-resistant prostate cancer and a possible therapeutic target. *J. Mol. Endocrinol.* 47 (1), R25–R41. doi:10.1530/JME-11-0018

Sutton, L. P., Orlandi, C., Song, C., Oh, W. C., Muntean, B. S., Xie, K., et al. (2018). Orphan receptor GPR158 controls stress-induced depression. *Elife* 7, e33273. doi:10.7554/eLife.33273

Toris, C. B. (2010). Pharmacotherapies for glaucoma. *Curr. Mol. Med.* 10 (9), 824–840. doi:10.2174/156652410793937778

Wagner, F., Bernard, R., Derst, C., French, L., and Veh, R. W. (2016). Microarray analysis of transcripts with elevated expressions in the rat medial or lateral habenula suggest fast GABAergic excitation in the medial habenula and habenular involvement in the regulation of feeding and energy balance. *Brain Struct. Funct.* 221 (9), 4663–4689. doi:10.1007/s00429-016-1195-z

Wang, B. D., Yu, X. J., Hou, J. C., Fu, B., Zheng, H., Liu, Q. K., et al. (2022). Bevacizumab attenuates osteosarcoma angiogenesis by suppressing MIAT encapsulated by serum-derived extracellular vesicles and facilitating miR-613-mediated GPR158 inhibition. *Cell Death Dis.* 13 (3), 272. doi:10.1038/s41419-022-04620-3

Wang, Q., Pronin, A. N., Levay, K., Almaca, J., Fornoni, A., Caicedo, A., et al. (2017). Regulator of G-protein signaling Gβ5-R7 is a crucial activator of muscarinic M3 receptor-stimulated insulin secretion. *Faseb J.* 31 (11), 4734–4744. doi:10.1096/fj.201700197RR

Wang, S., Gao, J., Lei, Q., Rozengurt, N., Pritchard, C., Jiao, J., et al. (2003). Prostate-specific deletion of the murine Pten tumor suppressor gene leads to metastatic prostate cancer. *Cancer Cell* 4 (3), 209–221. doi:10.1016/s1535-6108(03)00215-0

Yadav, V. K., Berger, J. M., Singh, P., Nagarajan, P., and Karsenty, G. (2022). Embryonic osteocalcin signaling determines lifelong adrenal steroidogenesis and homeostasis in the mouse. *J. Clin. Invest.* 132 (4), e153752. doi:10.1172/JCI153752

Zhao, H., Zhu, W., Li, J., Lin, J., Lei, X., Zhang, P., et al. (2021). *Metabolitin-based molecular drug delivery by targeting GPR158 in glioblastoma*. Cold Spring Harbor Laboratory. Available at: https://www.biorxiv.org/content/10.1101/2021.12.13.472376v1 (Accessed March 16, 2011.

frontiers | Frontiers in Cell and Developmental Biology

TYPE Mini Review
PUBLISHED 13 January 2023
DOI 10.3389/fcell.2023.1034455

OPEN ACCESS

EDITED BY
Huashan Zhao,
Shenzhen Institutes of Advanced Technology (CAS), China

REVIEWED BY
Ruan Degong,
The University of Hong Kong, Hong Kong SAR, China
Zhen Dong,
Southwest University, China

*CORRESPONDENCE
Min Chen,
edchen99@gmail.com

†These authors have contributed equally to this work.

SPECIALTY SECTION
This article was submitted to Cellular Biochemistry, a section of the journal Frontiers in Cell and Developmental Biology

RECEIVED 01 September 2022
ACCEPTED 03 January 2023
PUBLISHED 13 January 2023

CITATION
Kong J, Li S, Li Y and Chen M (2023), Effects of *Salvia miltiorrhiza* active compounds on placenta-mediated pregnancy complications. *Front. Cell Dev. Biol.* 11:1034455. doi: 10.3389/fcell.2023.1034455

Effects of *Salvia miltiorrhiza* active compounds on placenta-mediated pregnancy complications

Jingyin Kong[1†], Songjun Li[2†], Yingting Li[1] and Min Chen[1*]

[1]Department of Prenatal Diagnosis and Fetal Medicine, The Third Affiliated Hospital of Guangzhou Medical University, Guangzhou, China, [2]Department of Reproduction Medical Center, The Third Affiliated Hospital of Shenzhen University, Shenzhen, China

Placenta-mediated pregnancy complications (PMPCs), including preeclampsia (PE), fetal growth restriction (FGR), and recurrent spontaneous abortion (RSA), occur in approximately 5% of pregnancies and are caused by abnormal placenta development. The development of effective therapies for PMPCs is still challenging due to the complicated pathogenesis, such as disrupted vascular homeostasis and subsequent abnormal placentation. Synthetic drugs have been recommended for treating PMPCs; however, they tend to cause adverse reactions in the mother and fetus. *Salvia miltiorrhiza* (*S. miltiorrhiza*) has potential effects on PMPCs owing to its advantages in treating cardiovascular disorders. *S. miltiorrhiza* and its active compounds could attenuate the symptoms of PMPCs through anticoagulation, vasodilation, antioxidation, and endothelial protection. Thus, in this review, we summarize the literature and provide comprehensive insights on *S. miltiorrhiza* and its phytochemical constituents, pharmacological activities, and on PMPCs, which would be valuable to explore promising drugs.

KEYWORDS

placental pregnancy complications, *Salvia miltiorrhiza*, active compounds, placental development, preeclampsia

1 Introduction

The human placenta, a specialized organ that mediates exchanges between the mother and fetus, is essential for a successful pregnancy and fetal health. Its development begins during the implantation of the blastocyst (Hemberger et al., 2020). Chorionic villi, as structural and functional units of the placenta, are consisted of two layers of trophoblasts (James et al., 2022). The inner layer is composed of proliferative villous cytotrophoblasts (vCTBs), which can differentiate into outer layer villous syncytiotrophoblasts that form a physical barrier to pathogens (Turco and Moffett, 2019). Cytotrophoblast cells invade the maternal spiral arteries and replace the maternal endothelium. The remodeling of maternal spiral arteries reduces the resistance of blood flow to meet the nutrition transport for fetus (Turco and Moffett, 2019; James et al., 2022). Defective trophoblast differentiation and function cause incomplete spiral artery remodeling, contributing to PMPCs (Staff et al., 2022). However, the physiopathological mechanism of PMPCs has yet to be elucidated (Freitag et al., 2020; Wu et al., 2020; Staff et al., 2022).

PMPCs result in high maternal and neonatal morbidity rates as aforementioned (Kuwabara et al., 2020). Synthetic drugs have been recommended to treat PMPCs (Chappell et al., 2021). In particular, low-dose aspirin can attenuate the symptoms of PE (Hodgetts Morton and Stock, 2022; Walsh and Strauss, 2022). However, synthetic drugs have adverse reactions in the mother and fetus. In contrast, traditional Chinese medicine (TCM), with a long usage history, has drawn increasing attention in recent years due to its fewer side effects (Yang et al., 2022).

Clinicians have started treating PMPCs with TCM compounds, achieving satisfactory therapeutic effects (Zhang et al., 2006).

S. miltiorrhiza, known as Danshen in Chinese, is a perennial plant of the Lamiaceae family (Zeng et al., 2017). Modern pharmacological studies have found that *S. miltiorrhiza* affects the promotion of blood circulation, modulation of vascular endothelial cells, and reduction of immune interactions in the mother-fetus interface. *S. miltiorrhiza* injection, derived from *S. miltiorrhiza* extract, plays a remarkable role in treating PMPCs (Bai et al., 2019; Chen and Yang, 2019). Herein, we review the active compounds, potential effects, and the pharmacological mechanisms of *S. miltiorrhiza* in PMPCs (Figure 1).

2 Active compounds of *S. miltiorrhiza* in PMPCs

S. miltiorrhiza shows extensive biological activities, including antioxidant, antibacterial and anti-inflammatory. Thus, it is widely used for the treatment of various diseases, containing hyperlipidemia, stroke, and cardiovascular and cerebrovascular diseases (Chong et al., 2019). *S. miltiorrhiza* is first described in TCM in the *Compendium of Materia Medica* (Bencao Gangmu, Ming dynasty, 1596 AD). The primary bioactive compounds in *S. miltiorrhiza* are devided into two major groups of chemicals (Zhang et al., 2022). One group involves water-soluble phenolics, such as salvianolic acid A (Sal A), salvianolic acid B (Sal B), lithospermic acid and rosmarinic acid (Wang et al., 2019). The other group is consisting of lipophilic compounds, such as tanshinone I, tanshinone IIA (Tan IIA), tanshinone IIB, cryptotanshinone, and dihydrotanshinone I (Wang et al., 2020). Hence, we outline the valuable active compounds of *S. miltiorrhiza* associated with PMPCs, as listed in Table 1.

3 Effects of *S. miltiorrhiza* in PMPCs

3.1 *S. miltiorrhiza* ameliorates PE

PE is a serious condition characterized by hypertension and proteinuria after 20 weeks of pregnancy (Vata et al., 2015), with an incidence rate of 3%–5% and at least 42,000 maternal deaths yearly (Chappell et al., 2021). PE is a severe threat to maternal and fetal health during pregnancy and childbirth and increases the long-term risk of cardiovascular diseases in mothers and their fetuses (Staff, 2019). It is divided into early-onset and late-onset types (Lisonkova and Joseph, 2013). PE presents reduced trophoblast invasion and defective spiral artery remodeling, which triggers a series of pathophysiological processes, such as antiangiogenesis, vascular inflammation and oxidative stress, resulting in systemic endothelial dysfunction and clinical manifestations (Ortega et al., 2022). The blood vessels of a patient with PE narrowed because of impaired trophoblast invasion and incomplete spiral artery remodeling. The placenta is deprived of blood and oxygen, resulting in abnormal placentation (Hong et al., 2021). *S.*

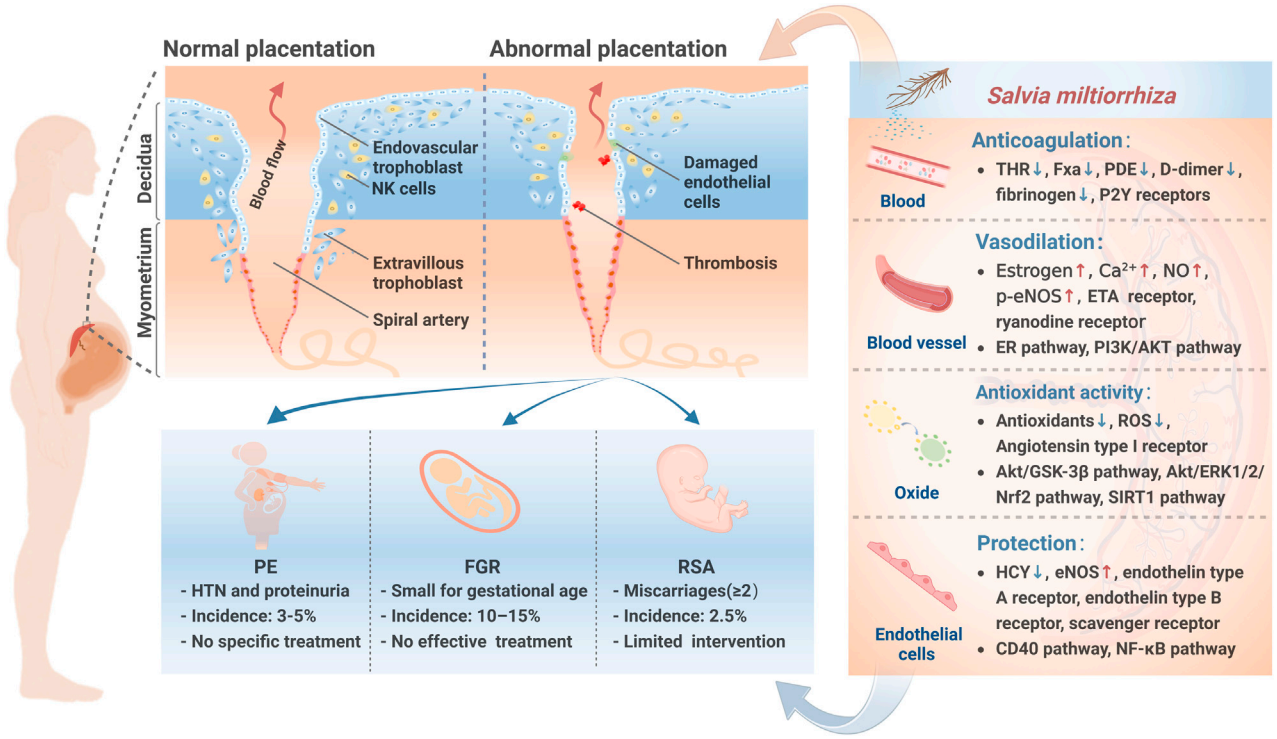

FIGURE 1
PMPCs pathophysiology and the mechanisms of *S. miltiorrhiza* in PMPCs. During normal placentation, extravillous cytotrophoblasts invade the uterine spiral arteries of the decidua andmyometrium, transforming the spiral arteries into large-caliber vessels. However, during abnormal placentation in PMPCs, failed spiral artery remodeling constrains maternal-fetal interface blood flow, which contributes to the pathogenesis of PMPCs. NK, natural killer; PE, preeclampsia; FGR, fetal growth restriction; RSA, recurrent spontaneous abortion; HTN, hypertension; THR, thrombin; Fxa, factor Xa; NO, nitric oxide; p-eNOS, phosnhorylation of endothelial nitric oxide synthase; ETA, endothelin A; ROS, reactive oxygen species; HCY, homocysteine.

TABLE 1 Active compounds and potential mechanisms of *S. miltiorrhiza* in PMPCs.

Classification	Active compound (Structure)	Potential mechanisms in PMPCs	References
water-soluble phenolics	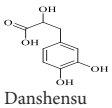 Danshensu	- Inhibit activated platelets	Shen et al. (2011)
		- Scavenge free radical	Zhang et al. (2010); Shen et al. (2011)
		- Protect the endothelial cells	Zhang et al. (2010)
	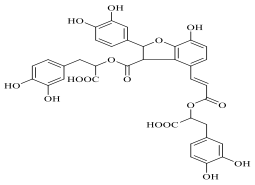 Salvianolic acid B	- Downregulate the expression of PAR-1 and phosphorylation of PKC	Zhang et al. (2021a)
		- Promote the vasodilation through nitric oxide	Shou et al. (2012)
		- Reduce the production of oxygen free radicals	Zhao et al. (2008); Xiao et al. (2020)
		- Regulate the gene expression of antioxidant enzymes	
		- Protect endothelial cells against apoptosis	Liu et al. (2007)
	 Protocatechualdehyde	- Have anticoagulant activity	Song Wang et al. (2008)
		- Decrease oxidative stress level	Ji et al. (2021)
		- Restore endothelial function	
	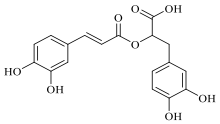 Rosmarinic acid	- Scavenge free radical	Lamaison et al. (1991); Huang and Zheng, (2006)
		- Reduce intracellular ROS	
		- Exhibit anti-angiogenic activity	Huang and Zheng, (2006)
	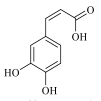 Caffeic acid	- Scavenge superoxide anion radical	Gülçin, (2006)
		- Modulate eNOS expression and phosphorylation	Migliori et al. (2015)
lipophilic tanshinones	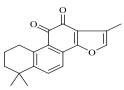 Tanshinone IIA	- Dilate the vessels *via* K^+ channel	Chan et al. (2011)
		- Inhibit CLIC1 expression level	Zhu et al. (2017)
		- Preserve umbilical vein endothelial cells	Lin et al. (2006)
	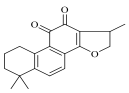 Cryptotanshinone	- Produce vasodilatation *via* decreased Ca^{2+} influx	Lam et al. (2008)
		- Regulate NF-κB and Nrf-2/HO-1 pathways	Wang et al. (2018)
		- Prohibit ET-1 secretion	Zhou et al. (2006)
		- Decrease ET-1 mRNA expression level	

miltiorrhiza has been used to treat PE because of its ability to increase blood flow; however, the mechanism is not fully understood (Zhang et al., 2006).

S. miltiorrhiza injection upregulates the serum insulin-like growth factor-1 and placental growth factor, which enhances the invasion and migration abilities of placental trophoblastic cells and improves the condition of patients with early-onset PE and the prognosis of the mother and the fetus (Li and Qiu, 2020). After the treatment, the systolic and diastolic blood pressures and 24 h urine protein levels decrease remarkably. *S. miltiorrhiza* also improves vascular endothelial function and ischemia-hypoxia status in patients with PE. And there is, abnormal expression of long-chain non-coding RNA (lncRNA) in the placenta of patients with PE (Liang and Meng, 2021). These lncRNAs may cause changes in the expression of downstream regulatory target genes, thereby reducing the invasion of trophoblasts and leading to uterine spiral artery remodeling disorders (Cheng et al., 2019). *S. miltiorrhiza* injection prevents PE from progressing to severe PE or eclampsia and improves maternal and infant outcomes through downregulating the expression of lncRNAs in the placental tissues (Ma et al., 2021). Furthermore, in PE animal models, *S. miltiorrhiza* injection effectively lower blood pressure and alleviate proteinuria to normal levels by increasing platelet count and reducing thrombomodulin expression in the placenta (Shen et al., 2011; Peng and Huang, 2021). The decrease of endogenous and exogenous coagulation factors, factor Xa (FXa), D-dimer, and fibrinogen indicates that the coagulation in PE rat models improved. And long-term low-dose Sal A administration exerts better efficacy through enhancing anticoagulant activity (Shen et al., 2011). Therefore, *S. miltiorrhiza* injection could effectively ameliorate placenta-related indicators and vascular endothelial function in PE (Jiao et al., 2021; Zhang et al., 2021b).

3.2 S. miltiorrhiza mitigates the severity of FGR

FGR is a severe pregnancy-related disease wherein fetuses cannot achieve the expected weight. It is a pivotal cause of stillbirths and an

essential factor affecting the long-term health of the fetus. FGR is mainly caused by abnormal placentation due to insufficient placental development and microvascular resistance, which causes blood circulation disorders in 10%–15% of pregnant women (Aplin et al., 2020; Wang et al., 2020; Ortega et al., 2022). It is divided into early-onset and late-onset according to the gestational age at onset. Early-onset FGR occurs before 32 weeks of pregnancy, accounting for 20% of all cases. Late-onset FGR (≥32 weeks) occurs in about 70% of patients and has a weak correlation with hypertension (approximately 10%) (Audette and Kingdom, 2018). FGR can be attributed to maternal (such as malnutrition, hypertension, PE) and fetal factors (such as chromosomal abnormalities and multiple births) and placental dysfunction. However, placental dysfunction is the most frequent underlying cause of FGR (Aplin et al., 2020; Freitag et al., 2020; Melamed et al., 2021). Incomplete invasion of vCTBs results in inhibition of placental growth, impairment of placental function, long-term hypoxia, and fetus malnutrition. The combination of sodium lactate Ringer's injection and *S. miltiorrhiza* is more effective than sodium lactate Ringer's injection alone (Wei et al., 2021).

3.3 *S. miltiorrhiza* improves the adverse symptoms of RSA

RSA, defined as the failure of two or more clinically recognized pregnancies before 20–24 weeks of gestation, occurs in nearly 2.5% of women trying to conceive. The etiology of RSA is still not fully understood. Trophoblast cells are the most critical cells in placental development, and their proliferation, migration, and invasion are essential for establishing and maintaining a successful pregnancy. Defective trophoblast function impairs uterine spiral artery reconstruction and is implicated in RSA (Wu et al., 2020). Currently, RSA is mainly treated with immunotherapy and anticoagulation, but these therapies have no specificity (Pan et al., 2022).

In RSA mouse models, Tan IIA is ascertained to reduce the rate of embryo loss (Tong et al., 2022). *S. miltiorrhiza* injection has a specific curative effect on patients with RSA through improving the trophoblast cell function and prethrombotic state (Liu et al., 2021). However, relevant studies remain limited and further studies are needed to elucidate the mechanism of *S. miltiorrhiza* in RSA.

4 Potential mechanisms of *S. miltiorrhiza* in PMPCs

4.1 Anticoagulation

The precise regulation of blood coagulation is critical in maintaining a successful pregnancy (True et al., 2022). The blood coagulation cascade is a complicated process regulated by plasma proteins and cofactors affected by different coagulation factors (Davie, 1995). Human pregnancy involves hemochorial placentation wherein the villous covered by a trophoblast layer is subdivided into functional units bathed by maternal blood, ensuring maternal-fetal exchanges (Kohli et al., 2022). Meanwhile, pregnant women are at high risk of hemorrhage, organ-specific thrombosis, and thromboinflammation (Kohli et al., 2022). Decidual thrombosis and spontaneous intrauterine umbilical artery thrombosis are associated with FGR, placental abruption, PE, and preterm birth (Vedmedovska et al., 2011). Thus, inhibiting coagulation is a promising strategy to treat PMPCs (Boeldt and Bird, 2017). Thrombin (THR), which is closely involved with the occurrence of thrombosis and embolism, and FXa, which is a common mediator of intrinsic and extrinsic coagulation, play crucial roles in the coagulation cascade (Yang et al., 2020). Some components of *S. miltiorrhiza* have been reported in response to these key events. Tan IIA, tanshinone I, dihydrotanshinone I, and cryptotanshinone, act as THR/FXa inhibitors, thereby destroying the coagulation cascade to achieve anticoagulation (Yang et al., 2020). Danshensu, one of the active compounds of *S. miltiorrhiza*, strongly mitigates blood viscosity and increases hematocrit levels due to its antithrombotic and antiplatelet aggregation effects (Yu et al., 2014). Moreover, *S. miltiorrhiza* injection substantially improves coagulation in PE rats (Peng and Huang, 2021). Notably, three major active compounds of *S. miltiorrhiza* (Sal A, B, and C) function by targeting the prothrombotic P2Y1 and P2Y12 receptors (Liu et al., 2018). Sal B inhibits platelet activation by decreasing phosphodiesterase activity and antagonizing the P2Y12 receptors (Liu et al., 2014). Coactivation of both P2Y receptors plays an essential role in ADP-induced platelet aggregation, whereas the inhibition of both receptors has a synergistic effect on antithrombotic therapy (Liu et al., 2018). However, to date, there are currently few commercial drugs targeting the P2Y receptors.

4.2 Vasodilation

A successful pregnancy is associated with dramatic changes in the uterine blood flow, facilitating the maternal-fetal exchanges of respiratory gas and meeting the needs of the developing fetus (Bowman et al., 2021). Impaired endothelium-dependent vasodilation has been implicated in the development of PE. Danshensu directly acts on vascular endothelial and smooth muscle cells to promote vascular relaxation (Wang et al., 2013; Lin et al., 2022). It also dilates the vessels and improves blood circulation to increase renal blood flow and improve renal function in PE rats (Peng and Huang, 2021). The mechanisms underlying pregnancy-associated uterine vasodilation are related to increased estrogen receptor (ER) levels, which drive the production of specific ER-dependent vasodilators in the uterine artery (Bai et al., 2020). Tan IIA exerts its vasodilation effect through activating the ER signal pathway and increasing endothelial nitric oxide synthase (eNOS) gene expression level, nitric oxide (NO) production, ERK1/2 phosphorylation, and Ca^{2+} mobilization (Fan et al., 2011). It also promotes vasodilatation by decreasing the expression of the endothelin A receptor, which is a primary receptor in modulating vasoconstriction (Chen et al., 2017). Magnesium acetate, an active compound of *S. miltiorrhiza*, dilates blood vessels through activating the PI3K/AKT pathway and increasing the phosphorylation of eNOS (Liu et al., 2019). Sal B is a potentially effective natural compound to lower blood pressure and alleviate hypertension-associated vascular dysfunctions (Ling et al., 2017). It mediates vasodilation by inhibiting extracellular calcium influx and intracellular calcium release. The calcium release mechanism relies on the ryanodine receptor family, one of the families of calcium release channels (Shou et al., 2012).

4.3 Antioxidant

Oxidative stress is widely believed to disrupt the balance between ROS and the antioxidant system (Hussain et al., 2021). During pregnancy, nutritional deficiencies result in adverse offspring outcomes (Sebastiani et al., 2019). Excessive oxidative stress impairs maternal and placental functions by limiting the antioxidant supply and eventually results in the decreased metabolic health of offspring (Schoots et al., 2018; Nadeem et al., 2019; Burton et al., 2021). Cryptotanshinone improves doxorubicin-induced oxidative damage and apoptosis through inhibiting the opening of the mitochondrial permeability transition pore *via* the Akt/GSK-3β pathway (Wang et al., 2021). Danshensu has a protective effect against oxidative stress during ischemia-reperfusion injury through ROS scavenging, and it enhances the activity of endogenous antioxidants, such as superoxide dismutase, catalase and malondialdehyde, through activating the Akt/ERK1/2/Nrf2 signaling pathway (Yu et al., 2015). Tan ⅡA exerts robust antioxidant activity through the SIRT1 signaling pathway (Feng et al., 2016). It also reduces the accumulation of free radicals in radioactive brain injuries (Sun et al., 2017). Sal A is essential to protect cells from damage caused by toxic stimuli (Wang and Xu, 2005). Sal B protects against oxidative damage by upregulating the Nrf2 antioxidant signaling pathway, which may be regulated by activating the SIRT1 pathway (Zhang et al., 2018). Through angiotensin type I receptors, angiotensin II activates the reduced nicotinamide adenine dinucleotide phosphate, which results in the formation of ROS in the vasculature (Gonzaga et al., 2018). In this progress, Sal B also downregulates angiotensin type I receptors in the vessel wall to alleviate the deleterious effect of angiotensin II, an essential stimulant for the production of ROS in the vascular system (Ling et al., 2017).

4.4 Endothelial protective effect

The endothelium, formed by a single endothelial cell layer, lines all blood vessels, such as arterioles, venules and veins (Lee et al., 2022). The endothelium regulates blood homeostasis *via* controlling blood fluidity, continuity, and fibrinolysis (Triggle et al., 2012). Endothelial cells have proteins involved in the various functions of leukocytes (Panés and Granger, 1998). Dysfunction and altered structure of the endothelial layer during pregnancy are associated with PMPCs (Ghafourian et al., 2022). Danshensu protects endothelial cells *via* the CD40 pathway and inhibition of apoptosis by downregulating the proportion of cells in the G(0)/G(1) phase (Yang et al., 2009). In addition, it reduces the serum levels of homocysteine, a substance damaging endothelial cells (Yang et al., 2010). Tan ⅡA inhibits endothelial cell apoptosis by reducing the expression of related apoptotic proteins *via* the NF-κB signaling pathway, thereby exerting a protective effect on vascular endothelial cells (Liu et al., 2021). It also protects endothelial function through inhibiting endothelin-1 expression, decreasing endothelin type A receptors, increasing endothelin type B receptors, and upregulating eNOS (Chen et al., 2017). Cryptotanshinone's endothelium protective action is mainly associated with the reduction of endothelial inflammation. In particular, cryptotanshinone blocks the scavenger receptor LOX1-mediated pro-inflammatory response in endothelial cells, preventing monocyte adhesion to endothelial cells (Li et al., 2018). Further researches are also necessary to determine the potential impact of cryptotanshinone on other crucial aspects of endothelium protection.

The above effects and mechanisms suggest that *S. miltiorrhiza* ameliorates adverse cardiovascular symptoms. Since PMPCs are characterized by insufficient blood perfusion, vascular endothelial dysfunction, and abnormal coagulation, *S. miltiorrhiza* and its active compounds can be applied in PMPCs (Bai et al., 2019). Thus, we profile the potential mechanisms of *S. miltiorrhiza* for PMPCs in Table 1.

5 Conclusion

In summary, PMPCs are a heterogeneous disease with similar mechanisms, including reduced trophoblast cell invasion and insufficient spiral artery remodeling, which results in placental hypoperfusion, endothelial dysfunction, and abnormal coagulation. *S. miltiorrhiza* effectively attenuates the symptoms of PMPCs through anticoagulation, vasodilation, inhibition of free radical formation, and protection of endothelial cells. Notebly, *S. miltiorrhiza* and its active compounds have been shown to treat PE, mitigate the severity of FGR, and improve the adverse symptoms of RSA. Hence, *S. miltiorrhiza* may be used to improve the pregnancy outcomes of pregnant women with PMPCs effectively. However, the specific effects of *S. miltiorrhiza* on PMPCs still need clinical verification, although animal models have provided much more valuable clues. *In vitro* and *in vivo* studies are required to clarify the related signaling pathways of. New techniques are needed to study human placental development and provide optimal therapy for patients with PMPCs.

Author contributions

MC and YL conceived the context. JK, SL, MC, and YL drafted the manuscript. JK prepared the figure and the table. All authors crucially revised the manuscript for important intellectual content and approved the final version to be published.

Funding

This study was partly supported by the Guangzhou Science and Technology Program (No. 202102010129).

Acknowledgments

Written informed consent was obtained from the BioRender (https://biorender.com/) for the publication of any potentially identifiable images or data included in this article.

Conflict of interest

The authors declare that the research was conducted in the absence of any commercial or financial relationships that could be construed as a potential conflict of interest.

Publisher's note

References

Aplin, J. D., Myers, J. E., Timms, K., and Westwood, M. (2020). Tracking placental development in health and disease. *Nat. Rev. Endocrinol.* 16 (9), 479–494. doi:10.1038/s41574-020-0372-6

Audette, M. C., and Kingdom, J. C. (2018). Screening for fetal growth restriction and placental insufficiency. *Semin. Fetal Neonatal Med.* 23 (2), 119–125. doi:10.1016/j.siny.2017.11.004

Bai, J., Qi, Q. R., Li, Y., Day, R., Makhoul, J., Magness, R. R., et al. (2020). Estrogen receptors and estrogen-induced uterine vasodilation in pregnancy. *Int. J. Mol. Sci.* 21 (12), 4349. doi:10.3390/ijms21124349

Bai, X., Huang, G., and Zhao, S. (2019). Clinical application prospect of Salvia miltiorrhiza combined with low molecular weight heparin in recurrent abortion based on prethrombotic state. *World Latest Med. Inf.* 19 (07), 6–8. doi:10.19613/j.cnki.1671-3141.2019.07.004

Boeldt, D. S., and Bird, I. M. (2017). Vascular adaptation in pregnancy and endothelial dysfunction in preeclampsia. *J. Endocrinol.* 232 (1), R27–R44. doi:10.1530/joe-16-0340

Bowman, C. E., Arany, Z., and Wolfgang, M. J. (2021). Regulation of maternal-fetal metabolic communication. *Cell. Mol. Life Sci.* 78 (4), 1455–1486. doi:10.1007/s00018-020-03674-w

Burton, G. J., Cindrova-Davies, T., Yung, H. W., and Jauniaux, E. (2021). Hypoxia and reproductive health: Oxygen and development of the human placenta. *Reproduction* 161 (1), F53–f65. doi:10.1530/rep-20-0153

Chan, P., Liu, I. M., Li, Y. X., Yu, W. J., and Cheng, J. T. (2011). Antihypertension induced by tanshinone IIA isolated from the roots of Salvia miltiorrhiza. *Evid. Based Complement. Altern. Med.* 2011, 392627. doi:10.1093/ecam/nep056

Chappell, L. C., Cluver, C. A., Kingdom, J., and Tong, S. (2021). Pre-eclampsia. *Lancet* 398 (10297), 341–354. doi:10.1016/s0140-6736(20)32335-7

Chen, L., Guo, Q. H., Chang, Y., Zhao, Y. S., Li, A. Y., and Ji, E. S. (2017). Tanshinone IIA ameliorated endothelial dysfunction in rats with chronic intermittent hypoxia. *Cardiovasc Pathol.* 31, 47–53. doi:10.1016/j.carpath.2017.06.008

Chen, W., and Yang, K. (2019). The influence of compound Danshen injection combined with low-molecular-weight heparin for treating women with early onset severe preeclampsia on their heart kidney function, and its mechanism. *Chin. J. Fam. Plan.* 27 (10), 1321–1325. doi:10.3969/j.issn.1004-8189.2007.04.027

Cheng, D., Jiang, S., Chen, J., Li, J., Ao, L., and Zhang, Y. (2019). Upregulated long noncoding RNA Linc00261 in pre-eclampsia and its effect on trophoblast invasion and migration via regulating miR-558/TIMP4 signaling pathway. *J. Cell. Biochem.* 120 (8), 13243–13253. doi:10.1002/jcb.28598

Chong, C. M., Su, H., Lu, J. J., and Wang, Y. (2019). The effects of bioactive components from the rhizome of Salvia miltiorrhiza (Danshen) on the characteristics of Alzheimer's disease. *Chin. Med.* 14, 19. doi:10.1186/s13020-019-0242-0

Davie, E. W. (1995). Biochemical and molecular aspects of the coagulation cascade. *Thromb. Haemost.* 74 (1), 001–006. doi:10.1055/s-0038-1642645

Fan, G., Zhu, Y., Guo, H., Wang, X., Wang, H., and Gao, X. (2011). Direct vasorelaxation by a novel phytoestrogen tanshinone IIA is mediated by nongenomic action of estrogen receptor through endothelial nitric oxide synthase activation and calcium mobilization. *J. Cardiovasc Pharmacol.* 57 (3), 340–347. doi:10.1097/FJC.0b013e31820a0da1

Feng, J., Li, S., and Chen, H. (2016). Tanshinone IIA inhibits myocardial remodeling induced by pressure overload via suppressing oxidative stress and inflammation: Possible role of silent information regulator 1. *Eur. J. Pharmacol.* 791, 632–639. doi:10.1016/j.ejphar.2016.09.041

Freitag, N., Tirado-Gonzalez, I., Barrientos, G., Powell, K. L., Boehm-Sturm, P., Koch, S. P., et al. (2020). Galectin-3 deficiency in pregnancy increases the risk of fetal growth restriction (FGR) via placental insufficiency. *Cell. Death Dis.* 11 (7), 560. doi:10.1038/s41419-020-02791-5

Ghafourian, M., Mahdavi, R., Akbari Jonoush, Z., Sadeghi, M., Ghadiri, N., Farzaneh, M., et al. (2022). The implications of exosomes in pregnancy: Emerging as new diagnostic markers and therapeutics targets. *Cell. Commun. Signal* 20 (1), 51. doi:10.1186/s12964-022-00853-z

Gonzaga, N. A., do Vale, G. T., Parente, J. M., Yokota, R., De Martinis, B. S., Casarini, D. E., et al. (2018). Ethanol withdrawal increases blood pressure and vascular oxidative stress: A role for angiotensin type 1 receptors. *J. Am. Soc. Hypertens.* 12 (7), 561–573. doi:10.1016/j.jash.2018.03.012

Gülçin, I. (2006). Antioxidant activity of caffeic acid (3, 4-dihydroxycinnamic acid). *Toxicology* 217 (2-3), 213–220. doi:10.1016/j.tox.2005.09.011

Hemberger, M., Hanna, C. W., and Dean, W. (2020). Mechanisms of early placental development in mouse and humans. *Nat. Rev. Genet.* 21 (1), 27–43. doi:10.1038/s41576-019-0169-4

Hodgetts Morton, V., and Stock, S. J. (2022). Low-dose aspirin for the prevention of preterm birth: More questions than answers. *PLoS Med.* 19 (2), e1003908. doi:10.1371/journal.pmed.1003908

Hong, K., Kim, S. H., Cha, D. H., and Park, H. J. (2021). Defective uteroplacental vascular remodeling in preeclampsia: Key molecular factors leading to long term cardiovascular disease. *Int. J. Mol. Sci.* 22 (20), 11202. doi:10.3390/ijms222011202

Huang, S. S., and Zheng, R. L. (2006). Rosmarinic acid inhibits angiogenesis and its mechanism of action *in vitro*. *Cancer Lett.* 239 (2), 271–280. doi:10.1016/j.canlet.2005.08.025

Hussain, T., Murtaza, G., Metwally, E., Kalhoro, D. H., Kalhoro, M. S., Rahu, B. A., et al. (2021). The role of oxidative stress and antioxidant balance in pregnancy. *Mediat. Inflamm.* 2021, 9962860. doi:10.1155/2021/9962860

James, J. L., Lissaman, A., Nursalim, Y. N. S., and Chamley, L. W. (2022). Modelling human placental villous development: Designing cultures that reflect anatomy. *Cell. Mol. Life Sci.* 79 (7), 384. doi:10.1007/s00018-022-04407-x

Ji, B., Yuan, K., Li, J., Ku, B. J., Leung, P. S., and He, W. (2021). Protocatechualdehyde restores endothelial dysfunction in streptozotocin-induced diabetic rats. *Ann. Transl. Med.* 9 (8), 711. doi:10.21037/atm-21-1431

Jiao, S., Sun, S., Ban, X., Zhang, Y., and Xing, H. (2021). Effect of compound danshen injection combined with magnesium sulfate on placental circulation in patients with preeclampsia. *China Pharm.* 30 (05), 45–47. doi:10.1155/2021/9026223

Kohli, S., Shahzad, K., Jouppila, A., Holthöfer, H., Isermann, B., and Lassila, R. (2022). Thrombosis and inflammation-A dynamic interplay and the role of glycosaminoglycans and activated protein C. *Front. Cardiovasc Med.* 9, 866751. doi:10.3389/fcvm.2022.866751

Kuwabara, Y., Yonezawa, M., Kubota, Y., Ichikawa, T., Ohashi, R., and Takeshita, T. (2020). Unique clinical and histological features of placental mesenchymal dysplasia complicated by severe preeclampsia in the midtrimester. *AJP Rep.* 10 (1), e113–e117. doi:10.1055/s-0040-1709186

Lam, F. F., Yeung, J. H., Chan, K. M., and Or, P. M. (2008). Mechanisms of the dilator action of cryptotanshinone on rat coronary artery. *Eur. J. Pharmacol.* 578 (2-3), 253–260. doi:10.1016/j.ejphar.2007.09.040

Lamaison, J. L., Petitjean-Freytet, C., and Carnat, A. (1991). Medicinal Lamiaceae with antioxidant properties, a potential source of rosmarinic acid. *Pharm. Acta Helv.* 66 (7), 185–188.

Lee, H. W., Shin, J. H., and Simons, M. (2022). Flow goes forward and cells step backward: Endothelial migration. *Exp. Mol. Med.* 54 (6), 711–719. doi:10.1038/s12276-022-00785-1

Li, J., and Qiu, R. (2020). Study on effect of compound Salvia miltiorrhiza injection on levels of IGF-1 and PLGF and pregnancy outcome of preeclampsia patients with critical early onset. *Chin. Archives Traditional Chin. Med.* 38 (11), 251–254. doi:10.13193/j.issn.1673-7717.2020.11.060

Li, Z. M., Xu, S. W., and Liu, P. Q. (2018). Salvia miltiorrhizaBurge (danshen): A golden herbal medicine in cardiovascular therapeutics. *Acta Pharmacol. Sin.* 39 (5), 802–824. doi:10.1038/aps.2017.193

Liang, X., and Meng, Q. (2021). Efficacy of compound Salvia miltiorrhiza injection combined with magnesium sulfate in the treatment of preeclampsia and its effect on serum PLGF, sFlt-1 and sEng. *Popular Sci. Technol.* 23 (09), 56–59. doi:10.7759/cureus.17322

Lin, R., Wang, W. R., Liu, J. T., Yang, G. D., and Han, C. J. (2006). Protective effect of tanshinone IIA on human umbilical vein endothelial cell injured by hydrogen peroxide and its mechanism. *J. Ethnopharmacol.* 108 (2), 217–222. doi:10.1016/j.jep.2006.05.004

Lin, Y. K., Chen, Y. J., Li, J. Y., Chen, Y. L., He, D., Zuo, R., et al. (2022). Salvianolic acid A from Danhong Injection induces vasorelaxation by Regulating L-type calcium channel in isolated mouse arteries. *J. Ethnopharmacol.* 296, 115431. doi:10.1016/j.jep.2022.115431

Ling, W. C., Liu, J., Lau, C. W., Murugan, D. D., Mustafa, M. R., and Huang, Y. (2017). Treatment with salvianolic acid B restores endothelial function in angiotensin II-induced hypertensive mice. *Biochem. Pharmacol.* 136, 76–85. doi:10.1016/j.bcp.2017.04.007

Lisonkova, S., and Joseph, K. S. (2013). Incidence of preeclampsia: Risk factors and outcomes associated with early-versus late-onset disease. *Am. J. Obstet. Gynecol.* 209 (6), 541–544. e512. doi:10.1016/j.ajog.2013.08.019

Liu, C. L., Xie, L. X., Li, M., Durairajan, S. S., Goto, S., and Huang, J. D. (2007). Salvianolic acid B inhibits hydrogen peroxide-induced endothelial cell apoptosis through regulating PI3K/Akt signaling. *PLoS One* 2 (12), e1321. doi:10.1371/journal.pone.0001321

Liu, L., Li, J., Zhang, Y., Zhang, S., Ye, J., Wen, Z., et al. (2014). Salvianolic acid B inhibits platelets as a P2Y12 antagonist and PDE inhibitor: Evidence from clinic to laboratory. *Thromb. Res.* 134 (4), 866–876. doi:10.1016/j.thromres.2014.07.019

Liu, X., Feng, J., Zhou, D., and Yu, G. (2021a). The protective effect of Tanshinone IIA on vascular endothelial cells in septic rats by regulating NF-κB signaling pathway. *Chin. J. Difficult Complicat. Cases* 20 (09), 935–938. doi:10.1080/17512433.2021.1878877

Liu, X., Gao, Z. G., Wu, Y., Stevens, R. C., Jacobson, K. A., and Zhao, S. (2018). Salvianolic acids from antithrombotic Traditional Chinese Medicine Danshen are antagonists of human P2Y(1) and P2Y(12) receptors. *Sci. Rep.* 8 (1), 8084. doi:10.1038/s41598-018-26577-0

Liu, Y., Liu, W., Ma, S., Kang, N., He, Y., and Zhang, W. (2021b). Clinical study on the therapeutic effect of Salvia miltiorrhiza injection in the early treatment of recurrent abortion. *Guangming J. Chin. Med.* 36 (06), 851–854. doi:10.3969/j.issn.1003-8914.2021.06.001

Liu, Y. L., Zhou, X. Y., and Xuan, L. J. (2019). Magnesium lithospermate B ameliorates microcirculation perfusion in rats by promoting vascular NO production via activating the PI3K/AKT pathway. *Acta Pharmacol. Sin.* 40 (8), 1010–1018. doi:10.1038/s41401-018-0203-7

Ma, Y., Liang, X., Wu, H., Li, J., Chen, H., and Li, P. (2021). Clinical efficacy of Danshen injection in the treatment of preeclampsia and its effect on lncRNA NR_002794 of placenta. *Chin. J. Woman Child Health Res.* 32 (04), 571–577. doi:10.3969/j.issn.1673-5293.2021.04.020

Melamed, N., Baschat, A., Yinon, Y., Athanasiadis, A., Mecacci, F., Figueras, F., et al. (2021). FIGO (international federation of gynecology and obstetrics) initiative on fetal growth: Best practice advice for screening, diagnosis, and management of fetal growth restriction. *Int. J. Gynaecol. Obstet.* 152 (1), 3–57. doi:10.1002/ijgo.13522

Migliori, M., Cantaluppi, V., Mannari, C., Bertelli, A. A., Medica, D., Quercia, A. D., et al. (2015). Caffeic acid, a phenol found in white wine, modulates endothelial nitric oxide production and protects from oxidative stress-associated endothelial cell injury. *PLoS One* 10 (4), e0117530. doi:10.1371/journal.pone.0117530

Nadeem, A., Ahmad, S. F., Al-Harbi, N. O., Attia, S. M., Alshammari, M. A., Alzahrani, K. S., et al. (2019). Increased oxidative stress in the cerebellum and peripheral immune cells leads to exaggerated autism-like repetitive behavior due to deficiency of antioxidant response in BTBR T + tf/J mice. *Prog. Neuropsychopharmacol. Biol. Psychiatry* 89, 245–253. doi:10.1016/j.pnpbp.2018.09.012

Ortega, M. A., Fraile-Martínez, O., García-Montero, C., Sáez, M. A., Álvarez-Mon, M. A., Torres-Carranza, D., et al. (2022). The pivotal role of the placenta in normal and pathological pregnancies: A focus on preeclampsia, fetal growth restriction, and maternal chronic venous disease. *Cells* 11 (3), 568. doi:10.3390/cells11030568

Pan, Q., Xu, H., Xu, L., and Mo, Z. (2022). Analysis on the effect of fuzheng huatan huoxue recipe in treating recurrent abortion of kidney deficiency and blood stasis type online first. *Chin. Archives Traditional Chin. Med.* 2022, 1–9. doi:10.3969/j.issn.1004-8189.2019.05.006

Panés, J., and Granger, D. N. (1998). Leukocyte-endothelial cell interactions: Molecular mechanisms and implications in gastrointestinal disease. *Gastroenterology* 114 (5), 1066–1090. doi:10.1016/s0016-5085(98)70328-2

Peng, Q., and Huang, M. (2021). Effect of Compound Danshen Injection on coagulation and renal function in preeclampsia rats. *J. Mod. Med. Health* 37 (23), 3989–3992. doi:10.3892/etm.2018.6173

Schoots, M. H., Gordijn, S. J., Scherjon, S. A., van Goor, H., and Hillebrands, J. L. (2018). Oxidative stress in placental pathology. *Placenta* 69, 153–161. doi:10.1016/j.placenta.2018.03.003

Sebastiani, G., Herranz Barbero, A., Borrás-Novell, C., Alsina Casanova, M., Aldecoa-Bilbao, V., Andreu-Fernández, V., et al. (2019). The effects of vegetarian and vegan diet during pregnancy on the health of mothers and offspring. *Nutrients* 11 (3), 557. doi:10.3390/nu11030557

Shen, Y., Hu, Y., and Zhang, Y. (2011). Favorable maternal and fetal effects of danshensu in an experimental mice model of preeclampsia. *Hypertens. Pregnancy* 30 (4), 465–480. doi:10.3109/10641955.2010.507842

Shou, Q., Pan, Y., Xu, X., Xu, J., Wang, D., Ling, Y., et al. (2012). Salvianolic acid B possesses vasodilation potential through NO and its related signals in rabbit thoracic aortic rings. *Eur. J. Pharmacol.* 697 (1-3), 81–87. doi:10.1016/j.ejphar.2012.09.044

Song Wang, Z. G., Li, E., Su, C., Zhu, H., and Zhu, H. (2008). The application with protocatechualdehyde to improve anticoagulant activity and cell affinity of silk fibroin. *Appl. Surf. Sci.* 255, 486–488. doi:10.1016/j.apsusc.2008.06.156

Staff, A. C., Fjeldstad, H. E., Fosheim, I. K., Moe, K., Turowski, G., Johnsen, G. M., et al. (2022). Failure of physiological transformation and spiral artery atherosis: Their roles in preeclampsia. *Am. J. Obstet. Gynecol.* 226 (2), S895–s906. doi:10.1016/j.ajog.2020.09.026

Staff, A. C. (2019). The two-stage placental model of preeclampsia: An update. *J. Reprod. Immunol.* 134-135, 1–10. doi:10.1016/j.jri.2019.07.004

Sun, Y., Xin, Q., Li, C., and Wang, N. (2017). Protective effect of Tan IIA on brain injury induced by radiation in mice and its molecular mechanism. *Pharmacol. Clin. Chin. Materia Medica* 33 (01), 66–70. doi:10.13412/j.cnki.zyyl.2017.01.019

Tong, X., Guo, Y., Nie, X., Yin, Y., and Tan, Y. (2022). Effects of tanshinone II A on the expression of annexin A2 mRNA and protein in decidua of mice with recurrent spontaneous abortion. *China J. Traditional Chin. Med. Pharm.* 2014, 308976. doi:10.1155/2014/308976

Triggle, C. R., Samuel, S. M., Ravishankar, S., Marei, I., Arunachalam, G., and Ding, H. (2012). The endothelium: Influencing vascular smooth muscle in many ways. *Can. J. Physiol. Pharmacol.* 90 (6), 713–738. doi:10.1139/y2012-073

True, H., Blanton, M., Sureshchandra, S., and Messaoudi, I. (2022). Monocytes and macrophages in pregnancy: The good, the bad, and the ugly. *Immunol. Rev.* 308 (1), 77–92. doi:10.1111/imr.13080

Turco, M. Y., and Moffett, A. (2019). Development of the human placenta. *Development* 146 (22), dev163428. doi:10.1242/dev.163428

Vata, P. K., Chauhan, N. M., Nallathambi, A., and Hussein, F. (2015). Assessment of prevalence of preeclampsia from Dilla region of Ethiopia. *BMC Res. Notes* 8, 816. doi:10.1186/s13104-015-1821-5

Vedmedovska, N., Rezeberga, D., Teibe, U., Melderis, I., and Donders, G. G. (2011). Placental pathology in fetal growth restriction. *Eur. J. Obstet. Gynecol. Reprod. Biol.* 155 (1), 36–40. doi:10.1016/j.ejogrb.2010.11.017

Walsh, S. W., and Strauss, J. F., 3rd (2022). Pregnancy-specific expression of protease-activated receptor 1: A therapeutic target for prevention and treatment of preeclampsia? *Am. J. Obstet. Gynecol.* 226 (2), S945–s953. doi:10.1016/j.ajog.2021.11.1367

Wang, D., Fan, G., Wang, Y., Liu, H., Wang, B., Dong, J., et al. (2013). Vascular reactivity screen of Chinese medicine danhong injection identifies Danshensu as a NO-independent but PGI2-mediated relaxation factor. *J. Cardiovasc Pharmacol.* 62 (5), 457–465. doi:10.1097/FJC.0b013e3182a29657

Wang, J., Xu, J., Gong, X., Yang, M., Zhang, C., and Li, M. (2019). Biosynthesis, chemistry, and pharmacology of polyphenols from Chinese Salvia species: A review. *Molecules* 24 (1), 155. doi:10.3390/molecules24010155

Wang, P., Li, H., and Wang, X. (2020a). Clinical study of Danshen Injection combined with magnesium sulfate in treatment of fetal growth restriction. *Drug Eval. Res.* 43 (11), 2263–2267. doi:10.7501/j.issn.1674-6376.2020.11.020

Wang, W., Wang, X., Zhang, X. S., and Liang, C. Z. (2018). Cryptotanshinone attenuates oxidative stress and inflammation through the regulation of nrf-2 and NF-κB in mice with unilateral ureteral obstruction. *Basic Clin. Pharmacol. Toxicol.* 123 (6), 714–720. doi:10.1111/bcpt.13091

Wang, X., Sun, Q., Jiang, Q., Jiang, Y., Zhang, Y., Cao, J., et al. (2021). Cryptotanshinone ameliorates doxorubicin-induced cardiotoxicity by targeting akt-GSK-3β-mPTP pathway *in vitro*. *Molecules* 26 (5), 1460. doi:10.3390/molecules26051460

Wang, X., and Xu, J. (2005). Salvianic acid A protects human neuroblastoma SH-SY5Y cells against MPP+-induced cytotoxicity. *Neurosci. Res.* 51 (2), 129–138. doi:10.1016/j.neures.2004.10.001

Wang, X., Yang, Y., Liu, X., and Gao, X. (2020b). Pharmacological properties of tanshinones, the natural products from Salvia miltiorrhiza. *Adv. Pharmacol.* 87, 43–70. doi:10.1016/bs.apha.2019.10.001

Wei, M., Wang, J., and Fu, J. (2021). Effect of danshen injection on fetal growth restriction and its influence on ultrasound parameters. *J. Rare Uncommon Dis.* 28 (01), 103–104. doi:10.3969/j.issn.1672-5131.2021.01.046

Wu, L., Cheng, B., Liu, Q., Jiang, P., and Yang, J. (2020). CRY2 suppresses trophoblast migration and invasion in recurrent spontaneous abortion. *J. Biochem.* 167 (1), 79–87. doi:10.1093/jb/mvz076

Xiao, Z., Liu, W., Mu, Y. P., Zhang, H., Wang, X. N., Zhao, C. Q., et al. (2020). Pharmacological effects of salvianolic acid B against oxidative damage. *Front. Pharmacol.* 11, 572373. doi:10.3389/fphar.2020.572373

Yang, G. D., Zhang, H., Lin, R., Wang, W. R., Shi, X. L., Liu, Y., et al. (2009). Down-regulation of CD40 gene expression and inhibition of apoptosis with Danshensu in endothelial cells. *Basic Clin. Pharmacol. Toxicol.* 104 (2), 87–92. doi:10.1111/j.1742-7843.2008.00342.x

Yang, R., Huang, S., Yan, F., Lu, X., Xing, Y., Liu, Y., et al. (2010). Danshensu protects vascular endothelia in a rat model of hyperhomocysteinemia. *Acta Pharmacol. Sin.* 31 (10), 1395–1400. doi:10.1038/aps.2010.167

Yang, Y. Y., Wu, Z. Y., Zhang, H., Yin, S. J., Xia, F. B., Zhang, Q., et al. (2020). LC-MS-based multivariate statistical analysis for the screening of potential thrombin/factor Xa inhibitors from Radix Salvia Miltiorrhiza. *Chin. Med.* 15, 38. doi:10.1186/s13020-020-00320-2

Yang, Z., Lin, S., Liu, Y., Ren, Q., Ge, Z., Wang, C., et al. (2022). Traditional Chinese medicine in coronary microvascular disease. *Front. Pharmacol.* 13, 929159. doi:10.3389/fphar.2022.929159

Yu, C., Qi, D., Lian, W., Li, Q. Z., Li, H. J., and Fan, H. Y. (2014). Effects of danshensu on platelet aggregation and thrombosis: *In vivo* arteriovenous shunt and venous thrombosis models in rats. *PLoS One* 9 (11), e110124. doi:10.1371/journal.pone.0110124

Yu, J., Wang, L., Akinyi, M., Li, Y., Duan, Z., Zhu, Y., et al. (2015). Danshensu protects isolated heart against ischemia reperfusion injury through activation of Akt/ERK1/2/Nrf2 signaling. *Int. J. Clin. Exp. Med.* 8 (9), 14793–14804.

Zeng, H., Su, S., Xiang, X., Sha, X., Zhu, Z., Wang, Y., et al. (2017). Comparative analysis of the major chemical constituents in Salvia miltiorrhiza roots, stems, leaves and flowers during different growth periods by UPLC-TQ-MS/MS and HPLC-ELSD methods. *Molecules* 22 (5), 771. doi:10.3390/molecules22050771

Zhang, J., Wu, T. X., and Liu, G. J. (2006). Chinese herbal medicine for the treatment of pre-eclampsia. *Cochrane Database Syst. Rev.* 2006 (2), Cd005126. doi:10.1002/14651858.CD005126.pub2

Zhang, N., Zou, H., Jin, L., Wang, J., Zhong, M. F., Huang, P., et al. (2010). Biphasic effects of sodium danshensu on vessel function in isolated rat aorta. *Acta Pharmacol. Sin.* 31 (4), 421–428. doi:10.1038/aps.2010.24

Zhang, T., Liu, M., Gao, Y., Li, H., Song, L., Hou, H., et al. (2021a). Salvianolic acid B inhalation solution enhances antifibrotic and anticoagulant effects in a rat model of pulmonary fibrosis. *Biomed. Pharmacother.* 138, 111475. doi:10.1016/j.biopha.2021.111475

Zhang, W., Li, J., Yang, P., Wang, G., Yue, Y., Zhong, Y., et al. (2022). Efficacy and safety of Salvia miltiorrhiza for treating chronic kidney diseases: A systematic review and meta-analysis. *Evid. Based Complement. Altern. Med.* 2022, 2117433. doi:10.1155/2022/2117433

Zhang, X., Wu, Q., Lu, Y., Wan, J., Dai, H., Zhou, X., et al. (2018). Cerebroprotection by salvianolic acid B after experimental subarachnoid hemorrhage occurs via Nrf2-and SIRT1-dependent pathways. *Free Radic. Biol. Med.* 124, 504–516. doi:10.1016/j.freeradbiomed.2018.06.035

Zhang, Y., Hao, Y., Li, Y., and Gao, Q. (2021b). Clinical analysis of compound Danshen injection combined with magnesium sulfate and nifedipine in the treatment of preeclampsia. *Chin. J. Hum. Sex.* 30 (03), 108–111. doi:10.3969/j.issn.1672-1993.2021.03.033

Zhao, G. R., Zhang, H. M., Ye, T. X., Xiang, Z. J., Yuan, Y. J., Guo, Z. X., et al. (2008). Characterization of the radical scavenging and antioxidant activities of danshensu and salvianolic acid B. *Food Chem. Toxicol.* 46 (1), 73–81. doi:10.1016/j.fct.2007.06.034

Zhou, Z., Wang, S. Q., Liu, Y., and Miao, A. D. (2006). Cryptotanshinone inhibits endothelin-1 expression and stimulates nitric oxide production in human vascular endothelial cells. *Biochim. Biophys. Acta* 1760 (1), 1–9. doi:10.1016/j.bbagen.2005.09.009

Zhu, J., Xu, Y., Ren, G., Hu, X., Wang, C., Yang, Z., et al. (2017). Tanshinone IIA Sodium sulfonate regulates antioxidant system, inflammation, and endothelial dysfunction in atherosclerosis by downregulation of CLIC1. *Eur. J. Pharmacol.* 815, 427–436. doi:10.1016/j.ejphar.2017.09.047

frontiers | Frontiers in Cell and Developmental Biology

TYPE Mini Review
PUBLISHED 10 February 2023
DOI 10.3389/fcell.2023.1115229

OPEN ACCESS

EDITED BY
Huashan Zhao,
Shenzhen Institutes of Advanced Technology (CAS), China

REVIEWED BY
Chunmei Li,
Institute of Food Science and Technology (CAAS), China
Qingqing Zhang,
The University of Hong Kong, Hong Kong SAR, China

*CORRESPONDENCE
Fang Deng,
fangdeng1997@126.com
Shuiping Lou,
1536498208@qq.com

†These authors have contributed equally to this work

SPECIALTY SECTION
This article was submitted to Cellular Biochemistry, a section of the journal Frontiers in Cell and Developmental Biology

RECEIVED 03 December 2022
ACCEPTED 02 February 2023
PUBLISHED 10 February 2023

CITATION
Zeng F, Zhang L, Deng F and Lou S (2023), Early-life exposure to di (2-ethyl-hexyl) phthalate: Role in children with endocrine disorders.
Front. Cell Dev. Biol. 11:1115229.
doi: 10.3389/fcell.2023.1115229

Early-life exposure to di (2-ethyl-hexyl) phthalate: Role in children with endocrine disorders

Fa Zeng[1†], Luodan Zhang[2†], Fang Deng[2*] and Shuiping Lou[1*]

[1]Shenzhen Longhua Maternity and Child Healthcare Hospital, Shenzhen, China, [2]Department of Nephrology, Anhui Provincial Children's Hospital, Children's Hospital of Anhui Medical University, Hefei, China

Di (2-ethyl-hexyl) phthalate (DEHP), one of endocrine-disrupting chemicals (EDCs), has widespread concern due to its serious health hazards. Exposure to DEHP in the early stage of life affects fetal metabolic and endocrine function, which even would cause genetic lesions. To date, it is widely believed that the increasing incidence of childhood obesity and diabetes in adolescents is related to the impact of DEHP on glucose and lipid homeostasis in children. However, there remains a knowledge gap to recognize these adverse effects. Thus, in this review, besides the exposure routes and levels of DEHP, we further outline the effects of early-life exposure to DEHP on children and potential mechanisms, focusing on the aspect of metabolic and endocrine homeostasis.

KEYWORDS

di (2-ethyl-hexyl) phthalate (DEHP), endocrine-disrupting chemicals (EDCs), early-life, placenta, offspring, lipid and glucose

1 Introduction

Di (2-ethyl-hexyl) phthalate (DEHP), belonging to the family of phthalates, is a plasticizer and solvent in polyvinyl chloride (PVC), which can be used to manufacture various products, such as cosmetics, toys, and medical tubing (Li et al., 2012). Through the widespread use of plastic products, phthalates would migrate to other products or the environment, indirectly or directly affecting human health (Cho et al., 2015). As endocrine-disrupting chemicals in the external environment, long-term exposure would have adverse effects on human health (Stojanoska et al., 2017). It is noted that DEHP shows obvious reproductive toxicity (Zhang et al., 2020) and results in much more problems, such as ovulation disorders, precocious puberty, and abnormal pregnancy. Endocrine and metabolic disorders have become risk factors for pregnancy complications, diabetes, and obesity (Huang et al., 2020; Zhang et al., 2022).

According to DOHaD theory, which is based on an epidemiological study about low birth weight and malnutrition (Barker, 2007), the effects of exposure before and during pregnancy would be reflected in the health status of offspring. If it is affected in the period of early life, it will interfere with the original growth process, resulting in incorrect coding and expression The DOHaD theory is now widely used in research on diseases, especially chronic diseases. This early-life nutritional theory is considered applicable to most chronic diseases. For organisms, the intrauterine period is the key phase of most organ development (Roseboom et al., 2001; Barker, 2007; Agarwal et al., 2018). In researches on chronic diseases, researchers often use the experimental method of maternal intervention during pregnancy to determine whether the research factors would produce the corresponding outcome by observing the performance of the offspring. DEHP exposure in early life can damage the endocrine system of offspring (Qian et al., 2020). DEHP could affect the fetal reproductive system by regulating the synthesis of hormones

during pregnancy (Liu et al., 2021a). In female offspring, DEHP exposure may regulate ovarian hormone production, thereby affecting the development of follicles (Liu et al., 2017; Liu et al., 2021b). Additionally, low-dose DEHP exposure is recognized as a potential risk factor for obesity and metabolic syndrome in offspring during early life stages (Fan et al., 2020). A prospective cohort study shows that maternal exposure to phthalates may affect glucose and lipid metabolic disorders, with potential persisting sex specificity in childhood (Sol et al., 2020). Understanding the detailed mechanisms that control endocrine metabolism is vital for improving the health of children.

Thus, in this review, we summarize the effects of early-life exposure to DEHP on endocrine homeostasis in offspring and the potential mechanism, and highlight the common connections existing in the current research, providing some insights for further scientific research and medical precaution.

2 Exposure routes and levels of DEHP

As general endocrine-disrupting chemicals, phthalates are common additive in the plastic manufacturing industry and are mainly used to increase the ductility, elasticity, and strength of plastic products, including food package, plastic utensils, agricultural plastic film, and medical PVC devices (Giuliani et al., 2020). As the combination of phthalates and the main body of the plastic matrix is non-covalent, phthalates would migrate out of various products and dissolve into the external environment, causing environmental pollution and affecting human health (Heudorf et al., 2007; Bolling et al., 2020). People are generally exposed to phthalates through soil pollution and air pollution in the external environment. Phthalates can enter the human body through the respiratory system, digestive system, and skin. Among them, absorption *via* the digestive tract through food intake is the largest intake route of phthalates (Wang et al., 2019). Besides, dust ingestion is also major exposure route of phthalates, with dosage in the range from 1.12 μg/kg in infants to 1.7 μg/kg in toddlers (Tran and Kannan, 2015). Table 1 shows the concentrations of various phthalates metabolites, including MEP, MBzP, MEHP, MEHHP, MEOHP and MECPP from DEHP, and MnBP, MIBP, MCPP in parent and child urine samples, respectively (Tellez-Rojo et al., 2013; Wu et al., 2017).

3 Effects of early-life exposure to DEHP on endocrine homeostasis in children

3.1 Early-life exposure to DEHP could cause childhood obesity

Childhood obesity has a great impact on health in adulthood, while adolescent obesity can also lead to psychological problems. People who were overweight or obese as children or adolescents are more likely to continue this trait in adulthood, and childhood obesity is associated with a variety of adverse outcomes (Di Cesare et al., 2019). A cohort study of 4,857 American Indian children without diabetes evaluated the association of body mass index (BMI), blood pressure level, cholesterol content, and premature death (Franks et al., 2010). Moreover, obesity in children and adolescence may be related to cardiovascular disease, diabetes, and various other causes (Bendor et al., 2020). These findings suggest that preventing obesity in the early stages of life is of great significance to health for the whole life cycle.

Increasing research on environmental endocrine disruptors has revealed that endocrine disruptors in the external environment are closely related to human glycolipids. A variety of established or potential environmental factors, including phthalate, polychlorinated biphenyls (PCBs), and perfluoroalkyl acids, can contribute to glucose and lipid metabolism in the body (Newbold et al., 2009; Do et al., 2017; Veiga-Lopez et al., 2018). Environmental factors can have an impact from the early stages of human life, and research in this field can help analyze the causes of obesity.

Perinatal exposure to DEHP may increase the incidence of obesity in offspring and DEHP may be a potential chemical stressor of obesity and obesity-related diseases (Hao et al., 2013). A meta-analysis summarizing original papers on the association between phthalate exposure and obesity in children and adults up to 2019 shows that there is an association between DEHP and adult obesity in general, but it was not conclusive (Ribeiro et al., 2019). Furthermore, the relationship between DEHP and childhood obesity has also been controversial in previous studies (Ribeiro et al., 2019). In a cohort study, the concentration of phthalates metabolites in urine collected twice during pregnancy is positively correlated with height, weight, waist circumference, body fat percentage, and other physical indicators of children aged 5–12 years (Harley et al., 2017). A cohort study of African American pregnant women shows that prenatal exposure to phthalates is associated with a lower BMI in early childhood (Maresca et al., 2016). In a cross-sectional study, an analysis of baseline data from 1,239 American girls between the ages of 6 and 8 years indicated that there is a weak but measurable relationship between phthalate exposure and BMI and waist circumference (Deierlein et al., 2016). A survey of middle-aged mothers shows that DEHP exposure before birth has a greater impact on the weight of male offspring, suggesting that prenatal DEHP exposure would affect the birth weight of the fetus and that there are gender differences in this effect (Zhang Y. W. et al., 2018b; Shafei et al., 2018). Collectively, these reports indicated that early-life exposure to DEHP could cause energy metabolism disorder, thereby disrupting endocrine homeostasis in children.

TABLE 1 Concentrations of various phthalate metabolites in urine (SG-corrected, ng/mL).

Source of sample	Phthalate metabolite (ng/ml)									References
	MEP	MnBP	MIBP	MBzP	MCPP	MEHP	MEHHP	MEOHP	MECPP	
Mother	138	85.61	2.30	3.54	1.75	6.56	22.08	14.23	39.65	Tellez–Rojo et al. (2013)
Children	30.8	61.2	17.2	2.90	5.8	10.4	40.66	10.8	12.6	Wu et al. (2017)

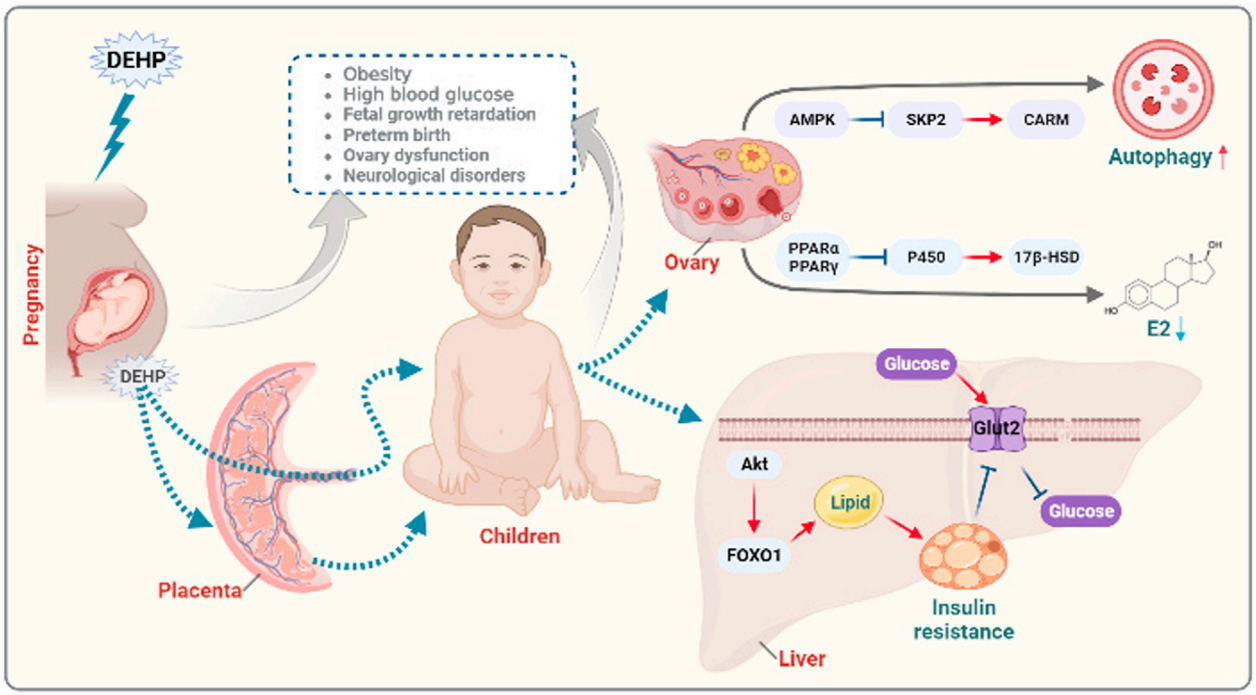

FIGURE 1
Diagram of the potential mechanisms of prenatal exposure to DEHP in offspring endocrine disorders. Functionally, DEHP could cross the placental barrier and directly or indirectly act on the fetus leading to growth retardation, preterm birth, ovary dysfunction and neurological disorders. Maternal exposure to DEHP could induce obesity and high blood glucose in offspring. Mechanically, maternal exposure to DEHP could activate AMPK-SKP2-CARM signaling to disrupt follicular development *via* autophagy in the offspring ovary. Moreover, DEHP can decrease P450 aromatase by activating PPARα and PPARγ, leading to the inhibition of ovarian secretion of hormones. Maternal DEHP exposure involving in regulating GLUT2 expression and in the liver leading to insulin resistance through FOXO1 signaling in immature male offspring. The figure was created with BioRender.com.

3.2 Early-life exposure to DEHP could disrupt endocrine homeostasis in children

In animal experiments involving metabolomics evaluation, the weight of offspring significantly increased after exposure to DEHP during pregnancy in mice, and the performance of the male offspring at low doses of DEHP is more obvious (Hao et al., 2013). Meanwhile, the liver metabolism of offspring is impaired in childhood, and glucose and lipid homeostasis are markedly abnormal (Hao et al., 2012; Rajagopal et al., 2019). These results suggest that maternal exposure to phthalates impairs liver function and metabolism in the offspring. However, a more detailed mechanism still needs to be elucidated.

Exposure to DEHP during pregnancy is associated with shortening of the pregnancy cycle, suggesting that exposure to DEHP during pregnancy can significantly increase the risk of preterm birth (Yu et al., 2018; Ferguson et al., 2019). It is reported that DEHP could cross the placental barrier and cause premature birth before 37 weeks. Infants whose gestational age is lower than MEHP negative (Huang et al., 2014). These studies indicate that the adverse effects of DEHP on fetal growth parameters may partly depend on the reduction of gestational age, rather than the direct effects of phthalates, since the gestational age of the fetus is also related to fetal growth parameters (Huang et al., 2014). In contrast, there are reports that DEHP exposure during pregnancy may have no physiological effects on the fetus. In a study of 404 multiethnic women in late pregnancy in New York, the establishment of phthalate biomarkers and multivariate adjustment model analysis reveal that DEHP-MWP and high MWP metabolites are associated with any birth outcome with no significant correlation (Patti et al., 2021).

4 Potential mechanisms of early-life exposure to DEHP affecting offspring health

DEHP not only directly affect the exposed population but also affect the offspring of the exposed population. The DOHaD theory proposes that there is a critical period of growth and development early in life, which is an important stage of fetal gene coding and expression. If environmental factors interfere with gene expression during this period, then the growth trajectory of life can be changed (Suzuki, 2018). DEHP has been reported to cross the placental barrier and directly or indirectly act on the fetus. The effect of DEHP on development is already in progress during the period of intrauterine growth (Latini et al., 2003). Maternal exposure to DEHP could activate AMPK-SKP2-CARM1 signaling to disrupt follicular development *via* autophagy in the fetal ovary in a mouse model (Zhang Y. et al., 2018a). Moreover, exposure of suckling mice to DEHP during lactation could affect hormone production, which is involved in the development of follicles, through the oxidative

stress pathway (Liu et al., 2021a). Previous studies have shown that phthalates can decrease P450 aromatase by activating PPARα and PPARγ, leading to the inhibition of ovarian secretion of hormones (Lovekamp-Swan and Davis, 2003; Ito et al., 2019; Li et al., 2020; Meling et al., 2022). Early-life exposure to phthalates is a potential risk factor for obesity and metabolic disorders in offspring (Fan et al., 2020). Maternal DEHP exposure also plays a significant role in metabolic disorders by regulating GLUT2 expression and epigenetics in the liver, which are involved in insulin resistance in immature male rat offspring (Rajagopal et al., 2019). Exposure to DEHP might induce glucose metabolic disorder in offspring through the JAK2/STAT3/SOCS3 pathway, which is involved in regulating insulin and leptin signaling pathways (Xu et al., 2018). In addition, DEHP was recently reported to promote the overexpression of FOXO1 to induce insulin resistance and hepatic lipid accumulation (Wei et al., 2022). An overview of the mechanism how exposure to DEHP affect offspring health is summarized in Figure 1.

5 Conclusion and perspectives

Existing research suggests there is a strong correlation between maternal exposure to DEHP and childhood obesity, in accord with the results observed in animal experiments. However, the exposure dose of DEHP s in each study was not identical, and the exposure dose of DEHP in animal experiments differs from the human exposure dose. Compared with rodents, primates are less sensitive to DEHP and this has been attributed to differences in the absorption, distribution, metabolism, and excretion of DEHP between these mammals (Matsumoto et al., 2008). Consequently, there may be some differences between the experimental results obtained in rodents and the actual situation in humans. Combining human and animal studies from a more specific molecular level would facilitate to explore the effects of DEHP exposure on endocrine metabolism in offspring. Evaluation of the clinical significance of DEHP exposure is difficult in epidemiological studies. Increasing studies that DEHP can cause changes in physiological functions analyze the effect of DEHP at the molecular mechanism level. Future work should also focus on related research in the field of epigenetics to explain the impact of DEHP on offspring.

Author contributions

FZ and LZ wrote this manuscript. FD and SL revised and edited this manuscript. All authors contributed to the article and approved the submitted version.

Funding

This study was supported by research on the clinical prevention and control model of birth defects based on accurate information management (2022061). Sanmin Project of Medicine in Shenzhen and Grants for New Technology and New Project of Anhui Provincial Children's Hospital (2022118).

Conflict of interest

The authors declare that the research was conducted in the absence of any commercial or financial relationships that could be construed as a potential conflict of interest.

Publisher's note

References

Agarwal, P., Morriseau, T. S., Kereliuk, S. M., Doucette, C. A., Wicklow, B. A., and Dolinsky, V. W. (2018). Maternal obesity, diabetes during pregnancy and epigenetic mechanisms that influence the developmental origins of cardiometabolic disease in the offspring. *Crit. Rev. Clin. Lab. Sci.* 55 (2), 71–101. doi:10.1080/10408363.2017.1422109

Barker, D. J. (2007). The origins of the developmental origins theory. *J. Intern Med.* 261 (5), 412–417. doi:10.1111/j.1365-2796.2007.01809.x

Bendor, C. D., Bardugo, A., Pinhas-Hamiel, O., Afek, A., and Twig, G. (2020). Cardiovascular morbidity, diabetes and cancer risk among children and adolescents with severe obesity. *Cardiovasc Diabetol.* 19 (1), 79. doi:10.1186/s12933-020-01052-1

Bolling, A. K., Sripada, K., Becher, R., and Beko, G. (2020). Phthalate exposure and allergic diseases: Review of epidemiological and experimental evidence. *Environ. Int.* 139, 105706. doi:10.1016/j.envint.2020.105706

Cho, Y. J., Park, S. B., and Han, M. (2015). Di-(2-ethylhexyl)-phthalate induces oxidative stress in human endometrial stromal cells *in vitro*. *Mol. Cell Endocrinol.* 407, 9–17. doi:10.1016/j.mce.2015.03.003

Deierlein, A. L., Wolff, M. S., Pajak, A., Pinney, S. M., Windham, G. C., Galvez, M. P., et al. (2016). Longitudinal associations of phthalate exposures during childhood and body size measurements in young girls. *Epidemiology* 27 (4), 492–499. doi:10.1097/Ede.0000000000000489

Di Cesare, M., Soric, M., Bovet, P., Miranda, J. J., Bhutta, Z., Stevens, G. A., et al. (2019). The epidemiological burden of obesity in childhood: A worldwide epidemic requiring urgent action. *BMC Med.* 17 (1), 212. doi:10.1186/s12916-019-1449-8

Do, M. T., Chang, V. C., Mendez, M. A., and de Groh, M. (2017). Urinary bisphenol A and obesity in adults: Results from the Canadian health measures survey. *Health Promot Chronic Dis. Prev. Can.* 37 (12), 403–412. doi:10.24095/hpcdp.37.12.02

Fan, Y., Qin, Y., Chen, M., Li, X., Wang, R., Huang, Z., et al. (2020). Prenatal low-dose DEHP exposure induces metabolic adaptation and obesity: Role of hepatic thiamine metabolism. *J. Hazard Mater* 385, 121534. doi:10.1016/j.jhazmat.2019.121534

Ferguson, K. K., Rosen, E. M., Rosario, Z., Feric, Z., Calafat, A. M., McElrath, T. F., et al. (2019). Environmental phthalate exposure and preterm birth in the PROTECT birth cohort. *Environ. Int.* 132, 105099. doi:10.1016/j.envint.2019.105099

Franks, P. W., Hanson, R. L., Knowler, W. C., Sievers, M. L., Bennett, P. H., and Looker, H. C. (2010). Childhood obesity, other cardiovascular risk factors, and premature death. *N. Engl. J. Med.* 362 (6), 485–493. doi:10.1056/NEJMoa0904130

Giuliani, A., Zuccarini, M., Cichelli, A., Khan, H., and Reale, M. (2020). Critical review on the presence of phthalates in food and evidence of their biological impact. *Int. J. Environ. Res. Public Health* 17 (16), 5655. doi:10.3390/ijerph17165655

Gupta, S. (2016). Obesity: The fat advantage. *Nature* 537 (7620), S100–S102. doi:10.1038/537S100a

Hao, C., Cheng, X., Guo, J., Xia, H., and Ma, X. (2013). Perinatal exposure to diethyl-hexyl-phthalate induces obesity in mice. *Front. Biosci. (Elite Ed.* 5, 725–733. doi:10.2741/e653

Hao, C., Cheng, X., Xia, H., and Ma, X. (2012). The endocrine disruptor mono-(2-ethylhexyl) phthalate promotes adipocyte differentiation and induces obesity in mice. *Biosci. Rep.* 32 (6), 619–629. doi:10.1042/BSR20120042

Harley, K. G., Berger, K., Rauch, S., Kogut, K., Henn, B. C., Calafat, A. M., et al. (2017). Association of prenatal urinary phthalate metabolite concentrations and childhood BMI and obesity. *Pediatr. Res.* 82 (3), 405–415. doi:10.1038/pr.2017.112

Heudorf, U., Mersch-Sundermann, V., and Angerer, J. (2007). Phthalates: Toxicology and exposure. *Int. J. Hyg. Environ. Health* 210 (5), 623–634. doi:10.1016/j.ijheh.2007.07.011

Huang, B., Zhu, W., Zhao, H., Zeng, F., Wang, E., Wang, H., et al. (2020). Placenta-derived osteoprotegerin is required for glucose homeostasis in gestational diabetes mellitus. *Front. Cell Dev. Biol.* 8, 563509. doi:10.3389/fcell.2020.563509

Huang, Y., Li, J., Garcia, J. M., Lin, H., Wang, Y., Yan, P., et al. (2014). Phthalate levels in cord blood are associated with preterm delivery and fetal growth parameters in Chinese women. *PLoS One* 9 (2), e87430. doi:10.1371/journal.pone.0087430

Ito, Y., Kamijima, M., and Nakajima, T. (2019). Di(2-ethylhexyl) phthalate-induced toxicity and peroxisome proliferator-activated receptor alpha: A review. *Environ. Health Prev. Med.* 24 (1), 47. doi:10.1186/s12199-019-0802-z

Latini, G., De Felice, C., Presta, G., Del Vecchio, A., Paris, I., Ruggieri, F., et al. (2003). *In utero* exposure to di-(2-ethylhexyl)phthalate and duration of human pregnancy. *Environ. Health Perspect.* 111 (14), 1783–1785. doi:10.1289/ehp.6202

Li, R., Yu, C., Gao, R., Liu, X., Lu, J., Zhao, L., et al. (2012). Effects of DEHP on endometrial receptivity and embryo implantation in pregnant mice. *J. Hazard Mater* 241-242, 231–240. doi:10.1016/j.jhazmat.2012.09.038

Li, X. N., Li, H. X., Yang, T. N., Li, X. W., Huang, Y. Q., Zhu, S. Y., et al. (2020). Di-(2-ethylhexyl) phthalate induced developmental abnormalities of the ovary in quail (*Coturnix japonica*) via disruption of the hypothalamic-pituitary-ovarian axis. *Sci. Total Environ.* 741, 140293. doi:10.1016/j.scitotenv.2020.140293

Liu, J. C., Lai, F. N., Li, L., Sun, X. F., Cheng, S. F., Ge, W., et al. (2017). Di (2-ethylhexyl) phthalate exposure impairs meiotic progression and DNA damage repair in fetal mouse oocytes *in vitro*. *Cell Death Dis.* 8 (8), e2966. doi:10.1038/cddis.2017.350

Liu, J. C., Xing, C. H., Xu, Y., Pan, Z. N., Zhang, H. L., Zhang, Y., et al. (2021a). DEHP exposure to lactating mice affects ovarian hormone production and antral follicle development of offspring. *J. Hazard Mater* 416, 125862. doi:10.1016/j.jhazmat.2021.125862

Liu, J. C., Yan, Z. H., Li, B., Yan, H. C., De Felici, M., and Shen, W. (2021b). Di (2-ethylhexyl) phthalate impairs primordial follicle assembly by increasing PDE3A expression in oocytes. *Environ. Pollut.* 270, 116088. doi:10.1016/j.envpol.2020.116088

Lovekamp-Swan, T., and Davis, B. J. (2003). Mechanisms of phthalate ester toxicity in the female reproductive system. *Environ. Health Perspect.* 111 (2), 139–145. doi:10.1289/ehp.5658

Maresca, M. M., Hoepner, L. A., Hassoun, A., Oberfield, S. E., Mooney, S. J., Calafat, A. M., et al. (2016). Prenatal exposure to phthalates and childhood body size in an urban cohort. *Environ. Health Perspect.* 124 (4), 514–520. doi:10.1289/ehp.1408750

Matsumoto, M., Hirata-Koizumi, M., and Ema, M. (2008). Potential adverse effects of phthalic acid esters on human health: A review of recent studies on reproduction. *Regul. Toxicol. Pharmacol.* 50 (1), 37–49. doi:10.1016/j.yrtph.2007.09.004

Meling, D. D., De La Torre, K. M., Arango, A. S., Gonsioroski, A., Deviney, A. R. K., Neff, A. M., et al. (2022). Phthalate monoesters act through peroxisome proliferator-activated receptors in the mouse ovary. *Reprod. Toxicol.* 110, 113–123. doi:10.1016/j.reprotox.2022.04.002

Newbold, R. R., Padilla-Banks, E., and Jefferson, W. N. (2009). Environmental estrogens and obesity. *Mol. Cell Endocrinol.* 304 (1-2), 84–89. doi:10.1016/j.mce.2009.02.024

Patti, M. A., Henderson, N. B., Gajjar, P., Eliot, M., Jackson-Browne, M., and Braun, J. M. (2021). Gestational triclosan exposure and infant birth weight: A systematic review and meta-analysis. *Environ. Int.* 157, 106854. doi:10.1016/j.envint.2021.106854

Qian, Y., Shao, H., Ying, X., Huang, W., and Hua, Y. (2020). The endocrine disruption of prenatal phthalate exposure in mother and offspring. *Front. Public Health* 8, 366. doi:10.3389/fpubh.2020.00366

Rajagopal, G., Bhaskaran, R. S., and Karundevi, B. (2019). Developmental exposure to DEHP alters hepatic glucose uptake and transcriptional regulation of GLUT2 in rat male offspring. *Toxicology* 413, 56–64. doi:10.1016/j.tox.2018.12.004

Ribeiro, C., Mendes, V., Peleteiro, B., Delgado, I., Araujo, J., Aggerbeck, M., et al. (2019). Association between the exposure to phthalates and adiposity: A meta-analysis in children and adults. *Environ. Res.* 179, 108780. ARTN 108780. doi:10.1016/j.envres.2019.108780

Roseboom, T. J., van der Meulen, J. H., Ravelli, A. C., Osmond, C., Barker, D. J., and Bleker, O. P. (2001). Effects of prenatal exposure to the Dutch famine on adult disease in later life: An overview. *Mol. Cell Endocrinol.* 185 (1-2), 93–98. doi:10.1016/s0303-7207(01)00721-3

Shafei, A. E., Nabih, E. S., Shehata, K. A., Abd Elfatah, E. S. M., Sanad, A. B. A., Marey, M. Y., et al. (2018). Prenatal exposure to endocrine disruptors and reprogramming of adipogenesis: An early-life risk factor for childhood obesity. *Child. Obes.* 14 (1), 18–25. doi:10.1089/chi.2017.0180

Shilian, H., Jing, W., Cui, C., and Xinchun, W. (2020). Analysis of epidemiological trends in chronic diseases of Chinese residents. *Aging Med. Milt.* 3 (4), 226–233. doi:10.1002/agm2.12134

Sol, C. M., Santos, S., Duijts, L., Asimakopoulos, A. G., Martinez-Moral, M. P., Kannan, K., et al. (2020). Fetal phthalates and bisphenols and childhood lipid and glucose metabolism. A population-based prospective cohort study. *Environ. Int.* 144, 106063. doi:10.1016/j.envint.2020.106063

Stojanoska, M. M., Milosevic, N., Milic, N., and Abenavoli, L. (2017). The influence of phthalates and bisphenol A on the obesity development and glucose metabolism disorders. *Endocrine* 55 (3), 666–681. doi:10.1007/s12020-016-1158-4

Suzuki, K. (2018). The developing world of DOHaD. *J. Dev. Orig. Health Dis.* 9 (3), 266–269. doi:10.1017/S2040174417000691

Tellez-Rojo, M. M., Cantoral, A., Cantonwine, D. E., Schnaas, L., Peterson, K., Hu, H., et al. (2013). Prenatal urinary phthalate metabolites levels and neurodevelopment in children at two and three years of age. *Sci. Total Environ.* 461-462, 386–390. doi:10.1016/j.scitotenv.2013.05.021

Tran, T. M., and Kannan, K. (2015). Occurrence of phthalate diesters in particulate and vapor phases in indoor air and implications for human exposure in Albany, New York, USA. *Arch. Environ. Contam. Toxicol.* 68 (3), 489–499. doi:10.1007/s00244-015-0140-0

Veiga-Lopez, A., Pu, Y., Gingrich, J., and Padmanabhan, V. (2018). Obesogenic endocrine disrupting chemicals: Identifying knowledge gaps. *Trends Endocrinol. Metab.* 29 (9), 607–625. doi:10.1016/j.tem.2018.06.003

Wang, Y., Zhu, H., and Kannan, K. (2019). A review of biomonitoring of phthalate exposures. *Toxics* 7 (2), 21. doi:10.3390/toxics7020021

Wei, X., Yang, D., Zhang, B., Fan, X., Du, H., Zhu, R., et al. (2022). Di-(2-ethylhexyl) phthalate increases plasma glucose and induces lipid metabolic disorders via FoxO1 in adult mice. *Sci. Total Environ.* 842, 156815. doi:10.1016/j.scitotenv.2022.156815

Wu, W., Zhou, F., Wang, Y., Ning, Y., Yang, J. Y., and Zhou, Y. K. (2017). Phthalate levels and related factors in children aged 6-12 years. *Environ. Pollut.* 220, 990–996. doi:10.1016/j.envpol.2016.11.049

Xu, J., Zhou, L., Wang, S., Zhu, J., Liu, T., Jia, Y., et al. (2018). Di-(2-ethylhexyl)-phthalate induces glucose metabolic disorder in adolescent rats. *Environ. Sci. Pollut. Res. Int.* 25 (4), 3596–3607. doi:10.1007/s11356-017-0738-z

Yu, Z., Han, Y., Shen, R., Huang, K., Xu, Y. Y., Wang, Q. N., et al. (2018). Gestational di-(2-ethylhexyl) phthalate exposure causes fetal intrauterine growth restriction through disturbing placental thyroid hormone receptor signaling. *Toxicol. Lett.* 294, 1–10. doi:10.1016/j.toxlet.2018.05.013

Zhang, L., Zeng, F., Jiang, M., Han, M., and Huang, B. (2022). Roles of osteoprotegerin in endocrine and metabolic disorders through receptor activator of nuclear factor kappa-B ligand/receptor activator of nuclear factor kappa-B signaling. *Front. Cell Dev. Biol.* 10, 1005681. doi:10.3389/fcell.2022.1005681

Zhang, Y., Mu, X., Gao, R., Geng, Y., Liu, X., Chen, X., et al. (2018a). Foetal-neonatal exposure of Di (2-ethylhexyl) phthalate disrupts ovarian development in mice by inducing autophagy. *J. Hazard Mater* 358, 101–112. doi:10.1016/j.jhazmat.2018.06.042

Zhang, Y., Mustieles, V., Yland, J., Braun, J. M., Williams, P. L., Attaman, J. A., et al. (2020). Association of parental preconception exposure to phthalates and phthalate substitutes with preterm birth. *JAMA Netw. Open* 3 (4), e202159. doi:10.1001/jamanetworkopen.2020.2159

Zhang, Y. W., Gao, H., Mao, L. J., Tao, X. Y., Ge, X., Huang, K., et al. (2018b). Effects of the phthalate exposure during three gestation periods on birth weight and their gender differences: A birth cohort study in China. *Sci. Total Environ.* 613, 1573–1578. doi:10.1016/j.scitotenv.2017.08.319

frontiers | Frontiers in Molecular Biosciences

TYPE Mini Review
PUBLISHED 20 March 2023
DOI 10.3389/fmolb.2023.1097018

OPEN ACCESS

EDITED BY
Huashan Zhao,
Shenzhen Institutes of Advanced Technology (CAS), China

REVIEWED BY
He Zhang,
Dalian Medical University, China
Yuanyi Zheng,
Shanghai Jiao Tong University, China

*CORRESPONDENCE
Zhen Zhang,
zhenshcc@163.com
Yunpeng Cao,
cypcmu@163.com
Yanbo Zhang,
yanbo.zhang@ualberta.ca

SPECIALTY SECTION
This article was submitted to Cellular Biochemistry, a section of the journal Frontiers in Molecular Biosciences

RECEIVED 13 November 2022
ACCEPTED 08 February 2023
PUBLISHED 20 March 2023

CITATION
Luo W, Yan Y, Cao Y, Zhang Y and Zhang Z (2023), The effects of GPER on age-associated memory impairment induced by decreased estrogen levels. *Front. Mol. Biosci.* 10:1097018. doi: 10.3389/fmolb.2023.1097018

The effects of GPER on age-associated memory impairment induced by decreased estrogen levels

Wenyu Luo[1], Yudie Yan[1], Yunpeng Cao[2]*, Yanbo Zhang[3]* and Zhen Zhang[1]*

[1]Department of Ultrasound, The First Hospital of China Medical University, Shenyang, Liaoning, China, [2]Department of Neurology, The First Hospital of China Medical University, Shenyang, Liaoning, China, [3]Department of Psychiatry, Faculty of Medicine and Dentistry, University of Alberta, Edmonton, AB, Canada

Estrogen, as a pleiotropic endocrine hormone, not only regulates the physiological functions of peripheral tissues but also exerts vital neuroregulatory effects in the central nervous system (CNS), such as the development of neurons and the formation of neural network connections, wherein rapid estrogen-mediated reactions positively stimulate spinogenesis and regulate synaptic plasticity and synaptic transmission to facilitate cognitive and memory performance. These fast non-genomic effects can be initiated by membrane-bound estrogen receptors (ERs), three best known of which are ERα, ERβ, and G protein-coupled estrogen receptor (GPER). To date, the effects of ERα and ERβ have been well studied in age-associated memory impairment, whereas there is still a lack of attention to the role of GPER in age-associated memory impairment, and there are still disputes about whether GPER indeed functions as an ER to enhance learning and memory. In this review, we provide a systematic overview of the role of GPER in age-associated memory impairment based on its expression, distribution, and signaling pathways, which might bring some inspiration for translational drugs targeting GPER for age-related diseases and update knowledge on the role of estrogen and its receptor system in the brain.

KEYWORDS

G protein-coupled estrogen receptor, estrogen, aging, memory impairment, neurogenesis, synaptic plasticity

1 Introduction

A dramatic decrease in estrogen synthesis and secretion during perimenopause in women is one of the characteristics of aging, which directly affects memory and cognitive function (van den Beld et al., 2018). Within the brain, estradiol (E2), the most potent and active form of estrogen, is well positioned on brain development, sex differentiation, reproductive behavior, and cognition (including learning and memory) (Vickers et al., 2016; Adhya et al., 2018). Preclinical evidence on the neuroprotective effects of 17β-E2 has also linked menopause to cognitive aging, with nearly twice as many women as men experiencing cognitive decline (Jett et al., 2022). E2 in the hippocampus, derived from the circulatory system and local synthesis, can promote hippocampal neurogenesis (Sager et al., 2018). E2 is also capable of regulating synaptic plasticity in both male and female rats, positively affecting hippocampus-dependent memory (Tuscher et al., 2016; Zhao et al.,

2018). Both nuclear- and membrane-associated ERs collaborate in mediating estrogenic actions within the CNS (Lai et al., 2017b).

As classical nuclear ERs, ERα and ERβ act as transcription factors *via* genomic pathways in the nuclear compartment of cells, which interact with nuclear estrogen response elements (EREs) and initiate transcription (O'Malley and Means, 1974). The identification of more ERs increases the complexity of estrogen-mediated signaling pathway network (Jacquot et al., 2021a). In 1990s, an orphan G protein-coupled receptor (GPCR) was named G protein-coupled receptor 30 (GPR30), and later in 2007, the International Union of Basic and Clinical Pharmacology assigned GPR30 as GPER, in concert with the observation of a high affinity for E2 (Thomas et al., 2005; Barton et al., 2018). The first credible genetic case for GPR30 as a novel ER was that rapid estrogen responses can be reproduced in non-responsive breast cancer cells *via* transfection with a GPR30 expression vector (Filardo et al., 2002). Among ERs, GPER seems unconventional, as it shares homology with the family of class A (rhodopsin) GPCRs, such as the angiotensin II 1A receptor and the interleukin 8A receptor (with 28% sequence similarity) (Carmeci et al., 1997; Prossnitz and Arterburn, 2015).

Given that GPER is capable of mediating estrogenic effects, most previous studies on GPER have focused on metabolic disorders, cancer, and cardiovascular function (Jacquot et al., 2021b). Thereafter, a notion is put forward that the effects of GPER can extend far beyond the gonads to the CNS, and experimental results have identified its neuroregulatory role in neurological disorders (Engler-Chiurazzi et al., 2017). Nevertheless, the ligands of GPER still need further investigated (Khan et al., 2022), several specific agonists [G1 (Bologa et al., 2006), CITFA (DeLeon et al., 2022), etc.] and antagonists [G15 (Dennis et al., 2009), G36 (Dennis et al., 2011), etc.] of GPER have been synthesized and characterized. The available application of these selective pharmacological tools in combination with GPER knockout mice may be of great importance to discern responses specific to ERs or GPER and unveil the functions of GPER (Prossnitz and Arterburn, 2015).

However, the investigation of GPER in the neuronal development and memory function is still relatively limited, and the understanding of its effects on age-associated memory impairment needs to be constantly updated. Thus, this review provides a profile of advances about GPER, including its expression, distribution, signaling pathways, and effects from the aspects of neurogenesis, synaptic plasticity and synaptic transmission.

2 Expression in memory-related tissues and subcellular distribution of GPER

GPER is ubiquitously expressed throughout the body (Prossnitz and Barton, 2011). In addition to peripheral tissues, such as the placenta, reproductive organs, heart, pancreas, and lung (Prossnitz and Barton, 2011), GPER is highly expressed in the CNS (Cooke et al., 2017), including the hippocampus, cortex, hypothalamus, striatum, and amygdala (Brailoiu et al., 2007; Llorente et al., 2020; Marraudino et al., 2021). Recent transcriptomic analysis of adult rats has shown that GPER transcripts are dominant in the brain compared to peripheral tissues and exhibit higher expression levels compared to classical ERs (Hutson et al., 2019).

Memory impairment induced by normal age or age-related diseases is the primary neurodegenerative symptom leading to biochemical changes in some brain regions, an imperative structure among which is the hippocampus (Wang et al., 2020). And the hippocampus is a brain region that is extremely sensitive to E2 (Uhl et al., 2022). Immunohistochemical studies in the rodent brain show that GPER is colocalized with pyramidal cells in every region of the hippocampus (CA1-3) and granule cells in the dentate gyrus (DG) and is especially dense in the stratum lucidum of CA3 (Waters et al., 2015; Mahmoud et al., 2016). The expression of GPER is influenced by sex and the estrous cycle, which is particularly evident in neurons of the CA1 and DG (Waters et al., 2015). In hippocampal CA1 neurons, GPER immunoreactivity is associated with dendrites, dendritic spines, and axons and is specifically localized to synaptic structures (Akama et al., 2013; Waters et al., 2015). Dual-fluorescent labeling studies of cortical neurons have also shown that GPER is expressed at synapses (Srivastava and Evans, 2013).

Regarding the subcellular distribution of GPER, some researchers have declared that it is expressed in the cell membrane (Thomas et al., 2005; Akama et al., 2013), while there is also evidence that GPER can be localized in the endoplasmic reticulum (Revankar et al., 2005; Camilletti et al., 2019), Golgi complex (Cheng et al., 2011b), and even the nucleus (Pupo et al., 2013). Thus far, the exact location of GPER is still unclear due to the exit of endocytic transport (Cheng et al., 2011a). Rapid endocytosis, rapid degradation, and slow transport experienced by GPER inside the cell may potentially explain the difficulty in detecting GPER on the cell surface (Cheng et al., 2011b). Additionally, the duration of GPER in the plasma membrane in different cell types may mainly depend on the extent of interaction with multiple scaffolding proteins, accessory proteins, and other GPCRs in the plasma membrane (West and Hanyaloglu, 2015). For example, the scaffolding protein PSD-95 can specifically bind to GPER at the postsynaptic density (PSD) region in dendritic spines and prevent its constitutive endocytosis, which extends the retention time of GPER in the membrane and increases its chance to interact with other GPCRs (Akama et al., 2013).

3 Signaling pathways of GPER

Despite the genomic and nongenomic responses initiated by estrogen almost ascribed to ERα and ERβ previously, accumulating evidence supports that GPER is capable of eliciting both rapid and transcriptional cellular events (Alexander et al., 2017; Feldman and Limbird, 2017). The non-genomic estrogenic responses encompass rapid activation of ion channels and intracellular second messenger signaling pathways, which occur in a time frame of seconds to minutes (Fuentes and Silveyra, 2019).

After GPER binding to estrogen or estrogen-like molecules, the heterotrimeric G protein splits into Gα and Gβγ subunits and further triggers multiplex intracellular signaling cascades that take part in systemic responses (Barton et al., 2018). Gαs accounts for estrogen-initiated activation of adenylyl cyclase (AC) and the ensuing increase in cAMP generation and protein kinase A (PKA) activity (Thomas et al., 2005). This process also results in intracellular calcium mobilization (Revankar et al., 2005). Gβγ recruits steroid receptor coactivator (SRC) to promote the activation of metalloproteinases (MMPs) and the subsequent cleaving of pro-heparan-bound epidermal growth factor

(pro-HB-EGF), releasing HB-EGF from the cell surface, which transactivates EGF receptor (EGFR) (Prossnitz et al., 2008). EGFR activation is accompanied by the activation of extracellular signal-regulated kinase 1/2 (ERK1/2) and phosphoinositide 3-kinase (PI3K) (Filardo et al., 2000; Bustamante-Barrientos et al., 2021). The cAMP-dependent signaling pathway has been shown to negatively regulate EGFR-induced ERK1/2 activity (Filardo, 2002). The details of phospholipase C (PLC) involvement need further investigation (Prossnitz et al., 2008; Lu and Herndon, 2017; Roque et al., 2019).

In the SRC/EGFR/mitogen-activated protein kinase (MAPK) pathway, when GPER couples to E2, phosphorylated c-Jun N-terminal kinase (JNK) regulates actin polymerization to promote dendritic spine formation and memory consolidation in the hippocampal CA1 region, which highlights the importance of actin polymerization in GPER-regulated hippocampal functions in female mice (Kim et al., 2019). On the other hand, ERK, another subfamily of MAPK, not only participates in the inhibitory effect of GPER on the neuronal stem/progenitor cells (NSPCs) proliferation (Zhong et al., 2019) but also activates and enhances synaptic transmission in the hippocampus (Kumar et al., 2015).

In addition, in the PI3K/Akt pathway, p-Akt inhibits GSK-3 to reduce neuronal loss and alleviate cognitive function (Wang et al., 2017). Activation of PI3K/Akt pathway by GPER is associated with the neuritogenesis in developing hippocampal neurons (Ruiz-Palmero et al., 2013). This pathway also engages in the process of axonal myelination and remyelination, which plays a neuroprotective role (Xiao et al., 2018). GPER can signal through PI3K/Akt/mammalian target of rapamycin (mTOR) pathway to reduce glutamate-induced excessive neuronal autophagy and protect neurons from excitotoxicity (Yue et al., 2019). Rapamycin complex 2 (mTORC2), an downstream target of SRC/EGFR/PI3K pathway, is capable of participating in actin cytoskeleton polymerization and long-term memory consolidation (Xing et al., 2018; Zhang Y. Y et al., 2019). Besides, GPER can downregulate ubiquitin-conjugating enzyme 9 (ubc9) expression, which is associated with synaptic plasticity, *via* E2 in cortical neurons through the PI3K pathway (Lai et al., 2017a).

Although GPER is well known for its nongenomic effects, it can mediate transcriptional events as well, which take place in the presence of kinase activation (Prossnitz et al., 2008; Feldman and Limbird, 2017). cAMP response element binding protein (CREB) and c-fos, representative transcription factors, have been implicated in several studies (Cheong et al., 2012). GPER activation can phosphorylate PKA and later stimulate CREB, contributing to learning and memory improvement and long-term memory consolidation in ovariectomized (OVX) rats (Lee et al., 2012; Koss et al., 2018; Machado et al., 2019). GPER-activated CREB can provoke acetylcholine (Ach) release (Filardo and Thomas, 2005; Liu et al., 2019). Phosphorylated CREB *via* cAMP/PKA pathway may also upregulate Bcl-2 expression and avoid oxidative stress-induced apoptosis, which is supposed to be mediated by GPER (Kanda and Watanabe, 2003). Transcriptional activation of c-fos occurs in the downstream of GPER-mediated EGFR/ERK1/2 pathway (Cirillo et al., 2019). As mentioned above, PI3K/Akt pathway can inhibits GSK-3 and ensuingly activate Nrf2, which transfers into the nucleus and combines with transcriptional factors to initiate the transcription of antioxidant enzymes (Wang et al., 2017). In addition, the GPER-initiated PI3K/Akt pathway can also phosphorylate intracellular ERα/β, denoting the beginning of the genomic pathway (Bustamante-Barrientos et al., 2021).

4 The effects of GPER on memory impairment

4.1 GPER affects memory and cognition by engaging in neurogenesis and reducing neuronal loss

Hippocampal neurogenesis plays an integral role in synaptic plasticity and function, and its perturbation can result in learning and memory impairment (Hollands et al., 2016; Kempermann, 2019). Adult hippocampal neurogenesis declines with age, as has been well established in rodents (Demars et al., 2013) and humans (Khan et al., 2015). Given that newborn neurons are capable of maintaining hippocampal functions and have a positive impact on spatial memory (Kathner-Schaffert et al., 2019), E2 can counteract age-associated memory impairment by promoting neurogenesis in the hippocampus (Sager et al., 2018; Sahab-Negah et al., 2020). In contrast, the degraded regeneration capacity of compromised neurons in mice contributes to long-term cognitive deficits (Kathner-Schaffert et al., 2019).

GPER is universally expressed in NSPCs (Zhang L. et al., 2019; Zhong et al., 2019). Activation of GPER *via* the specific agonist G1 dose-dependently suppresses the proliferation of mouse-derived NSPCs, and this inhibitory effect can be reversed by G15 (Zhong et al., 2019). However, a contradictory finding shows that long-term administration of G1 can promote neurogenesis and ameliorate neuronal damage in CA1 region of the hippocampus in OVX rats, improving spatial memory after neuronal injury (Wang et al., 2021). To investigate the effects of GPER on the estrogen-mediated proliferation of NSPCs, E2 conjugated with bovine serum albumin (E2-BSA) is used to prevent E2 from entering the cell, leading to the conclusion that GPER indirectly engages in the proliferation of NSPCs (Okada et al., 2010). In addition, the region-specific effect of GPER on neurogenesis has been explored, and the results showed that G1 reduces the proliferation of neurons and downregulates the expression of GPER in the DG of adult female rats, whereas G15 increases the number of proliferating neurons in the dorsal DG and decreases their number in the ventral DG (Duarte-Guterman et al., 2015). G15 in combination with E2 only partially counteracts the pro-proliferative effect of E2, indicating that the effect of GPER on neurogenesis is not completely dependent on E2 (Duarte-Guterman et al., 2015). Additionally, GPER does not colocalize with progenitor cells in the subgranular zone of the DG, revealing that the effects of GPER on neurogenesis may be indirect (Duarte-Guterman et al., 2015).

However, accumulating data have shown that GPER can inhibit apoptosis, neuroinflammation, neurotoxicity, and other detrimental factors that result in neuronal damage and degeneration to reduce neuronal loss and improve cognitive function (Huang et al., 2017; Sarchielli et al., 2020). *In vitro* studies have shown that activated GPER can upregulate antiapoptotic proteins such as Bcl-2 and downregulate apoptotic proteins in neurons by stimulating ERs, thereby alleviating neuronal degeneration (Zhou et al., 2018). Cholinergic neurons regulate hippocampal and neocortical learning and memory circuits, and GPER can respond to estrogen to attenuate inflammation in brain cholinergic neurons,

TABLE 1 The effects of GPER in memory impairment.

	Estrogen or estrogen-like molecules	Models	Cells/Tissues	Main findings	References
Neurogenesis	E2	E12.5 fetal mice	NSPCs from cortex	GPER expresses in NPSCs and its activation inhibits the proliferation in a dose-dependent manner	Okada et al. (2010)
	G1				Zhang L. et al. (2019)
	G15				Zhong et al. (2019)
	E2	Adult female rats	NSPCs from hippocampus	GPER region-specifically impacts cell proliferation in hippocampal DG. G1 reduces the proliferation of neurons, whereas G15 increases the number of proliferating neurons in the dorsal DG and decreases the number of them in the ventral DG	Duarte-Guterman et al. (2015)
	G1				
	G15				
	E2	OVX rats with GCI	NSC in the hippocampal SGZ and CA1 regions	Long-term GPER activation promotes neurogenesis	Wang et al. (2021)
	G1				
Neuroprotection	Raloxifene	ALS	TDP-25 cells	Raloxifene provides neuroprotection through GPER by increasing autophagy, decreasing apoptosis and enhancing cell viability	Zhou et al. (2018)
	E2				
	G1				
	G15				
	E2	Neuroinflammation	primary hfNBM	GPER activation attenuates inflammation in brain cholinergic neurons and improves cognitive deficits	Sarchielli et al. (2020)
	G1				
	G15				
	E2	Male rats after TBI	Hippocampal neurons	GPER activation can improve early-onset cognitive deficits and neuronal death	Wang et al. (2017)
	G1				
	E2	OVX rats with GCI	Hippocampal neurons	E2 has a therapeutic window to exert neuroprotection and declining expression of GPER reduces the responsiveness of neurons to E2	Wu et al. (2018)
	G1				
	G15				
	G1	5XFAD mice	Primary rat cortex neurons	GPER activation markedly attenuates Aβ1-42-induced neuronal toxicity and mitigates impairment of novel object recognition memory in female 5XFAD mice	Kubota et al. (2016)
	G15				Kurt et al. (2019)
Synaptic plasticity	G1	OVX female mice	Hippocampal neurons	GPER-induced rapid increase of dendritic spine density in CA1 correlates with the facilitation of learning and memory	Gabor et al. (2015)
	CITFA	E18 fetal rats	Hippocampal neurons	CITFA can significantly promote axonal and dendritic growth	DeLeon et al. (2022)
	E2	OVX rhesus monkeys	Neurons from the DPC	The higher expression levels of GPER adjacent to PSD means the higher synaptic density in this region	Crimins et al. (2017)
	G1				
	G1	OVX female rats	Hippocampal CA1 neurons	GPER activation increases dendritic spine density and enhances memory consolidation through a pathway in which JNK and cofilin phosphorylation contribute to actin polymerization	Kim et al. (2016)
					Kim et al. (2019)
	G1	OVX female mice	mHippoE-14 from embryonic mouse	GPER regulates learning and memory through ERα/ERβ/SRC and PI3K pathways, followed by activation of mTORC2 and downstream actin polymerization	Zhang Y. Y et al. (2019)
	G15				
	E2	Mice expressing eGFP	Organotypic entorhinal-hippocampal cultures; Hippocampal CA1 neurons	GPER activation only affects the structural plasticity of the developing hippocampal CA1 region, and this effect is gender-specific	Li et al. (2021)
	G1				

(Continued on following page)

TABLE 1 (*Continued*) The effects of GPER in memory impairment.

	Estrogen or estrogen-like molecules	Models	Cells/Tissues	Main findings	References
	G1	OVX female rats	Hippocampal CA3 neurons	GPER activation induces a rapid release of BDNF and promotes the internalization and degradation of GluA1, triggering LTD.	Briz et al. (2015)
	G1	Middle-aged mice	Hippocampal slices	GPER activation enhances mGluR-LTD in mossy fiber-CA3 synapses and ameliorates fear and spatial memory	Xu et al. (2018)
	G15				
	E2	OVX APP/PS1 mice	Cortical neurons	GPER activation downregulates the mRNA and protein levels of ubc9 and reduces SUMOylation of it	Lai et al. (2017a)
Synaptic transmission	E2	OVX female rats	Hippocampal neurons	Both short-term and long-term G1 treatment can strengthen the function of hippocampal cholinergic neurons and improve learning and memory, while long-term G15 has the opposite effect	Hammond et al. (2011)
	G1				Hammond et al. (2012)
	G15				Gibbs et al. (2014)
					Hawley et al. (2014)
	E2	Adult male rats	—	Cholinergic neurons in the basal forebrain may participate in GPER-mediated early consolidation of object recognition memory and emotional memory	de Souza et al. (2021)
	G1				
	G15				

Notes: NSPCs: Neural stem/progenitor cells; GCI: Global cerebral ischemia; DPC: Dorsolateral prefrontal cortex; SGZ: Subgranular zone; OVX: Ovariectomy; hfNBM: Human cholinergic neurons from the fetal nucleus basalis of meynert; TBI: Traumatic brain injury; ALS: Amyotrophic lateral sclerosis; PSD: Postsynaptic density; eGFP: enhanced green fluorescence protein.

contributing to the improvement of cognitive deficits (Sarchielli et al., 2020).

The long-term impact of ischemic injury in hippocampal neurons is a decrease in neurogenesis in the DG, accompanied by a degradation in learning and relearning ability and memory function (Kathner-Schaffert et al., 2019). However, short-term increased neurons after stroke exhibit the characteristics of abnormal basal dendrite morphology and mislocalization to the hilus of the DG. They either integrate into the established hippocampal circuits but have a shortened lifespan or fail to integrate correctly into the preexisting network, both of which can potentially result in hippocampus-dependent memory impairment (Niv et al., 2012; Woitke et al., 2017). The declining expression of GPER mRNA and protein in the hippocampal CA1 region after stroke reduces the responsiveness of neurons to E2, but E2 treatment immediately after ovariectomy can restore GPER mRNA and protein levels and alleviate ischemic-induced hippocampal neuronal loss, suggesting that GPER mediates the protective effects of E2 on neurons and reduces neuronal loss after neuronal injury (Wu et al., 2018). Single-onset traumatic brain injury is also associated with acute neuronal loss in the hippocampus, and G1 can ameliorate early-onset cognitive deficits and neuronal death by activating the PI3K/Akt pathway (Wang et al., 2017). G1 also significantly mitigates Aβ1-42-induced neuronal toxicity (Kurt et al., 2019) and alleviates the impairment of novel object recognition memory in female 5XFAD mice (Kubota et al., 2016).

Although there still exist some contradictions in the role of GPER in hippocampal neurogenesis, the fact cannot be excluded that GPER indeed participates in the protective process of damaged neurons, elongating neuronal survival to reduce neuronal loss and further improving cognitive function after neuronal injury.

4.2 GPER affects memory and cognition by regulating synaptic plasticity

Remodeling of synaptic structure and upkeep of synaptic function are essential to the cognitive function (Srivastava et al., 2013). GPER is enriched at synapses in the brain and is involved in the rapid regulation of hippocampal dendritic morphology and synaptic plasticity (Alexander et al., 2017). G1 treatment can increase dendritic spine density in the hippocampal CA1 region in a non-genomic way (Gabor et al., 2015). The newly identified GPER-specific agonist CITFA can significantly promote axonal and dendritic growth in hippocampal neurons of E18 fetal rats (DeLeon et al., 2022). In addition, overexpression of GPER in cortical neurons leads to an increase in spine synaptic density (Srivastava and Evans, 2013). Further research performed in monkeys shows that a higher expression of GPER adjacent to the PSD corresponds to a higher synaptic density of dendritic spines in this region, revealing the critical role of GPER in synaptic plasticity (Crimins et al., 2017). The increased dendritic spine density in CA1 may be strongly linked to the facilitation of learning and memory by GPER (Gabor et al., 2015). Actin polymerization underlies GPER-mediated dendritic spine generation and memory consolidation in the hippocampal CA1 region (Kim et al., 2019). GPER is reported to regulate learning and memory through the ERα/ERβ/SRC and PI3K/Akt pathways, followed by activation of mTORC2 and downstream actin polymerization to govern synaptic protein expression, suggesting that GPER can modulate structural plasticity in the hippocampal CA1 region (Zhang Y. Y et al., 2019; Li et al., 2021). mTORC2 activation can remarkably rescue the G15-induced decrease in dendritic spine density and spatial memory disorder (Xing et al., 2018). GPER activation can also increase dendritic spine density and enhance memory consolidation through a

10.3389/fmolb.2023.1097018

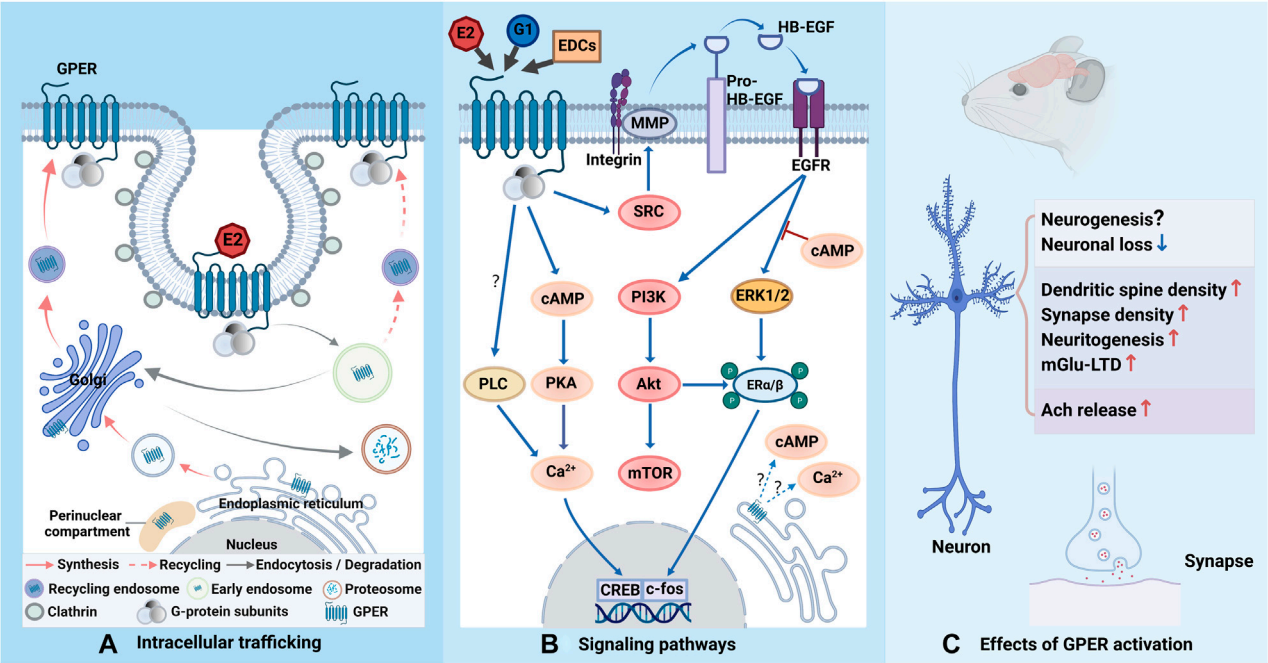

FIGURE 1
Schematic representation of GPER trafficking, related signaling pathways and effects. **(A)** GPER is biosynthesized in the endoplasmic reticulum and processed in the Golgi apparatus before its trafficking to the plasma membrane. When binding to estrogen or estrogen-like molecules, GPER is constitutively endocytosed into cells *via* clathrin-coated vesicles and enters the early endosome. The majority of GPERs are transported to the Golgi apparatus and degraded *via* the ubiquitin-proteasomal system, while a minority of them are recycled back to the cell membrane. GPER is also reported to accumulate in the perinuclear compartment. **(B)** Upon activation, the G protein departs into Gα and Gβγ subunits and further triggers complicated signaling cascades. Gβγ stimulates SRC-activated MMPs, leading to the release of HB-EGF from the cell surface, which transactivates EGFR and subsequently triggers ERK1/2 and PI3K. Gαs activates AC and increases cAMP generation, which results in intracellular calcium mobilization. cAMP also recruits PKA to activates CREB in the nucleus to initiate transcription, which can also be potentiated by phosphorylated ERα/β *via* ERK and Akt. The cAMP-related signaling pathway can regulate EGFR-induced ERK1/2 activity. It is not yet clear whether GPER signaling can be observed from intracellular receptors. The involvement of PLC may depend on cell type (question marks). **(C)** Activation of GPER can exert neuroprotection to reduce neuronal loss, but the role of GPER in neurogenesis necessities further investigation. Activation of GPER can positively regulate synaptic formation and plasticity. GPER can also mediate E2 effect to increase Ach release. The figure was created with BioRender.com.

pathway where JNK phosphorylation and cofilin phosphorylation contribute to actin polymerization (Kim et al., 2016; Kim et al., 2019) but not through E2-mediated ERK phosphorylation (Kim, 2014). Intriguingly, in the developing hippocampus, GPER activation markedly increases the density of dendritic spines and alters the expression of related synaptic proteins in the stratum lacunosum moleculare (SLM) of the hippocampal CA1 in female rats (Li et al., 2021). However, these increased dendritic spines do not translate into increased synaptic density, implying that GPER activation only modifies the structural plasticity of the developing hippocampal CA1 region, and this effect is gender-specific (Li et al., 2021).

Dendritic spines are specialized projections of neurons, and alterations in dendritic spine function directly affect synaptic plasticity (Dorostkar et al., 2015). Memory is encoded by changing synaptic strength through long-term potentiation (LTP) and long-term depression (LTD) (Nabavi et al., 2014). GPER-mediated mGluR-LTD in CA3 represents a novel estrogen-mediated regulation of synaptic plasticity (Briz et al., 2015). GPER activation by G1 induces a rapid release of brain-derived neurotrophic factor (BDNF) that transiently stimulates the translation of activity-regulated cytoskeleton-associated protein (Arc) and internalization of GluA1-containing AMPA receptor in the CA3 region (Briz et al., 2015). However, unlike the induction of mGluR-LTD *via* E2 in CA1, mGluR activation in CA3 does not increase the synthesis of Arc; instead, it promotes the internalization of GluA1 under the premise of GPER activation and causes GluA1 to be rapidly degraded by the ubiquitin-proteasome system, triggering LTD (Briz et al., 2015). That GPER activation enhances mGluR-LTD in mossy fiber-CA3 synapses also explains the improving effects of G1 on contextual and spatial memory in middle-aged mice (Xu et al., 2018). LTD plays a role in regulating the transcription, translation, and recycling of receptors, which results in the downregulation of cellular excitability and affects learning and memory (Mahmoud et al., 2016). Thus, GPER-induced mGluR-LTD in CA3 lends support to the modulation of synaptic functional plasticity *via* GPER in the hippocampus.

Ubc9 plays an indispensable role in synaptic functional plasticity (Lai et al., 2017a). GPER can reduce the interaction of ubc9 with the postsynaptic protein PSD-95 and increase its interaction with the presynaptic protein synaptophysin *via* the PI3K pathway, and the accumulation of presynaptic ubc9 may inhibit synaptic transmission (Lai et al., 2017a). G1 can increase the expression of PSD-95 in the CA3 region of the mouse hippocampus (Waters et al., 2015). Overexpression of PSD-95 promotes the maturation of glutamatergic synapses and enhances the activity of postsynaptic

glutamate receptors, indicating that PSD-95 coordinates synaptic development (El-Husseini et al., 2000). PSD-95 also increases the number and size of dendritic spines, suggesting its role in synaptic stability and plasticity (El-Husseini et al., 2000).

4.3 GPER affects memory and cognition by enhancing synaptic transmission

The anatomical localization of GPER at synapses suggests that GPER may play a role in regulating neurotransmission (Wang et al., 2007; Akama et al., 2013). By applying 17β-E2-3-benzoate (EB) and agonists and antagonists of ERs to investigate the contribution of each ER, it was found that ERα, ERβ, and GPER are all involved in EB-mediated enhancement of synaptic transmission (Kumar et al., 2015). However, among them, GPER is the leading contributor to the EB-mediated increase in ERK activation and the CA3-CA1 synaptic response in the hippocampus of OVX female mice (Kumar et al., 2015). GPER can also alter the efficacy of excitatory synaptic transmission at Schaffer-collateral-CA1 synapses. Indeed, G1 is reported to mirror the actions of E2 to constantly potentiate excitatory synaptic transmission at CA1 synapses (Smejkalova and Woolley, 2010).

There is a strong connection between cholinergic signaling and cognitive function in the CNS (Ballinger et al., 2016). Levels of choline acetyltransferase (ChAT) and acetylcholinesterase (AchE), major markers of cholinergic neuronal activity, are reduced in the late stage of Alzheimer's disease, which contributes to cognitive deficits (H. Ferreira-Vieira et al., 2016). GPER is expressed in the majority of cholinergic neurons in the basal forebrain, and GPER activation effectively improves the function of hippocampal cholinergic neurons in OVX rats (Hammond et al., 2011).

Experimental results demonstrate that short-term G1 treatment in OVX rats productively enhances spatial recognition memory relying on environmental novelty, which may be based on the fact that GPER activation increases the release of Ach from the basal forebrain to the hippocampus and that elevated Ach levels in the hippocampus can lead to an increase in synaptic connectivity and interneuron communication during learning (Hawley et al., 2014). Moreover, long-term G1 administration in OVX rats increases hippocampal potassium-stimulated Ach release by 3-fold and improves rat performance in a maze test (Hammond et al., 2011). Thereafter, this team extended their previous conclusion and illustrated that E2 treatment can improve task-specific learning by activating GPER and enhancing Ach release associated with food reward (Gibbs et al., 2014), which suggests that both short-term and long-term G1 treatment can strengthen hippocampal cholinergic neuronal function and improve learning and memory. In contrast, long-term G15 administration impairs the performance in the maze test and slows the rate of spatial memory acquisition, which is similar to the effect of removing cholinergic inputs to the hippocampus and frontal cortex, suggesting that GPER may mediate the effects of E2 on basal forebrain cholinergic function to modulate spatial memory (Hammond et al., 2012). Cholinergic neurons in the basal forebrain also engage in GPER-mediated early consolidation of object recognition memory and emotional memory in adult male rats (de Souza et al., 2021).

Followed by the activation of cAMP and CREB, GPER increases the activity of the AchE promoter in PC12 neurons, while GPER increases miR-132 levels, which is associated with the inhibition of AchE translation (Liu et al., 2019). Thus, GPER may maintain the homeostasis between Ach synthesis and degradation to improve cognitive and memory function in neurodegenerative diseases (Liu et al., 2019).

5 Conclusion and perspectives

In summary, GPER can trigger a rapid estrogenic response to improve hippocampal memory and cognitive function, either by acting on the neurogenesis or by affecting hippocampal synaptic function and the activity of cholinergic input into the hippocampus (Table 1). The emergence of GPER fills the gap in the mechanisms of estrogen-mediated neuroprotection, suggesting that GPER can be applied as a promising target to alleviate aging-induced memory decline and cognitive dysfunction. Since GPER can elicit both non-genomic signaling and transcriptional progress, further studies are needed to clarify the precise subcellular localization of GPER and identify the potential interactions between membrane-associated signaling pathways and nuclear-associated signaling pathways to provide a robust theoretical basis for the therapeutic role of GPER in aging-induced memory impairments. Future studies may also require the discovery or synthesis of more agonists, antagonists, and modulators with higher affinity and specificity for GPER to deeply explore its regulatory mechanisms. Another urgent issue is the lack of a crystal structure for GPER. Furthermore, considering that most studies of estrogen and GPER are performed in cellular models and OVX female rodents, more researches are needed to understand how GPER regulates memory in the human CNS in normal and pathological conditions (Figure 1).

Author contributions

ZZ, YC and YZ made substantial contributions to the conception of the manuscript. WL, YY and ZZ wrote the manuscript. YC and YZ made careful revision and provided valuable suggestions. WL prepared the figure and the table. All authors contributed to the paper and approved the submitted version.

Funding

This work was supported by the National Natural Science Foundation of China (81971639).

Conflict of interest

The authors declare that the research was conducted in the absence of any commercial or financial relationships that could be construed as a potential conflict of interest.

Publisher's note

References

Adhya, D., Annuario, E., Lancaster, M. A., Price, J., Baron-Cohen, S., and Srivastava, D. P. (2018). Understanding the role of steroids in typical and atypical brain development: Advantages of using a "brain in a dish" approach. *J. Neuroendocrinol.* 30, e12547. doi:10.1111/jne.12547

Akama, K. T., Thompson, L. I., Milner, T. A., and McEwen, B. S. (2013). Post-synaptic density-95 (PSD-95) binding capacity of G-protein-coupled receptor 30 (GPR30), an estrogen receptor that can Be identified in hippocampal dendritic spines. *J. Biol. Chem.* 288, 6438–6450. doi:10.1074/jbc.M112.412478

Alexander, A., Irving, A. J., and Harvey, J. (2017). Emerging roles for the novel estrogen-sensing receptor GPER1 in the CNS. *Neuropharmacology* 113, 652–660. doi:10.1016/j.neuropharm.2016.07.003

Ballinger, E. C., Ananth, M., Talmage, D. A., and Role, L. W. (2016). Basal forebrain cholinergic circuits and signaling in cognition and cognitive decline. *Neuron* 91, 1199–1218. doi:10.1016/j.neuron.2016.09.006

Barton, M., Filardo, E. J., Lolait, S. J., Thomas, P., Maggiolini, M., and Prossnitz, E. R. (2018). Twenty years of the G protein-coupled estrogen receptor GPER: Historical and personal perspectives. *J. Steroid Biochem. Mol. Biol.* 176, 4–15. doi:10.1016/j.jsbmb.2017.03.021

Bologa, C. G., Revankar, C. M., Young, S. M., Edwards, B. S., Arterburn, J. B., Kiselyov, A. S., et al. (2006). Virtual and biomolecular screening converge on a selective agonist for GPR30. *Nat. Chem. Biol.* 2, 207–212. doi:10.1038/nchembio775

Brailoiu, E., Dun, S. L., Brailoiu, G. C., Mizuo, K., Sklar, L. A., Oprea, T. I., et al. (2007). Distribution and characterization of estrogen receptor G protein-coupled receptor 30 in the rat central nervous system. *J. Endocrinol.* 193, 311–321. doi:10.1677/JOE-07-0017

Briz, V., Liu, Y., Zhu, G., Bi, X., and Baudry, M. (2015). A novel form of synaptic plasticity in field CA3 of hippocampus requires GPER1 activation and BDNF release. *J. Cell Biol.* 210, 1225–1237. doi:10.1083/jcb.201504092

Bustamante-Barrientos, F. A., Méndez-Ruette, M., Ortloff, A., Luz-Crawford, P., Rivera, F. J., Figueroa, C. D., et al. (2021). The impact of estrogen and estrogen-like molecules in neurogenesis and neurodegeneration: Beneficial or harmful? *Front. Cell. Neurosci.* 15, 636176. doi:10.3389/fncel.2021.636176

Camilletti, M. A., Abeledo-Machado, A., Ferraris, J., Pérez, P. A., Faraoni, E. Y., Pisera, D., et al. (2019). Role of GPER in the anterior pituitary gland focusing on lactotroph function. *J. Endocrinol.* 240, 99–110. doi:10.1530/JOE-18-0402

Carmeci, C., Thompson, D. A., Ring, H. Z., Francke, U., and Weigel, R. J. (1997). Identification of a gene (GPR30) with homology to the G-protein-coupled receptor superfamily associated with estrogen receptor expression in breast cancer. *Genomics* 45, 607–617. doi:10.1006/geno.1997.4972

Cheng, S.-B., Graeber, C. T., Quinn, J. A., and Filardo, E. J. (2011a). Retrograde transport of the transmembrane estrogen receptor, G-protein-coupled-receptor-30 (GPR30/GPER) from the plasma membrane towards the nucleus. *Steroids* 76, 892–896. doi:10.1016/j.steroids.2011.02.018

Cheng, S.-B., Quinn, J. A., Graeber, C. T., and Filardo, E. J. (2011b). Down-modulation of the G-protein-coupled estrogen receptor, GPER, from the cell surface occurs via a trans-golgi-proteasome pathway. *J. Biol. Chem.* 286, 22441–22455. doi:10.1074/jbc.M111.224071

Cheong, R. Y., Kwakowsky, A., Barad, Z., Porteous, R., Herbison, A. E., and Ábrahám, I. M. (2012). Estradiol acts directly and indirectly on multiple signaling pathways to phosphorylate cAMP-response element binding protein in GnRH neurons. *Endocrinology* 153, 3792–3803. doi:10.1210/en.2012-1232

Cirillo, F., Lappano, R., Bruno, L., Rizzuti, B., Grande, F., Guzzi, R., et al. (2019). AHR and GPER mediate the stimulatory effects induced by 3-methylcholanthrene in breast cancer cells and cancer-associated fibroblasts (CAFs). *J. Exp. Clin. Cancer Res.* 38, 335. doi:10.1186/s13046-019-1337-2

Cooke, P. S., Nanjappa, M. K., Ko, C., Prins, G. S., and Hess, R. A. (2017). Estrogens in male physiology. *Physiol. Rev.* 97, 995–1043. doi:10.1152/physrev.00018.2016

Crimins, J. L., Wang, A. C.-J., Yuk, F., Puri, R., Janssen, W. G. M., Hara, Y., et al. (2017). Diverse synaptic distributions of G protein-coupled estrogen receptor 1 in monkey prefrontal cortex with aging and menopause. *Cereb. Cortex* 27, 2022–2033. doi:10.1093/cercor/bhw050

de Souza, L. O., Machado, G. D. B., de Freitas, B. S., Rodrigues, S. L. C., Severo, M. P. A., Molz, P., et al. (2021). The G protein-coupled estrogen receptor (GPER) regulates recognition and aversively–motivated memory in male rats. *Neurobiol. Learn. Mem.* 184, 107499. doi:10.1016/j.nlm.2021.107499

DeLeon, C., Pemberton, K., Green, M., Kalajdzic, V., Rosato, M., Xu, F., et al. (2022). Novel GPER agonist, CITFA, increases neurite growth in rat embryonic (E18) hippocampal neurons. *ACS Chem. Neurosci.* 13, 1119–1128. doi:10.1021/acschemneuro.1c00811

Demars, M. P., Hollands, C., Zhao, K. D., Tommy)and Lazarov, O. (2013). Soluble amyloid precursor protein-α rescues age-linked decline in neural progenitor cell proliferation. *Neurobiol. Aging* 34, 2431–2440. doi:10.1016/j.neurobiolaging.2013.04.016

Dennis, M. K., Burai, R., Ramesh, C., Petrie, W. K., Alcon, S. N., Nayak, T. K., et al. (2009). *In vivo* effects of a GPR30 antagonist. *Nat. Chem. Biol.* 5, 421–427. doi:10.1038/nchembio.168

Dennis, M. K., Field, A. S., Burai, R., Ramesh, C., Petrie, W. K., Bologa, C. G., et al. (2011). Identification of a GPER/GPR30 antagonist with improved estrogen receptor counterselectivity. *J. Steroid Biochem. Mol. Biol.* 127, 358–366. doi:10.1016/j.jsbmb.2011.07.002

Dorostkar, M. M., Zou, C., Blazquez-Llorca, L., and Herms, J. (2015). Analyzing dendritic spine pathology in Alzheimer's disease: Problems and opportunities. *Acta Neuropathol. (Berl.)* 130, 1–19. doi:10.1007/s00401-015-1449-5

Duarte-Guterman, P., Lieblich, S. E., Chow, C., and Galea, L. A. M. (2015). Estradiol and GPER activation differentially affect cell proliferation but not GPER expression in the Hippocampus of adult female rats. *PLOS ONE* 10, e0129880. doi:10.1371/journal.pone.0129880

El-Husseini, A. E., Schnell, E., Chetkovich, D. M., Nicoll, R. A., and Bredt, D. S. (2000). PSD-95 involvement in maturation of excitatory synapses. *Science* 290, 1364–1368. doi:10.1126/science.290.5495.1364

Engler-Chiurazzi, E. B., Brown, C. M., Povroznik, J. M., and Simpkins, J. W. (2017). Estrogens as neuroprotectants: Estrogenic actions in the context of cognitive aging and brain injury. *Prog. Neurobiol., New Perspect. Healthy Aging* 157, 188–211. doi:10.1016/j.pneurobio.2015.12.008

Feldman, R. D., and Limbird, L. E. (2017). Gper (GPR30): A nongenomic receptor (GPCR) for steroid hormones with implications for cardiovascular disease and cancer. *Annu. Rev. Pharmacol. Toxicol.* 57, 567–584. doi:10.1146/annurev-pharmtox-010716-104651

Ferreira-Vieira, H., Guimaraes, T., M., Silva, I., R., and Ribeiro, F., M. F. (2016). Alzheimer's disease: Targeting the cholinergic system. *Curr. Neuropharmacol.* 14, 101–115. doi:10.2174/1570159X13666150716165726

Filardo, E. J. (2002). Epidermal growth factor receptor (EGFR) transactivation by estrogen via the G-protein-coupled receptor, GPR30: A novel signaling pathway with potential significance for breast cancer. *J. Steroid Biochem. Mol. Biol.* 80, 231–238. doi:10.1016/s0960-0760(01)00190-x

Filardo, E. J., Quinn, J. A., Bland, K. I., and Frackelton, A. R. (2000). Estrogen-induced activation of Erk-1 and Erk-2 requires the G protein-coupled receptor homolog, GPR30, and occurs via trans-activation of the epidermal growth factor receptor through release of HB-EGF. *Mol. Endocrinol. Balt. Md* 14, 1649–1660. doi:10.1210/mend.14.10.0532

Filardo, E. J., Quinn, J. A., Frackelton, A. R., and Bland, K. I. (2002). Estrogen action via the G protein-coupled receptor, GPR30: Stimulation of adenylyl cyclase and cAMP-mediated attenuation of the epidermal growth factor receptor-to-MAPK signaling axis. *Mol. Endocrinol. Balt. Md* 16, 70–84. doi:10.1210/mend.16.1.0758

Filardo, E. J., and Thomas, P. (2005). GPR30: A seven-transmembrane-spanning estrogen receptor that triggers EGF release. *Trends Endocrinol. Metab.* 16, 362–367. doi:10.1016/j.tem.2005.08.005

Fuentes, N., and Silveyra, P. (2019). Estrogen receptor signaling mechanisms. *Adv. Protein Chem. Struct. Biol.* 116, 135–170. doi:10.1016/bs.apcsb.2019.01.001

Gabor, C., Lymer, J., Phan, A., and Choleris, E. (2015). Rapid effects of the G-protein coupled oestrogen receptor (GPER) on learning and dorsal hippocampus dendritic spines in female mice. *Physiol. Behav.* 149, 53–60. doi:10.1016/j.physbeh.2015.05.017

Gibbs, R. B., Nelson, D., and Hammond, R. (2014). Role of GPR30 in mediating estradiol effects on acetylcholine release in the hippocampus. *Horm. Behav.* 66, 339–345. doi:10.1016/j.yhbeh.2014.06.002

Hammond, R., Nelson, D., and Gibbs, R. B. (2011). GPR30 co-localizes with cholinergic neurons in the basal forebrain and enhances potassium-stimulated acetylcholine release in the hippocampus. *Psychoneuroendocrinology* 36, 182–192. doi:10.1016/j.psyneuen.2010.07.007

Hammond, R., Nelson, D., Kline, E., and Gibbs, R. B. (2012). Chronic treatment with a GPR30 antagonist impairs acquisition of a spatial learning task in young female rats. *Horm. Behav.* 62, 367–374. doi:10.1016/j.yhbeh.2012.07.004

Hawley, W. R., Grissom, E. M., Moody, N. M., Dohanich, G. P., and Vasudevan, N. (2014). Activation of G-protein-coupled receptor 30 is sufficient to enhance spatial recognition memory in ovariectomized rats. *Behav. Brain Res.* 262, 68–73. doi:10.1016/j.bbr.2014.01.006

Hollands, C., Bartolotti, N., and Lazarov, O. (2016). Alzheimer's disease and hippocampal adult neurogenesis; exploring shared mechanisms. *Front. Neurosci.* 10, 178. doi:10.3389/fnins.2016.00178

Huang, Y., Todd, N., and Thathiah, A. (2017). The role of GPCRs in neurodegenerative diseases: Avenues for therapeutic intervention. *Curr. Opin. Pharmacol. Neurosci.* 32, 96–110. doi:10.1016/j.coph.2017.02.001

Hutson, D. D., Gurrala, R., Ogola, B. O., Zimmerman, M. A., Mostany, R., Satou, R., et al. (2019). Estrogen receptor profiles across tissues from male and female *Rattus norvegicus*. *Biol. Sex. Differ.* 10, 4. doi:10.1186/s13293-019-0219-9

Jacquot, Y., Kampa, M., and Lindsey, S. H. (2021b). Editorial: GPER and human pathologies. *Front. Endocrinol.* 12, 794332. doi:10.3389/fendo.2021.794332

Jacquot, Y., Kampa, M., and Lindsey, S. H. (2021a). Editorial: Gper: Control and functions. *Front. Endocrinol.* 12, 794344. doi:10.3389/fendo.2021.794344

Jett, S., Schelbaum, E., Jang, G., Boneu Yepez, C., Dyke, J. P., Pahlajani, S., et al. (2022). Ovarian steroid hormones: A long overlooked but critical contributor to brain aging and Alzheimer's disease. *Front. Aging Neurosci.* 14, 948219. doi:10.3389/fnagi.2022.948219

Kanda, N., and Watanabe, S. (2003). 17α-estradiol inhibits oxidative stress-induced apoptosis in keratinocytes by promoting Bcl-2 expression. *J. Invest. Dermatol.* 121, 1500–1509. doi:10.1111/j.1523-1747.2003.12617.x

Kathner-Schaffert, C., Karapetow, L., Günther, M., Rudolph, M., Dahab, M., Baum, E., et al. (2019). Early stroke induces long-term impairment of adult neurogenesis accompanied by hippocampal-mediated cognitive decline. *Cells* 8, 1654. doi:10.3390/cells8121654

Kempermann, G. (2019). Environmental enrichment, new neurons and the neurobiology of individuality. *Nat. Rev. Neurosci.* 20, 235–245. doi:10.1038/s41583-019-0120-x

Khan, M. M., Wakade, C., de Sevilla, L., and Brann, D. W. (2015). Selective estrogen receptor modulators (SERMs) enhance neurogenesis and spine density following focal cerebral ischemia. *J. Steroid Biochem. Mol. Biol., Sex steroids Brain Disord.* 146, 38–47. doi:10.1016/j.jsbmb.2014.05.001

Khan, S. U., Ahemad, N., Chuah, L.-H., Naidu, R., and Htar, T. T. (2022). G protein-coupled estrogen receptor-1: homology modeling approaches and application in screening new GPER-1 modulators. *J. Biomol. Struct. Dyn.* 40, 3325–3335. doi:10.1080/07391102.2020.1844059

Kim, J. K. (2014). "The role of G-protein coupled estrogen receptor (GPER/GPR30) in hippocampal memory and cell signaling in female mice,". Theses Diss.

Kim, J., Schalk, J. C., Koss, W. A., Gremminger, R. L., Taxier, L. R., Gross, K. S., et al. (2019). Dorsal hippocampal actin polymerization is necessary for activation of G-protein-coupled estrogen receptor (GPER) to increase CA1 dendritic spine density and enhance memory consolidation. *J. Neurosci.* 39, 9598–9610. doi:10.1523/JNEUROSCI.2687-18.2019

Kim, J., Szinte, J. S., Boulware, M. I., and Frick, K. M. (2016). 17 -estradiol and agonism of G-protein-coupled estrogen receptor enhance hippocampal memory via different cell-signaling mechanisms. *J. Neurosci.* 36, 3309–3321. doi:10.1523/JNEUROSCI.0257-15.2016

Koss, W. A., Haertel, J. M., Philippi, S. M., and Frick, K. M. (2018). Sex differences in the rapid cell signaling mechanisms underlying the memory-enhancing effects of 17β-estradiol. *Eneuro* 5, ENEURO.0267-18.2018. doi:10.1523/ENEURO.0267-18.2018

Kubota, T., Matsumoto, H., and Kirino, Y. (2016). Ameliorative effect of membrane-associated estrogen receptor G protein coupled receptor 30 activation on object recognition memory in mouse models of Alzheimer's disease. *J. Pharmacol. Sci.* 131, 219–222. doi:10.1016/j.jphs.2016.06.005

Kumar, A., Bean, L. A., Rani, A., Jackson, T., and Foster, T. C. (2015). Contribution of estrogen receptor subtypes, ERα, ERβ, and GPER1 in rapid estradiol-mediated enhancement of hippocampal synaptic transmission in mice. *Hippocampus* 25, 1556–1566. doi:10.1002/hipo.22475

Kurt, A. H., Yuksel, K. Z., Uremis, N., Uremis, M. M., Altun, I., Bosnak, M., et al. (2019). Protective effects of G protein-coupled estrogen receptor 1 (GPER1) on β-amyloid-induced neurotoxicity: Implications for Alzheimer's disease. *Neurochem. J.* 13, 99–104. doi:10.1134/S1819712419010148

Lai, Y-J., Liu, L., Hu, X.-T., He, L., and Chen, G.-J. (2017a). Estrogen modulates ubc9 expression and synaptic redistribution in the brain of APP/PS1 mice and cortical neurons. *J. Mol. Neurosci.* 61, 436–448. doi:10.1007/s12031-017-0884-2

Lai, Y-J., Yu, D., Zhang, J. H., and Chen, G.-J. (2017b). Cooperation of genomic and rapid nongenomic actions of estrogens in synaptic plasticity. *Mol. Neurobiol.* 54, 4113–4126. doi:10.1007/s12035-016-9979-y

Lee, E., Sidoryk-Wêgrzynowicz, M., Wang, N., Webb, A., Son, D.-S., Lee, K., et al. (2012). GPR30 regulates glutamate transporter GLT-1 expression in rat primary astrocytes. *J. Biol. Chem.* 287, 26817–26828. doi:10.1074/jbc.M112.341867

Li, X., Johann, S., Rune, G. M., and Bender, R. A. (2021). Sex-specific regulation of spine density and synaptic proteins by G-protein-coupled estrogen receptor (GPER)1 in developing Hippocampus. *Neuroscience* 472, 35–50. doi:10.1016/j.neuroscience.2021.07.035

Liu, E. Y. L., Xu, M. L., Xia, Y., Kong, X., Wu, Q., Dong, T. T. X., et al. (2019). Activation of G protein-coupled receptor 30 by flavonoids leads to expression of acetylcholinesterase in cultured PC12 cells. *Chem. Biol. Interact.* 306, 147–151. doi:10.1016/j.cbi.2019.04.031

Llorente, R., Marraudino, M., Carrillo, B., Bonaldo, B., Simon-Areces, J., Abellanas-Pérez, P., et al. (2020). G protein-coupled estrogen receptor immunoreactivity fluctuates during the estrous cycle and show sex differences in the amygdala and dorsal Hippocampus. *Front. Endocrinol.* 11, 537. doi:10.3389/fendo.2020.00537

Lu, C.-L., and Herndon, C. (2017). New roles for neuronal estrogen receptors. *Neurogastroenterol. Motil.* 29, e13121. doi:10.1111/nmo.13121

Machado, G. D. B., Freitas, B. S., Florian, L. Z., Monteiro, R. T., Gus, H., and Schröder, N. (2019). G protein-coupled oestrogen receptor stimulation ameliorates iron- and ovariectomy-induced memory impairments through the cAMP/PKA/CREB signalling pathway. *J. Neuroendocrinol.* 31, e12780. doi:10.1111/jne.12780

Mahmoud, R., Wainwright, S. R., and Galea, L. A. M. (2016). Sex hormones and adult hippocampal neurogenesis: Regulation, implications, and potential mechanisms. *Front. Neuroendocrinol.* 41, 129–152. doi:10.1016/j.yfrne.2016.03.002

Marraudino, M., Carrillo, B., Bonaldo, B., Llorente, R., Campioli, E., Garate, I., et al. (2021). G protein-coupled estrogen receptor immunoreactivity in the rat hypothalamus is widely distributed in neurons, astrocytes, and oligodendrocytes, fluctuates during the estrous cycle, and is sexually dimorphic. *Neuroendocrinology* 111, 660–677. doi:10.1159/000509583

Nabavi, S., Fox, R., Proulx, C. D., Lin, J. Y., Tsien, R. Y., and Malinow, R. (2014). Engineering a memory with LTD and LTP. *Nature* 511, 348–352. doi:10.1038/nature13294

Niv, F., Keiner, S., Krishna, -K., Witte, O. W., Lie, D. C., and Redecker, C. (2012). Aberrant neurogenesis after stroke: A retroviral cell labeling study. *Stroke* 43, 2468–2475. doi:10.1161/STROKEAHA.112.660977

Okada, M., Makino, A., Nakajima, M., Okuyama, S., Furukawa, S., and Furukawa, Y. (2010). Estrogen stimulates proliferation and differentiation of neural stem/progenitor cells through different signal transduction pathways. *Int. J. Mol. Sci.* 11, 4114–4123. doi:10.3390/ijms11104114

O'Malley, B. W., and Means, A. R. (1974). Female steroid hormones and target cell nuclei. *Science* 183, 610–620. doi:10.1126/science.183.4125.610

Prossnitz, E. R., and Arterburn, J. B. (2015). International union of basic and clinical Pharmacology. XCVII. G protein–coupled estrogen receptor and its pharmacologic modulators. *Pharmacol. Rev.* 67, 505–540. doi:10.1124/pr.114.009712

Prossnitz, E. R., and Barton, M. (2011). The G-protein-coupled estrogen receptor GPER in health and disease. *Nat. Rev. Endocrinol.* 7, 715–726. doi:10.1038/nrendo.2011.122

Prossnitz, E. R., Arterburn, J. B., Smith, H. O., Oprea, T. I., Sklar, L. A., and Hathaway, J. J. (2008). Estrogen signaling through the transmembrane G protein–coupled receptor GPR30. *Annu. Rev. Physiol.* 70, 165–190. doi:10.1146/annurev.physiol.70.113006.100518

Pupo, M., Vivacqua, A., Perrotta, I., Pisano, A., Aquila, S., Abonante, S., et al. (2013). The nuclear localization signal is required for nuclear GPER translocation and function in breast Cancer-Associated Fibroblasts (CAFs). *Mol. Cell. Endocrinol.* 376, 23–32. doi:10.1016/j.mce.2013.05.023

Revankar, C. M., Cimino, D. F., Sklar, L. A., Arterburn, J. B., and Prossnitz, E. R. (2005). A transmembrane intracellular estrogen receptor mediates rapid cell signaling. *Science* 307, 1625–1630. doi:10.1126/science.1106943

Roque, C., Mendes-Oliveira, J., Duarte-Chendo, C., and Baltazar, G. (2019). The role of G protein-coupled estrogen receptor 1 on neurological disorders. *Front. Neuroendocrinol.* 55, 100786. doi:10.1016/j.yfrne.2019.100786

Ruiz-Palmero, I., Hernando, M., Garcia-Segura, L. M., and Arevalo, M.-A. (2013). G protein-coupled estrogen receptor is required for the neuritogenic mechanism of 17α-estradiol in developing hippocampal neurons. *Mol. Cell. Endocrinol.* 372, 105–115. doi:10.1016/j.mce.2013.03.018

Sager, T., Kashon, M. L., and Krajnak, K. (2018). Estrogen and environmental enrichment differentially affect neurogenesis, dendritic spine immunolabeling and synaptogenesis in the Hippocampus of young and reproductively senescent female rats. *Neuroendocrinology* 106, 252–263. doi:10.1159/000479699

Sahab-Negah, S., Hajali, V., Moradi, H. R., and Gorji, A. (2020). The impact of estradiol on neurogenesis and cognitive functions in Alzheimer's disease. *Cell. Mol. Neurobiol.* 40, 283–299. doi:10.1007/s10571-019-00733-0

Sarchielli, E., Guarnieri, G., Idrizaj, E., Squecco, R., Mello, T., Comeglio, P., et al. (2020). The G protein-coupled oestrogen receptor, GPER1, mediates direct anti-inflammatory effects of oestrogens in human cholinergic neurones from the nucleus basalis of Meynert. *J. Neuroendocrinol.* 32, e12837. doi:10.1111/jne.12837

Smejkalova, T., and Woolley, C. S. (2010). Estradiol acutely potentiates hippocampal excitatory synaptic transmission through a presynaptic mechanism. *J. Neurosci.* 30, 16137–16148. doi:10.1523/JNEUROSCI.4161-10.2010

Srivastava, D. P., and Evans, P. D. (2013). G-protein oestrogen receptor 1: Trials and tribulations of a membrane oestrogen receptor. *J. Neuroendocrinol.* 25, 1219–1230. doi:10.1111/jne.12071

Srivastava, D. P., Woolfrey, K. M., and Penzes, P. (2013). Insights into rapid modulation of neuroplasticity by brain estrogens. *Pharmacol. Rev.* 65, 1318–1350. doi:10.1124/pr.111.005272

Thomas, P., Pang, Y., Filardo, E. J., and Dong, J. (2005). Identity of an estrogen membrane receptor coupled to a G protein in human breast cancer cells. *Endocrinology* 146, 624–632. doi:10.1210/en.2004-1064

Tuscher, J. J., Szinte, J. S., Starrett, J. R., Krentzel, A. A., Fortress, A. M., Remage-Healey, L., et al. (2016). Inhibition of local estrogen synthesis in the hippocampus impairs hippocampal memory consolidation in ovariectomized female mice. *Horm. Behav.* 83, 60–67. doi:10.1016/j.yhbeh.2016.05.001

Uhl, M., Schmeisser, M. J., and Schumann, S. (2022). The sexual dimorphic synapse: From spine density to molecular composition. *Front. Mol. Neurosci.* 15, 818390. doi:10.3389/fnmol.2022.818390

van den Beld, A. W., Kaufman, J.-M., Zillikens, M. C., Lamberts, S. W. J., Egan, J. M., and van der Lely, A. J. (2018). The physiology of endocrine systems with ageing. *Lancet Diabetes Endocrinol.* 6, 647–658. doi:10.1016/S2213-8587(18)30026-3

Vickers, C., Mitew, S., Woodhouse, A., Fernandez-Martos, M., Kirkcaldie, T., Canty, M., J., et al. (2016). Defining the earliest pathological changes of Alzheimer's disease. *Curr. Alzheimer Res.* 13, 281–287. doi:10.2174/1567205013666151218150322

Wang, C., Prossnitz, E. R., and Roy, S. K. (2007). Expression of G protein-coupled receptor 30 in the hamster ovary: Differential regulation by gonadotropins and steroid hormones. *Endocrinology* 148, 48534853–48534864. doi:10.1210/en.2007-0727

Wang, L., Liu, J., Xu, J., Zhang, W., and Wang, R. (2021). Coupling of GPR30 mediated neurogenesis and protection with astroglial Aromatase-STAT3 signaling in rat hippocampus after global cerebral ischemia. *Mol. Cell. Endocrinol.* 535, 111394. doi:10.1016/j.mce.2021.111394

Wang, X., Xu, W., Chen, H., Li, W., Li, W., and Zhu, G. (2020). Astragaloside IV prevents Aβ1-42 oligomers-induced memory impairment and hippocampal cell apoptosis by promoting PPARγ/BDNF signaling pathway. *Brain Res.* 1747, 147041. doi:10.1016/j.brainres.2020.147041

Wang, Z.-F., Pan, Z.-Y., Xu, C.-S., and Li, Z.-Q. (2017). Activation of G-protein coupled estrogen receptor 1 improves early-onset cognitive impairment via PI3K/Akt pathway in rats with traumatic brain injury. *Biochem. Biophys. Res. Commun.* 482, 948–953. doi:10.1016/j.bbrc.2016.11.138

Waters, E. M., Thompson, L. I., Patel, P., Gonzales, A. D., Ye, H., Filardo, E. J., et al. (2015). G-Protein-Coupled estrogen receptor 1 is anatomically positioned to modulate synaptic plasticity in the mouse Hippocampus. *J. Neurosci.* 35, 2384–2397. doi:10.1523/JNEUROSCI.1298-14.2015

West, C., and Hanyaloglu, A. C. (2015). Minireview: Spatial programming of G protein-coupled receptor activity: Decoding signaling in health and disease. *Mol. Endocrinol. Balt. Md* 29, 1095–1106. doi:10.1210/ME.2015-1065

Woitke, F., Ceanga, M., Rudolph, M., Niv, F., Witte, O. W., Redecker, C., et al. (2017). Adult hippocampal neurogenesis poststroke: More new granule cells but aberrant morphology and impaired spatial memory. *PLOS ONE* 12, e0183463. doi:10.1371/journal.pone.0183463

Wu, Y., Feng, D., Lin, J., Qu, Y., He, S., Wang, Y., et al. (2018). Downregulation of G-protein-coupled receptor 30 in the hippocampus attenuates the neuroprotection of estrogen in the critical period hypothesis. *Mol. Med. Rep.* 17, 5716–5725. doi:10.3892/mmr.2018.8618

Xiao, Q., Luo, Y., Lv, F., He, Q., Wu, H., Chao, F., et al. (2018). Protective effects of 17β-estradiol on hippocampal myelinated fibers in ovariectomized middle-aged rats. *Neuroscience* 385, 143–153. doi:10.1016/j.neuroscience.2018.06.006

Xing, F.-Z., Zhao, Y.-G., Zhang, Y.-Y., He, L., Zhao, J.-K., Liu, M.-Y., et al. (2018). Nuclear and membrane estrogen receptor antagonists induce similar mTORC2 activation-reversible changes in synaptic protein expression and actin polymerization in the mouse hippocampus. *CNS Neurosci. Ther.* 24, 495–507. doi:10.1111/cns.12806

Xu, W., Cao, J., Zhou, Y., Wang, L., and Zhu, G. (2018). GPR30 activation improves memory and facilitates DHPG-induced LTD in the hippocampal CA3 of middle-aged mice. *Neurobiol. Learn. Mem.* 149, 10–19. doi:10.1016/j.nlm.2018.02.005

Yue, J., Wang, X., Feng, B., Hu, L., Yang, L., Lu, L., et al. (2019). Activation of G-protein-coupled receptor 30 protects neurons against excitotoxicity through inhibiting excessive autophagy induced by glutamate. *ACS Chem. Neurosci.* 10, 4227–4236. doi:10.1021/acschemneuro.9b00287

Zhang, L., Ma, Y., Liu, M., Ma, Y., and Guo, H. (2019). The effects of various estrogen doses on the proliferation and differentiation of cultured neural stem cells. *Gen. Physiol. Biophys.* 38, 417–425. doi:10.4149/gpb_2019022

Zhang, Y. Y., Liu, M.-Y., Liu, Z., Zhao, J.-K., Zhao, Y.-G., He, L., et al. (2019). GPR30-mediated estrogenic regulation of actin polymerization and spatial memory involves SRC-1 and PI3K-mTORC2 in the hippocampus of female mice. *CNS Neurosci. Ther.* 25, 714–733. doi:10.1111/cns.13108

Zhao, J., Bian, C., Liu, M., Zhao, Y., Sun, T., Xing, F., et al. (2018). Orchiectomy and letrozole differentially regulate synaptic plasticity and spatial memory in a manner that is mediated by SRC-1 in the hippocampus of male mice. *J. Steroid Biochem. Mol. Biol.* 178, 354–368. doi:10.1016/j.jsbmb.2018.02.007

Zhong, J., Ge, H., Zhang, C., Chen, J., Li, H., Fang, X., et al. (2019). G protein-coupled estrogen receptor 1 negatively regulates the proliferation of mouse-derived neural stem/progenitor cells via extracellular signal-regulated kinase pathway. *Brain Res.* 1714, 158–165. doi:10.1016/j.brainres.2019.02.024

Zhou, F., Dong, H., Liu, Y., Yan, L., Sun, C., Hao, P., et al. (2018). Raloxifene, a promising estrogen replacement, limits TDP-25 cell death by enhancing autophagy and suppressing apoptosis. *Brain Res. Bull.* 140, 281–290. doi:10.1016/j.brainresbull.2018.05.017

Frontiers in
Cell and Developmental Biology

Explores the fundamental biological processes of life, covering intracellular and extracellular dynamics.

The world's most cited developmental biology journal, advancing our understanding of the fundamental processes of life. It explores a wide spectrum of cell and developmental biology, covering intracellular and extracellular dynamics.

Discover the latest Research Topics

See more →

Frontiers

Avenue du Tribunal-Fédéral 34
1005 Lausanne, Switzerland
frontiersin.org

Contact us

+41 (0)21 510 17 00
frontiersin.org/about/contact